U.PORTO

DOUTORAMENTO EM CIÊNCIAS FARMACÊUTICAS
ESPECIALIZAÇÃO EM QUÍMICA ANALÍTICA

Self-contained heterogeneous separation/potentiometric sensing devices for the screening of alike compounds in food matrices

Renato Lopes Gil

D

2022

Renato Lopes Gil

Self-contained heterogeneous separation/potentiometric sensing devices for the screening of alike compounds in food matrices

Tese do 3º Ciclo de Estudos Conducente ao Grau de Doutor
em Ciências Farmacêuticas na Especialidade de Química Analítica

Trabalho realizado sob a orientação do Professor Doutor Alberto Nova Araújo e coorientação da Professora Doutora Maria Conceição Branco Silva e da Professora Doutora Célia Gomes Amorim.
No âmbito do Doutoramento Europeu, o trabalho foi realizado sob a orientação do Professor Doutor Gastón Adrián Crespo Paravano

Março 2022

Caminhos difíceis sempre levam a belos destinos.

O melhor está por vir.

This Doctoral Thesis was financially supported by a research Ph.D. Grant (SFRH/BD/131504/2017) provided by Fundação para a Ciência e Tecnologia (FCT, Portugal) from the Minister of Science, Technology and Higher Education (MCTES, Portugal) and European Social Fund through Programa Operacional Capital Humano (POCH).

This Thesis was also supported by the LAQV/REQUIMTE unit, which is financed by Portuguese national funds (FCT/MCTES) through the project UIDB/50006/2020.

The experimental work presented in this Doctoral Thesis was performed in the Laboratory of Applied Chemistry, Department of Chemical Sciences of the Faculty of Pharmacy, University of Porto, Portugal, and in the Department of Chemistry of the School of Engineering Science in Chemistry, Biotechnology, and Healthcare, Royal Institute of Technology, Sweden.

Acknowledgments

Firstly, I would like to express my gratitude to my Supervisor, Professor Alberto Araújo (Ph.D.), for the scientific guidance, consideration, trust, and friendship, providing me with all the conditions to perform this Thesis.

I would also like to express my gratitude to my Co-Supervisor, Professor Maria Conceição Branco Silva (Ph.D.), for the transmitted knowledge, consideration, availability, and friendship. In addition, I am grateful for the challenge of going abroad as a research visitor at the Royal Institute of Technology, Stockholm, Sweden.

A special thank you to my Co-Supervisor, Professor Célia Gomes Amorim (Ph.D.), for the complete availability, guidance, challenge, and trust me throughout this journey. Her scientific and personal teachings have been really important in my personal development, since 2010 when she invited me to join the Sensors and Biosensors Group as a junior researcher. I would like to express my gratitude for her encouragement in the pursuit of a career in research and for the support in each moment of my life.

To Professor Gaston Crespo (Ph.D.) for the supervision of the European Doctorate and for having me as a research visitor in his group at the Royal Institute of Technology, Stockholm, Sweden, for four months, providing me with all the conditions to perform the work.

To Professor Maria Cuartero (Ph.D.) for all teachings, availability, and friendship during my stay at the Royal Institute of Technology. A special thank you for the useful discussions about potentiometry that contributed to my scientific development.

To Professor Irene Rebelo (Ph.D.) and Professor Natércia Teixeira (Ph.D.) for their valuable contribution in providing me with the HPLC instrumentation used throughout this Thesis.

To all the professors of the Applied Chemistry lab of the Faculty of Pharmacy of the University of Porto for the excellent welcome and support, especially to Professor Marcela Segundo (Ph.D.) for the availability in exchanging ideas and to Professor Beatriz Quinaz (Ph.D.) for the opportunity to be a monitor of electrochemistry classes.

To Engenheira Manuela Barros, Ms. Vânia Dias, Ms. Ana Paula Ribeiro, and Ms. Sara Cravo for the friendship and help in logistic issues, always cheerful attending my requests.

To all Sensors and Biosensors Group members for the great working environment, always with good music in the background. A special thanks to Álvaro, Lucho, Jaime, Micha, Diana, and Carina for all the great moments.

To all the next-door colleagues for sharing reagents and materials as well as for their availability and help in technical issues. A special thanks to Bruno, Sarah, Ana Isabel, Andreia M., and Pedro for their enthusiastic friendship, good moments, and words of encouragement.

To all the Crespo Group members for the hospitality, kindness, and friendship during my stay in the Royal Institute of Technology. A special thanks to Kequan, Clara, Bibiana, Noemi, and Alex for all the good moments.

To the IB2 group members, especially Rafael and Sara, for the friendship and work collaboration.

To the Faculty of Pharmacy of the University of Porto and LAQV/REQUIMTE for providing me with the necessary conditions for my work.

To Fundação para a Ciência e Tecnologia (FCT), to Programa Operacional Capital Humano (POCH), and to European Union for the Ph.D. grant SFRH/BD/131504/2017. The financial support for the research stay in the Royal Institute of Technology, in Stockholm, is also acknowledged.

To all my friends for the friendship and support. A special thanks to Liliane, Melânia, Pedro, Ana Rita, Rafael, and Sara for the great moments and words of encouragement.

To my family for backing me up at all times. A special thanks to my parents, Hélder and Maria, and my brother, Pedro, for their unconditional support and for believing in me. Without them (and my grandfather, wherever he is), I would have never reached where I am now. I also thanks to my parents in law, Abílio and Maria José, and to my brothers in law, Carlos and Sofia, for their friendship and support.

To all those who crossed my path and somehow helped me to complete this project.

Finally, I would like to express my deep and sincere gratitude to my wife, Bárbara Loureiro, who has constantly supported me in each moment of my life. Thank you for the love, friendship, trust, and for making me feel happy to be at your side.

Abstract

The present thesis addresses the synergic coupling of potentiometric detection with liquid chromatography (LC) for the development of simple, cost-effective, and robust analytical methodologies applied to food and water quality monitoring.

LC is probably the most common technique used in routine analytical laboratories, being generally combined with UV-Vis or fluorimetric detectors. However, derivatization steps are usually required to increase sensitivity and detectability, involving time-consuming procedures with toxic reagents. On the other hand, mass spectrometry detectors have been used for the determination of trace levels, though the high cost of analysis and the requirement of skilled technicians for operation hinder their availability for most laboratories.

Alternatively, electroanalytical detection provides versatile tools that offer high selectivity and sensitivity in a short time, using simple and affordable instrumentation. While amperometric and conductimetric detectors are well-established, with commercially available instrumentation, the use of potentiometric detectors seems to be overlooked. Potentiometric detection coupled to chromatographic separation techniques started decades ago by using metallic copper electrodes for the determination of inorganic ions in ion chromatography (IC) systems and later extended to organic ionic substances, resorting to polymeric membrane electrodes based on a solid conductive support. Despite their powerful features, potentiometric sensors are still not used as routine detectors in LC. Particularly in the food sector, researchers should put more effort into demonstrating their competitiveness with other detectors.

In this context, the challenge analytical determination of hydrophilic organic compounds in food samples by LC-potentiometric detector is here discussed, particularly the biogenic amines (BAs) and tetracycline antibiotics (TCs), due to their harmful effects on public health. All-solid state ion-selective electrodes (ISEs) were used due to their simple fabrication process, robust analytical performance, and the ability for miniaturization. A wall-jet potentiometric flow-cell, assembling the miniaturized indicator and reference electrodes, was easily integrated into the chromatographic system. A full analysis concerning the determining factors that affected both separation and detection conditions are reported, namely the type of stationary phase, the mobile phase composition, hydrodynamic conditions, and the composition of the sensing membranes in terms of recognition element and use of nanomaterials. The developed ISEs based on polymeric membranes contain cucurbit[n]urils (CB[n]) as recognition elements, whose potentiometric response to

compounds with alike chemical structures (i.e. BAs and TCs) was undertaken. The analytical methodologies were validated according to the requirements of the International Conference on Harmonization, EuraChem, and the European Union.

The determination of BAs in tomato products and alcoholic beverages was achieved by using an amine-selective electrode combined with ion-pair chromatography. The potentiometric detector was based on CB[6] and a lipophilic ion-exchanger as sensing elements, whose analytical performance was improved by the incorporation of multi-walled carbon nanotubes. Aliphatic, aromatic, and heterocyclic amines were successfully quantified without any chemical derivatization procedure, enabling fast and eco-friendly measurements. The chromatographic separation of all studied amines was obtained in less than 25 min using a gradient mobile phase of acetic acid, acetonitrile, and butane-sulfonic acid. Detection and quantification limits ranged from 9.3 to 60.7 μg L^{-1} and from 31.1 to 202.3 μg L^{-1}, respectively.

An analytical method based on a tetracycline-selective electrode coupled to reversed-phase LC for the determination of TCs (chlortetracycline, doxycycline, oxytetracycline, and tetracycline) around the maximum residue limits in milk samples was also developed. The detector was based on CB[8], a lipophilic ion-exchanger, and multi-walled carbon nanotubes. The separation was attained in less than 30 min using a gradient mobile phase of sulphuric acid and acetonitrile. The limits of detection and quantification ranged from 13.3 to 46.0 μg L^{-1} and 44.4 to 92.1 μg L^{-1}, respectively.

Finally, the benefits of LC in the determination of (sub)micromolar levels of ammonium ions in water samples using nonactin-based electrodes, in the presence of high levels of potassium ions, were demonstrated. In this strategy, ammonium-selective electrodes were assembled in a thin-layer flow cell, which was implemented as a detector of IC. The separation of both cations was achieved in less than 15 min by isocratic elution with a mobile phase of nitric acid. Detection and quantification limits were 5.4 and 18.0 μg L^{-1}, respectively.

All the LC-potentiometry methods were successfully applied to the analysis of real samples, highlighting the competitiveness of potentiometric detectors with other techniques. The portability and miniaturization ability of potentiometric sensors, combined with the downsizing of chromatographic columns, will certainly leverage the development of an integrated lab-on-chip platform for the remote screening of different samples.

Keywords: Potentiometric detectors; Ion-selective electrodes; Liquid chromatography; Microfluidics; Food analysis.

Resumo

A presente tese aborda o acoplamento sinérgico da deteção potenciométrica com a cromatografia líquida (CL) para o desenvolvimento de metodologias analíticas simples, económicas e robustas que sejam aplicadas na monitorização da qualidade de alimentos e água.

A CL é provavelmente a técnica mais usada em laboratórios analíticos, sendo geralmente combinada com detetores UV-Vis ou fluorimétricos. No entanto, a derivatização química é geralmente necessária para aumentar a sensibilidade e a detetabilidade, envolvendo procedimentos demorados com reagentes tóxicos. Por outro lado, os detetores de espectrometria de massa têm sido usados para determinações a níveis vestigiais, embora o preço elevado e a necessidade de técnicos qualificados para a operação dificultem a sua disponibilidade para a maioria dos laboratórios.

Em alternativa, a deteção eletroanalítica fornece ferramentas versáteis que oferecem alta seletividade e sensibilidade num curto espaço de tempo, utilizando instrumentação simples e acessível. Embora os detetores amperométricos e condutimétricos estejam devidamente estabelecidos, com equipamento comercialmente disponível, o uso de detetores potenciométricos parece ser negligenciado. O acoplamento da deteção potenciométrica à CL foi inicialmente estudado usando elétrodos metálicos de cobre para a determinação de iões inorgânicos em cromatografia iónica (CI) e posteriormente alargado para substâncias iónicas orgânicas através de elétrodos de membrana polimérica em suporte condutor sólido. Apesar das suas vantagens, os sensores potenciométricos ainda não são vistos como detetores de rotina em CL. Em particular no sector alimentar, um maior esforço de investigação é necessário para demonstrar a competitividade com outros detetores.

Neste contexto, a determinação analítica de compostos hidrofílicos orgânicos em alimentos por CL com deteção potenciométrica é aqui apresentada, nomeadamente aminas biogénicas e tetraciclinas, devido ao seu impacto na saúde pública. Elétrodos-seletivos de iões (ESIs) de suporte condutor sólido foram usados devido à sua construção simples, desempenho analítico robusto e à capacidade de miniaturização. A célula de deteção potenciométrica em *wall-jet*, integrando o elétrodo indicador e de referência, foi acoplada ao sistema cromatográfico. Uma análise completa dos fatores determinantes que afetam as condições de separação e deteção é descrita, nomeadamente o tipo de fase estacionária, a composição da fase móvel, as condições hidrodinâmicas e a composição

das membranas sensoras relativamente ao elemento de reconhecimento e ao uso de nanomateriais. Os ESIs desenvolvidos baseavam-se em membranas poliméricas contendo cucurbit[n]urilos (CB[n]) como elementos de reconhecimento molecular, cuja resposta potenciométrica foi avaliada relativamente a compostos com estruturas químicas semelhantes. As metodologias analíticas foram validadas de acordo com os requisitos da Conferência Internacional de Harmonização, EuraChem e União Europeia.

A determinação de aminas biogénicas em derivados de tomate e bebidas alcoólicas foi proposta usando um elétrodo-seletivo a aminas acoplado a cromatografia de par iónico. O detetor potenciométrico baseia-se em CB[6] e um permutador iónico, cujo desempenho analítico foi melhorado pela incorporação de nanotubos de carbono. Aminas alifáticas, aromáticas e heterocíclicas foram quantificadas sem recurso a qualquer procedimento de derivatização química, permitindo medições rápidas e ecológicas. A separação cromatográfica foi obtida em menos de 25 minutos, usando uma eluição em gradiente com ácido acético, acetonitrilo e ácido butano-sulfónico. Os limites de deteção e quantificação variam de 9,3 a 60,7 μg L^{-1} e de 31,1 a 202,3 μg L^{-1}, respetivamente.

Um elétrodo-seletivo a tetraciclinas acoplado a CL também foi proposto para a determinação de tetraciclinas em amostras de leite. O detetor baseia-se em CB[8], um permutador iónico e nanotubos de carbono. Os analitos foram separados em menos de 30 minutos através de uma eluição em gradiente com ácido sulfúrico e acetonitrilo. Os limites de deteção e quantificação variam de 13,3 a 46,0 μg L^{-1} e 44,4 a 92,1 μg L^{-1}, respetivamente.

Por fim, a determinação de amónio em amostras de água usando elétrodos baseados em nonactina demonstrou os benefícios da CL para superar os problemas de seletividade dos sensores potenciométricos. Nesta abordagem, os elétrodos-seletivos de amónio foram integrados numa célula de fluxo *thin-layer*, que foi implementada como detetor de CI. A separação foi obtida em menos de 15 minutos através de eluição isocrática com ácido nítrico. Os limites de deteção e quantificação são 5,4 e 18,0 μg L^{-1}, respetivamente.

Todos os métodos aqui propostos foram aplicados com sucesso á análise de amostras reais, destacando-se a competitividade dos detetores potenciométricos com outras técnicas analíticas.

Palavras-chave: Detetores potenciométricos; Elétrodos-seletivos de iões; Cromatografia líquida; Análises alimentares; Microfluídica.

Graphical Abstract

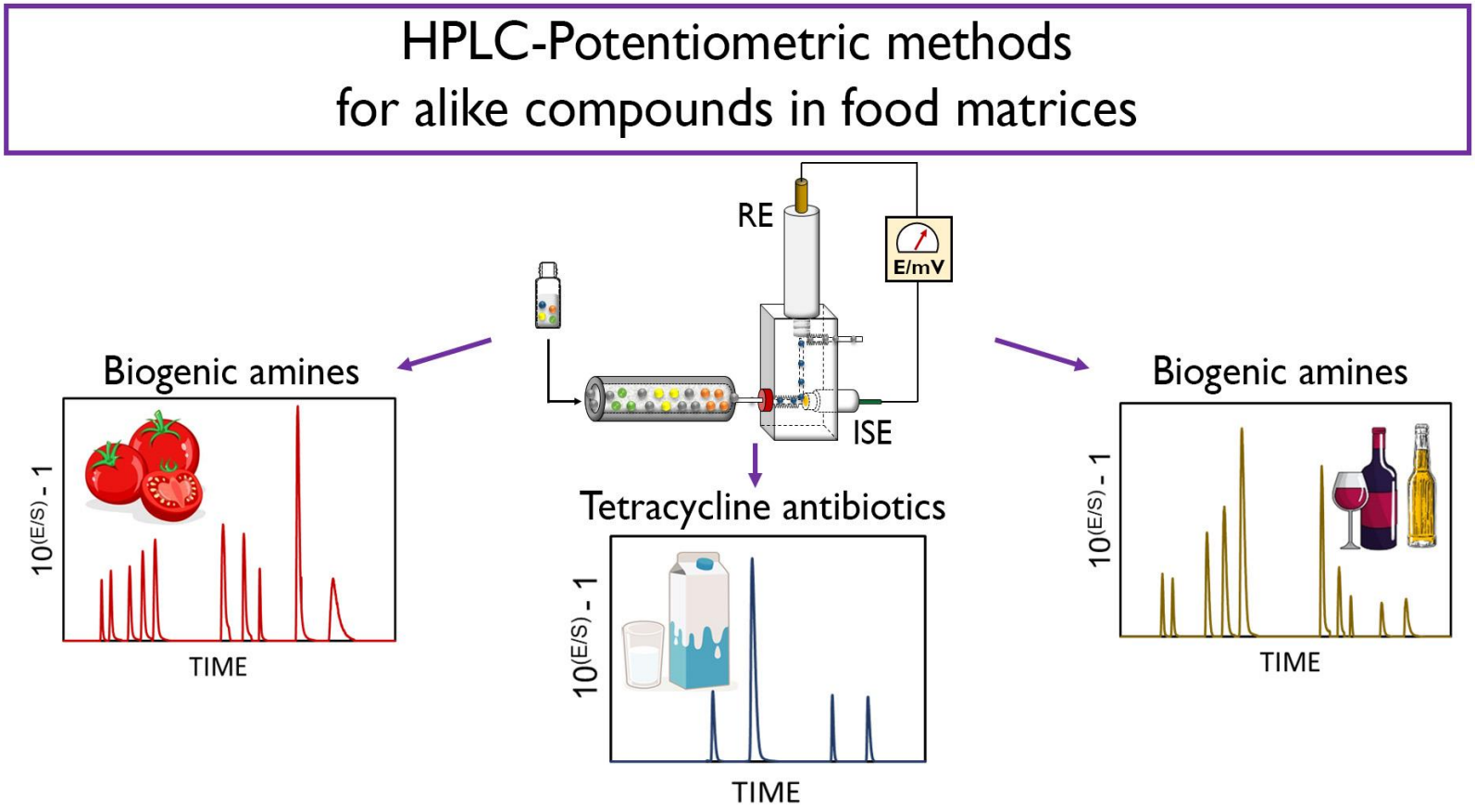

Organization of the Thesis

This Doctoral Thesis in Pharmaceutical Sciences – specialization branch of Analytical Chemistry, entitled "*Self-contained heterogeneous separation/potentiometric sensing devices for the screening of alike compounds in food matrices"*, is divided into five main chapters, each one containing the following information:

- **Chapter 1** – Introduction, which provides a general introduction and the general/specific objectives of this Thesis;
- **Chapter 2** – State-of-the-art, which contains a literature overview about the theoretical background of potentiometry, particularly to the potentiometric response mechanisms in both metallic and ion-selective electrodes. The progress of potentiometry in flow systems is briefly described, highlighting the study of different electrodes constructions and flow-cells designs. Finally, the use of potentiometric detection in liquid chromatographic systems is reported, enhancing its great potential for new analytical applications;
- **Chapter 3** – Experimental section, which describes an overview of the potentiometric measurements in both steady-state and flow conditions. The potentiometric flow cells and the construction of the solid-contact electrodes are fully described. The method validation strategies and the chromatographic parameters are also provided in this chapter;
- **Chapter 4** – Development of four different analytical methodologies based on LC-potentiometry and their application. In sections 4.2 and 4.3, it is stated the development of an amine-selective electrode assembled in a wall-jet flow-cell to be used as a detector of ion-pair chromatography for the determination of underivatized biogenic amines in foodstuff, particularly tomato products and alcoholic beverages. In section 4.4, it is described the development of a tetracycline-selective electrode, assembled in a wall-jet flow-cell, used as a detector in reversed-phase chromatography for the determination of tetracycline residues in milk samples. In section 4.5, ammonium-selective electrodes were incorporated in a thin-layer flow-cell to be implemented as a detector of ion-chromatography for the determination of (sub)micromolar levels of ammonium ions in water samples. As a proof-of-concept, multi-ion detection in the same samples is also described resorting to three different ion-selective electrodes assembled in the flow cell;

- **Chapter 5** – Conclusion, which integrates all the obtained results of the developed analytical methodologies along with the main contributions for electrochemistry and liquid chromatography. Prospects are suggested considering the potential of lab-on-chip chromatography with potentiometric detection in food and environmental analysis.

Table of Contents

List of Figures

Chapter 2. State-of-art

Chapter 3. Experimental section

Section 4.3.

Section 4.4.

Section 4.5.

List of Tables

Section 4.3.

Section 4.4.

Section 4.5.

Abbreviations

α	Separation factor
a_i	Activity of primary ion
a_j	Activity of interfering ion
A_s	Asymmetry factor
E	Potential
F	Faraday constant
G	Gibbs energy
I	Ionic strength
k	Retention factor
$K_{I,J}^{pot}$	Potentiometric selectivity coefficient
N_{eff}	Effective plate number
R	Gas constant
R_s	Peak resolution
T	Absolute temperature
T_f	Tailing factor
tR	Transformed response
t_R	Retention time
ACN	Acetonitrile
BAs	Biogenic amines
CB[n]	Cucurbit[n]uril
CAD	Cadaverine
CTC	Chlortetracycline
DXC	Doxycycline
EFSA	European food safety authority
EMF	Electromotive force
ETH	Ethylamine
EU	European union
FC	Flow-cell
FDA	US Food and Drug Administration
FNDPE	2-fluorophenyl 2-nitrophenyl ether
IC	Ion-chromatography
ICH	International council for harmonisation of technical requirements for pharmaceuticals for human use

ISE	Ion-selective electrode
ISFET	ion-sensitive field-effect transistor
ISM	Ion-selective membrane
IUPAC	International union of pure and applied chemistry
HIS	Histamine
HPLC	High performance liquid chromatography
LC	Liquid chromatography
LLD	Lower limit of detection
LLLR	Lower limit of linear response
LRR	Linear response range
LOD	Limit of detection
LOQ	Limit of quantification
LRR	Linear range of response
MET	Methylamine
MetOH	Methanol
MRL	Maximum residue limit
MS	Mass spectrometry
MWCNTs	Multi-walled carbon nanotubes
NE	Nikolsky-Eisenman
ONPOE	O-nitrophenyloctyl ether
OTC	Oxytetracycline
PDL	Practical detection limit
PEEK	Polyether ether ketone
PHE	Phenylethylamine
POT	Potentiometric detection
PTFE	Polytetrafluoroethylene
PUT	Putrescine
PVC	Polyvinyl chloride
RE	Reference electrode
RM	Reference membrane
RSD	Relative standard deviation
S/N	Signal-to-noise ratio
SBS	Butanesulfonic acid sodium salt
SHS	Heptanesulfonic acid sodium salt
SMS	Methanesulfonic acid sodium salt
SPE	Solid-phase extraction

SPM	Spermine
SPMD	Spermidine
TAN	Total ammonia nitrogen
TC	Tetracycline antibiotic
TCPB	Potassium tetrakis(4-chlorophenyl)borate
THF	Tetrahydrofuran
TRYP	Tryptamine
TTC	Tetracycline
TYR	Tyramine
ULD	Upper limit of detection
UHPLC	Ultra-high performance liquid chromatography
UV-Vis	Ultraviolet-visible

Chapter 1

Introduction

1.1. General introduction

Analytical techniques are extensively used to evaluate the quality and safety of goods and consumables. Between those, liquid chromatography (LC) is today the premier technique for chemical analysis and related applications, with an ability to separate, analyze, and/or purify virtually any sample. LC is a broad classification used to encompass different chromatographic configurations using liquid mobile phases. Paper, thin-layer, and classical column chromatography techniques as well as high-performance liquid chromatography (HPLC) belong to the group of LC. On the other hand, a variety of separation mechanisms can be used within LC, including adsorption, ion-exchange, size-exclusion, affinity, and ion-pair formation. Deep and extensive descriptions of these separation mechanisms can be found in excellent books (1-3) to improve theoretical background and expertise.

HPLC is the most used chromatographic technique in routine analytical laboratories for the separation and analysis of chemical mixtures. Compared to other separation techniques, HPLC presents remarkable assay precision, a broad range of equipment and instrumentation commercially available, and almost universal applicability (2). Notably, only a few samples are excluded from HPLC separation, which combined with the automation and low samples volumes required, makes it the first choice when the analysis of chemical mixtures is required. Moreover, the high versatility is demonstrated by the analysis of a wide type of samples from different industrial sectors. The assessment of the quality of drinking water, the presence of drugs in biological fluids, and the identification of trace contaminants in the pharmaceutical industry, are some of the examples (4). On the other hand, the separation and quantification of vitamins, proteins, carbohydrates, nutraceuticals, allergens, additives, preservatives, toxins, and other contaminants in food has been fully accomplished in the food industry sector (5).

HPLC has been mostly coupled with spectrophotometric detection techniques (i.e. UV-Vis and fluorimetry) for the routine determination of organic species. However, many substances present high polarity and/or do not absorb in the UV region, which hinders its separation and detection by traditional reversed-phase chromatographic columns coupled with spectrophotometric detectors. Chemical derivatization procedures are thus required to increase both sensitivity and detectability, though involving time-consuming sample processing, instability of the chemical products, the toxicity of derivatization agents, and variability of reaction completeness. To mitigate that, LC with tandem mass spectrometry (LC/MS/MS) has been used due to their powerful analytical features such as high sensitivity and selectivity, accuracy, great resolution, and mass spectral identity confirmation (6). Nonetheless, the high cost of the instrumentation (acquisition and maintenance), the use for internal standards, and the need for highly skilled technicians hinder its use in routine quality assays for the quantification of chemical species. The need for sensitive but simpler, fast, reliable, and less expensive detection techniques in LC is thus justified.

Electroanalytical detection has great potential to fulfill these requirements (7), offering high selective and sensitive analysis in a short time, using simple and affordable instrumentation (8). Detection limits in the nanomolar and even picomolar range are readily achieved, making possible the determination of extremely low levels of biochemical compounds. Notably, electroanalytical detection is an ideal candidate for *on-field* chemical analysis because of its portability and miniaturization features without compromising sensitivity and detectability.

While amperometric, coulometric, and conductimetric detectors are well established in LC with commercially available instrumentation (7), the use of potentiometric detectors seems to be overlooked. Potentiometric detection is inexpensive and enables simple determination procedures when compared with previous electroanalytical techniques. As a consequence, potentiometric measurements have been highlighted in small benchtop laboratory apparatus as well as in automated flow equipment (9). Determination of electrolytes in blood samples, heavy metals in natural water samples, and pharmaceutical drugs in bulk drug materials are some of the examples where ion-selective electrodes (ISEs) have been successfully applied (10).

Despite the broad range of applications of potentiometric sensors and the well-known use for the determination of ionizable substances, references to their use as detectors in liquid chromatographic procedures are scarce (11, 12). The first use of potentiometric detection coupled to ion chromatography (IC) systems occurred in the 1970s resorting to liquid membrane electrodes (13). Later, other constructions such as metallic copper (14-17) and

tungsten oxide (18) electrodes were reported. Additionally, ISEs coupled to HPLC were also described by different authors (19-24). Until 2000, the total number of publications was no more than fifty papers, most of them restricted to classical potentiometric detection of metal cations and small inorganic anions (25). Luc Nagels and his group showed new potentialities for coated-wire electrodes based on solid conductive support (26, 27). The group extended the applications to organic ionic substances using polymeric membrane electrodes (28, 29) or conducting oligomer/polymer electrodes (30, 31), mostly in the pharmaceutical field. Meanwhile, the coupling of potentiometric detection with ultra-high performance liquid chromatography (UHPLC) was proposed for the determination of cocaine in biological samples (32).

All the research efforts were focused on coupling the potentiometric detection with LC, searching the most favorable indicator electrodes (metallic or ISE) as well as on demonstrating the detection of analytes from different chemical groups after chromatographic separation (12). The developments achieved so far proved the great potential of potentiometry to become a competitive detection technique with many others. Apart from that, only a few analytical applications in real samples have been reported, particularly in the food sector, where the coupling of potentiometric detection with LC still needs to be evaluated.

1.2. Objectives

The main objective of the present thesis is to show the feasibility of the synergic coupling of potentiometric detection with LC, particularly to achieve simple, cost-effective, and reliable analytical methodologies for the assessment of food and water quality. This approach will extend the application of the potentiometric sensors because many ions usually regarded as interferences in potentiometric measurements will be simultaneously detected and quantified after chromatographic separation. On the other hand, LC enables the determination of new targets for potentiometric sensors, such as bioorganic compounds, which are available in very small quantities and often in admixture with other substances.

All-solid state ISEs were used as indicator electrodes due to their simplicity of fabrication, good potential stability, and the ability for miniaturization. Hydrophilic organic compounds were settled as target analytes, namely biogenic amines, and tetracycline antibiotics, due to their toxicity for public health. Resorting to the powerful features of chromatographic

separation, combined with the versatility of potentiometric sensors, the main objectives of this thesis are:

1. perform a state-of-art overview concerning the use of potentiometric detection in liquid chromatographic systems, highlighting the theoretical background of potentiometry, the potentiometric flow-through detectors already reported, and analytical applications with typical examples;
2. Design and construct of new microfluidic flow-cells to accommodate the ion-selective and the reference electrode, to be used as potentiometric detectors of liquid chromatographic systems;
3. Study the potentiometric response of ISEs based on neutral macrocyclic hosts as ionophores (i.e. cucurbit[n]urils) and/or only on lipophilic ion-exchangers to compounds with alike chemical structures;
4. Integration of the miniaturized ISEs in the constructed microfluidic flow-cells to be used as potentiometric detectors;
5. Optimization of separation and detection conditions, namely stationary phase (i.e. reversed-phase or ion-exchange mode), mobile phase composition (i.e. organic modifier, acidifying agent, and ionic strength), hydrodynamic conditions (flow-rate and injection volume). Evaluation of the use of carbon nanotubes in the preparation of ISEs;
6. Analytical validation of the developed methodologies, including the assessment of the range, linearity, precision, limits of detection and quantification, accuracy, and selectivity.
7. Application of the full validated procedures to the analysis of real samples;
8. Comparison of the proposed LC-potentiometry methodologies with well-established techniques, namely UV-Vis and conductimetric detection.

1.3. References

1. Lundanes E, Reubsaet L, Greibrokk T. Chromatography: Basic Principles, Sample Preparations and Related Methods: Wiley; 2013.

2. Snyder LR, Kirkland JJ, Dolan JW. Introduction to Modern Liquid Chromatography. Third, editor. Hoboken, N.J: Wiley; 2009. 960 p.

3. Ståhlberg J. Chromatography: liquid | Ion pair liquid chromatography. In: Poole C, Cooke M, Wilson ID, editors. Encyclopedia of separation science. First Ed. ed. Oxford: Academic Press; 2000. p. 676-84.

4. Swadesh JK. HPLC: Practical and Industrial Applications, Second Edition: CRC Press; 2000.

5. Nie Q, Nie S. 13 - High-performance liquid chromatography for food quality evaluation. In: Zhong J, Wang X, editors. Evaluation Technologies for Food Quality: Woodhead Publishing; 2019. p. 267-99.

6. Zimmer D. Introduction to quantitative liquid chromatography-tandem mass spectrometry (LC-MS-MS). Chromatographia. 2003;57(1):S325-S32.

7. Erickson BE. Electrochemical detectors for liquid chromatography. Anal Chem. 2000;72(9):353A-7A.

8. Gil R, Amorim CG, Araújo AN, Montenegro MCBSM. Process Analysis: Electroanalytical Techniques. In: Worsfold P, Poole C, Townshend A, Miró M, editors. Encyclopedia of Analytical Science, (3rd ed): Elsevier; 2018. p. 384–8.

9. Montenegro MCBSM, Araújo AN. Flow Potentiometry. In: Trojanowicz M, editor. Advances in Flow Analysis: Wiley-VCH; 2008.

10. Zdrachek E, Bakker E. Potentiometric Sensing. Anal Chem. 2019;91(1):2-26.

11. Trojanowicz M. Recent developments in electrochemical flow detections--a review: part I. Flow analysis and capillary electrophoresis. Anal Chim Acta. 2009;653(1):36-58.

12. Trojanowicz M. Recent developments in electrochemical flow detections--a review part II. Liquid chromatography. Anal Chim Acta. 2011;688(1):8-35.

13. Schultz FA, Mathis DE. Ion-selective electrode detector for ion-exchange liquid chromatography. Anal Chem. 1974;46(14):2253-5.

14. Alexander PW, Haddad PR, Trojanowicz M. Potentiometric detection in ion chromatography using a metallic copper indicator electrode. Chromatographia. 1985;20(3):179-84.

15. Haddad PR, Alexander PW, Trojanowicz M. Ion chromatography of Mg, Ca, Sr and Ba ions using a metallic copper electrode as a potentiometric detector. J Chromatogr A. 1984;294:397-402.

16. Haddad PR, Alexander PW, Trojanowicz M. Ion chromatography of inorganic anions with potentiometric detection using a metallic copper electrode. J Chromatogr. 1985;321(2):363-74.

17. Haddad PR, Alexander PW, Trojanowicz M. Application of indirect potentiometric detection with a metallic copper electrode to ion chromatography of transition metal ions. J Chromatogr A. 1985;324:319-32.

18. Chen ZL, Alexander PW, Haddad PR. Liquid chromatography of carboxylic acids using potentiometric detection with a tungsten oxide electrode. Anal Chim Acta. 1997;338(1-2):41-9.

19. Manz A, Simon W. Potentiometric detector for fast high-performance open-tubular column liquid chromatography. Anal Chem. 2002;59(1):74-9.

20. Isildak I, Covington AK. Ion-selective electrode potentiometric detection in ion-chromatography. Electroanalysis 1993;5(9-10):815-24.

21. Isildak I, Asan A. Simultaneous detection of monovalent anions and cations using all solid-state contact PVC membrane anion and cation-selective electrodes as detectors in single column ion chromatography. Talanta. 1999;48(4):967-78.

22. Trojanowicz M, Meyerhoff ME. Replacement ion chromatography with potentiometric detection using a potassium-selective membrane-electrode. Anal Chim Acta. 1989;222(1):95-107.

23. Trojanowicz M, Meyerhoff ME. Potentiometric pH detection in suppressed ion chromatography. Anal Chem. 1989;61(7):787-9.

24. Hong US, Kwon HK, Nam H, Cha GS, Kwon KH, Paeng KJ. Simultaneous determination of alkali and alkaline-earth metals by ion chromatography with neutral carrier-based ion-selective electrode detector. Anal Chim Acta. 1995;315(3):303-10.

25. Nagels LJ. Potentiometric detection for high-performance liquid chromatography is a reality: Which classes of organic substances are the targets? Pure Appl Chem. 2004;76(4):839–45.

26. Vissers B, Everaert J, Sekula J, Malak A, Bohets H, Bazylak G, et al. Unique potentiometric detection systems for HPLC determination of some steroids in human urine. J Sep Sci. 2009;32(2):167-79.

27. Zielinska D, Gil A, Pietraszkiewicz M, Pietraszkiewicz O, Van de Vijver D, Nagels LJ. Podand and macrocyclic amine receptors with urea functionalities for potentiometric detection of organic acids in HPLC. Anal Chim Acta. 2004;523(2):177-84.

28. B. L. De Backer LJN. Potentiometric detection for capillary electrophoresis: Determination of organic acids. Anal Chem. 1996;68(24):4441-5.

29. De Backer BL, Nagels LJ. Potentiometric detection of organic acids in ion-exclusion chromatography using different types of liquid-membrane electrodes. Anal Chim Acta. 1994;290(3):259-67.

30. Poels I, Nagels LJ, Verreyt G, Geise HJ. Potentiometric detection of organic acids in liquid chromatography using conducting oligomer electrodes. Anal Chim Acta. 1998;370(2-3):105-13.

31. Poels I, Nagels LJ, Verreyt G, Geise HJ. Conducting polymer based potentiometric detection applied to the determination of organic acids with narrow-bore LC systems. Biomed Chromatogr. 1998;12(3):124-5.

32. Daems D, van Nuijs AL, Covaci A, Hamidi-Asl E, Van Camp G, Nagels LJ. Potentiometric detection in UPLC as an easy alternative to determine cocaine in biological samples. Biomed Chromatogr. 2015;29(7):1124-9.

Chapter 2

State-of-art

Chapter 2 gives a brief tutorial about potentiometric detection and an overview of its use in liquid chromatographic systems to enhance its importance for future analytical applications[1].

[1] This is a partial transcription of the article *Renato L. Gil, Célia G. Amorim, Maria C.B.S.M. Montenegro, Alberto N. Araújo; Potentiometric detection in liquid chromatographic systems: an overview; Journal of Chromatography A, 2019, 1602, 326-340; doi: 10.1016/j.chroma.2019.06.006*;

2.1. Introduction

Liquid chromatography (LC) is one of the most used techniques in routine analytical laboratories, usually coupled with spectrophotometric detection techniques. Different electroanalytical techniques have been also used in HPLC but only a small fraction of commercial instruments are covered by electrochemical detectors (1). Electroanalytical techniques offer plenty of information ranging from chemical speciation to thermodynamic and kinetic data derived from phenomena taking place at the bulk solution or in the vicinity of a heterogeneous interface (**Figure 2.1**). Simple measurement of ion content in the sample through the ability to carry electric charges is an example of a bulk solution phenomenon (conductimetry). In turn, the measurement of the physical properties such as impedance, current and potential is related to the amount of analyte present in an electrode interface.

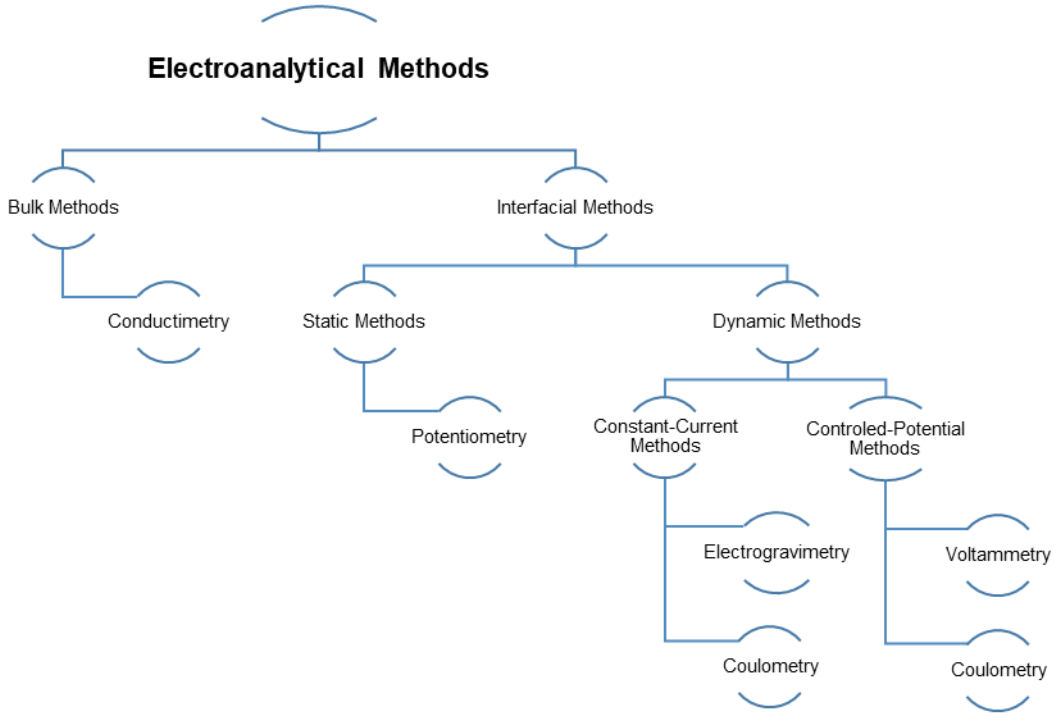

Figure 2.1 Classification of electroanalytical methods.

These techniques are interesting and attractive once they can offer better selectivity and sensitivity than other models of detection. Besides, electroanalytical detection is an ideal candidate for miniaturized analytical systems because of its ability to portability and miniaturization without compromising sensitivity. These advantages are well demonstrated by the numerous reported applications in environmental, clinical, pharmaceutical, and food

analysis (2-9). Electrochemical detectors are thus more selective than UV-Vis and refractive index detectors because analytes that do not absorb in the UV-Vis region are measurable within a large linear dynamic range with high sensitivity. Moreover, they can provide low detection limits in the nanomolar and even picomolar range, making possible the determination of extremely low levels of biochemical compounds (1). The relatively low-cost instrumentation and the short time of analysis make electrochemical detectors very attractive for new analytical applications.

Although the described great advantages, electroanalytical detection has not been widely used in hydrodynamic separation methods as much as spectrophotometric detection. Furthermore, while amperometric, coulometric, and conductimetric detectors are well established in HPLC, with commercially available instrumentation, potentiometric detectors have been only scarcely used (1, 10-16). The number of references is negligible but the results reported therein prove the otherwise great potential for routine applications. Therefore, the present article gives a brief tutorial about potentiometric detection and an overview of its use in liquid chromatographic systems.

2.2. Potentiometry and potentiometric detectors

Potentiometry is a well-established technique boosted by routine use of pH electrodes (glass electrodes) and by the use of ion-selective electrodes for clinical (17), environmental (18, 19), food (20), and pharmaceutical applications (21, 22). At modest costs, the potentiometric detection provides direct or indirect determination of ionizable species within a wide linear dynamic range (23). Two equally important advantages over spectrophotometric methods are the high-quality measurements that do not depend on the optical pathway in the sample bulk, nor are compromised by the background staining or turbidity of the sample matrix. Other key aspects can be better understood by following over time what was the technological development of ion-selective electrodes (24-28).

Potentiometry is an analytical technique based on the measurement of the potential difference between two interfaces in thermodynamic equilibrium when the analyte ion is in simultaneously contact with the reference electrode and the indicator electrode (**Figure 2.2**). The electrodes are in turn connected to a high impedance electrometer instead of a ubiquitous voltage meter, to avoid equilibrium disruption by meaningful electronic currents. Silver-silver chloride and saturated calomel electrodes contacting directly with the sample via double junction are the most used reference electrodes (29). With the trend toward

miniaturization of analytical instrumentation and searching for predictable thermodynamic potentials, reference electrodes based on membranes doped with high lipophilic salts will emerge in routine analysis (30). In turn, the indicator electrodes can range from the classical metallic type electrodes to the ion-selective electrodes with a liquid inner solution or solid-contact – conventional, tubular, coated-wire electrodes and screen-printed electrodes; ion-sensitive field-effect transistors (ISFETs), light addressable potentiometric sensors, and other types of platforms.

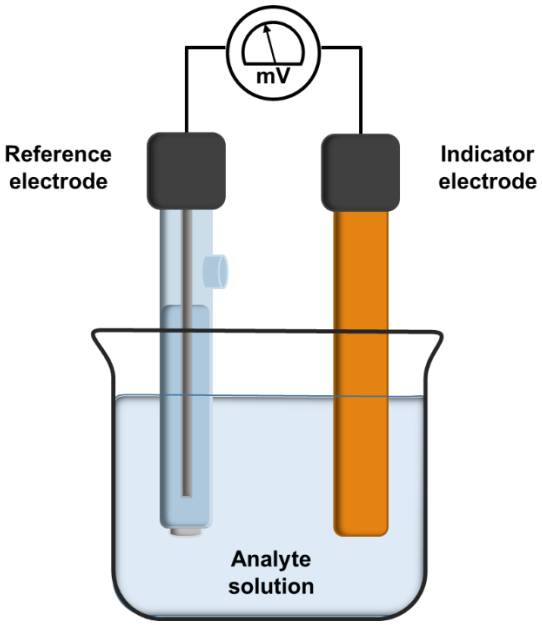

Figure 2.2 Potentiometric cell with a reference electrode and an indicator electrode.

It is the potential at the indicator electrode, and the corresponding potential difference regarding the reference electrode, that contains information about the amount of analyte in a sample. The response mechanisms for the electrodes are very diverse and have been well documented in various review articles (29-33). The first-class electrodes, divided from first to third kind metallic electrodes as well as the redox electrodes, are responsive to the activities of the oxidized and reduced forms of the redox couple near the electrode surface. The developed potential (E), in volts, is related with the extension of the redox reaction, which is expressed by the Gibbs energy (ΔG) through the relationship $\Delta G = -nFE$. Since both ΔG and E depend on the logarithm of the activities of the redox couple, the electrode response can be translated by the Nernst equation:

$$E = E^0 + \frac{RT}{nF} ln \frac{a_{Ox}}{a_{Red}} \qquad (1)$$

where E^0 is the potential difference of the indicator and reference electrodes under standard conditions plus liquid-junction and material interfacial potentials, R is the gas constant, T is the absolute temperature, n is the number of electrons involved in the reaction and F is the Faraday constant. The activities of the oxidized and reduced forms of the compound are denoted by a_{Ox} and a_{Red}, respectively. Therefore, it is easy to understand that redox potentiometry is dependent on the redox ability of target compounds. However, this could be a disadvantage because many analytes are non-redox ionic compounds and hence these potentiometric electrodes are rarely used as detectors in chromatographic systems.

In contrast with conventional metallic electrodes, ion-selective electrodes present high chemical versatility since their response mechanism does not result from any redox reaction. The sensing membranes are based on a hydrophobic charged ion-exchanger and/or a selective complexing agent, called ionophore, which may be (or not) immobilized in a polymeric matrix. The analyte ions can be selectively extracted into the organic membrane phase or adsorbed on the membrane surface, depending on the type of electrode construction. In both cases, they thereby change the chemical surface potential as a result of either an ion-exchange process or an ion transport process occurring between the organic phase and the aqueous phase solution. Considering the anion-exchange process displayed in **Figure 2.3**, the tendency of analyte anion X^- to move from one phase to the other is expressed by ΔG between the ion in the aqueous phase and the ion in the membrane phase:

$$\Delta G_{tr} = \Delta G_{hydr} - \left(\Delta G_{solv} + \Delta G_{ion} + \Delta G_{complex}\right) \qquad (2)$$

where ΔG_{tr} is the Gibbs energy difference of the ion between the aqueous phase and the membrane phase; ΔG_{hydr} is the hydration energy of the ion in the aqueous phase; ΔG_{solv} is the solvation energy of the ion in the membrane phase; ΔG_{ion} refers to the ion-ion interactions in the membrane and $\Delta G_{complex}$ reflects the formation of the complex with the ionophore. Considering that ΔG_{tr} is related to the electrode potential by the expression $E = -\Delta G_{tr}/nF$, it can be assumed that this thermodynamic parameter is the major contributor to the potentiometric signal. When the analyte distributes itself favorably between the sample and the membrane surface, the ΔG_{tr} is high and hence the ion will induce a substantial change in surface potential. Therefore, the sensor responds with high sensitivity to the analyte ion and low detection limits can be achieved.

For an “ideal” ion-selective electrode, the potential would change only when the analyte ions go through the membrane. However, other background ions contribute to the

potentiometric signal when they are present in the sample matrix. The Nikolsky-Eisenman equation translates how interfering ions introduced a signal bias for low analyte concentrations:

$$E\ (mV) = E^0 + S\log\left(c_{analyte} + Cst\right) \qquad (3)$$

Where S is the slope of the linear relationship between $E\ (mV)$ and $\log\ c_{analyte}$ (for a monovalent ion, S is equal to 59 mV at 25ºC) and Cst is the value expressing the contribution of interfering ions to the analytical signal. This contribution depends on the concentration of the interfering ions, their charge, and on the potentiometric selectivity coefficients ($K_{I,J}^{pot}$), which is a numerical measure of the sensor's ability to discriminate the main ion *I* from the interfering one *J* (31, 32). Once each sample has its ionic composition, the values of the coefficients for interfering ions must be small enough for a sensitive determination of the analyte ion. When $c_{analyte}$ >> Cst the electrode potential varies linearly with $\log c_{analyte}$. However, when $c_{analyte}$ < Cst, the potentiometric response becomes constant and independent of the analyte concentration.

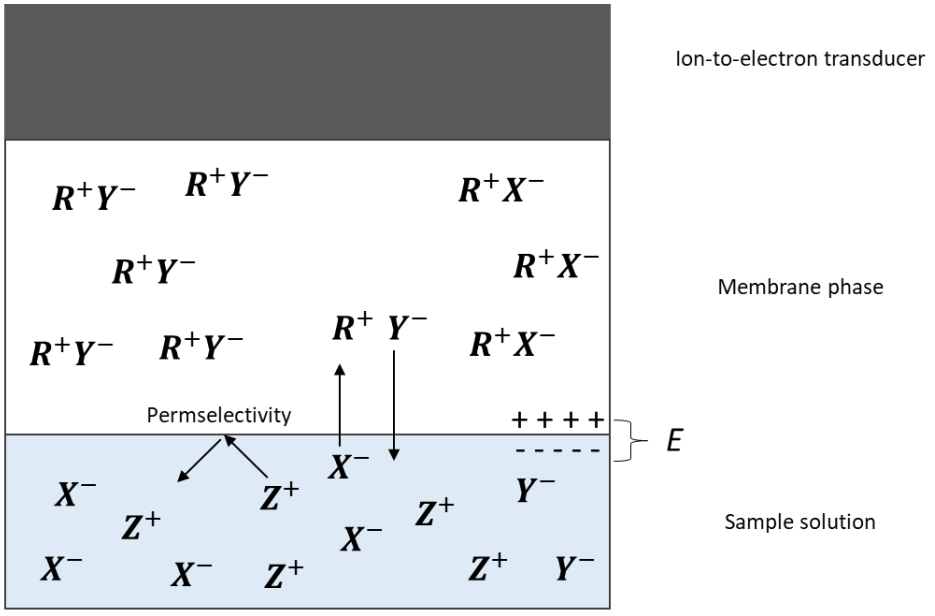

$$X^-_{(aq)} + R^+Y^-_{(membrane)} \leftrightarrow R^+X^-_{(membrane)} + Y^-_{(aq)}$$

Figure 2.3 Diagram interface of the equilibria between the sample and ion-selective membrane. Analyte ion (X^-); lipophilic anion-exchanger (R^+); counter anion (Y^-); counter cation (Z^+).

To obtain high sensitivity, Cst is minimized by a careful choice of a lipophilic ion-exchanger and/or a selective ionophore. The former, usually phenyl borate derivatives or quaternary

ammonium salts, improve ΔG_{ion} by pulling the main ion through the membrane while keeping the counter ion outside. This important property represents the perm-selectivity of the membrane. In turn, the choice of a suitable ionophore favors the complexation with the main ion, improving the $\Delta G_{complex}$. This brings high versatility to potentiometric sensors once the selectivity and sensitivity of the measurements can be modulated according to the application. Furthermore, the ΔG_{solv} also represents an important factor in the potential development because sensing membranes are usually lipophilic and therefore tend to attract lipophilic compounds (high *logP* values) (33).

According to the discussion before, the potentiometric response is not derived from a simple mechanism (34) once it is dependent on the properties of the sensing membrane that are managed by its composition, thermodynamics, and kinetics (35). Theoretical modeling of ion-selective membranes response is very recent (49, 54-57) and it enables the understanding of ions dynamics across the selective membrane (55, 58). Such models guide the management of ion fluxes from the membrane into the sample solution which is very important when detection of sub-nanomolar levels is intended (38, 59). Therefore, the detection limit attained is at least three orders of magnitude better than those obtained with optical detectors (60). The dramatic improvement of detection limits and discrimination of interfering ions allow the application of potentiometry in fields such as environmental trace analysis and biosensing (61).

The evolution of potentiometric techniques over the years allowed its large-scale introduction in routine process analysis through commercially available devices. However, despite its great success, a significant number of chemical assays worldwide are still carried out manually under static batch conditions. Therefore, automation of potentiometric detection in process analysis is highly required, whenever many samples must be processed, or when continuous monitoring is desired. Indeed, a laboratory should be able to analyze many samples in a fast, accurate, reproducible, and economic way.

2.2.1. Potentiometric flow-through detectors

The introduction of laboratory flow analysis was an important landmark for the automation of chemical procedures. The first automatic instrument was proposed by Leonard Skeggs in the middle of the 1950s to perform typical clinical determinations (36, 37). His design of an automatic analyzer was based on the segmentation of the flowing stream with air bubbles, allowing it to achieve an attractive sampling rate due to the limitation of analyte

dispersion during liquid transport. This concept was the basis of flow injection analysis proposed by Ruzicka and Hansen in 1975 (38) wherein a sample solution was aspirated into a carrier stream and transported to a detector. The transient analytical signal was then recorded as a peak instead of a steady-state equilibrium signal with plateau value and was used with satisfactory accuracy in quantitative analysis. The several advantages over the conventional methodologies and the new instrumentation brought speed, automated solution handling, miniaturization, and low cost to the analytical laboratories (39) and were subject to comprehensive and detailed reviews published in the literature (3, 39-44).

Due to the simple construction of flow-through detectors as well as the easy miniaturization of ion-selective electrodes, potentiometric detection was used in the pioneering works on flow injection measurements (38, 45-47). This coupling results in important benefits, demonstrated by the publication of more than 200 research papers (48). In these cases, fast and reliable measurements were focused on the selectivity of the electrode used. Different authors (49-51) reported lower selectivity coefficients measured under transient flow injection conditions than those measured under batch conditions. This is explained by the short time of interaction between the membrane surface and the interfering ions under transient flow injections. Besides, the interference process is highly dependent on the ratio of diffusion and the ion-exchange reaction of the interfering ion (52). Therefore, the selectivity of certain ion-selective electrodes was improved by their use in flow injection conditions, such as in the measurement of chloride levels in tap and sewage water samples (50) and lithium levels in biological samples (53). Over several decades, the great progress of potentiometry has been reflected in the applications in flow systems, studying different electrodes constructions and flow-cells designs. Those development trends are well illustrated by review papers (2, 40, 42, 48, 54-56) and different analytical applications (18, 57-59).

In recent years, it was shown that ISEs without inner electrolyte reference solution and based on polymeric membranes are the most favorable for potentiometric measurements (60-63). Their great figures of merit as well as their robustness and simple fabrication process make them the first choice for flow applications. The easy preparation of the coated-wire electrodes with metal as membrane support could favor its application in flow measurements (16). However, the poor adhesion of the membranes, usually prepared with polyvinyl chloride (PVC) and, above all, the resulting electrical noise of the metal exposed to the flow, contributed to the replacement by other more robust electrode designs with better analytical signals. Accordingly, the direct deposition of the membrane on conductive support was proposed to overpass these coated-wire electrodes drawbacks (64). Moreover,

the flow-through cells design is important for the dynamic characteristics of detection, which include the stability and detection limit of the recorded signal (10). Various potentiometric flow-cells have been described in the literature since the 1970s, namely thin-layer (65), cascade (46), sandwich (66), tubular (67), wall-jet (68) cells, and others with coated-wire electrodes (69). Differences in the length, diameter, and geometry of the channels in the cells were explored, determining the inner dead volume and the transport mechanism of the sample to the membrane electrode interface. Depending on how the sample solution reaches the sensing surface of the electrode, different flow configurations can be adopted. In the wall-jet cell, the electrode is located perpendicularly to the flow and the sample solution spreads uniformly over the entire membrane, creating a minimal diffusion film thickness. Thin-layer and tubular cells are alternative configurations where the sample solution can reach the surface of the sensing membrane through a tangential flow along the membrane.

At the end of the seventies, Ruzicka *et al.* reported a very simple cascade flow-cell for rapid analysis of nitrate and potassium ions in soil extracts (46). The main drawback of this set-up is its deficient mechanical stability. Afterward, a flow-through sandwich potentiometric detector was constructed with a commercial nitrate sensor (66). It allowed simple replacement of the sensing membrane and showed good mechanical and electric stability. The tubular cell has been also used for analytical applications, where the flow channel is made through a longitudinal hole drilled in the conductive support (70-74). Then, the sensing membrane is deposited in the inner walls of the drilled channel and the electrode is inserted in the flow manifold. This detector allows easy change of the membrane and reduces the inner dead volume of the detection cell. These advantages have been demonstrated by several authors for the determination of substances in pharmaceutical formulations, namely penicillin-G (71), clavulanic acid (72), diclofenac (75), and acetylsalicylic acid (76). A classic design of a thin-layer flow-cell was adopted for epinephrine determination in pharmaceutical formulations with great sensitivity but with reduced lifetime when compared with other designs (77). The wall-jet flow configuration has been also used in flow analysis manifolds with a significant increase of durability and stability, namely for the determination of monovalent cations (78, 79), pharmaceutical drugs (80), and histamine content in food products (81). However, none of these flow-through arrangements were highlighted in flow potentiometric analysis, as each of them exhibits some advantages and drawbacks.

All this evolution in the potentiometric flow measurements, through the development of more automated techniques and miniaturization of ion-selective electrodes, contribute to the increase of analytical applications. Although the enormous success is evidenced for millions

of assays every year, potentiometric detection in hydrodynamic separation systems has been neglected and only a limited number of research groups worked on this promising approach (10, 16). The easy and low-cost fabrication of flow detection cells with controlled dead-volumes and the possibility of modulating sensitivity and selectivity should favor the use of potentiometric detectors in liquid chromatography. However, only a few flow-through cells have been tested in liquid chromatographic systems (**Figure 2.4**), with special emphasis on the wall-jet design with coated-wire electrodes. The following section will describe the evolution of potentiometric detection in chromatographic methods of analysis, enhancing its importance for future analytical applications.

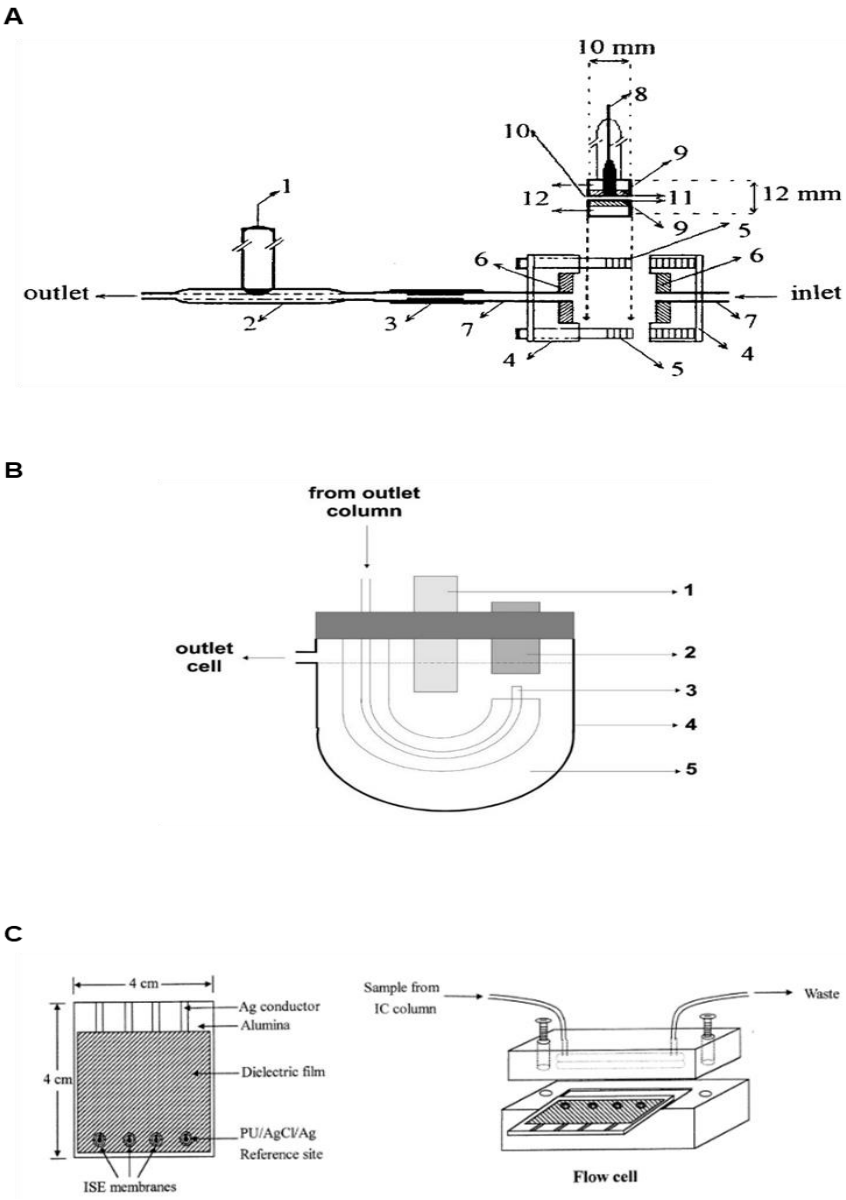

Figure 2.4 Examples of detection cells with potentiometric detectors developed for liquid chromatographic detection. **A –** Detection cell with a tubular ion-selective electrode. (1) reference

electrode; (2) glass holder; (3) adapter; (4) perspex holders; (5) screws; (6) O-rings; (7) PTFE-tubing; (8) electric cable; (9) conducting epoxy cylinder; (10) channel; (11) PVC-matrix membrane; (12) perspex cylinder body. Reprinted with permission from (82). **B –** Schematic presentation of the laboratory-made large-volume wall-jet detector. (1) reference electrode; (2) indicator electrode; (3) LC tubing outlet; (4) large-volume cell in glass; (5) eluent solution. Reprinted with permission from (83). **C** – Detection cell with screen-printed ion-selective electrodes array. Reprinted with permission from (84).

2.3. Potentiometric detection in liquid chromatographic systems

Despite the great potential of potentiometric detectors for the determination of ionizable substances in liquid chromatography, the number of references available is incomparably smaller than those concerning other electrochemical detectors (2, 10). The first uses of potentiometric detection occurred in the 1970s resorting to liquid membrane electrodes (85) but also by using metallic copper (86-89) and tungsten oxide electrodes (90) in ion chromatography (IC) systems. Other groups also implemented diverse applications after coupling ion-selective electrodes to HPLC systems, such as referred by Manz and Simon (91), Isildak and Covington (92, 93), Trojanowicz and Meyerhoff (68, 94), and Hong (95). Until 2000, the total number of publications was no more than fifty papers, most of them restricted to classical potentiometric detection of metal cations and small inorganic anions (96). Luc Nagels and his group showed new potentialities for coated-wire electrodes based on conductive support (97, 98). The group extended the applications to organic ionic substances using polymeric membrane electrodes (99, 100) or conducting oligomer/polymer electrodes (101, 102), mostly in the pharmaceutical field. A summary of the applications found in the literature concerning the use of potentiometric detection in liquid chromatography is described in **Table 2.1**.

As stated before, the first attempts to explore the use of potentiometric detection in liquid chromatography used metallic electrodes, particularly the copper electrode. The potentiometric response of this electrode relied either on the potential determined by the concentration of cuprous or cupric ions in equilibrium at the electrode surface or on direct oxidation or reduction of analytes (88). The copper wire electrode has been extensively used in the determination of a wide variety of chemical species such as inorganic ions (88), carbohydrates (103), organic acids (104), aliphatic amines (105), amino acids (106), and carboxylic acids (107) by chromatographic systems. The determination of aliphatic amines in the range of 0.5 – 1.0 nmol without any sample pre-treatment was noteworthy, since they

do not absorb in the UV region and usually require chemical derivatization to increase detectability (105). Another example concerns the determination of carbohydrates (103), wherein the obtained low detection limits in nanomole range (0.6 – 6.7 nmol) were one order of magnitude smaller than those obtained by refractive index detection (15 – 40 nmol). Less used, the tubular-shaped copper electrode allowed direct determination of amino acids in HPLC, showing comparable response time and sensitivity with UV detection (108). A tungsten oxide wire electrode was also reported for the determination of carboxylic acids by a chromatographic system operating in different modes such as reversed-phase (RP), ion-interaction, and ion-exclusion (90). The detection limits were similar to those obtained with UV detector but the authors have not been successful in uncovering the mechanism of potentiometric response. A different approach to the use of metallic electrodes was tested with a second kind of silver-based electrode for halides determination (109). An Ag/AgBr electrode was used for direct measurement of anions at concentrations lower than those enabled by conductimetric detection in a non-suppressed ion chromatography system (110). The same electrode was also used in replacement ion chromatography for the determination of different anions separated in a suppressed system, which were quantitatively replaced by bromide ions before the effluent passed through the detector. Afterward, the Ag/AgBr electrode shown to be useful for cations detection by monitoring the exchange of co-eluting counter hydroxide ions by bromide ions in the replacement stage of the system.

The low cost of ion-selective electrodes with improved detection limits and fast response time, though with less selectivity for compounds with similar structure led to their assessment as detectors in liquid chromatography (93). The first examples referred to the use of commercial nitrite, nitrate, and phthalate-selective electrodes based on liquid membranes (85). The detector presented a linear range in low nanomole levels for inorganic anions, achieving detection limits of 0.1 and 0.3 nmol for nitrate and nitrite, respectively. The introduction of polymeric membranes based on PVC led to the development of new detectors based on different ion-exchanger or ionophores. The first attempts regarded the use of conventionally-shaped electrodes with inner reference solution, such as the examples reported for the determination of inorganic cations (111) and anions (112) as well as organic acids (100, 112). Low-molecular-weight organic acids only absorb in the low-wavelength UV (210 nm) resulting in high detection limits and frequent matrix interferences. The post-column derivatization increases the sensitivity but with a more laborious method. Hence, the use of potentiometry as an alternative detection method was explored in ion chromatography. A detector based on a PVC membrane with a quaternary ammonium salt achieved detection limits at least 100 times better than those obtained with the UV detector

in the determination of organic acids in red wine and coffee samples (100). Using a similar electrodes configuration, the determination of alkali metal ions and ammonium ions after separation by ion chromatography was evidenced by using different membranes based on neutral carrier type ionophores (113). The results proved that ISE detectors could be looked at as an alternative towards conductimetric detectors, generally used in IC, for monitoring monovalent cations. Subsequently, research has continued in the direction of miniaturization and simplification of the fabrication process by incorporating suitable solid internal contact rather than aqueous inner reference solution (114, 115). For this purpose, the great development achieved with potentiometric detection in flow analysis systems, previously reported in this review, was advantageous. On the one hand, the construction of suitable flow-cell designs to minimize dead-volume and the high availability of sensitive ISEs for different groups of analytes, led to increase the use of solid-contact electrodes in liquid chromatography, especially tubular (82, 93) and coated-wire electrodes (83, 116-118).

In the former case, a solid-contact tubular electrode was reported for simultaneous detection of various inorganic and organic anions after ion chromatography separation (82). The detector was based on a PVC membrane and provided detection limits in sub-ppb levels for most of the analyzed ions. This great sensitivity for the most constructed detectors remained almost constant for at least 2.5 months. The proposed method was then successfully tested through the determination of chloride and nitrate ions in river, rain, and drinking water samples without any sample preconcentration. In another case, the determination of eleven monovalent anions and seven cations by ion chromatography was reported, incorporating different polymeric membranes in tubular-shaped electrodes (92). The author also proposed a system for independent separation and simultaneous detection of both inorganic and organic monovalent anions and cations (**Figure 2.5**). The system included a tubular anion-selective electrode at the end of an anion-exchange column, and a tubular cation-selective electrode at the end of a second one (cation-exchange column), both connected in series. This arrangement enabled a detection limit of ppb levels for all ions. Afterward, the same author proposed the simultaneous separation and detection of monovalent anions and cations but, contrarily to the previous system, the detectors were placed at the end of a single ion chromatography column (93). The system presented a reproducibility better than 2% and a constant sensitivity for almost 2 months in ppb levels. In addition, most anions do not interfere in the detection of cations and most cations do not affect the detection of anions. This represents a real advantage against optical detection because allows the determination of oppositely charged analytes even with similar retention times. The proposed system was then successfully tested through the determination of ions

in environmental water samples without any pre-treatment such as river, sea, and tap waters.

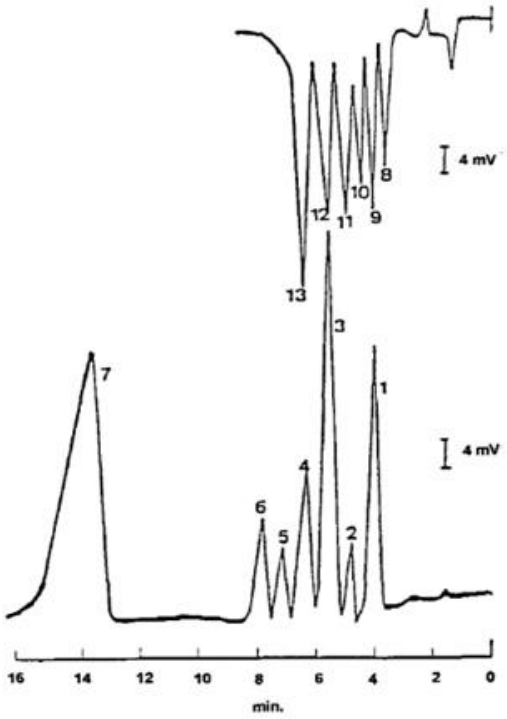

Figure 2.5 Simultaneous separation of anions and cations by ion chromatography followed by potentiometric detection with monovalent anion and cation-selective electrodes in series. Peaks: (1) sodium; (2) ammonium; (3) potassium; (4) rubidium; (5) tetramethylammonium; (6) caesium; (7) thallium; (8) chloride; (9) nitrite; (10) cyanate; (11) benzoate; (12) bromide; (13) nitrate. Injected volume: 20 µL. Columns: Dionex HPIC-AS4A and -CS3. Flow-rate: 1.2 mL min^{-1}. Reprinted with permission from (92).

Another example of solid-contact electrodes used as detectors in liquid chromatography concerns the coated-wire electrodes. The arrangement described and widely explored by Luc Nagels and co-workers consist of a polymeric membrane cast (or deposited) in a solid conductive surface and placed in a large volume wall-jet flow-cell (83, 116-120), similar to the one previously developed independently by Frenzel and Trojanowicz and validated by flow injection potentiometry (121, 122). The eluent contacts perpendicularly with the coated-wire electrode, wherein the distance from the LC tubing-outlet to the sensitive membrane is 100µm. This arrangement was tested for the determination of organic anions of biological interest, using a PVC membrane electrode based on a lipophilic anion-exchanger (116). Different metabolic intermediates (mono-, di-. and tricarboxylic acids, sugar phosphates, and nucleotides) were detected after separation in anion-exchange chromatography. Under isocratic conditions with sodium hydroxide as eluent, this potentiometric detector has

increased sensitivity over other detection methods, achieving detection limits of $5.0x10^{-7}$ mol L^{-1} for fumaric acid. The system was highly reproducible and the electrode sensitivity was maintained for at least 2 months. Using a similar set-up, a membrane containing macrocyclic hexamines as neutral ionophores were used for the determination of organic acids after separation in reversed-phase LC with aqueous phosphoric acid as eluent (83). The great sensitivity of the detector was demonstrated by the detection limits of 6 pmol for malonic acid and 2 pmol for maleic acid. Another work reported the determination of organic amines in ion chromatography, using a detector based on a cation-exchanger combined with a macrocyclic ionophore (119). Without any sample pre-treatment, the potentiometric detector demonstrated a sensitivity 20 times better than the obtained with indirect UV detection, achieving detection limits of $1.0x10^{-6}$ mol L^{-1} (injected concentrations).

Afterward, Bazylak and Nagels's groups extended the analysis to more complex organic ionic substances in the pursuit of new applications. One of the first examples was the analysis of exogenic beta-adrenergic substances in cation-exchange HPLC and RP-HPLC systems (117, 123). Various polymeric membranes containing a cation-exchanger alone or combined with different macrocyclic neutral ionophores (α-cyclodextrin, dibenzo-18-crown-6, or calix[6]arene) were prepared and compared with UV detection. The results showed competitive sensitivity against the traditional spectrophotometric detection, even for strongly UV absorbing compounds. The use of α-cyclodextrin yielded the lowest detection limits, down to 10^{-7}-10^{-8} mol L^{-1} (injected concentrations) for many beta-adrenergic substances. Moreover, the use of eluents with high concentrations of acetonitrile (up to 55%) attained detection limits down to 10^{-9} mol L^{-1} (injected concentrations) but the detector performance was lost after 3 days of continuous use. Maintaining the same cation-exchanger and the same ionophores, the authors also proposed the determination of lysosomotropic amino alcohols and alkyl amines in cation-exchange-HPLC systems (124). In this work, the combination with calix[6]arene yielded the most sensitive detection, achieving detection limits of $1.1x10^{-8}$ and $2.4x10^{-8}$ mol L^{-1} for *N*-methylaminoethanol and hexylamine, respectively. Under isocratic conditions with a mobile phase composed of aqueous phosphoric acid modified with acetonitrile, the separation of a mixture of five standard amino alcohols takes less than 4 minutes (**Figure 2.6**). The viability of the proposed system was then tested by determination of *N,N'*-diethylaminoethanol, a local anesthetic agent, in fortified bovine serum samples after liquid-liquid or solid-phase extraction. The results showed the sensitive and reliable assessment of the target analyte, demonstrated by the detection limit of $1.5x10^{-7}$ mol L^{-1} with the detector based on dibenzo-18-crown-6 as macrocyclic ionophore. In both cases, it was found that an appropriate choice of an ionophore combined (or not) with an ion-exchanger as well as a suitable organic modifier

content in the mobile phase are critical factors to obtaining low detection limits with potentiometric sensors. Therefore, the results obtained by the authors were competitive or even better than those provided by the traditional UV-Vis detection.

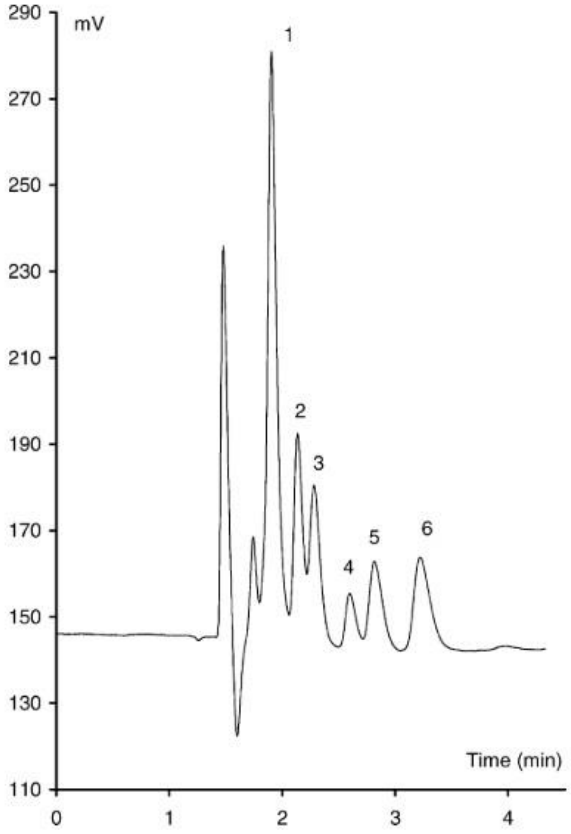

Figure 2.6 Isocratic separation of lysosomotropic amino alcohols by cation exchange HPLC with potentiometric detection using liquid membrane glassy-carbon electrode containing calix[6]arene hexaethylacetate ester. Peaks: (1) aminoethanol; (2) *N*-methylaminoethanol; (3) *N*-ethylaminoethanol; (4) *N,N'*-dimethylaminoethanol; (5) *N,N'*-dimethylaminoisopropanol; (6) *N,N'*-diethylaminoethanol. Injected volume: 20 µL; Injected concentration: 2.0×10^{-4} mol L^{-1}. Column: Alltech universal cation exchange (100mm x 4.6mm i.d.) with pre-column. Mobile phase: acetonitrile-40 mmol L^{-1} phosphoric acid (15:85, v/v), pH 2.30; flow rate: 1 mL min^{-1}. Reprinted with permission from (124).

The same authors also developed a system for reliable HPLC determination of clenbuterol, ambroxol, and bromhexine in commercial pharmaceutical formulations using podant- and macrocyclic-type neutral ionophores (125). A detection limit of 2.6×10^{-10} mol L^{-1} was achieved for the highly hydrophobic bromhexine with a cyanic reversed-phase column and a mobile phase composed by acetonitrile:ethanol:perchloric acid (60:2:38, v/v/v). Although the improved sensitivity for very lipophilic compounds by using high acetonitrile or methanol concentrations (60-75%, v/v) in the mobile phase, the electrodes lifetime was drastically

reduced for just 3 days (when used 3 hours/day). This was explained probably due to the leaching of the ionophores from the PVC matrix (117, 119) and to the increased PVC membrane swelling in the mobile phase containing a high concentration of organic modifier (126). Another application reported in the literature was the determination of triphosphate nucleotides and oligo-nucleotides with a detector based on synthetic macrocyclic amine – and podand ureum receptors (118). The HPLC system consisted of a reversed-phase column and a mobile phase composed of a phosphate buffer, triethylammonium acetate, and acetonitrile in gradient mode. Despite the great sensitivity and long-term stability of the detector (at least 3 months), the long response time and the runs (of almost 60 minutes) had to be improved.

As described above, the results obtained by the sensitive HPLC determination of organic ionizable substances with ion-selective electrodes demonstrate the great potential of potentiometric detection in liquid chromatography. However, there are not yet enough arguments found in the literature that proves the commercial instrumentation development with this detection technique. One reason for this lack of market penetration may be attributed to the reduced electrodes lifetime when using high concentrations of organic modifiers or even because there are not a sufficient number of applications that demonstrate the advantages of potentiometric detection in chromatography. Another reason may be related to the interaction time between the analyte and the membrane surface in flow conditions that contribute to the limited response rate and hence to the peak broadening and loss of sensitivity (10, 127). To understand the potentiometric response in hydrodynamic systems, K. De Wael *et al.* studied the molecular interactions between the analyte and the sensor membrane at the electrode surface (120). The potentiometric signal, in millivolts, was first converted to a signal that expressed the surface concentration of adsorbed ions and a linearization method was then used to measure the binding kinetics. In another work, the adsorption/desorption rates of alkaloid metergoline were also studied and the experimentally determined ΔG values of the analyte-surface interaction showed a linear relation to the response of the sensor (128). A Langmuir adsorption was experienced and the diffusion process through the membrane was negligible. Indeed, the diffusion process only appears if the analyte molecule has long contact times with the sensor membrane. This knowledge about kinetics behavior was applied to optimize the potentiometric detection for other plant alkaloids down to sub-micromolar levels by ultra-high performance liquid chromatography (UHPLC) (128). Moreover, the results obtained by UHPLC/potentiometry method yielded a high correlation with those provided by UHPLC/MS method but presented ten times higher detection limits (**Figure 2.7**). Using the proposed adsorption-based model, the usefulness of a potentiometric detector was later tested to

determine cocaine in complex matrices in UHPLC (129). The system comprised a reversed-phase column eluted with a mixture of acidified water (0.1% formic acid) and methanol under isocratic conditions. Detection limits of 6.3 ng mL^{-1} were attained in serum and urine without any sample pre-treatment, which are below the maximum residue limit of 25 ng mL^{-1}.

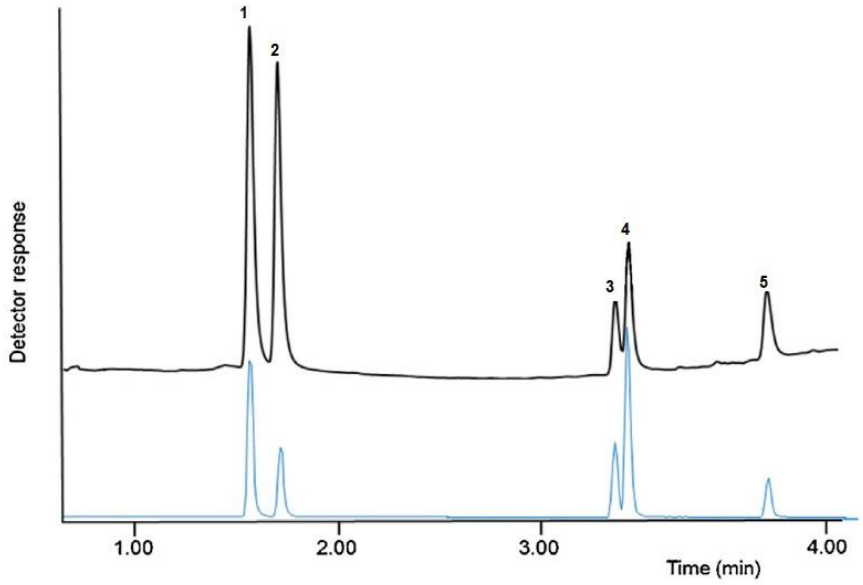

Figure 2.7 Chromatograms obtained from an UHPLC measurement with potentiometric detection (upper curve, black) and mass spectrometry (lower curve, blue). (1) cocaine; (2) papaverine; (3) metergoline; (4) solanidine; (5) drophenine. Injected volume: 6 µL; Injected concentration: $2.0x10^{-5}$ mol L^{-1}. Reprinted with permission from (128).

The use of electroactive conducting polymers in the preparation of conventionally-shaped potentiometric membrane electrodes has been an increasing number of applications (130). Therefore, Luc Nagels and his group tested these materials as an alternative to plasticized PVC membranes for the construction of sensitive potentiometric detectors. An example reported an electroactive oligomer compound for the determination of organic acids by reversed-phase liquid chromatography (101). A membrane-based on a mixture of a phenylene vinylene trimer with a polycarbonate host polymer and iodine in a chloroform solution was directly deposited on the electrode surface. The developed detector allowed to obtain detection limits in the nanogram levels for monocarboxylic acids under isocratic elution with an aqueous-organic solution, which were 10 times better than those obtained with UV detection. The detector showed a rapid response and good reproducibility, maintaining the sensitivity for several months. The ion-exchange properties of these electroactive conducting materials for a broad range of ionic species make them very suitable for use in liquid chromatography (102). However, this approach had a greater

impact on other analytical separation techniques, in particular in miniaturized systems such as capillary electrophoresis (131). Other potentiometric arrangements were also described for the development of miniaturized systems coupled with chromatographic columns such as polymeric membrane ion-selective field-effect transistors. An example was reported for the determination of alkali-metal cations in injected samples with less than 1µL using a miniaturized cation-exchange column eluted with aqueous nitric acid (132). The system was applied for sodium and potassium determination in serum, presenting a good agreement with the results obtained by flame photometry. In another work, an ISFET-based anion sensor was reported for the determination of organic acids by ion-exchange and reversed-phase chromatography (133). The analytical characteristics were compared with those obtained with coated-wire and conventionally-shaped electrodes when using an anion-exchange column eluted with sodium hydroxide, showing similar detection limits of around 100 pmol. Despite the ISFETs being interesting devices for use in miniaturized separation systems of analysis (16), the poor adhesion of the membrane to the gate part of the ISFET made this approach not suitable for chromatographic applications.

Another arrangement described in the literature for potentiometric detection in miniaturized separation systems concerns the chemical sensors arrays, using solid-state screen-printed electrodes (84, 134). Instead of a nonselective ionophore for different ionic species, a variety of neutral carrier type ionophores was used to prepare selective membranes for the determination of monovalent cations by ion chromatography. The potentiometric sensor array provided not only the overall chromatogram for the separated ionic species (lithium, sodium, ammonium, and potassium ions) but also the enhanced chromatogram for specific ions (valinomycin for potassium ions and nonactin for ammonium ions). For the determination of sodium, ammonium, potassium, magnesium, and calcium ions in water samples, a sensor array was directly coupled in a flow system that accommodate a chromatographic column, providing detection limits down to 0.02-0.1 mg L^{-1} level (134). The most significant advantage of these sensor arrays is their ability to determine simultaneously cations and anions in a sample by using the appropriate selective membranes, even when the separation efficiency is not sufficient. However, this approach has been rarely applied in hydrodynamic separation systems but it has been highlighted in the development of electronic tongues for sensory analysis (135, 136).

As stated throughout this overview, various attempts have been carried out to develop new analytical applications, either through the assessment of various potentiometric electrodes or through different flow cells. Despite the different approaches for using potentiometric detection in liquid chromatography, it did not achieve the stage of routine applications with

commercially available instruments, contrary to other electrochemical detectors. Therefore, future studies should be carried out to fulfill the gap of potentiometric detectors in LC.

Table 2.1 Applications of potentiometric detection in liquid chromatography.

Year	*Analyte*	*Sample*	*Type of Electrode*	*Construction*	*Flow-cell*	*Chromatographic Technique*	*Detection Limit*	*Ref.*
1974	Inorganic anions	–	ISE (liquid)	Conventional (inner solution)	Wall-jet	IC	1 – 3 µmol L^{-1}	(85)
1985	Alkaline earth and transition metal ions	–	Metallic (1º kind) Cu	Wire	Cell with wire electrode	IC	0.16 – 9 mg L^{-1}	(86)
1985	Inorganic and organic anions	–	Metallic (1º kind) Cu	Wire	Cell with wire electrode	IC	14 – 87 µg L^{-1}	(86)
1986	Carbohydrates	–	Metallic (1º kind) Cu	Wire	Cell with wire electrode	IC	0.6 – 6.7 nmol (injected amount)	(103)
1987	Inorganic anions	–	ISE (glass)	Conventional (inner solution)	Wall-jet	IC	0.05 – 0.2 mg L^{-1}	(137)
1989	Inorganic anions	–	Metallic (2º kind) Ag/AgBr	Wire	Cell with wire electrode	IC	0.25 – 160 µmol L^{-1}	(110)
1991	Alkali metal ions Potassium	Serum	ISFET (PVC)	Chips	–	IC	10 µmol L^{-1}	(132)
1993	Inorganic anions	–	ISE (PVC)	Conventional (inner solution)	Wall-jet	IC	30 – 60 nmol (injected amount)	(112)
1993	Organic acids	–	ISE (PVC)	Conventional (inner solution)	Wall-jet	IC	30 – 45 ng (injected amount)	(112)
1994	Alkali metal ions and ammonium ion	–	ISE (PVC)	Conventional (inner solution)	Wall-jet	IC	0.42 – 84 µmol L^{-1}	(113)
1995	Alkali and alkaline earth metal ions	Commercial mineral waters	ISE (PVC)	Conventional (inner solution)	Wall-jet	IC	0.77 – 665 ng (injected amount)	(95)
1997	Aliphatic amines	–	Metallic (1º kind) Cu	Wire	Cell with wire electrode	IC	35 µmol L^{-1}	(105)
1997	Carboxylic acids	–	Metallic (1º kind) Cu	Wire	Cell with wire electrode	IC	10 – 50 µmol L^{-1}	(107)
1997	Metal ions	–	Metallic (1º kind) WO_3	Wire	Cell with wire electrode	IC	1 – 10 µmol L^{-1}	(138)

Table 2.1 Continued.

Year	*Analyte*	*Sample*	*Type of Electrode*	*Construction*	*Flow-cell*	*Chromatographic Technique*	*Detection Limit*	*Ref.*
1997	Carboxylic acids	–	Metallic (1º kind) WO_3	Wire	Cell with wire electrode	RP-LC	10 – 50 µmol L^{-1}	(107)
1998	Alkali, alkaline earth metal ions, and ammonium ion	Commercial and natural waters	ISE (PVC)	Screen-printed (array)	Thin-layer cell	IC	0.02 – 0.10 mg L^{-1}	(134)
1998	Organic acids	Wine, orange juice	ISE (Conducting oligomer film)	Coated-wire	Wall-jet	RP-LC	0.09 – 1.10 mg L^{-1}	(101)
1999	Organic and inorganic anions	River, sea, and tap waters	ISE (PVC)	Tubular	Tubular	IC	10 – 500 µg L^{-1}	(93)
1999	Organic and inorganic anions	River, rain, and drinking waters	ISE (PVC)	Tubular	Tubular	IC	few to tens µg L^{-1}	(82)
1999	Inorganic cations	River, sea, and tap waters	ISE (PVC)	Tubular	Tubular	IC	20-120 µg L^{-1}	(93)
2000	Carboxylic acids, phosphate esters, and nucleotides	–	ISE (PVC)	Coated-wire	Wall-jet	LC	0.5 µmol L^{-1}	(116)
2000	Organic acids Fumaric acid	–	ISFET (PVC)	Chips	Wall-jet	RP-LC	 5 µmol L^{-1}	(133)
2000	Alkali metals ions and ammonium ion	–	ISE (PVC)	Screen-printed (array)	Thin-layer cell	IC	0.8-4 µmol L^{-1}	(84)
2001	Organic acids	–	ISE (PVC)	Coated-wire	Wall-jet	RP-LC	2 – 30 pmol (injected amount)	(83)
2001	Amines Aliphatic Biogenic Neurochemical	–	ISE (PVC)	Coated-wire	Wall-jet	Cation-exchange	 0.21 – 2.9 µmol L^{-1} 0.65 – 1 µmol L^{-1} 17 – 50 µmol L^{-1}	(119)
2002	Amino alcohols	–	ISE (PVC)	Coated-wire	Wall-jet	Cation-exchange	11 nmol L^{-1}	(124)
2002	*N,N'*-diethylaminoethanol	Bovine serum	ISE (PVC)	Coated-wire	Wall-jet	Cation-exchange	0.15 µmol L^{-1}	(124)

Table 2.1 Continued.

Year	*Analyte*	*Sample*	*Type of Electrode*	*Construction*	*Flow-cell*	*Chromatographic Technique*	*Detection Limit*	*Ref.*
2003	Pharmaceutical drugs	Pharmaceutical formulations	ISE (PVC)	Coated-wire	Wall-jet	RP-HPLC		(125)
	Ambroxol						3.7 nmol L^{-1}	
	Bromhexine						0.26 nmol L^{-1}	
	Clenbuterol						16 nmol L^{-1}	
2004	Organic acids	–	ISE (PVC)	Coated-wire	Wall-jet	RP-HPLC	1 nmol L^{-1}	(98)
2005	Mononucleotides, oligonucleotides	–	ISE (PVC)	Coated-wire	Wall-jet	RP-HPLC	Low µmol L^{-1}	(118)
2006	Pharmaceutical drugs	–	ISE (PVC)	Coated-wire	Wall-jet	HPLC		(33)
	Bromhexine						0.3 µmol L^{-1}	
	Drofenine						0.41 µmol L^{-1}	
	Fluphenazine						0.25 µmol L^{-1}	
2009	Steroids	Urine	ISE (PVC)	Coated-wire	Wall-jet	HPLC	0.11 – 0.25 µmol L^{-1}	(97)
2009	Ascorbic acid	Pharmaceutical formulations	ISE (polypyrrole film)	Coated-wire	–	IC	70 nmol L^{-1}	(139)
2013	Plant alkaloids	–	ISE (PVC)	Coated-wire	Wall-jet	UHPLC	0.25 – 35.8 µmol L^{-1}	(128)
2014	Cocaine	Serum and urine	ISE (PVC)	Coated-wire	Wall-jet	UHPLC	6.3 ng mL^{-1}	(129)

2.4. Future trends

Potentiometry based on polymeric ion-selective electrodes has improved its analytical performance throughout the years, in part to the coupling with automated flow analysis manifolds and well-succeeded modeling of response using thermodynamic and kinetic approaches. Consequently, competitive detection limits in sub-nanomolar combined with the ability of miniaturization, rapidity, and inexpensive operation turned ISEs into an attractive and powerful tool to be taken into account on a similar basis as is, for instance, UV-Vis or fluorometric methods.

These advantages associated with suitable flow-through detection cells support their use as detectors in liquid chromatography. Nevertheless, this method was not yet accepted as a routine electrochemical detector in liquid chromatographic systems. The question is why? What are the major hindrances superimposing its generalized usage? The high content of organic modifiers in mobile phases decreases the reproducibility and lifetime of detectors based on PVC membranes, which are the most commonly used in analytical applications. On the other hand, contributions evidencing real management of ion fluxes to improve the detection limits of ISEs in chromatographic detection need to be urgently validated, instead of passively accepting the idea that potentiometric detectors only allow detections in the order of micromolar.

The recent knowledge on the adsorption-based model at the electrode surface allowed a better understanding of binding kinetics in flow conditions and hence the optimization of potentiometric response to different analytes in UHPLC (120, 129). On the other hand, nanomaterials play an important role in the fabrication of sensors due to their attractive properties, such as the large surface area/volume ratio and the excellent electrical properties (140). Accordingly, different approaches about their use have been described in the literature, namely the functionalization of nanomaterials to develop stable ISEs with longer lifetime, the application of nanomaterials as alternative receptors layers to avoid the leaching of the membrane components, and the incorporation of nanomaterials to increase the sensitivity (141). These great advances associated with the great versatility of potentiometric arrangements will certainly leverage the more and more realistic use of this detection technique in hydrodynamic separation methods of analysis. Using robust forms of ion-selective electrodes, the potential for new analytical applications in food, industrial, and biotech fields is very high. Potentiometry coupled to LC can give access to the determination of many bioorganic compounds, such as proteins, hormones, and vitamins, which are available only in a few quantities and often in admixture with other substances.

To improve the “extraction” of the analyte ion into the membrane and minimize the response to interfering ions, different membrane materials such as polymer matrix, plasticizers and ion-exchangers should have to be tested to demonstrate the advantage of potentiometry in flow separation systems. The interaction of the analyte and interfering ions with the sensor surface must be studied wherein the molecular dynamics simulations can be helpful in the future. The selectivity and sensitivity as determining factors should also be tested concerning the type of chromatographic columns and mobile phase composition to achieve the best analytical features of the method. These successful studies will make the HPLC/Potentiometry technique a promising approach for sensitive, simple, and low-cost analysis in different areas of interest.

2.5. References

1. Erickson BE. Electrochemical detectors for liquid chromatography. Anal Chem. 2000;72(9):353A-7A.

2. Trojanowicz M. Recent developments in electrochemical flow detections--a review: part I. Flow analysis and capillary electrophoresis. Anal Chim Acta. 2009;653(1):36-58.

3. Trojanowicz M, Kolacinska K. Recent advances in flow injection analysis. Analyst. 2016;141(7):2085-139.

4. Hanrahan G, Patil DG, Wang J. Electrochemical sensors for environmental monitoring: design, development and applications. J Environ Monit. 2004;6(8):657-64.

5. Wang Y, Xu H, Zhang JM, Li G. Electrochemical sensors for clinic analysis. Sensors-Basel. 2008;8(4):2043-81.

6. Viswanathan S, Radecka H, Radecki J. Electrochemical biosensors for food analysis. Monatsh Chem. 2009;140(8):891-9.

7. Kimmel DW, LeBlanc G, Meschievitz ME, Cliffel DE. Electrochemical sensors and biosensors. Anal Chem. 2012;84(2):685-707.

8. Rapini R, Marrazza G. Electrochemical aptasensors for contaminants detection in food and environment: Recent advances. Bioelectrochemistry. 2017;118:47-61.

9. Felix FS, Angnes L. Electrochemical immunosensors - A powerful tool for analytical applications. Biosens Bioelectron. 2018;102:470-8.

10. Trojanowicz M. Recent developments in electrochemical flow detections--a review part II. Liquid chromatography. Anal Chim Acta. 2011;688(1):8-35.

11. Wang C, Xu J, Zhou G, Qu Q, Yang G, Hu X. Electrochemical detection coupled with high-performance liquid chromatography in pharmaceutical and biomedical analysis: A mini review. Comb Chem High T Scr. 2007;10(7):547-54.

12. Kusu F. Development and application of electroanalytical methods in biomedical fields. Yakugaku Zasshi. 2015;135(3):415-30.

13. Cheng J, Liu Y. Electrochemical detection in high performance liquid chromatography for analysis of pharmaceutical drugs. Chin Pharm J. 2017;52(20):1753-71.

14. Sontag G, Pinto MI, Noronha JP, Burrows HD. Analysis of food by high performance liquid chromatography coupled with coulometric detection and related techniques: a review. J Agr Food Chem. 2019;67(15):4113-44.

15. Hori H, Hayakawa E, Yamashita N, Taniyasu S, Nakata F, Kobayashi Y. High-performance liquid chromatography with conductimetric detection of perfluorocarboxylic acids and perfluorosulfonates. Chemosphere. 2004;57(4):273-82.

16. L.J. Nagels IP. Solid state potentiometric detection systems for LC, CE and µTAS methods. Trac-Trend Anal Chem. 2000;19(7):410-7.

17. Lewenstam A. Chapter 1 Clinical analysis of blood gases and electrolytes by ion-selective sensors. In: S. Alegret AM, editor. Comprehensive Analytical Chemistry. 49: Elsevier; 2007. p. 5-24.

18. De Marco R, Clarke G, Pejcic B. Ion-Selective Electrode Potentiometry in Environmental Analysis. Electroanalysis 2007;19(19-20):1987-2001.

19. Radu A, Radu T, McGraw C, Dillingham P, Anastasva-Ivanova S, Diamond D. Ion selective electrodes in environmental analysis. J Serb Chem Soc. 2013;78(11):1729-61.

20. Viswanathan S, Radecka H, Radecki J. Electrochemical biosensors for food analysis. Monatshefte für Chemie - Chemical Monthly. 2009;140(8):891-9.

21. K. Gupta V, Nayak A, Agarwal S, Singhal B. Recent advances on potentiometric membrane sensors for pharmaceutical analysis. Comb Chem High T Scr. 2011;14(4):284-302.

22. Siddiqui MR, AlOthman ZA, Rahman N. Analytical techniques in pharmaceutical analysis: A review. Arab J Chem. 2017;10:S1409-S21.

23. Bratov A, Abramova N, Ipatov A. Recent trends in potentiometric sensor arrays--a review. Anal Chim Acta. 2010;678(2):149-59.

24. Lindner E, Toth K. To the memory of Erno Pungor: a subjective view on the history of ion-selective electrodes. Electroanalalysis 2009;21(17-18):1887-94.

25. Buck RP, Lindner E. Peer reviewed: Tracing the history of selective ion sensors. Anal Chem. 2001;73(3):88 A-97 A.

26. Frant MS. History of the early commercialization of ion-selective electrodes. Analyst. 1994;119(11):2293-301.

27. Fernandes JCBK, Lauro Tatsuo, Oliveira Neto, Graciliano. Eletrodos íon-seletivos: histórico, mecanismo de resposta, seletividade e revisão dos conceitos. Quim Nova. 2001;24(1):120-30.

28. Frant MS. Where did ion selective electrodes come from? The story of their development and commercialization. J Chem Educ. 1997;74(2):159-66.

29. Guth U, Gerlach F, Decker M, Oelßner W, Vonau W. Solid-state reference electrodes for potentiometric sensors. J Solid State Electr. 2008;13(1):27-39.

30. Mattinen U, Bobacka J, Lewenstam A. Solid-contact reference electrodes based on lipophilic salts. Electroanalysis 2009;21(17-18):1955-60.

31. Bakker E, Pretsch E, Buhlmann P. Selectivity of potentiometric ion sensors. Anal Chem. 2000;72(6):1127-33.

32. Macca C. Determination of potentiometric selectivity. Anal Chim Acta. 1996;321(1):1-10.

33. Vissers B, Bohets H, Everaert J, Cool P, Vansant EF, Du Prez F, et al. Characteristics of new composite- and classical potentiometric sensors for the determination of pharmaceutical drugs. Electrochim Acta. 2006;51(24):5062-9.

34. Bobacka J, Ivaska A, Lewenstam A. Potentiometric ion sensors. Chem Rev. 2008;108(2):329-51.

35. Eric Bakker PB, Erno Pretsch. Polymer membrane ion-selective electrodes - What are the limits? Electroanalysis 1999;11(3):915-32.

36. Skeggs LT, Jr. An automatic method for colorimetric analysis. Clin Chem. 1956;2:241.

37. Skeggs LT, Jr. An automatic method for colorimetric analysis. Am J Clin Pathol. 1957;28(3):311-22.

38. J.Ŗužička EHH. Flow injection analyses: Part I. A new concept of fast continuous flow analysis. Anal Chim Acta. 1975;78(1):145-57.

39. Ruzicka J, Hansen EH. Retro-review of flow-injection analysis. Trac-Trend Anal Chem. 2008;27(5):390-3.

40. Trojanowicz M, Szewczynska M, Wcislo M. Electroanalytical flow measurements – recent advances. Electroanalysis 2003;15(5-6):347-65.

41. Trojanowicz M. Advances in Flow Analysis: Wiley; 2008.

42. Batista AD, Sasaki MK, Rocha FRP, Zagatto EAG. Flow analysis in Brazil: contributions over the last four decades. Analyst. 2014;139(15):3666-82.

43. Trojanowicz M, Kaniewska M. Flow methods in chiral analysis. Anal Chim Acta. 2013;801:59-69.

44. Chocholous P, Solich P, Satinsky D. An overview of sequential injection chromatography. Anal Chim Acta. 2007;600(1-2):129-35.

45. J.W.B. Stewart JR, H. Bergamin Filho, E.A. Zagatto. Flow injection analysis : Part III. Comparison of continuous flow spectrophotometry and potentiometry for the rapid determination of the total nitrogen content in plant digests. Anal Chim Acta. 1976;81(2):371-86.

46. J. Ruzicka EHH, E.A. Zagatto. Flow injection analysis: Part VII. Use of ion-selective electrodes for rapid analysis of soil extracts and blood serum. Determination of potassium, sodium and nitrate. Anal Chim Acta. 1977;88(1):1-16.

47. E. Pungor ZF, G. Nagy. Application of silicone rubber-based graphite electrodes for continuous flow measurements: Part I. general relationships. Anal Chim Acta. 1970;51(3):431-6.

48. Couto CMCM, Montenegro MCBSM. Potentiometric detectors for flow injection analysis systems, evolution and application. Quim Nova. 2000;23(6):774-84.

49. Trojanowicz M, Matuszewski W. Potentiometric flow-injection determination of chloride. Anal Chim Acta. 1983;151:77-84.

50. Ilcheva L, Cammann K. Flow injection analysis of chloride in tap and sewage water using ion-selective electrode detection. Fresenius Z Anal Chem. 1985;322(3):323-6.

51. Shpigun LK, Basanova OV, Zolotov YA. Performance of solid-membrane cation-selective electrodes for flow-injection potentiometry. Sens Actuators B: Chem. 1992;10(1):15-20.

52. Hulanicki A, Lewenstam A. Model for treatment of selectivity coefficients for solid-state ion-selective electrodes. Anal Chem. 1981;53(9):1401-5.

53. Coldur F, Andac M. A flow-injection potentiometric system for selective and sensitive determination of serum lithium level. Electroanalysis 2013;25(3):732-40.

54. Perez-Olmos R, Soto JC, Zarate N, Araujo AN, Montenegro MCBSM. Sequential injection analysis using electrochemical detection: a review. Anal Chim Acta. 2005;554(1-2):1-16.

55. Chailapakul O, Ngamukot P, Yoosamran A, Siangproh W, Wangfuengkanagul N. Recent electrochemical and optical sensors in flow-based analysis. Sensors-Basel. 2006;6(10):1383-410.

56. Tóth K, Fucskó J, Lindner E, Fehér Z, Pungor E. Potentiometric detection in flow analysis. Anal Chim Acta. 1986;179:359-70.

57. Mesquita RB, Rangel AO. A review on sequential injection methods for water analysis. Anal Chim Acta. 2009;648(1):7-22.

58. Pimenta AM, Montenegro MC, Araujo AN, Calatayud JM. Application of sequential injection analysis to pharmaceutical analysis. J Pharm Biomed Anal. 2006;40(1):16-34.

59. Simkova D, Labuda J. Electrochemical DNA biosensors and flow-through analysis. A review. Curr Anal Chem. 2011;7(1):2-7.

60. Pungor E. The new theory of ion-selective electrodes. Sensors. 2001;1(1):1-12.

61. Bakker E, Buhlmann P, Pretsch E. Carrier-based ion-selective electrodes and bulk optodes. 1. General characteristics. Chem Rev. 1997;97(8):3083-132.

62. Sokalski T, Zwickl T, Bakker E, Pretsch E. Lowering the detection limit of solvent polymeric ion-selective electrodes. 1. Modeling the influence of steady-state ion fluxes. Anal Chem. 1999;71(6):1204-9.

63. Sutter J, Radu A, Peper S, Bakker E, Pretsch E. Solid-contact polymeric membrane electrodes with detection limits in the subnanomolar range. Anal Chim Acta. 2004;523(1):53-9.

64. Montenegro MCBSM, Araújo AN. Flow Potentiometry. In: Trojanowicz M, editor. Advances in Flow Analysis: Wiley-VCH; 2008.

65. Yildiz A, Kissinge.Pt, Reilley CN. Evaluation of an improved thin-layer electrode. Anal Chem. 1968;40(7):1018-24.

66. Alegret S, Alonso J, Bartroli J, Lima JLFC, Machado AASC, Paulis JM. Flow-through sandwich PVC matrix membrane electrode for flow injection analysis. Anal Lett. 2006;18(18):2291-303.

67. Alegret S, Alonso J, Bartrolí J, Paulis JM, Lima JLFC, Machado AASC. Flow-through tubular PVC matrix membrane electrode without inner reference solution for flow injection analysis. Anal Chim Acta 1984;164:147-52.

68. Trojanowicz M, Meyerhoff ME. Potentiometric Ph detection in suppressed ion chromatography. Anal Chem. 1989;61(7):787-9.

69. Alexander PW, Haddad PR, Trojanowicz M. Potentiometric flow-injection determination of copper-complexing inorganic anions with a copper-wire indicator electrode. Anal Chem. 2002;56(13):2417-22.

70. Pimenta AM, Araujo AN, Montenegro MC, Pasquini C, Rohwedder JJ, Raimundo IM, Jr. Chloride-selective membrane electrodes and optodes based on an indium(III)

porphyrin for the determination of chloride in a sequential injection analysis system. J Pharm Biomed Anal. 2004;36(1):49-55.

71. Santos EM, Araujo AN, Couto CM, Montenegro MC, Kejzlarova A, Solich P. Ion selective electrodes for penicillin-G based on Mn(III)TPP-Cl and their application in pharmaceutical formulations control by sequential injection analysis. J Pharm Biomed Anal. 2004;36(4):701-9.

72. Pimenta AM, Araujo AN, Conceicao M, Montenegro BSM. A sequential injection analysis system for potassium clavulanate determination using two potentiometric detectors. J Pharm Biomed Anal. 2002;30(4):931-7.

73. Kamel AH, Soror TY, Al Romian FM. Flow through potentiometric sensors based on molecularly imprinted polymers for selective monitoring of mepiquat residue, a quaternary ammonium herbicide. Anal Methods-Uk. 2012;4(9):3007-12.

74. Fernandes RN, Sales MG, Reis BF, Zagatto EA, Araujo AN, Montenegro MC. Multi-task flow system for potentiometric analysis: its application to the determination of vitamin B6 in pharmaceuticals. J Pharm Biomed Anal. 2001;25(5-6):713-20.

75. Pimenta AM, Araujo AN, Montenegro MCBSM. Simultaneous potentiometric and fluorimetric determination of diclofenac in a sequential injection analysis system. Anal Chim Acta. 2002;470(2):185-94.

76. Pasekova H, Sales MG, Montenegro MC, Araujo AN, Polasek M. Potentiometric determination of acetylsalicylic acid by sequential injection analysis (SIA) using a tubular salicylate-selective electrode. J Pharm Biomed Anal. 2001;24(5-6):1027-36.

77. Amorim CG, Araujo AN, Montenegro MC. Exploiting sequential injection analysis with lab-on-valve and miniaturized potentiometric detection epinephrine determination in pharmaceutical products. Talanta. 2007;72(4):1255-60.

78. Gyurcsanyi RE, Nyback AS, Toth K, Nagy G, Ivaska A. Novel polypyrrole based all-solid-state potassium-selective microelectrodes. Analyst. 1998;123(6):1339-44.

79. Quan DP, Quang CX, Duan LT, Viet PH. A conductive polypyrrole based ammonium ion selective electrode. Environ Monit Assess. 2001;70(1-2):153-65.

80. Amorim CG, Araujo AN, Montenegro MC, Silva VL. Cyclodextrin-based potentiometric sensors for midazolam and diazepam. J Pharm Biomed Anal. 2008;48(4):1064-9.

81. Amorim CG, Souza RC, Araujo AN, Montenegro MCBSM, Silva VL. SI lab-on-valve analysis of histamine using potentiometric detection for food quality control. Food Chem. 2010;122(3):871-6.

82. Isildak I. Potentiometric detection of monovalent anions separated by ion chromatography using all solid-state contact PVC matrix membrane electrode. Chromatographia. 1999;49(5-6):338-42.

83. Zielinska D, Poels I, Pietraszkiewicz M, Radecki J, Geise HJ, Nagels LJ. Potentiometric detection of organic acids in liquid chromatography using polymeric liquid membrane electrodes incorporating macrocyclic hexaamines. J Chromatogr A. 2001;915(1-2):25-33.

84. Lee DK, Lee HJ, Cha GS, Nam H, Paeng KJ. Ion chromatography detector based on solid-state ion-selective electrode array. J Chromatogr A. 2000;902(2):337-43.

85. Schultz FA, Mathis DE. Ion-selective electrode detector for ion-exchange liquid chromatography. Anal Chem. 1974;46(14):2253-5.

86. Alexander PW, Haddad PR, Trojanowicz M. Potentiometric detection in ion chromatography using a metallic copper indicator electrode. Chromatographia. 1985;20(3):179-84.

87. Haddad PR, Alexander PW, Trojanowicz M. Ion chromatography of Mg, Ca, Sr and Ba ions using a metallic copper electrode as a potentiometric detector. J Chromatogr A. 1984;294:397-402.

88. Haddad PR, Alexander PW, Trojanowicz M. Ion chromatography of inorganic anions with potentiometric detection using a metallic copper electrode. J Chromatogr 1985;321(2):363-74.

89. Haddad PR, Alexander PW, Trojanowicz M. Application of indirect potentiometric detection with a metallic copper electrode to ion chromatography of transition metal ions. J Chromatogr A. 1985;324:319-32.

90. Chen ZL, Alexander PW, Haddad PR. Liquid chromatography of carboxylic acids using potentiometric detection with a tungsten oxide electrode. Anal Chim Acta. 1997;338(1-2):41-9.

91. Manz A, Simon W. Potentiometric detector for fast high-performance open-tubular column liquid chromatography. Anal Chem. 2002;59(1):74-9.

92. Isildak I, Covington AK. Ion-selective electrode potentiometric detection in ion-chromatography. Electroanalysis 1993;5(9-10):815-24.

93. Isildak I, Asan A. Simultaneous detection of monovalent anions and cations using all solid-state contact PVC membrane anion and cation-selective electrodes as detectors in single column ion chromatography. Talanta. 1999;48(4):967-78.

94. Trojanowicz M, Meyerhoff ME. Replacement ion chromatography with potentiometric detection using a potassium-selective membrane-electrode. Anal Chim Acta. 1989;222(1):95-107.

95. Hong US, Kwon HK, Nam H, Cha GS, Kwon KH, Paeng KJ. Simultaneous determination of alkali and alkaline-earth metals by ion chromatography with neutral carrier-based ion-selective electrode detector. Anal Chim Acta. 1995;315(3):303-10.

96. Nagels LJ. Potentiometric detection for high-performance liquid chromatography is a reality: Which classes of organic substances are the targets? Pure Appl Chem. 2004;76(4):839–45.

97. Vissers B, Everaert J, Sekula J, Malak A, Bohets H, Bazylak G, et al. Unique potentiometric detection systems for HPLC determination of some steroids in human urine. J Sep Sci. 2009;32(2):167-79.

98. Zielinska D, Gil A, Pietraszkiewicz M, Pietraszkiewicz O, Van de Vijver D, Nagels LJ. Podand and macrocyclic amine receptors with urea functionalities for potentiometric detection of organic acids in HPLC. Anal Chim Acta. 2004;523(2):177-84.

99. B. L. De Backer LJN. Potentiometric Detection for Capillary Electrophoresis: Determination of Organic Acids. Anal Chem. 1996;68(24):4441-5.

100. De Backer BL, Nagels LJ. Potentiometric detection of organic acids in ion-exclusion chromatography using different types of liquid-membrane electrodes. Anal Chim Acta. 1994;290(3):259-67.

101. Poels I, Nagels LJ, Verreyt G, Geise HJ. Potentiometric detection of organic acids in liquid chromatography using conducting oligomer electrodes. Anal Chim Acta. 1998;370(2-3):105-13.

102. Poels I, Nagels LJ, Verreyt G, Geise HJ. Conducting polymer based potentiometric detection applied to the determination of organic acids with narrow-bore LC systems. Biomed Chromatogr. 1998;12(3):124-5.

103. Cowie CE, Haddad PR, Alexander PW. The determination of reducing carbohydrates using a cation-exchange column and potentiometric detection with a metallic copper electrode. Chromatographia. 1986;21(7):417-9.

104. Haddad PR, Alexander PW, Trojanowicz M. High-performance liquid-chromatography of organic-acids with potentiometric detection using a metallic copper electrode. J Chromatogr 1984;315(Dec):261-70.

105. Chen ZL, Alexander PW. Potentiometric detection of aliphatic amines by flow injection analysis and ion-interaction chromatography with a metallic copper electrode. J Chromatogr A. 1997;758(2):227-33.

106. Trojanowicz M, Martin GB, Meyerhoff ME. Reversed-phase HPLC of peptides with tetraphenylporphyrin-based stationary phase and potentiometric detection with a copper electrode. Chem Anal-Warsaw. 1996;41(4):521-30.

107. Z.-L Chen DBH. Simultaneous amperometric and potentiometric detection of sugars, polyols and carboxylic acids in flow systems using copper wire electrodes. J Chromatogr A. 1997;766:27–33.

108. Alexander PW, Haddad PR, Low GKC, Maitra C. Application of a copper tubular electrode as a potentiometric detector in the determination of amino-acids by high-performance liquid-chromatography. J Chromatogr. 1981;209(1):29-39.

109. Franks MC, Pullen DL. A technique for the determination of trace anions by the combination of a potentiometric sensor and liquid chromatography, with particular reference to the determination of halides. Analyst. 1974;99(1181).

110. Trojanowicz M, Pobozy E, Meyerhoff ME. Direct and replacement ion chromatography with potentiometric detection using a silver silver bromide electrode. Anal Chim Acta. 1989;222(1):109-19.

111. Hyun Han S, Shin Lee K, Sig Cha G, Liu D, Trojanowicz M. Potentiometric detection in ion chromatography using multi-ionophore membrane electrodes. J Chromatogr A. 1993;648(1):283-8.

112. De Backer BL, Nagels LJ, Alderweireldt FC, Van Bogaert PP. Liquid chromatographic determination of acids and anions using liquid membrane ion-selective electrodes in a potentiometric flow-through detector. Anal Chim Acta. 1993;273(1-2):449-56.

113. Kwon KH, Paeng KJ, Lee DK, Lee IC, Hong US, Cha GS. Neutral carrier-based ion-selective electrode with similar sensitivity to different monovalent cations as a detector in ion chromatography. J Chromatogr A. 1994;688(1-2):350-6.

114. Nagels LJ, Bazylak G, Zielinska D. Designing potentiometric sensor materials for the determination of organic ionizable substances in HPLC. Electroanalysis. 2003;15(5-6):533-8.

115. Cadogan A, Gao Z, Lewenstam A, Ivaska A, Diamond D. All-solid-state sodium-selective electrode based on a calixarene ionophore in a poly(vinyl chloride) membrane with a polypyrrole solid contact. Anal Chem. 2002;64(21):2496-501.

116. Picioreanu S, Poels I, Frank J, van Dam JC, van Dedem GWK, Nagels LJ. Potentiometric detection of carboxylic acids, phosphate esters, and nucleotides in liquid chromatography using anion-selective coated-wire electrodes. Anal Chem. 2000;72(9):2029-34.

117. Bazylak G, Nagels LJ. Potentiometric detection of exogenic beta-adrenergic substances in liquid chromatography. J Chromatogr A. 2002;973(1-2):85-96.

118. Bao Y, Everaert J, Pietraszkiewicz M, Pietraszkiewicz O, Bohets H, Geise HJ, et al. Behaviour of nucleotides and oligonucleotides in potentiometric HPLC detection. Anal Chim Acta. 2005;550(1-2):130-6.

119. Poels I, Nagels LJ. Potentiometric detection of amines in ion chromatography using macrocycle-based liquid membrane electrodes. Anal Chim Acta. 2001;440(2):89-98.

120. De Wael K, Daems D, Van Camp G, Nagels LJ. Use of potentiometric sensors to study (bio)molecular interactions. Anal Chem. 2012;84(11):4921-7.

121. Trojanowicz M, Frenzel W. Flow injection potentiometry for low level measurements in the presence of sensed ion in the carrier. Fresenius Z Anal Chem. 1987;328(8):653-6.

122. Matuszewski W, Trojanowicz M, Frenzel W. Computerized flow-injection potentiometric stripping analysis with large-volume wall-jet cell. Fresenius Z Anal Chem. 1988;332(2):148-52.

123. Bazylak G, Nagels L, Geise H. Potentiometric quasi-array employing calixarene derivatives for the highthroughput similarity / diversity screening of beta-adrenergic and beta- blocking chiral drugs by HPLC. Comb Chem High T Scr. 2004;7(4):345-59.

124. Bazylak G, Nagels LJ. Potentiometric detection of N,N-diethylaminoethanol and lysosomotropic amino alcohols in cation exchange high-performance liquid chromatography systems. Anal Chim Acta. 2002;472(1-2):11-26.

125. Bazylak G, Nagels LJ. Simultaneous high-throughput determination of clenbuterol, ambroxol and bromhexine in pharmaceutical formulations by HPLC with potentiometric detection. J Pharm Biomed Anal. 2003;32(4-5):887-903.

126. Sun YM, Hsu SC, Lai JY. Transport properties of ionic drugs in the ammonio methacrylate copolymer membranes. Pharm Res. 2001;18(3):304-10.

127. Nagels LJ, Vissers B, Bohets H, Everaert J, Robbens J. Potentiometric sensors for organic analytes: insights to proceed to miniaturization. Curr Pharm Anal. 2009;5(2):120-6.

128. Daems D, Van Camp G, Fernandez M, Guisez Y, Prinsen E, Nagels LJ. Use of potentiometric detection in (ultra) high performance liquid chromatography and modelling with adsorption/desorption binding kinetics. Anal Chim Acta. 2013;777:25-31.

129. Daems D, van Nuijs AL, Covaci A, Hamidi-Asl E, Van Camp G, Nagels LJ. Potentiometric detection in UPLC as an easy alternative to determine cocaine in biological samples. Biomed Chromatogr. 2015;29(7):1124-9.

130. Trojanowicz M, Krawczyk T, Alexander PW. Organic conducting polymers as active materials in electrochemical chemo-sensors and biosensors. Chem Anal. 1997;42(2):199-213.

131. Poels I, Nagels LJ. Conducting polymer and oligomer micro-electrodes for the potentiometric detection of anions in capillary electrophoresis. Anal Chim Acta. 1999;401(1-2):21-7.

132. Watanabe K, Tohda K, Sugimoto H, Eitoku F, Inoue H, Suzuki K, et al. Ion-sensitive field-effect transistor as a monovalent cation detector for ion chromatography and its application to the measurement of Na^+ and K^+ concentrations in serum. J Chromatogr-Biomed. 1991;566(1):109-16.

133. Poels I, Schasfoort RBM, Picioreanu S, Frank J, van Dedem GWK, van den Berg A, et al. An ISFET-based anion sensor for the potentiometric detection of organic acids in liquid chromatography. Sensor Actuat B-Chem. 2000;67(3):294-9.

134. Shen HD, Cardwell TJ, Cattrall RW. The application of a chemical sensor array detector in ion chromatography for the determination of Na^+, NH_4^+, K^+, Mg^{2+} and Ca^{2+} in water samples. Analyst. 1998;123(10):2181-4.

135. Hruskar M, Major N, Krpan M. Application of a potentiometric sensor array as a technique in sensory analysis. Talanta. 2010;81(1-2):398-403.

136. Janczyk M, Kutyla-Olesiuk A, Ceto X, del Valle M, Ciosek P, Wroblewski W. Resolution of amino acid mixtures by an array of potentiometric sensors based on boronic acid derivative in a SIA flow system. Sensor Actuat B-Chem. 2013;189:179-86.

137. Nomura T, Nakagawa G. Properties of alkali-free lead phosphate-glasses as an ion-selective electrode and their application to a potentiometric detector for ion chromatography. B Chem Soc Jpn. 1987;60(8):2861-4.

138. Chen Z, Alexander PW. Potentiometric detection of metal ions separated by liquid chromatography using a tungsten oxide electrode. Electroanalysis 1997;9(11):818-21.

139. Sahin M, Ozcan L, Usta B, Sahin Y. Determination of ascorbic acid by polypyrrole potentiometric detector in ion chromatography. Biosens Bioelectron. 2009;24(12):3492-7.

140. Düzgün A, Zelada-Guillén GA, Crespo GA, Macho S, Riu J, Rius FX. Nanostructured materials in potentiometry. Anal Bioanal Chem. 2011;399(1):171-81.

141. Yin T, Qin W. Applications of nanomaterials in potentiometric sensors. Trac-Trend Anal Chem. 2013;51:79-86.

Chapter 3

Experimental section

3.1. Introduction

Chapter 3 provides information related to the experimental part of the thesis, including the analytical techniques, procedures, and instrumentation used. Firstly, an overview of the potentiometric measurements is introduced. Secondly, a description of the two flow-cells (FC) used and lastly, the construction of the solid-state ion-selective and reference electrodes is reported. More detailed information on chemical reagents, specific materials, standard solutions, mobile phases, chromatographic conditions, and sample pre-treatment are given in the corresponding subsections of the next chapter.

3.2. Overview of potentiometric measurements

The output signal of the potentiometric cell, expressed as electromotive force (EMF, E_{cell}), is related to the activity of the target ion (or molar concentration if the ionic strength is adjusted) by the Nikolsky-Eisenman (NE) equation:

$$E_{cell} = E^0 + \frac{2.303RT}{z_i F} \log \left(a_i + \sum_{n=1}^{x} K_{i,j}^{pot} \left(a_j\right)^{z_i/z_j} \right) \qquad (1)$$

wherein a_i and a_j are the activities of the target ion and interfering ion, respectively; E^0 is a constant that represents the sum of all generated potentials in the potentiometric cell, i.e. the standard potential of the indicator electrode, the standard potential of the reference electrode, and the phase boundary potential between the membrane/sample solution; R is the gas constant, 8.3144 J K^{-1} mol^{-1}; T is the absolute temperature; F is the Faraday

constant, 9.64846x10^4 C mol^{-1}; z_i and z_j are the charges of the target ion and interfering ion, respectively; and $K_{i,j}^{pot}$ is the potentiometric selectivity coefficient.

According to the International Union of Pure and Applied Chemistry (IUPAC) recommendations, a Nernstian response is revealed when a plot of the E_{cell} value *vs*. the logarithm of the activity of the target ion is linear with a slope of $^{RT}/_{z_iF}$ over a certain range of activity (2). Therefore, the theoretical sensitivity is $^{59.2}/_{z_i}$ mV per decade of a_i at 298.15 K, depending on the charge number of the target ion. Nonetheless, from practical point of view useful electrodes with super and sub-Nernstian sensitivity have been also described in the literature, though they are not discussed here.

Typical calibration charts for cation- and anion-selective electrodes are depicted in **Figure 3.1**. In both cases, it is possible to identify three distinct regions: i) to the left of the lower limit of detection (LLD) interception, where the electrode potential remains constant; ii) between LLD and the upper limit of detection (ULD), where a steep variation of the electrode potential with the activity of the primary ion follow the NE equation, though this variation does not follow it near the LLD or ULD; and iii) to the right of ULD interception where the electrode potential no longer depends on *log* a_i.

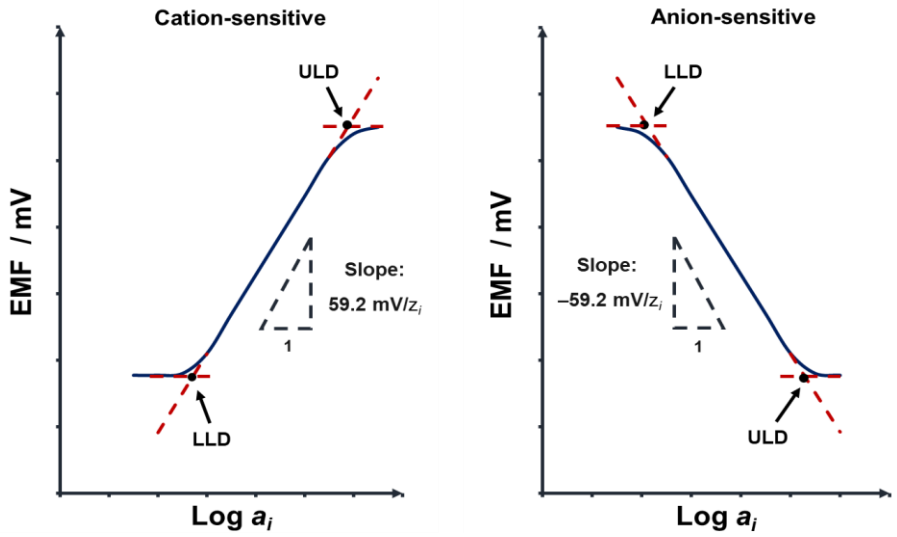

Figure 3.1 Typical calibration graphs for cation- and anion-selective electrodes. LLD – Lower limit of detection; ULD – Upper limit of detection.

The characterization of ion-selective electrodes (ISEs) at steady-state conditions was accomplished following the IUPAC recommendations (1), by the assessment of six main parameters, namely sensitivity, selectivity, range, the limit of detection, stability, and response time.

3.2.1. Sensitivity

The sensitivity of each ISE was obtained from the slope of the calibration curve. The dynamic potentiometric response was measured after the addition of discrete volumes of a concentrated solution containing the target ions under constant stirring. All experiments were carried out at room temperature of 22±1°C.

Activity coefficients were calculated based on the Debye-Hückel theory (equation 2), taking into account both the ion concentrations and the total ionic strength (3).

$$\log y_i = -\frac{A\,.\,|z_+\,.\,z_-|.\sqrt{I}}{1 + B.\sqrt{I}} + C.I \qquad (2)$$

in which y_i is the activity coefficient (dimensionless), I is the ionic strength, z is the charge of ions. A is a constant that is a function of temperature (0.5108 at 25°C) while B and C are empirical parameters that depend on the electrolyte under study.

Alternatively, the potential value of the potentiometric cell (E_{cell}) was related to the main ion concentration and fitted to the Nernst equation to obtain the sensitivity (slope) and intercept (4). To do this, the ISE and the reference electrode were immersed in an accurate solution volume with the ionic strength and/or pH adjusted to ensure a constant activity coefficient for the target species, according to equation 3:

$$a_i = y_i\,.\,C_i \qquad (3)$$

in which a_i and C_i are the activity and concentration of the target ion, respectively, and y_i is the activity coefficient (dimensionless).

The ionic strength of all solutions was adjusted using an electrolyte whose composition did not represent a significant chemical interference for the proposed potentiometric detectors. The calculation of the ionic strength of the respective solutions was carried out through equation 4:

$$I = \frac{1}{2}\sum(C_i.z^2) \qquad (4)$$

in which I is the ionic strength, C_i is the concentration, and z is the charge of the ion.

3.2.2. Selectivity

The presence of other ions in the analyzed solutions, even in small concentrations, can interfere with the potentiometric signal and thus the evaluation of the potentiometric selectivity coefficients $K_{i,j}^{pot}$ is mandatory to know the behavior of the sensor in real samples. The $K_{i,j}^{pot}$ defines the ability of an ISE to distinguish a particular ion from the others and can be measured by different methods that fall into two main groups: (i) fixed interference method, and (ii) separate solution method (5).

In the fixed interference method, the EMF of a potentiometric cell comprising an ISE and a reference electrode is measured in solutions with the constant activity of interfering ion (a_j), and changing the activity of the primary ion (a_i). The EMF values obtained are plotted *vs* the logarithm of a_i and the intersection of the extrapolation of the linear portions of this plot indicates the value of a_i that is used to calculate $K_{i,j}^{pot}$ according to equation 5:

$$K_{i,j}^{pot} = \frac{a_i}{a_j^{z_i/z_j}} \qquad (5)$$

In the separate solution method, the EMF of a potentiometric cell is measured in each solution, one containing only the primary ion (a_i) and other containing the interfering ion (a_j) at the same activity. If the measured values are E_i and E_J, respectively, the $K_{i,j}^{pot}$value may be calculated from equation 6:

$$K_{i,j}^{pot} = \frac{(E_j - E_i)z_i F}{2.303RT} + \left(1 - \frac{z_i}{z_j}\right) log a_i \qquad (6)$$

Nonetheless, the theory and experimental determination of the selectivity have been discussed for a long time (6-8), namely to establish how they reflect true thermodynamic $K_{i,j}^{pot}$ values.

3.2.3. Limit of detection

The ISEs calibration obtained in broad concentration ranges allows identifying the presence of lower and upper limits of analytical usefulness. According to the IUPAC recommendations, these limits are defined by the cross-section of the two extrapolated linear segments of the calibration plot (**Figure 3.1**) (1).

The LLD was determined as the activity at the point of intersection of the extrapolated linear midrange and final low concentration level segments of the calibration plot. It corresponds to the least ion concentration in the vicinity of the lipophilic membrane in equilibrium with the free ion in the membrane. On the other hand, the ULD was calculated on a similar basis but at the point of the intersection of the extrapolated linear midrange and final high concentration level segments. The ULD is a consequence of a simultaneous coextraction process of primary and their counter ions from the sample into the ion-selective membrane, thereby leading to a loss of membrane permselectivity (2).

3.2.4. Range

The range of response (activity or concentration of the main ions) is defined between the lower and upper detections limits (1), which are determined as described above in section 3.2.3.

3.2.5. Stability

The evaluation of the potentiometric signal along short and long periods is one of the most important parameters to characterize the sensor performance. Therefore, the nonrandom change in the E_{cell} with time assembled in a solution of constant composition and temperature is usually expressed as a *drift* (1). Its value was determined by the slope of the potential *vs* time curve over a given period, being expressed in μV h^{-1} or mV h^{-1} unit.

3.2.6. Response time

According to the IUPAC recommendations, the response time of a given ISE is the time elapsed from the instant when an ISE and a reference electrode are brought into contact with a sample solution (or at which the activity of the ion of interest in a solution is changed) and the first instant at which the E_{cell}/time slope ($^{\Delta E}/_{\Delta t}$) reaches a limiting value selected based on the experimental conditions (1). Although this approach was accepted by the IUPAC in 1994, more recent studies pointed out the use of the “differential criterion” as a more convenient approach to evaluate polymeric-membrane electrodes, according to equation 7 (9):

$$t^* = t'\left(\frac{\Delta E}{\Delta t}\right) \qquad (7)$$

in which t^* is the response time of the electrode; t' is the reading time, corresponding to the recorded time distance between two additions; and ΔE is the potential increment over a certain period; Δt is the time needed to reach steady-state after each activity change. However, this criterion is not being widely used today by the electrochemistry community. Therefore, the response time of the potentiometric electrodes was herein determined as t_{95}, which is the time that elapses between the instant at which the activity of the target ion is changed in the solution and the first instant at which the measured E_{cell} becomes equal to 95% of the signal at a steady-state (1). This last value was considered when E_{cell} variations were less than ± 0.1mV.

3.2.7. Potentiometric measurements in LC

The practical aspects of the potentiometric measurements described before are important for the characterization of ISEs. However, for applications under flow conditions, namely in liquid chromatographic methods, the determination of low concentrations near the LLD, requires an analytical signal linearly dependent of $c_{analyte}$. Therefore, the potential output ($E\ (mV)$) must be first transformed, as suggested by Luc Nagels and co-workers. They demonstrated a linear correlation between $E\ (mV)$ and the $c_{analyte}$ when $c_{analyte} << k_{i,j}^{pot} c_j$ (10, 11). To attain that condition the mobile phase must be the only source of interfering compounds, hence with known composition (Cst). The corresponding NE equation becomes simplified according to equation 8 (11):

$$E\ (mV) = E^0 + S\log(c_{analyte} + Cst) \qquad (8)$$

in which S is the slope of the calibration curve ($E\ (mV)$ *vs* $log\ c_{analyte}$,) and Cst accounts for the contribution of interfering ions of the mobile phase to the analytical signal (11).

The detector output $E\ (mV)$ is set to 0 mV when $c_{analyte} = 0$ (offset of the baseline signal) by the subtraction of a constant value. In this case, the subtraction of E_0 and $S\ \log(Cst)$, which are constant values, enables to convert the equation 8 in a more useful form:

$$c_{analyte} = Cst\left(10^{E/S} - 1\right) \qquad (9)$$

Finally, the $10^{E/S} - 1$ function is a transformed response (tR) obtained from the rearrangement of the NE equation. The application of tR was successfully demonstrated in the use of potentiometric detection in liquid chromatography for the screening of nucleotides and oligonucleotides (12), pharmaceutical drugs (13), steroids (14), and alkaloids (15).

3.3. Apparatus

The HPLC comprised a Waters 600E Multisolvent Delivery System (Waters®), equipped with a Waters 600 controller, a Waters 600E pump, a Waters 2487 Dual Absorbance Detector, and a Rheodyne 7725i six-port external manual injector (IDEX Health & Science, LLC) (**Figure 3.2)**. Millennium 32 Chromatography Manager Software (Waters, USA) was used to control the HPLC components and data processing in the UV detector.

The potentiometric measurements were carried out using a 6-Channel Precision Electrochemistry EMF Interface (LawsonLabs, Inc. USA). The equipment was connected to a computer equipped with the graphics software from LawsonLabs, Inc. USA, enabling recording the potentiometric signals *vs*. time (**Figure 3.2**).

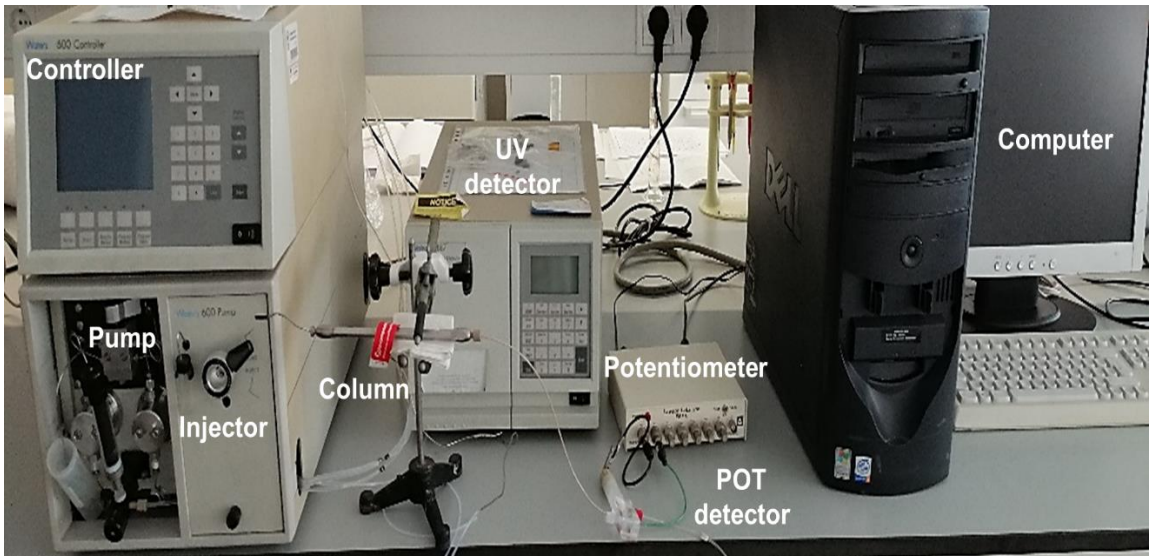

Figure 3.2 HPLC-potentiometry workstation includes the controller, pump, injector, chromatographic column, potentiometric (POT) detector, UV absorption detector, potentiometer, and computer.

3.3.1. Flow-cells

Both indicator and reference electrodes referred to in chapter 4, sections 4.2, 4.3, and 4.4, were assembled on a microfluidic wall-jet flow cell (**Figure 3.3**). The flow-cell consisted of an acrylic block (length – 40 mm, width – 22 mm, and height – 22 mm) incorporating four single holes: two enabling the inlet and outlet of the mobile phase, the third where the reference electrode is screwed, and the last for coupling the miniaturized ISE. The internal channel was drilled with an internal diameter of 0.8 mm and a length of 17mm, enabling a cell volume of 8.5 µL. For the inlet and outlet, a blue ferrule and male red nut (1/16) were used to connect the PEEK tubing.

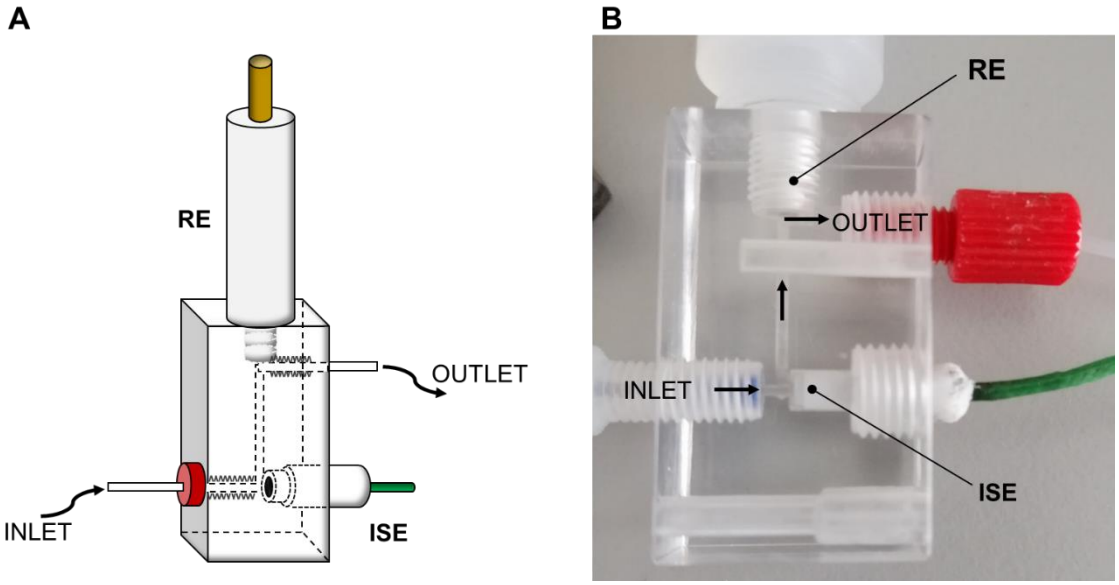

Figure 3.3 Wall-jet flow-cell assembled with the potentiometric electrodes. **A** – Schematic representation; **B** – Real picture. ISE – Ion-selective electrode; RE – Commercial Ag/AgCl (KCl 3 mol L^{-1}) reference electrode.

A microfluidic thin-layer flow cell was used as a potentiometric detector in section 4.5. The cell consisted of an acrylic hexagonal prism (25 mm side length) with six drilled holes: two on opposite faces for eluent inlet and outlet, one for the reference electrode, and three others to host ISEs (**Figure 3.4**). The electrodes were concentrically placed around an inner chamber of the cell (20 µL volume) and were attached using plastic end-fits (flangeless yellow ferrule and a male green nut, 1/8). The electrical connection was ensured using small crocodile clamps connected to each electrode. For the inlet and outlet, a blue ferrule, and a male red nut (1/16) were used to connect the PTFE tubing.

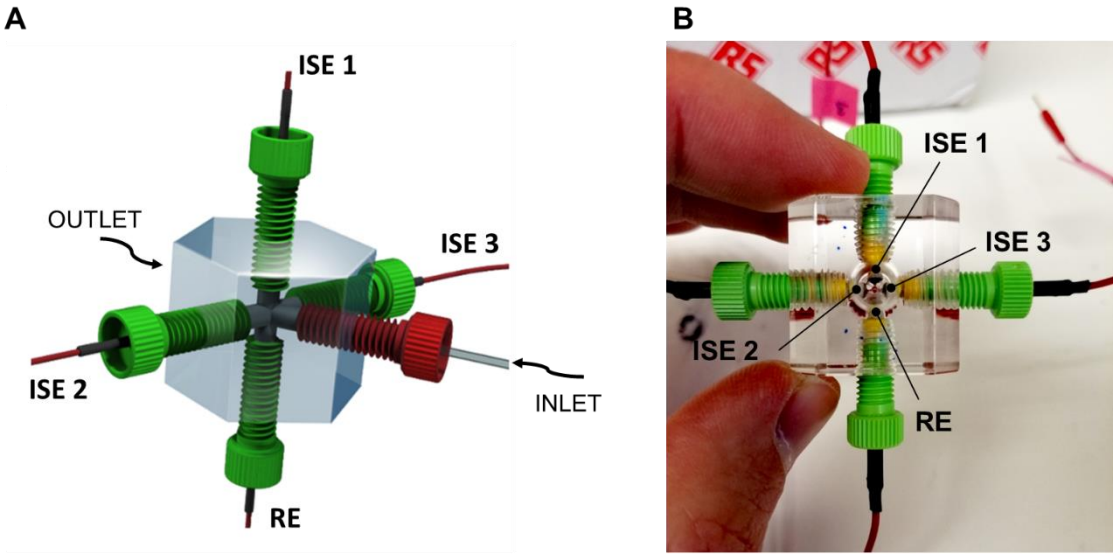

Figure 3.4 Thin-layer flow-cell assembled with the potentiometric electrodes. **A** – Schematic representation; **B** – Real picture. ISE – Ion-selective electrodes (1, 2, and 3); RE – Handmade Ag/AgCl solid-state reference electrode.

3.3.2. Electrodes

The potentiometric measurements were carried out using handmade conventionally-shaped (**Figure 3.5A**) and miniaturized indicator electrodes (**Figure 3.5B** and **C**). The conductive support of the miniaturized electrodes was based on a graphite substrate (**Figure 3.5B**) or a glassy carbon rod (**Figure 3.5C**). The fabrication processes are detailed in section 3.4. As reference electrodes, commercial double-junction Ag/AgCl electrodes were used. The external compartment of the Orion 90-02-00 (Thermo Scientific) electrode was filled with a 1.0×10^{-2} M KCl solution (**Figure 3.6A**). A 3.0 M KCl/1.0 M lithium acetate (LiOAc) solution was used in the 6.0726.100 - Metrohm electrode (**Figure 3.6B**). One commercial miniaturized reference electrode filled with a 3.0 M KCl (model 6.0727.000, Metrohm) (**Figure 3.6C**) and a handmade solid-state reference electrode were additionally utilized (**Figure 3.6D**).

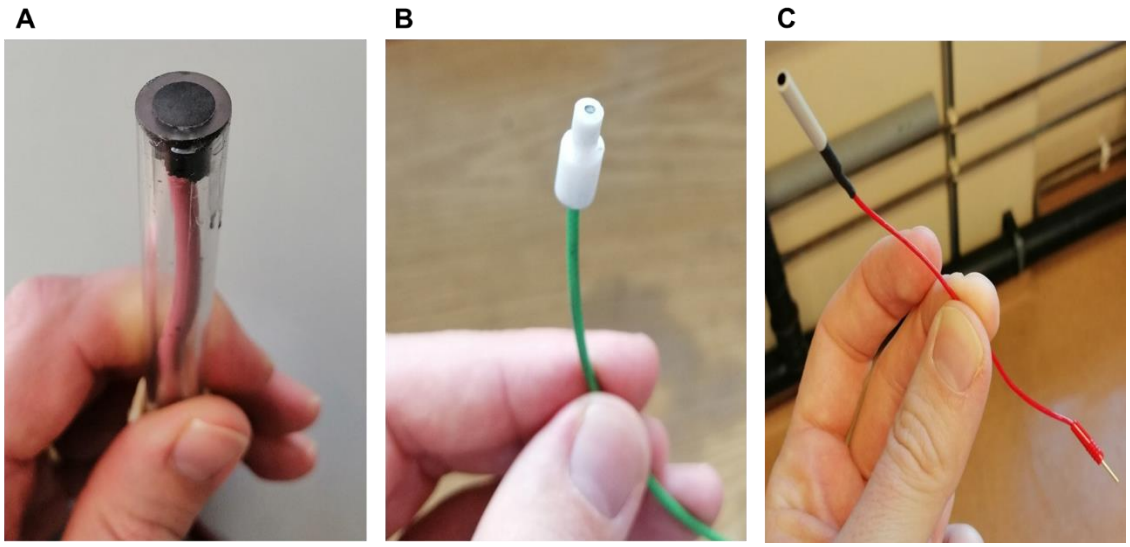

Figure 3.5 Indicator electrodes. **A** – Conventionally-shaped electrode based on a graphite substrate; **B** – Miniaturized electrode based on graphite substrate; **C** – Miniaturized electrode based on glassy carbon.

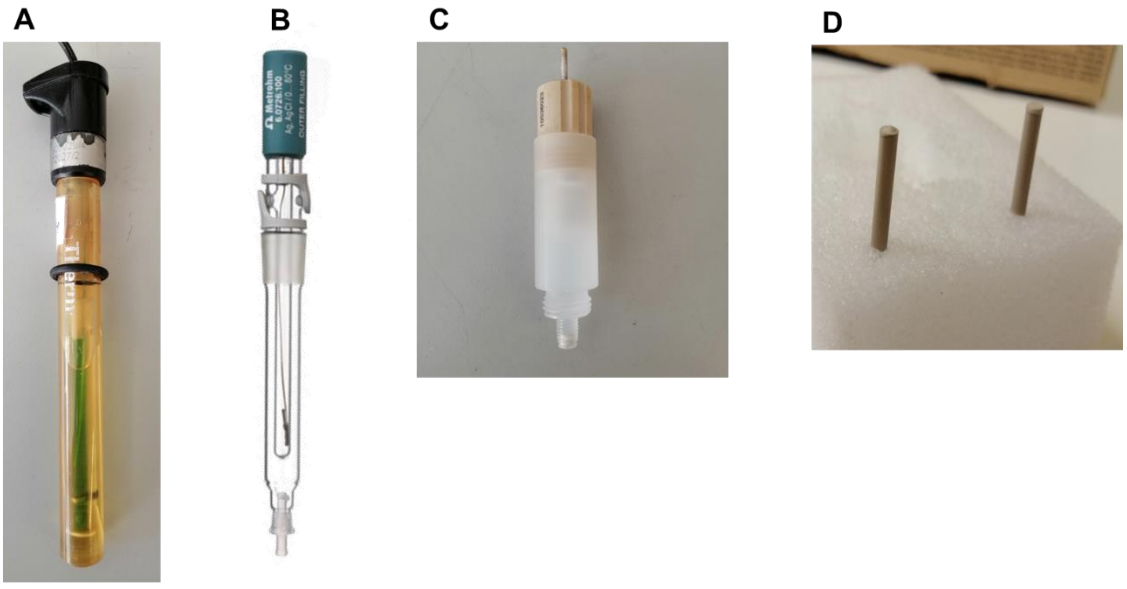

Figure 3.6 Reference electrodes. **A** – Commercial double-junction Ag/AgCl/0.01M KCl reference electrode; **B** – Commercial double-junction Ag/AgCl/3.0 M KCl/1.0 M LiOAc reference electrode; **C** – Commercial reference electrode filled with a 3.0 M KCl; **D** – Handmade miniaturized Ag/AgCl reference electrode.

3.4. Construction of solid-state electrodes

3.4.1. Conventionally-shaped ion-selective electrodes

Handmade indicator electrodes of solid contact based on graphite conductive substrate were fabricated following a procedure described by Lima et al. (16). Firstly, a non-conductive epoxy resin was prepared by mixing Araldite-M and hardener Ren HY 5162 (1:0.4 w/w), which was blended with graphite powder to obtain a composite with appropriate homogeneity and consistency. The final proportion was 1:1.85 w/w of epoxy resin and graphite, respectively. A portion of the conductive composite was introduced in one end of a common Perspex tube with 6.0 mm of internal diameter, 10.0 mm of external diameter, and 150.0 mm of length (**Figure 3.7a** and **b**). An electrically shielded cable with the copper wire exposed was inserted in the opposite ending to establish the electrical contact (**Figure 3.7c**) and the electrodes were left to dry over 24h at room temperature (**Figure 3.7d**). Finally, the electrically shielded cable was fixed with plastic tape (**Figure 3.7e**) and the conductive surface was polished with sandpaper of different grit sizes until a specular gloss was obtained (**Figure 3.7f**). The remaining solid residues were removed with paper embedded in tetrahydrofuran.

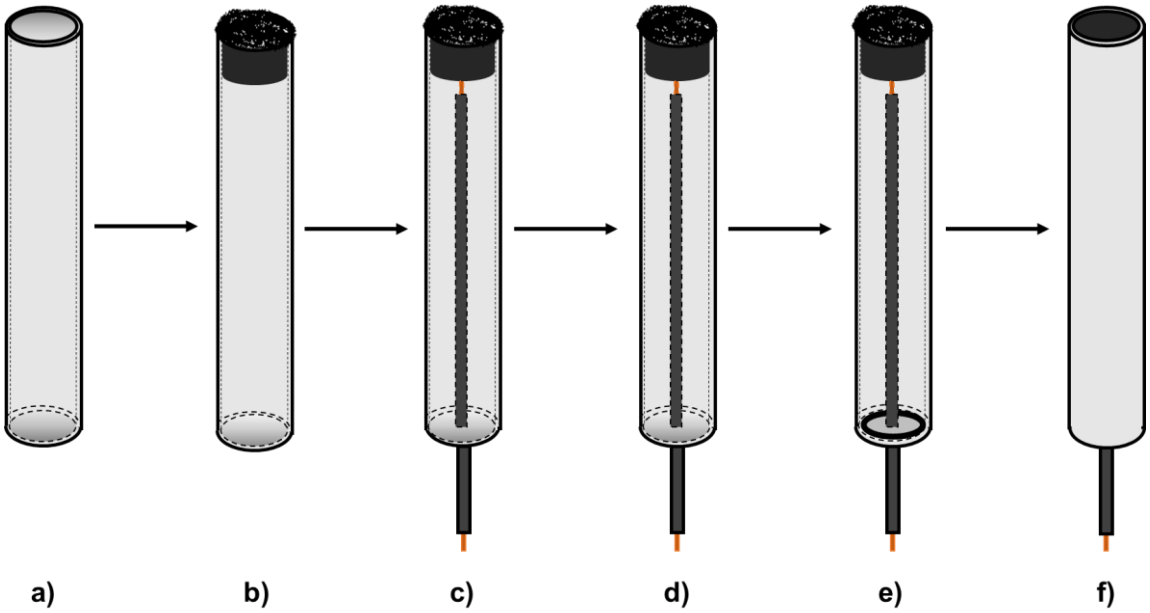

Figure 3.7 Construction of conventionally-shaped electrodes based on a graphite substrate. **a)** Perspex tube; **b)** Introduction of the conductive composite; **c)** Introduction of the electrically shielded cable; **d)** Polymerization and drying of the conductive composite; **e)** Fixation of the electrically shielded cable with plastic tape; **f)** Polishing of the surface until specular gloss.

3.4.2. Miniaturized ion-selective electrodes

Miniaturized handmade electrodes based on graphite conductive substrate and glassy carbon substrate were fabricated following the procedure described by Gil et. al (17) and Cuartero et. al (18), respectively.

For the graphite-based electrodes, a conductive composite was firstly prepared as described in the above section (3.4.1.) and packed in one end of a polytetrafluoroethylene (PTFE) rod (teflon®), properly machined, with 1.6 mm of internal diameter, 4.0 mm of external diameter, and 15.0 mm of length (**Figure 3.8a** and **b**). An electrically shielded cable with the copper wire exposed was inserted in the opposite ending to establish the electrical contact (**Figure 3.8c**) and the electrodes were left to dry over 24h at room temperature (**Figure 3.8d**). Finally, the conductive surface was polished with smooth sandpaper until a specular gloss was obtained (**Figure 3.8e**). The remaining solid residues were removed with paper, previously embedded in tetrahydrofuran.

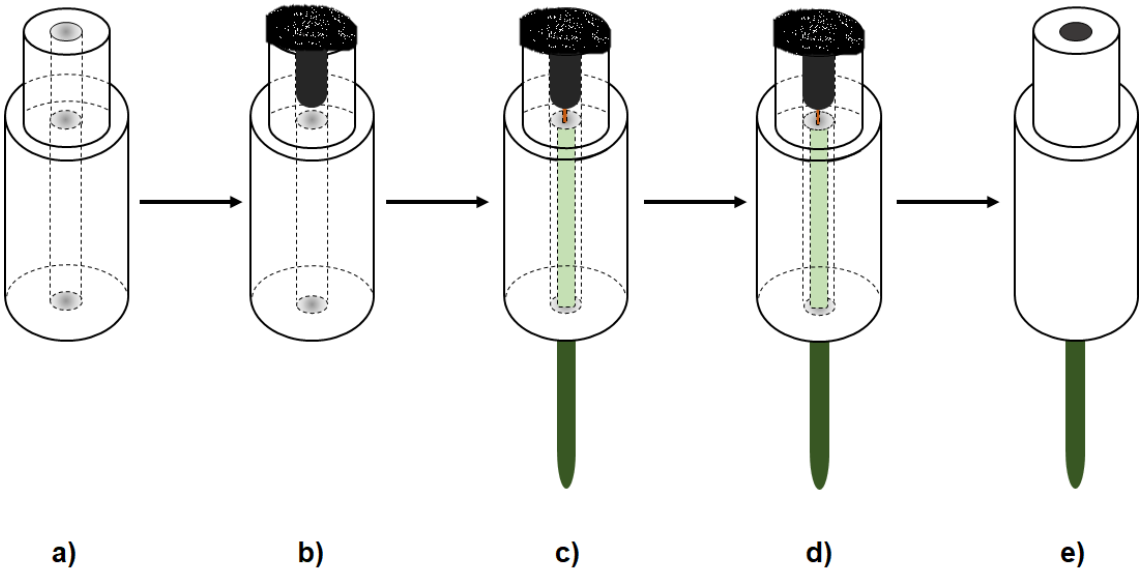

Figure 3.8 Construction of the miniaturized electrodes based on a graphite substrate. **a)** Polytetrafluoroethylene rod tube; **b)** Filling with conductive composite; **c)** Introduction of the electrically shielded cable; **d)** Polymerization and drying of the conductive composite; **e)** Polishing of the surface until specular gloss.

On the other hand, for the glassy carbon-based electrodes, a carbon rod with 1.98 mm of internal diameter and 20.0 mm length was glued inside a polyether ether ketone (PEEK) tube. A length of 5 mm of the carbon rod was maintained outside the PEEK tube to allow the electrical connections (**Figure 3.9a** and **b**). The surface of the carbon rod inside the PEEK was firstly polished with sandpaper until a flat surface was reached and then with

alpha-alumina (0.5 microns) to reach a specular brightness of the glassy carbon material (**Figure 3.9c**).

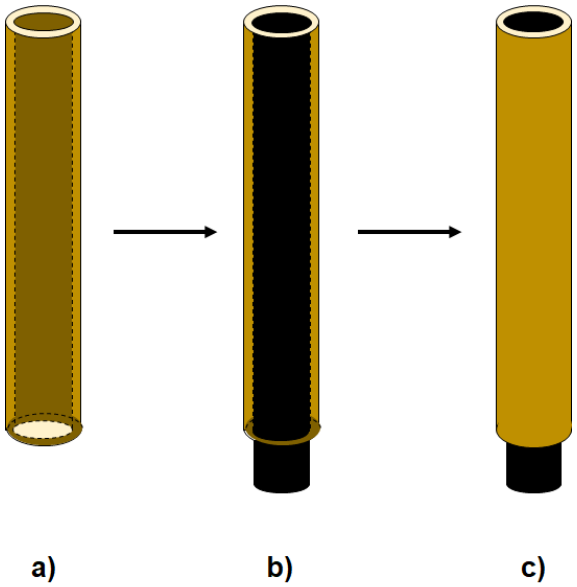

Figure 3.9 Construction of miniaturized electrodes based on a glassy carbon substrate. **a)** PEEK tube; **b)** Gluing the glassy carbon rod inside the peak tube; **c)** Polishing of the surface until specular gloss.

3.4.3. Miniaturized solid-state reference electrode

The handmade solid-state reference electrode was fabricated following the procedure described elsewhere (18). Firstly, the surface of the miniaturized glassy carbon electrode was modified with a silver/silver chloride (Ag/AgCl) ink (C21310007D3, GWENT Group, UK), followed by oven-curing at 100°C for 10 min. A reference membrane (50 mg of sodium chloride and 78 mg of polyvinyl butyral in 1 mL of methanol) was dropped (4 x 5 µL) on the top of an Ag/AgCl layer, previously cured, being each layer dried for 10 min before another depositing. The reference electrode was left to dry overnight and conditioned in 3.0 M KCl for at least 48 h. When not in use, the electrode was kept in a 3.0 M KCl solution.

3.4.4. Preparation of ion-selective membranes

The ion-selective membranes (ISMs) were prepared by mixing accurate amounts of the polymer, plasticizer, ionophore, ionic additive, and carbon nanotubes (when applicable) in

glass vials. All the ISM composition used throughout this thesis is described in the corresponding section of chapter 4. Nonetheless, the sensing elements incorporated in the different ISMs, namely the ionophores and the lipophilic additives, are summarized in **Table 3.1.**

Table 3.1 Sensing elements used in the development of ion-selective electrodes.

Sensing element	ISEs	Section
Potassium tetrakis (4-chlorophenyl)borate	Biogenic amines	4.2, 4.3
	Tetracycline antibiotics	4.4
Sodium tetrakis[3,5-bis(trifluoromethyl)phenyl]borate	Ammonium	4.5
	Sodium	4.5
	Potassium	4.5
Cucurbit[6]uril	Biogenic amines	4.2, 4.3
Cucurbit[8]uril	Tetracycline antibiotics	4.4
Ammonium ionophore I (nonactin)	Ammonium	4.5
Potassium ionophore I (valinomycin)	Potassium	4.5
Sodium ionophore X (4-tert-Butylcalix[4]arene-tetraacetic acid tetraethyl ester)	Sodium	4.5

The homogenized ISMs were deposited on the conductive surface of the electrodes. For conventionally-shaped electrodes, the surface was modified by dropping 5 x 100 µL of the corresponding ISMs to cover all the support contact areas. The THF was left to evaporate for 30 min between each deposition. Finally, the electrodes were left to dry overnight before conditioning. For miniaturized electrodes based on a graphite substrate, 4 x 5 µL of the corresponding ISM was dropped onto the conductive support with an automatic pipette. Each layer was allowed to dry for 20 min before the next addition. Regarding the miniaturized glassy carbon electrodes, its surface was firstly modified by drop-casting 4 x 5 µL of 1 mg mL^{-1} multi-walled carbon nanotubes solution in ethanol (19). Each layer was allowed to dry for 10 min before the next addition. Then, the ISM was formed by drop-casting 4 x 5 µL of the corresponding membrane cocktail on top of the MWCNT film. Each layer was allowed to dry for 20 min.

Finally, the electrodes were conditioned overnight on appropriate solutions. When not in use, each electrode was kept immersed in the corresponding conditioning solution.

3.5. Analytical validation of LC-potentiometric methods

The proposed analytical methodologies were validated in compliance with the Eurachem (20), International Council for Harmonisation of Technical Requirements for Pharmaceuticals for Human Use (21), European Union (22), and IUPAC (23) guidelines. The IUPAC technical report about the use of electrochemical detection in liquid flow analytical techniques was also followed to assess the potentiometric detector performance (24). Accordingly, the range, linearity, limits of detection (LOD) and quantification (LOQ), precision, and accuracy were evaluated.

3.5.1. Range

The range of an analytical procedure is the interval between the lower and upper concentration of analyte in the sample for which it has been demonstrated a suitable level of precision, accuracy, and linearity (22). The range established along this thesis was based on the linear relation between the transformed response, $tR = 10^{E/S} - 1$, and the analyte concentration (see section 3.2.7).

3.5.2. Linearity

The linearity was evaluated across the range (section 3.5.1.) in which a linear relationship was established between the potentiometric detector output and the analyte concentration. For that, a minimum of five concentrations was used and the coefficients of determination, y-intercepts, and slopes of the regression lines were investigated (21).

3.5.3. Precision

Precision is defined as the closeness of agreement between the detector responses obtained by several individual measurements of a homogeneous sample, under the same stipulated conditions (23). It was assessed through repeatability and intermediate precision of the potentiometric signal and retention time. The repeatability values were obtained after triplicate analysis of standard solutions of the analytes at three concentration levels performed on the same day, whereas the intermediate precision was evaluated by the triplicate analysis at three concentration levels (or quintuplicate analysis at one

concentration level) performed on consecutive days. The inter-electrode reproducibility was also evaluated by triplicate analysis of standard solutions of analytes at three concentration levels using three different sensor units. All the obtained results were expressed as relative standard deviation values (RSD%).

3.5.4. Accuracy

Accuracy is the closeness between the concentration provided by the analytical assay and the true value (23). It was determined through the triplicate analysis of spiked samples at three fortification levels and expressed as percent recovery regarding the known added amount of analyte to the sample (22).

In the case of biogenic amines (chapter 4, sections 4.2 and 4.3), the recovery values were calculated accordingly to the Waters Company Protocol (25):

$$Recovery\ (\%) = \frac{Analyte_{Recovered}}{Analyte_{Post\ spiked}}\ x\ 100\% \qquad (10)$$

with $Analyte_{Recovered}$ corresponding to the concentration in the samples spiked before the solid-phase extraction and $Analyte_{Post\ spiked}$ corresponding to the concentration of the spiked extracts.

In the assessment of the proposed methods for the determination of tetracycline antibiotics (chapter 4, section 4.4) and ammonium ions (chapter 4, section 4.5), the recoveries were calculated according to the following equation:

$$Recovery\ (\%) = \frac{Analyte_{Found} - Analyte_{Initial}}{Analyte_{Spiked}}\ x\ 100 \qquad (11)$$

in which $Analyte_{Found}$ is the concentration measured in the spiked samples, $Analyte_{Initial}$ is the concentration present in each sample, and $Analyte_{spiked}$ corresponds to the concentration added to the samples, respectively.

3.5.5. Limit of detection

For each particular method, the limit of detection (LOD) or minimum detectable value corresponds to the lowest concentration, or quantity, that can be determined with reasonable certainty based on a statistical basis (24, 26-28). Particularly for analytical methods that exhibit baseline noise (21), such as liquid chromatography coupled to either

spectroscopic or electrochemical detection, the measured signals (i.e. peak height) of standard solutions with known low concentrations of analyte were compared with blank solutions, enabling to establish the minimum concentration at which the analyte can be reliably detected (29). Accordingly, a signal-to-noise ratio (S/N) of 3:1 was used throughout this thesis to estimate the LOD (21).

3.5.6. Limit of quantification

The limit of quantitation (LOQ) is the lowest level of an analyte that can be determined with acceptable performance (20), which includes precision and accuracy (28). The LOQ was herein determined using the S/N ratio of 10:1 (21), by comparing measured signals from standard solutions with known low concentrations of analyte with those of blank solutions and by establishing the minimum concentration at which the analyte can be reliably quantified (29).

3.5.7. Robustness

The evaluation of the robustness of the analytical method was considered during all the development processes to ensure the reliability of the analysis concerning deliberate variations in method parameters (21). Accordingly, the main parameters investigated whose variation can affect the measurable signal were the composition of the mobile phase (i.e. ionic strength and organic modifier), type of stationary phase, flow rate, and injection volume.

3.6. Chromatographic parameters

The chromatographic parameters, namely retention time, retention factor, separation factor, effective plate number, peak resolution, and asymmetry factor were calculated using standard formulas about the liquid chromatographic process (30-33).

3.6.1. Retention time and retention factor

The retention time (t_R) is the time that a given compound spends in a chromatographic column. On the other hand, the retention factor (k) is a dimensionless parameter of

measuring the retention of an analyte on the chromatographic column, which is expressed by the following equation:

$$k = \frac{(t_R - t_0)}{t_0} \qquad (12)$$

in which t_R is the retention time of the analyte and t_0 is the retention time of a non-retained compound. The non-retained compound has no affinity for the stationary phase and elutes with the solvent front at a time t_0, which is also known as the “dead time”.

A k value between 1 and 10 is considered satisfactory among the chromatography community. For instance, if k < 1 means that the analyte is eluted together with the solvent front and thus no separation is achievable. On the other hand, a k > 10 indicates strong retention of the analyte in the column, which demands adjustments in the separation conditions to decrease the total run time.

3.6.2. Separation factor

The separation factor (α) is the ability of the chromatographic system to ‘chemically’ distinguish the sample components. It is usually measured as a ratio of the retention factors of the two peaks in question and can be visualized as the distance between the apices of the two peaks. The equation for calculating α is expressed as follow:

$$\alpha = \frac{k_2}{k_1} = \frac{t_{R2} - t_0}{t_{R1} - t_0} \qquad (13)$$

in which k_2 is the retention factor of the second peak, k_1 is the retention factor of the first peak, t_{R2} is the retention time of the second peak, t_{R1} is the retention time of the first peak, and t_0 is the retention time of a non-retained compound.

By definition, the separation factor is always greater than one because when α is equal to one means that the two peaks are co-eluting (i.e. their retention factor values are identical). Therefore, high α values indicate good separating power and good separation between the apices of each peak.

3.6.3. Efficiency

The efficiency of a chromatographic peak is a measure of the dispersion of the analyte band as it travels through the HPLC system and column. Ideally, the peaks would be defined as pencil lines but a Gaussian shape is usually observed as a result of diverse kinetic factors including liquid-solid mass transfer, forward and backward axial dispersion, and non-ideal distribution of liquid around the column packing (30). Accordingly, this peak dispersion on the chromatographic column is expressed by the effective plate number index (N_{eff}), which is calculated by the following equation:

$$N_{eff} = 16\left(\frac{t_R}{w_b}\right)^2 = 5.54\left(\frac{t_R}{w_{1/2}}\right)^2 \qquad (14)$$

in which t_R is the retention time, w_b, is the peak width at base, and $w_{1/2}$ is the peak width at half height.

The plate concept derives historically from the theory on analyte separation by distillation and corresponds to the distance over which the sample component achieves a perfect partition equilibrium between the stationary and mobile phase in the column. Therefore, the high number of plates available for highly efficient columns indicates more equilibration possibilities, which improves the quality of separation.

3.6.4. Resolution

The peak resolution (R_s) represents the separation of two peaks in terms of their average peak width at the base ($t_{R2} > t_{R1}$) and maybe calculated by the following equation:

$$R_s = \frac{t_{R2} - t_{R1}}{\frac{w_{b1} + w_{b2}}{2}} = \frac{2\,(t_{R2} - t_{R1})}{w_{b1} + w_{b2}} \qquad (15)$$

in which t_{R2} is the retention time of the second peak, t_{R1} is the retention time of the first peak, w_{b2} is the peak width at the base of the second peak, and w_{b1} is the peak width at the base of the first peak.

A peak resolution value ≥1.5 between two adjacent peaks will ensure that the sample components are well separated to a degree at which the area or height of each peak may be accurately measured. The main goal is to obtain the optimum resolution in the shortest time possible.

The peak resolution is affected by the efficiency (N_{eff}), separation factor (α), and retention factor (k), as demonstrated by the following equation:

$$R_s = \frac{1}{4}\sqrt{N_{eff}} \times \frac{\alpha - 1}{\alpha} \times \frac{k}{1+k} \qquad (18)$$

3.6.5. Peak symmetry

The peak symmetry represents the closeness of chromatographic peaks to a symmetric or Gaussian shape. The tailing describes an asymmetric peak reflecting a longer delay in returning to the baseline. It may be affected by the instrument dead-volume, adsorptive effects of the stationary phase, and the quality of the column packing. In contrast, fronting peak shapes may also occur, particularly if the sample concentration is too high or if the sample solvent is stronger than the mobile phase.

The peak symmetry is evaluated by the asymmetry factor (A_s), which is obtained by drawing a horizontal line at 10% of the peak's maximum height and measuring the distance from each side of the peak to a line drawn vertically through the peak's maximum (**Figure 3.10**). The equation for calculating A_s is expressed as follow:

$$A_S = \frac{b}{a} \qquad (16)$$

in which a and b are the distance from the points at 10% of the peak's maximum height to the center in both left and right sides of the peak, respectively.

On the other hand, the tailing factor (T_f) has also been used to evaluate the peak symmetry, mostly by the pharmaceutical industry. It is obtained by drawing a horizontal line at 5% of the peak's maximum height and measuring the distance from each side of the peak to a line drawn vertically through the peak's maximum (**Figure 3.10**). The equation for calculating T_f is expressed as follow:

$$T_f = \frac{c+d}{2c} \qquad (17)$$

in which c and d are the distance from the points at 5% of the peak's maximum height to the center in both left and right sides of the peak, respectively.

In both cases, T_f and A_s give approximately the same tailing values, though T_f is the standard measurement in the pharmaceutical industry while A_s is often used in other applications (33). Values between 1.0 and 1.05 indicate the symmetric Gaussian shape of an ideal chromatographic peak. Nonetheless, $T_f \approx A_s \leq 1.5$ are usually acceptable. However, values > 2.0 are undesirable, which hinders the resolution and the quantification of the peaks, and thus corrective actions are recommended.

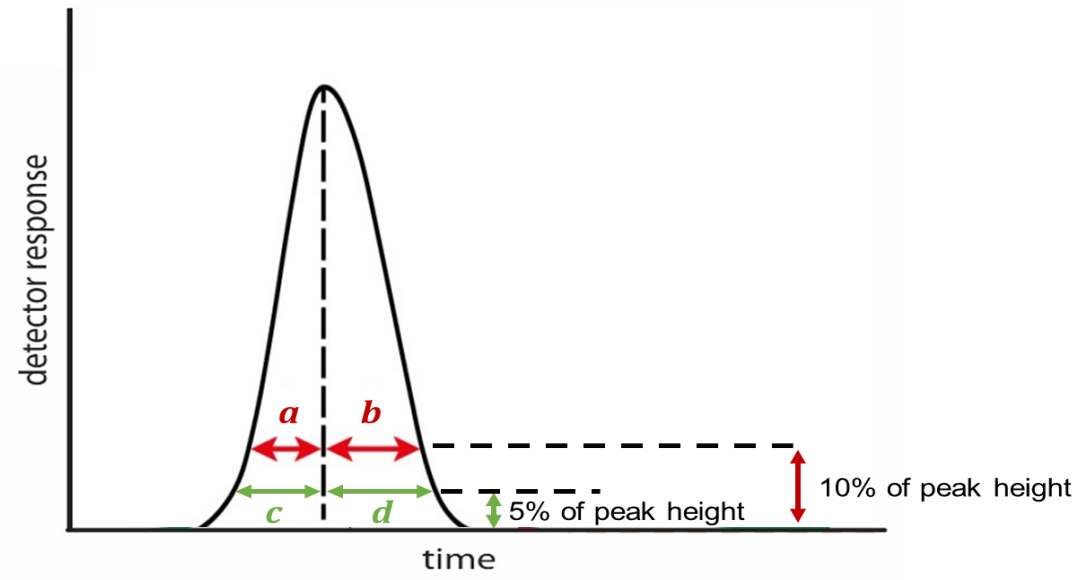

Figure 3.10 Illustration of the calculation of the tailing factor and asymmetry factor for a chromatographic peak.

3.7. Assessment of real samples

The fully validated analytical methodologies developed throughout this thesis were applied for the analysis of different samples. To increase the robustness of the LC-potentiometric methods, the results were compared, whenever possible, with routine and well-established detectors placed in line with the potentiometric one. In chapter 4, section 4.4, the determination of tetracycline antibiotics in milk samples was also performed with a UV detector (Waters®) while in section 4.5, the determination of ammonium ions in environmental water samples was performed with a conductimetric detector (Metrohom®).

3.8. Statistical analysis

Despite the evaluation of the repeatability and intermediate precision during the analytical method validation, it was also performed Fischer's two-sided test to compare the precision between two detectors, whenever possible, for a level of confidence of 95% (35).

The accuracy was statistically assessed by the two-tail paired *t*-student, determining the differences between two means obtained by the proposed and the reference methodologies, for a level of confidence of 95%.

3.9. References

1. Richard P. Buch EL. Recommendations for nomenclature of ion-selective electrodes (IUPAC Recommendations 1994). Pure Appl Chem. 1994;66(12):2527-36.

2. Bakker E, Buhlmann P, Pretsch E. Carrier-based ion-selective electrodes and bulk optodes. 1. General characteristics. Chem Rev. 1997;97(8):3083-132.

3. Meier PC. Two-parameter debye-hückel approximation for the evaluation of mean activity coefficients of 109 electrolytes. Anal Chim Acta. 1982;136:363-8.

4. Bakker E, Pretsch E. Modern potentiometry. Angew Chem Int Ed Engl. 2007;46(30):5660-8.

5. Umezawa Y, Buhlmann P, Umezawa K, Tohda K, Amemiya S. Potentiometric selectivity coefficients of ion-selective electrodes Part I. Inorganic cations - (Technical report). Pure Appl Chem. 2000;72(10):1851-2082.

6. Bakker E. Determination of improved selectivity coefficients of polymer membrane ion-selective electrodes by conditioning with a discriminated ion. J Electrochem Soc. 1996;143(4):L83-L5.

7. Bakker E, Pretsch E, Buhlmann P. Selectivity of potentiometric ion sensors. Anal Chem. 2000;72(6):1127-33.

8. Bakker E. Determination of unbiased selectivity coefficients of neutral carrier-based cation-selective electrodes. Anal Chem. 1997;69(6):1061-9.

9. Maccà C. Response time of ion-selective electrodes: Current usage versus IUPAC recommendations. Anal Chim Acta. 2004;512(2):183-90.

10. De Backer BL, Nagels LJ. Potentiometric detection for capillary electrophoresis: determination of organic acids. Anal Chem. 1996;68(24):4441-5.

11. Sekula J, Everaert J, Bohets H, Vissers B, Pietraszkiewicz M, Pietraszkiewicz O, et al. Coated wire potentiometric detection for capillary electrophoresis studied using organic amines, drugs, and biogenic amines. Anal Chem. 2006;78(11):3772-9.

12. Bao Y, Everaert J, Pietraszkiewicz M, Pietraszkiewicz O, Bohets H, Geise HJ, et al. Behaviour of nucleotides and oligonucleotides in potentiometric HPLC detection. Anal Chim Acta. 2005;550(1-2):130-6.

13. Vissers B, Bohets H, Everaert J, Cool P, Vansant EF, Du Prez F, et al. Characteristics of new composite- and classical potentiometric sensors for the determination of pharmaceutical drugs. Electrochim Acta. 2006;51(24):5062-9.

14. Vissers B, Everaert J, Sekula J, Malak A, Bohets H, Bazylak G, et al. Unique potentiometric detection systems for HPLC determination of some steroids in human urine. J Sep Sci. 2009;32(2):167-79.

15. Daems D, Van Camp G, Fernandez M, Guisez Y, Prinsen E, Nagels LJ. Use of potentiometric detection in (ultra) high performance liquid chromatography and modelling with adsorption/desorption binding kinetics. Anal Chim Acta. 2013;777:25-31.

16. Lima JLFC, Machado AASC. Procedure for the construction of all-solid-state PVC membrane electrodes. Analyst. 1986;111(7):799-802.

17. Gil RL, Amorim CG, Montenegro MCBSM, Araújo AN. HPLC-potentiometric method for determination of biogenic amines in alcoholic beverages: A reliable approach for food quality control. Food Chem. 2022;372:131288.

18. Cuartero M, Pankratova N, Cherubini T, Crespo GA, Massa F, Confalonieri F, et al. In situ detection of species relevant to the carbon cycle in seawater with submersible potentiometric probes. Environ Sci Tech Let. 2017;4(10):410-5.

19. Liu Y, Cánovas R, Crespo GA, Cuartero M. Thin-Layer potentiometry for creatinine detection in undiluted human urine using ion-exchange membranes as barriers for charged interferences. Anal Chem. 2020;92(4):3315-23.

20. Magnusson B, Örnemark U. Eurachem Guide: The fitness for purpose of analytical methods – A laboratory guide to method validation and related topics 2014 [Available from: https://www.eurachem.org/images/stories/Guides/pdf/MV_guide_2nd_ed_EN.pdf.

21. ICH. ICH harmonised tripartite guideline: Validation of analytical procedures: text and methodology Q2 (R1) ICH, Geneva, Switzerland, 2005 [Available from: https://www.ich.org/page/quality-guidelines.

22. Union E. Commission Decision of 12 August 2002 implementing Council Directive 96/23/EC concerning the performance of analytical methods and the interpretation of results. Off J Eur Communities; 2002. p. 8-36.

23. Thompson M, Ellison SLR, Wood R. Harmonized guidelines for single-laboratory validation of methods of analysis (IUPAC Technical Report). Pure Appl Chem. 2002;74(5):835-55.

24. Toth K, Stulik K, Kutner W, Feher Z, Lindner E. Electrochemical detection in liquid flow analytical techniques: characterization and classification - (IUPAC Technical Report). Pure Appl Chem. 2004;76(6):1119-38.

25. Waters. Taking the complexity out of SPE method development 2017 [Available from: http://www.waters.com/webassets/cms/library/docs/720005685en.pdf.

26. Inczedy J, Lengyel T, Ure AM. Compendium of Analytical Nomenclature (definitive rules 1998) (the “Orange Book”),. 3rd ed. Oxford: Blackwell Science.

27. Currie LA. Nomenclature in evaluation of analytical methods including detection and quantification capabilities (IUPAC Recommendations 1995). Pure Appl Chem. 1995;67(10):1699-723.

28. Shrivastava A, Gupta V. Methods for the determination of limit of detection and limit of quantitation of the analytical methods. Chronicles of Young Scientists. 2011;2(1).

29. Dolan J. Enhancing Signal-to-Noise. LCGC North America. 2010;28(3):212–6.

30. Pool CF. The Essence of Chromatography. 1st ed. Amsterdam: Elsevier; 2003.

31. Scientific C. HPLC Chromatographic parameters 2021 [Available from: https://www.chromacademy.com/.

32. Snyder LR, Kirkland JJ, Dolan JW. Introduction to Modern Liquid Chromatography. 3rd ed, editor. Hoboken. New Jersey: Wiley; 2009.

33. Maryutina TA, Savonina EY, Fedotov PS, Smith RM, Siren H, Hibbert DB. Terminology of separation methods (IUPAC Recommendations 2017). Pure Appl Chem. 2018;90(1):181-231.

34. Dolan J. Detective Work, Part II: Physical Problems with the Column. LCGC North America. 2015;33(12):894–9.

35. James NM, Jane CM. Statistics and Chemometrics for Analytical Chemistry. 6th ed. New Jersey: Prentice Hall; 2010.

Chapter 4

Development and application of LC-Potentiometry analytical methodologies

4.1. Introduction

The state-of-the-art, described in chapter 2 of the present thesis, elucidated the progress about the use of potentiometric detection in liquid chromatographic systems. Notably, different electrodes constructions and flow-cells designs have been investigated in the search of the most favorable potentiometric detector as well as in the extension of the target analytes. The advancements achieved so far in chromatography proved the great potential of potentiometry to become a competitive detection technique compared to classical ones such as conductimetry in ion-chromatography and UV-Vis in reversed-phase liquid chromatography (LC). Therefore, the research must be conducted in the development of new analytical applications, especially involving analytes of interest in food, pharmaceutical, and biotechnology industries but also environmental analysis. Interestingly, the successful coupling of different kinds of potentiometric sensors to chromatographic systems overcomes the lack of selectivity because interferences are easily separated. On the other hand, LC enables new targets for potentiometric determinations, such as bioorganic compounds, which are available in very small quantities and often in admixture with other substances.

Taking these assumptions into account, new fully validated analytical methodologies based on the synergic coupling of potentiometric detection and LC are presented in the next sections. All the LC-potentiometric methods are applied to the analysis of real samples to demonstrate the competitiveness of potentiometric detection when compared with other techniques for the development of simple, cost-effective, and robust analytical methodologies.

Sections 4.2 and 4.3 describe an amine-selective electrode coupled to ion-pair chromatography for the determination of underivatized biogenic amines in foodstuff, particularly tomato products and alcoholic beverages. Further insight on chemical structure subdivides them between aliphatic, aromatic, or heterocyclic amines to which one or more amino groups are attached. According to the number of reactive amino groups, amines can be subdivided in monoamines (e.g. ethylamine – Eth, methylamine – Met, phenylethylamine – Phe, tryptamine – Tryp, and tyramine – Tyr), diamines (e.g. cadaverine – Cad, putrescine – Put, and histamine – His) or polyamines (e.g. spermine – Spm and spermidine – Spmd). The amine-selective electrode is based on a macrocyclic host (cucurbit[6]uril) and a lipophilic ion-exchanger as sensing elements (section 4.2), whose analytical performance is improved by the incorporation of multi-walled carbon nanotubes in the sensing membrane (section 4.3).

On a similar basis, section 4.4 shows a tetracycline-selective electrode as a detector of reversed-phase liquid chromatography for the determination of tetracycline antibiotics in milk samples. The most representative and regulated tetracycline antibiotics were selected, including the monovalent cations chlortetracycline – CTC, doxycycline – DXC, oxytetracycline – OTC, and tetracycline – TTC. The tetracycline-selective electrode is based on a macrocyclic host (cucurbit[8]uril), a lipophilic ion-exchanger, and multi-walled carbon nanotubes.

On the other hand, section 4.5 shows the benefits of chromatographic separation to overcome specific drawbacks in terms of selectivity of potentiometric sensors, by addressing the challenging detection of ammonium ions using nonactin-based electrodes, in the presence of high levels of potassium ions. In this latter section, ammonium-selective electrodes are implemented as a detector of ion-chromatography for the determination of (sub)micromolar levels of ammonium ions in water samples. As a proof-of-concept, multi-ion detection in the same samples is also described resorting to three different ion-selective electrodes assembled in the microfluidic flow cell.

4.2. Determination of biogenic amines in tomato by ion-pair chromatography coupled to an amine-selective potentiometric detector

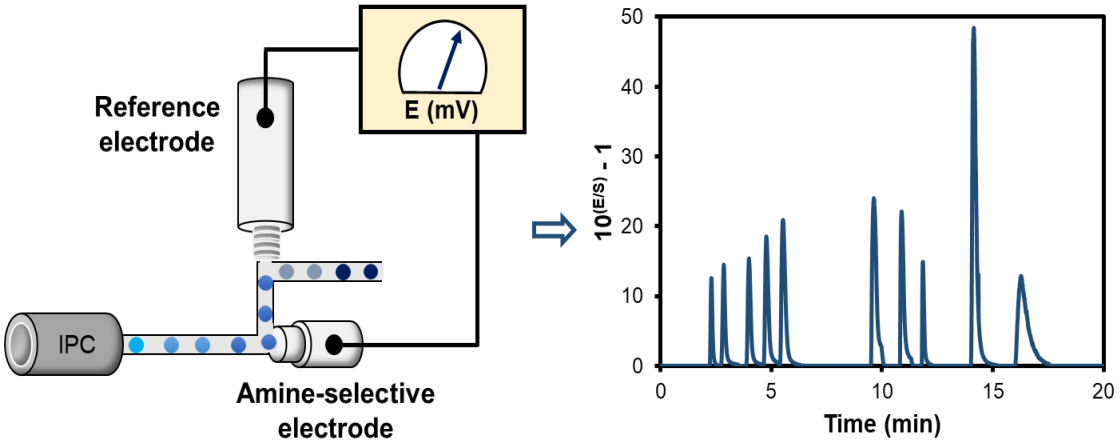

Section 4.2 describes the development of an HPLC-Potentiometric method based on ion-pair chromatography coupled to an amine-selective electrode for the determination of biogenic amines in tomato samples[2].

[2] This is a partial transcription of the article *Renato L. Gil, Célia G. Amorim, Maria C.B.S.M. Montenegro, Alberto N. Araújo; Determination of biogenic amines in tomato by ion-pair chromatography coupled to an amine-selective potentiometric detector; Electrochimica Acta, 2021, 378, 138134; doi: 10.1016/j.electacta.2021.138134*;

4.2.1. Introduction

The coupling of potentiometric detection to chromatographic separation techniques has been studied since the seventies (1, 2). First trials reported the use of metallic copper (3-5) and tungsten oxide electrodes (6, 7) in ion chromatographic (IC) systems. Later on, applications comprising ion-selective electrodes (ISEs) and HPLC were also described (8, 9). The total number of publications was no more than fifty papers at the dawn of the new century, most of them restricted to classical potentiometric detection of metal cations and small inorganic anions (10). The remaining resulted from important contributions of Luc Nagels´research group and included organic acids (11), basic drugs (12), and alkaloids (13).

Potentiometric sensors are currently not viewed as routine detectors for LC, which might be mainly explained by robustness issues (14). The use of organic modifiers in reversed-phase chromatography decreases the reproducibility and the lifetime of the sensors. These also exhibit longer response times for low concentrations of analytes (10). The proposal of new procedures should attend not only to those hindrances along with the optimization of chromatographic conditions but also to the construction of the sensors and respective flow-cells, difficult to be found in the market. The trade-off is the achievement of simpler and friendlier procedures to the environment, where chemical derivatization steps are eliminated and tedious sample preparation is minimized by the typical enlarged analytical range of potentiometric sensors. The henceforth reported determination of biogenic amines (BAs) in foodstuff has high evidence potential in this respect.

BAs are low molecular weight organic bases usually found in food products and beverages (15-19), which are produced by enzymatic decarboxylation of amino acids in the course of bacterial growth (20). The high content of these compounds in food might put sensorial properties in jeopardy and its intake can even trigger toxic effects to the consumer (21, 22). For instance, some of them may react with nitrite salts, especially used in smoked meat products, producing nitrosamines that are carcinogenic compounds (23). As such, the presence of BAs in foodstuff indicates spoilage and its determination is important for public health risk assessment (22). Excellent reviews of available methods for BAs detection and quantification were previously published by others (24, 25), and emphasize mostly the ones based on reversed-phase chromatography coupled to either UV/Vis (26, 27) or fluorometric detection (28, 29). Nonetheless, chemical derivatization of the amine group with the involvement of toxic reagents is usually performed to improve the resolution and detection

limits (30). Alternatively, direct BAs analysis is feasible in mass spectrometry hyphenated methods operated by skilled technicians but at a high-cost expense (31-33).

Electroanalytical detectors have been also proposed for the determination of BAs in food matrices. Conductivity is the traditional method of detection in ion chromatography (34, 35), though a suppressor system is usually required to improve sensitivity. Amperometric detection with gold electrodes was also used in ion chromatography but a post-column addition of sodium hydroxide was necessary to provide the required alkaline conditions (36, 37).

Concerning potentiometric detectors, many papers have been demonstrating their ability to detect underivatized BAs after their separation by ion chromatography, for food quality control. Chen and Alexander (38) reported the use of a metallic copper indicator electrode, as a detector in ion-pair chromatography, for the determination of four aliphatic amines. However, the resolution was poor and the high detection limits were hurdles difficult to transpose regarding useful real applications. Poels and Nagels showed for the first time the use of macrocycle-based ISEs for the detection of several amines in chromatographic separation, highlighting the importance of the membrane composition to improve the sensitivity and detection limits (39). Afterward, the analysis of aliphatic amines in cheese serum by ion-pair chromatography was proposed (40). Some of the BAs investigated during the method development gave only reasonable detector responses and hence were not further studied in the chromatographic experiments. To our knowledge, no other reports show the advantages of using potentiometric detectors in LC to detect BAs, especially histamine, which has been targeted as a toxin by the Food and Drug Administration (41) and the European Food Safety Authority (42). Besides, aliphatic polyamines such as putrescine, cadaverine, spermidine, and spermine are also important because of their toxicity but a simultaneous determination was not accomplished in LC potentiometry systems, yet. This fact justifies the development of novel potentiometric detectors and analytical methodologies that allow the determination of these important amines in foodstuffs.

Cucurbit[n]urils (CB[n]) belong to a family of toroid-shaped macrocyclic structures with superior molecular recognition ability in aqueous media (43). The well-established ability to interact and form complexes with positively charged guests (44, 45) highlights their use as ionophores in potentiometric sensing membranes. Recently, a histamine- selective electrode based on CB[6] was proposed by our group for the analysis of biological samples (46). Therefore, the authors aim to study the potentiometric response for a wider range of BAs (aliphatic, aromatic, heterocyclic), some of them not yet investigated, to be separated

in hydrodynamic conditions resorting to an ion-pair reagent. This challengeable strategy has a tremendous effect on the potentiometric response of the sensor by the use of the ion-pair reagent and by the use of organic solvents that affect the polymeric membrane viability of the sensor. So, a careful study was followed to find the best chemical and hydrodynamic conditions for the determination of ten BAs in the desired concentration range. The proposed methodology was validated and applied to the analysis of tomato samples.

4.2.2. Materials and methods

4.2.2.1. Reagents, chemicals, and standard solutions

Ultra-pure water with conductivity <0.055 µS cm^{-1} and p. a. grade chemicals were used. Acetonitrile (ACN from Merck, ref. 1.00029.2500P) and methanol (MetOH from Fisher Chemical, ref. 1.06035.2500P) of HPLC Gradient grade were acquired from VWR. Mixed cellulose ester membranes, 0.22 µm, from Millipore (GSWP04700) were used to filter the mobile phases. Ammonium hydroxide solution (NH_4OH, ref. 320145), methanesulfonic acid sodium salt (SMS, ref. 304506), butane-1-sulfonic acid sodium salt (SBS, ref. 1183030025), 1-heptanesulfonic acid sodium salt (SHS, ref. H2766), o-nitrophenyloctyl ether (o-NPOE, ref. 365130), cucurbit[6]uril hydrate (ref. 94544), high molecular weight polyvinyl chloride (PVC, ref. 81392) and tetrahydrofuran (THF, ref. 186562) were purchased from Sigma-Aldrich. Potassium tetrakis(p-chlorophenyl)borate (TCPB, ref. 60591) was from Fluka.

Lithium formate buffer solution (pH=4) was prepared by mixing a $1.0x10^{-2}$ mol L^{-1} formic acid solution (HCOOH, ≥98% from Fluka, ref. 06450) with $1.0x10^{-2}$ mol L^{-1} lithium hydroxide solution (LiOH from Merck, ref. 1127980). Methylamine hydrochloride (Met, ≥98%, ref. M0505), ethylamine hydrochloride (Eth, 98%, ref. 232831), putrescine dihydrochloride (Put, ≥97%, P5780), cadaverine dihydrochloride (Cad, 95%, D22606), histamine dihydrochloride (His, ≥99%, H7250), spermidine trihydrochloride (Spmd, ≥98%, ref. S2501), spermine tetrahydrochloride (Spm, ≥99%, ref. 85610), tyramine hydrochloride (Tyr, ≥98%, ref. T2879), 2-phenylethylamine hydrochloride (Phe, ≥98%, ref. P6513) and tryptamine hydrochloride (Tryp, ≥99%, ref. 246557) were obtained from Sigma-Aldrich. Stock solutions of amines were prepared in lithium formate buffer and stored in the fridge at 4 °C. Dilutions of the stock solutions in solvent A of the mobile phase were made daily before injection.

4.2.2.2. Sample preparation

Different types of tomato samples were purchased from the local market: fresh tomato, canned chopped tomato, and canned pulp tomato. All samples were firstly homogenized in a domestic mill and then centrifuged (3000g for 15 min) to eliminate suspended particles. The supernatants were filtered through 0.45 µm Nylon membranes (Millipore) and stored at 4° C (no more than one week). Before analysis, further cleanup was proceeded by solid-phase extraction using cartridges Water Oasis PRIME MCX (3cc, 60mg, ref. 186008918) according to Zhang Y. et al (27). About 1.0 mL of each sample percolated the cartridge, afterward washed twice with 1.0 mL of ultra-pure water. The compounds of interest were quantitatively recovered after triplicate elution with 1.0 mL of a MetOH: NH_4OH solution (95:5, v/v). The eluate was dried under N_2 flow and finally reconstituted in 1.0 mL of the initial mobile phase. All solutions were passed through 0.22 µm Nylon filters before injection in the chromatographic system.

Recovery experiments were performed according to the protocol described by Waters Company (47) by adding known amounts of a standard mixture of BAs to the sample. The content of BAs was further determined using the proposed methodology.

4.2.2.3. Chromatographic conditions

The HPLC system consisted of a Waters 600 Solvent Delivery Pump (Waters Liquid Chromatography) equipped with a Rheodyne 7725i six-port external sample injector (IDEX Health & Science, LLC). A sample loop of 100 µL was used unless otherwise stated. The chromatographic column was a Luna® Omega 5 µm Polar C18 100A, LC Column 150 x 4.6 mm (Phenomenex). Another Luna® 5 µm C8(2) 100 Å, LC Column 150 x 4.6 mm (Phenomenex) was also used during the method development. The mobile phase used for gradient elution comprised the solvent A ($5.0x10^{-3}$ mol L^{-1} SBS in $1.0x10^{-2}$ mol L^{-1} lithium formate buffer, pH=4) and the solvent B ($1.0x10^{-3}$ mol L^{-1} lithium formate buffer: ACN, 90:10 v/v, pH=4). The fixed flow rate of 1.2 mL min^{-1} was used throughout unless otherwise stated.

4.2.2.4. Detection cell

The column outlet was connected to the low-dead volume wall-jet flow-cell depicted in **Figure 4.1**. It consisted of an acrylic block incorporating four single holes: two for the inlet

and outlet of the mobile phase; one enabling to screw the commercial reference electrode (model 6.0727.000, Metrohm, Switzerland), and the last for coupling the miniaturized indicator electrode. Both electrodes were connected to a 6-Channel Precision Electrochemistry EMF Interface (LawsonLabs, Inc. USA). The chromatograms, i.e., potentiometric signals vs. time were recorded by the graphics software from LawsonLabs, Inc. USA.

As an indicator electrode, a polytetrafluoroethylene rod (1.6 mm I.D. x 4.0 mm O.D. x 15 mm length) having its axis filled with a conductive graphite composite material (48) was used. An electrical shielded cable was connected to one of its endings while the sensing polymeric membrane was dripped on the other ending surface. It consisted of 1.0% (w/w) of CB[6] as an ionophore, 0.3% (w/w) of TCPB as an ionic additive, 68.7% (w/w) of o-NPOE as a plasticizer and 30.0% (w/w) of PVC as polymer. The molar ratio between the ionic additive and the ionophore was 60TCPB:100CB[6] and the structures of the sensing elements are displayed in **Figure 4.2**.

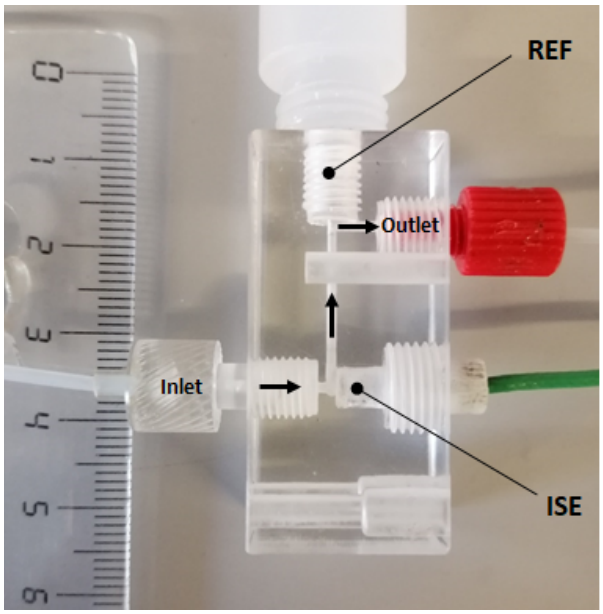

Figure 4.1 Wall-jet flow-cell assembled with the potentiometric electrodes. ISE – Ion-selective electrode. REF – Ag/AgCl (KCl 3 mol L^{-1}) reference electrode.

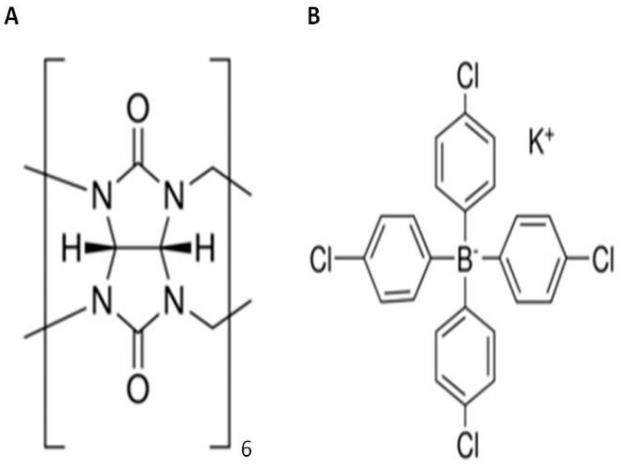

Figure 4.2 Structures of the membrane sensing elements. **(A)** Cucurbit[6]uril and **(B)** potassium tetrakis(p-chlorophenyl)borate.

The solution used in the membrane preparation was obtained by initial mixing of the ionophore and the lipophilic ion-exchanger in the plasticizer solvent. The mixture was poured on PVC previously dissolved in THF. For electrode preparation, the membrane solution was dripped directly on the conductive surface of the miniaturized electrodes (4 x 5 µL). The solvent was allowed to evaporate for 20 min at room temperature between each drop and finally left to dry for at least 2 h.

The electrodes were soaked in buffer solution when not in use. Before HPLC measurements, the electrode was firstly inserted in the wall-jet flow-cell and conditioned with the running mobile phase until a stable baseline was observed (~30 min). For a better comparison between the different chromatograms obtained during the method development, the sensor response was offset to 0 mV at the injection moment.

4.2.3. Results and discussion

It is well-known that CB[n]s macrocyclic compounds form inclusion complexes with positively charged guests (44, 45). Therefore, the authors aimed to study the high potential of CB[6] as a molecular recognition element to develop an amine-selective electrode capable of detecting different BAs after their separation by LC. To ensure the perm-selectivity and to improve the ion extraction, an ionic additive (TCPB) was added to the

sensing membrane. As such, the potentiometric response towards BAs was firstly assessed under static conditions by using the membrane formulation previously reported (46). The figures of merit for the electrode towards each amine are summarized in **Table 4.1**, using the lithium formate buffer (pH=4) as a background electrolyte to guarantee the ionized form of all amines.

Table 4.1 Summary of the analytical figures of merit of the proposed detector under static conditions.

Amine	Slope (mV dec^{-1})	R^2	LLLR (mol L^{-1})	PDL (mol L^{-1})	Linear Range (mol L^{-1})	Ref
Put	24.8±0.9	0.9910±0.0016	4.0x10^{-6}	(2.7±1.1)x10^{-6}	4.0x10^{-6} – 1.0x10^{-2}	(46)
Cad	28.4±0.4	0.9954±0.0011	2.2x10^{-6}	(1.4±0.7)x10^{-6}	2.2x10^{-6} – 1.0x10^{-2}	(46)
His	30.9±1.2	0.9988±0.0011	3.0x10^{-7}	(3.0±0.6)x10^{-7}	3.0x10^{-7} – 1.0x10^{-2}	(46)
Spmd	20.2±1.8	0.9962±0.0010	1.0x10^{-5}	(5.7±1.5)x10^{-6}	1.0x10^{-5} – 1.0x10^{-2}	This work
Spm	13.8±1.0	0.9936±0.0018	5.0x10^{-7}	(4.4±0.8)x10^{-7}	5.0x10^{-7} – 1.0x10^{-2}	This work
Tyr	53.3±1.2	0.9978±0.0012	1.0x10^{-5}	(8.1±2.7)x10^{-6}	1.0x10^{-5} – 1.0x10^{-2}	This work
Phe	62.7±2.5	0.9969±0.0045	1.0x10^{-5}	(3.2±2.2)x10^{-7}	1.0x10^{-5} – 1.0x10^{-2}	This work

LLLR – Lower limit of linear response; PDL – practical detection limit.

The corresponding calibration curves are displayed in **Figure 4.3**. Nernstian responses were obtained for all assayed amines in the range of 1.0x10^{-5} and 1.0x10^{-2} mol L^{-1} with R^2 higher than 0.9910. Differences in the slope values were due to the number of amine groups in each BA and to the nature of the potentiometric response. For instance, spermine presents four positive charges while phenylethylamine presents only one, and thus, according to the Nikolsky-Eisenman equation, slopes of 13.8 and 62.7 mV dec^{-1} were attained, respectively. Noteworthy, the analytical range was wider for histamine and spermine, over almost five orders of magnitude. These figures of merit enabled to anticipate the ability of the electrode to detect each one of those amines after its separation by LC.

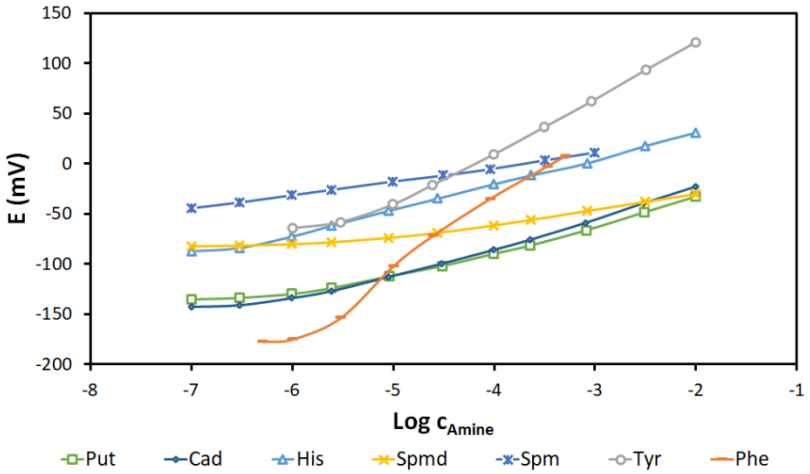

Figure 4.3 Individual calibration curves obtained for putrescine, cadaverine, histamine, spermidine, spermine, tyramine, and phenylethylamine under static conditions.

4.2.3.1. Ion-pair chromatography performance

To attain the separation of the desired set of high polar BAs in LC, different approaches based on previously reported works were analyzed (34, 36, 39). In such cases, the use of ion chromatography was considered though leading to irreproducible measurements because of the low capacity of ion-exchange materials. This also results in poor chromatographic mass-transfer characteristics and therefore in broader peaks (49). Besides, ion-exchange columns are much more expensive than the reversed-phase columns, which increases the price of the analysis.

To overcome these limitations, a different strategy based on ion-pair chromatography with reliable and stable hydrophobic columns was considered. The addition of an ion-pair agent to the mobile phase improves the retention of polar analytes (organic or inorganic) on reversed-phase columns (e.g. C18 or C8) (50). Sulfonic acid derivatives, quaternary ammonium salts, and volatile agents have been reported (51), and their usefulness to separate BAs and amino acids was evidenced before (32, 40, 52, 53).

In this work, methyl sulfonate (SMS), butyl sulfonate (SBS), and heptyl sulfonate (SHS) sodium salts were assessed as ion-pair agents. Concentrations ranging from (1 to 15)x10^{-3} mol L^{-1} were prepared in the mobile phase made up of lithium formate buffer and ACN (97.5:2.5, v/v, pH=4). The retention capacity of a Luna® C8 column to the hydrophilic spermine (XLogP3 = -1.1), spermidine (XLogP3 = -1.0), putrescine (XLogP3 = -0.9), histamine (XLogP3 = -0.7), ethylamine (XLogP3 = -0.7), cadaverine (XLogP3 = -0.6) and

ethylamine (XLogP3 = -0.3) (54) generally improved with the increase in concentration of the ion-pair agent, especially for SBS and SHS, as also reported by others (50, 55). However, the baseline of the potentiometric detector shifted to more positive potentials and worsened the detection limits for the BAs when the highest concentrations of the ion-pair agent were used. This was due to the amount of sodium counter-ion, which while competing with lithium was extracted to a greater extent into the electrode membrane (46). Therefore, a concentration of 5.0×10^{-3} mol L^{-1} was selected as an ideal compromise for BAs resolution and the detector performance. Moreover, there was a positive correlation between the length of the alkyl chain of the ion-pair agent and the retention of BAs due to the stronger hydrophobic interactions with the reversed-phase column (**Figure 4.4**).

While SMS showed no efficient retention of hydrophilic amines, the strong retention of histamine observed with the SHS (28 min) invalidated its choice as an ion-pair agent due to the unacceptable long-run times. In turn, the addition of SBS enabled the separation and elution of the BAs in less than 20 min, though signals overlapped regarding the histamine, cadaverine, and putrescine, as confirmed by their similar values of *k* (1.3) and *α* (4.9). Longer run times (40 min) and peak broadening were also inevitable when the lipophilic tyramine (XLogP3 = 1.1), phenylethylamine (XLogP3 = 1.4), and tryptamine (XLogP3 = 1.6) (54) were included in the set. Increment of the ACN content in the mobile phase from 2.5 to 10% (v/v) was beneficial but with hydrophilic amines being more co-eluted. Thus, gradient elution to address these issues was instead considered.

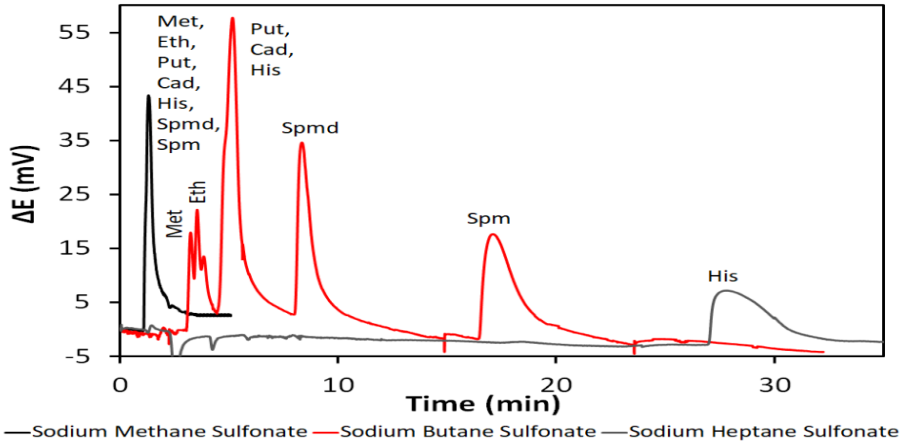

Figure 4.4 Effect of type of ion-pair agent in the separation of a mixture of biogenic amines. Chromatographic conditions: Injected concentration: 1.0×10^{-4} mol L^{-1}; Isocratic elution: mobile phase A – 5.0×10^{-3} mol L^{-1} of ion-pair agent in 1.0×10^{-2} mol L^{-1} lithium formate buffer: ACN (v/v, 97.5:2.5, pH=4). Column: Luna® 5 µm C8(2), 150 x 4.6 mm I.D. (Phenomenex). Flow-rate: 1.0 mL min^{-1}. Injection volume: 100 µL.

4.2.3.2. Gradient method optimization

Two solvents were firstly selected: the solvent A with added SBS – $5.0x10^{-3}$ mol L^{-1} SBS in $1.0x10^{-2}$ mol L^{-1} lithium formate buffer: ACN (97.5:2.5, v/v, pH=4) and solvent B with higher ACN content – $1.0x10^{-2}$ mol L^{-1} lithium formate buffer: ACN (90:10, v/v, pH=4).

During the optimization process (the optimal hydrodynamic conditions are addressed in supplementary material) a constant elution pattern emerged for sample injection volumes of 100 µL and the eluent flow-rate of 1.2 mL min^{-1}. The hydrophilic mono and diamines, such as methylamine and histamine, were firstly eluted in solvent A, due to poor interaction with the stationary phase. The polyamines, such as spermidine and spermine, were eluted between the most hydrophilic and lipophilic amines. Despite the hydrophilic properties (XLogP3 < 1) of the multi charged amines, they showed higher interaction with the negative sulfonic group of the ion-pair agent thus increasing the *k* values. Finally, the lipophilic amines were the most retained, and solvent B was required for efficient elution, respecting the order of their XLogP3.

ACN and MetOH are often used as organic modifiers in reversed-phase chromatography. The first is an aprotic solvent with high elution strength. The second, can increase analyte retention and promote large changes in the chromatographic selectivity (56). Accordingly, the effect of these two organic modifiers was assessed regarding the separation of a standard mixture with nine BAs (**Figure 4.5**).

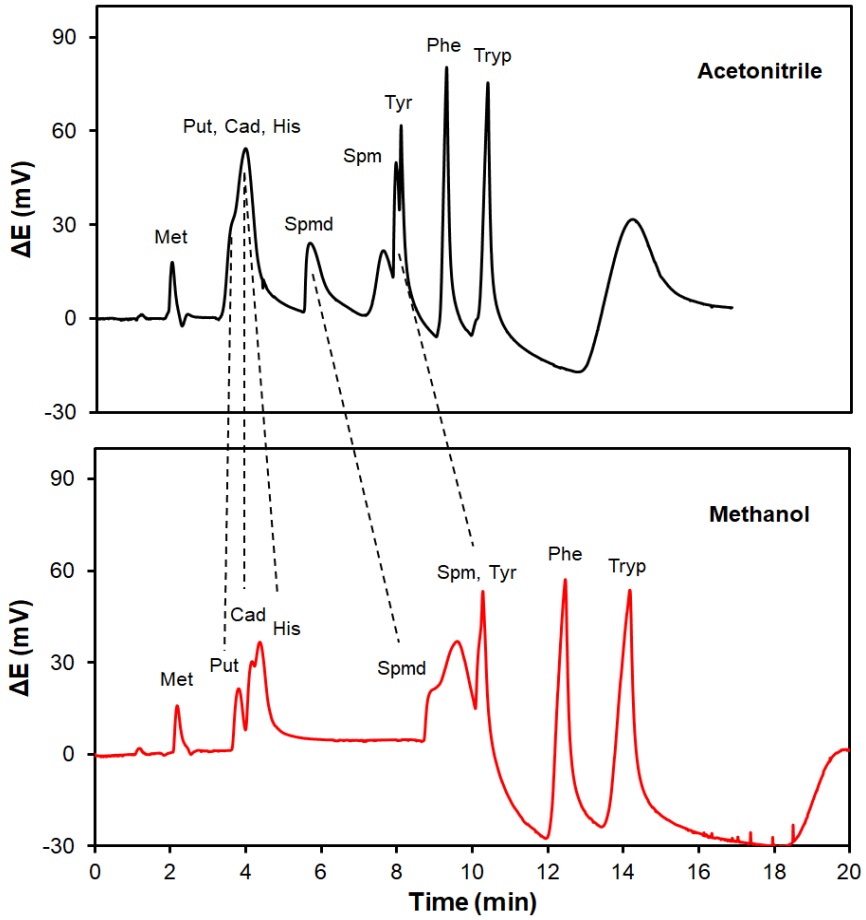

Figure 4.5 Organic modifier effect in the separation of a mixture of biogenic amines. Chromatographic conditions: Injected concentration: $1.0x10^{-4}$ mol L^{-1}; Gradient elution: solvent A – $5.0x10^{-3}$ mol L^{-1} SBS in $1.0x10^{-2}$ mol L^{-1} lithium formate buffer: organic modifier (v/v, 97.5:2.5, pH=4) and solvent B – $1.0x10^{-3}$ mol L^{-1} lithium formate buffer: organic modifier (v/v, 90:10, pH=4). Column: Luna® 5 µm C8(2), 150 x 4.6 mm I.D. (Phenomenex). Flow-rate: 1.2 mL min^{-1}. Injection volume: 100 µL.

The resolution of putrescine, cadaverine, and histamine signals improved when MetOH was used. However, spermidine was eluted during the transition of solvent A to B, and spermine and tyramine were co-eluted. Peak broadening was further observed for phenylethylamine and tryptamine. Although both *k* and α improved with the use of MetOH, especially for hydrophilic amines, the use of ACN was needed for a better peak shape of the lipophilic amines. Therefore, MetOH was chosen as an organic modifier in solvent A and ACN in solvent B.

The hydrophobicity of the stationary phase increases with functional carbon chain groups, which is even boosted by the increase of their length (57). The hydrophobic interaction with the ion-pair agent can thus be improved, modulating the retention parameters for BAs. So, a Luna® Omega Polar C18 column was equated and compared with the Luna® C8 in use, while maintaining the column dimensions (150 x 4.6 mm, 5 µm) (**Figure 4.6**). Higher resolutions were obtained for putrescine, cadaverine, histamine, spermine, and tyramine, which were even boosted by the elimination of the MetOH from solvent A. In turn, a large broadening of the potentiometric signals of phenylethylamine and tryptamine caused by their strong retention in the stationary phase was observed, which also affected the peak height. Nevertheless, the complete separation of ten BAs was feasible with the new column using a gradient elution which comprised 100% of solvent A for 3.0 min, followed by a linear increase from 0 to 100% of solvent B during 5.0 min, then kept for more 8.0 min. Initial eluent conditions were resumed after linear return in 0.5 min to 100% of A, which was maintained during 7.0 min for column conditioning. During each run, it was observed a small variation in the baseline signal when the mobile phase changes from solvent A to B due to potentiometric sensitivity to solvent ionic changes.

An important aspect regarding the performance of the proposed methodology concerns the response time of the potentiometric detector, which affects the peak height and the peak symmetry. To account for its impact, the time to reach the maximum peak height was investigated for standard mixtures of BAs at concentrations ranging from 1.0×10^{-5} up to 1.0×10^{-4} mol L^{-1}, and it was found to be less than 15 s for all amines. With the new conditions, the proposed analytical methodology was further validated.

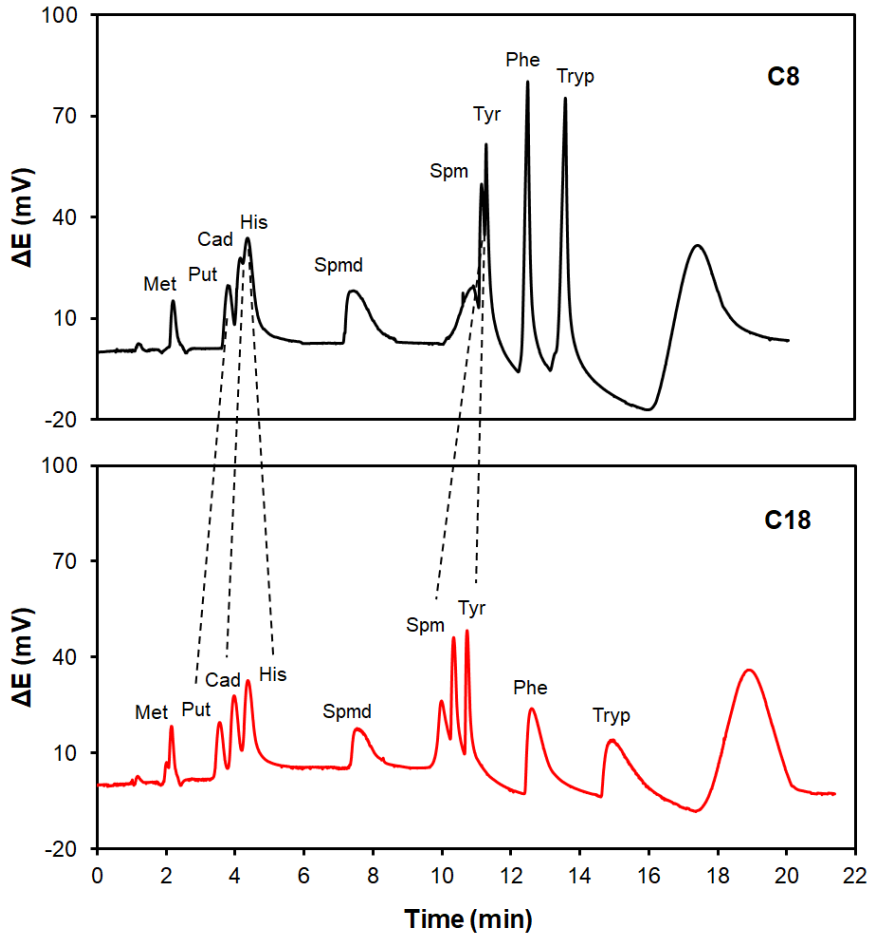

Figure 4.6 Effect of the stationary phase in the separation of a mixture of biogenic amines. Chromatographic conditions: Injected concentration: $1.0x10^{-4}$ mol L^{-1}; Gradient elution: solvent A – $5.0x10^{-3}$ mol L^{-1} SBS in $1.0x10^{-2}$ mol L^{-1} lithium formate buffer: MetOH (v/v, 97.5:2.5, pH=4) and solvent B – $1.0x10^{-3}$ mol L^{-1} lithium formate buffer: ACN (v/v, 90:10, pH=4). Columns: see experimental section. Flow-rate: 1.2 mL min^{-1}. Injection volume: 100 µL.

4.2.3.3. Validation of the proposed method for biogenic amines determination

The validation of the proposed method was done following the guidelines of the International Council for Harmonisation of Technical Requirements for Pharmaceuticals for Human Use (ICH) (58), namely in assessing specificity, range, linearity, the limit of detection (LOD), and quantification (LOQ), precision and accuracy. Confirmation of the parameters was done for relative standard deviations (RSD%) lower than 15%.

The retention parameters and analytical figures of merit for each amine are summarized in **Table 4.2**. The k and α values obtained for all amines are fairly good, ranging from 0.9 to 13.3 and 1.1 to 1.9, respectively. Only the low k value obtained for methylamine (0.9) indicates poor interaction with the stationary phase and thus care should be taken in the presence of other compounds eluted with the dead volume. Besides, the peak resolution (R_s) obtained for all BAs ranged from 2.2 to 11.9, which is above the acceptable criteria (R_s ≥ 1.5), proving the great resolution of the proposed method.

The analytical figures of merit of the detector were assessed by multilevel standard solutions of BAs covering the concentration range of 1.0x10^{-6} to 1.0x10^{-4} mol L^{-1} (*n=5*). A typical linear Nernstian response was obtained plotting the peak height as a function of the logarithmic concentration at the range of 1.0x10^{-5} to 1.0x10^{-4} mol L^{-1}. To improve the determination at lower concentrations a transformed response $tR = 10^{E/S} - 1$ was used as an analytical signal, wherein E is the potential (mV) and S is the slope of the Nikolsky-Eisenman equation (59). This transformed response is linearly related to the analyte concentration and it was recently employed in the determination of cocaine in biological samples using a UHPLC/potentiometry system (60). Following this approach, the tR was plotted against the BAs concentration and linear regression models were obtained for all amines with R^2 varying from 0.9804 to 0.9972 (*n=4*). The LOD and LOQ were calculated based on a signal-to-noise ratio of three and ten, obtaining values ranged from 0.03 to 0.20 mg L^{-1} and 0.09 to 0.61 mg L^{-1}, respectively.

The reproducibility of the proposed methodology was evaluated through the within-run precision (repeatability) after 8 replicate injections of a standard mixture of BAs at 1.0x10^{-4} mol L^{-1} (*n=8*). Two lower concentration levels were also injected in triplicate (1.0x10^{-5} and 1.0x10^{-6} mol L^{-1}). The RSD% of the peak heights was lower than 9.1%, 11.7%, and 13.8% at 1.0x10^{-4}, 1.0x10^{-5}, and 1.0x10^{-6} mol L^{-1}, respectively, proving the good precision of the proposed system. The between-run precision (intermediate precision) was also evaluated for the higher concentration by the injection of a standard mixture at 1.0x10^{-4} mol L^{-1} (*n=5*) on consecutive days. RSD% lower than 13.3% were obtained for all amines. Nonetheless, an increase of the peak heights for lipophilic amines and a decrease for the hydrophilic ones was observed between injections, which negatively affected the RSD%. This gradual shift of the response pattern, also reported by Luc Nagels in previous work with macrocycle-based electrodes (39), can be explained by the partial leakage of the membrane compounds when exposed to organic modifiers. Therefore, sensor calibration should be performed before sample analysis for more accurate measurements. The inter-electrode

reproducibility was also investigated (*n=3*) for $1.0x10^{-4}$ and $1.0x10^{-5}$ mol L^{-1} standard mixture of BAs, showing RSD% lower than 8.3% and 11.2%.

The accuracy of the method was assessed by recoveries criteria. Tomato samples were spiked with three BAs levels: $3.0x10^{-6}$, $1.0x10^{-5}$, and $3.0x10^{-5}$ mol L^{-1} being each sample processed in triplicate. The obtained recoveries ranged from 85.8±0.0% to 108.5±0.0% with RSD% values lower than 9.4%, which demonstrates the great accuracy of the proposed method. Detailed information on recoveries and RSD% obtained for each sample is further summarized in **Table S1.** However, the low capacity factor of methylamine hinders its quantification in the real samples due to its elution with unretained components.

Comparing the obtained figures of merit with those previously reported in the literature (**Table 4.3**), the proposed method provides higher detection limits than those based on fluorimetry or mass spectrometry. Nonetheless, especially for histamine, the attained detection limits cover the minimum admissible values referred to in the guidance and regulation information (42), being this method very attractive for BAs screening in food samples. The absence of derivatization procedures contributes to a more environmentally friendly analytical methodology for the determination of this set of amines. On the other hand, the proposed method presents similar figures of merit when compared with analytical methods based on electrochemical detectors (**Table 4.3**). However, the common post-column reaction with hydroxide in the amperometric detection (36, 37), to alkalinize the eluent pH to allow the oxidation of the amine group on the gold electrode, is avoided with the potentiometric detector. In the case of the conductivity detector, a suppressor system is required for the amine determination at low levels, which affects the reproducibility and increases the price of apparatus; moreover, the gradient concentrations of methane sulfonic acid for the separation of BAs usually used can negatively affect the resolution of the peaks.

Therefore, the proposed potentiometric detector enables a simpler analytical procedure by suppressing additional steps such as derivatization and post-column reactions. The simple preparation of the electrodes and the precise and accurate amine determination makes this detection procedure very promising for food quality control by chromatography.

Table 4.2 Summary of validation results obtained with the proposed amine-selective electrode in HPLC.

Amine	Retention parameters[a]				Linear Equations[b] (*y=mx+b*)	R^2	Reproducibility %RSD				LOD[e] mg L^{-1}	LOQ[f] mg L^{-1}	Accuracy[g] %
							Intra-day[c]			Inter-day[d]			
	t_R	k	α	R_s			1	10	100	100			
Met	2.3	0.9	1.5	2.3	147.7x-1.05	0.9818	11.7	5.1	6.0	13.3	0.03	0.09	-
Eth	2.9	1.4	1.8	4.6	166.1x-0.95	0.9915	11.9	2.4	3.5	6.7	0.05	0.14	85.8-102.0
Put	4.2	2.5	1.3	3.0	222.2x-0.57	0.9937	8.4	11.2	9.1	11.7	0.03	0.09	86.3-105.9
Cad	5.1	3.2	1.2	2.2	271.4x-0.54	0.9951	7.7	9.6	9.1	12.6	0.03	0.10	86.0-106.7
His	5.9	3.9	1.9	10.8	306.4x-0.52	0.9939	12.9	11.7	4.8	10.2	0.03	0.11	86.5-108.5
Spmd	10.0	7.3	1.1	3.2	467.4x-1.70	0.9931	13.8	7.8	7.8	12.7	0.15	0.44	87.5-100.3
Spm	11.0	8.2	1.1	4.7	199.5x-0.64	0.9972	13.6	9.7	8.8	12.4	0.20	0.61	97.6-106.0
Tyr	12.0	9.0	1.2	11.9	128.8x-0.87	0.9904	11.2	4.3	6.3	11.7	0.14	0.41	85.6-98.9
Phe	14.5	11.1	1.2	5.8	128.3x-1.04	0.9804	10.4	11.4	8.5	11.6	0.12	0.36	86.2-100.0
Tryp	17.1	13.3	-	-	180.7x-0.76	0.9901	10.6	10.9	7.4	13.1	0.16	0.48	86.3-106.8

[a] BAs concentration 10 µmol L^{-1}; t_R – retention time (min); k – retention factor; α – separation factor related to the next peak; R_s – peak resolution; t_0 – 1.2 min; [b] *n = 4*; [c] *n = 8* for 100 µmol L^{-1} and *n = 3* for the other two levels; [d] *n = 5* in two consecutive days for 100 µmol L^{-1}; [e] LOD based on S/N=3 (injected concentration); [f] LOQ based on S/N=10 (injected concentration); [g] *n = 3*

Table 4.3 General comparison of different analytical methods based on HPLC for BAs determination.

Amines	Derivatization	Separation Technique	Detection	LOD/LOQ	Reproducibility Spiked Sample (RSD)	Ref
Amy, But, Cad, Eth, Hex, His, Phe, Prop, Put, Spm, Spmd, Tryp	Yes benzoyl chloride	RP-HPLC (column: C18 250x4.6mm)	UV	LOD: 0.13-0.51 mg L^{-1} LOQ: 0.33-1.54 mg L^{-1}	1.8-28.7%	(61)
Agm, Cad, His, Phe, Put, Spm, Spmd, Tryp, Tyr, 5-HT	Yes benzoyl chloride	RP-HPLC (column: ODS-3 250x4.6 mm)	UV	LOD: 0.01-0.03 mg kg^{-1} LOQ: 0.03-0.10 mg kg^{-1}	-	(62)
Agm, Cad, His, Phe, Put, Spmd, Tyr	Yes AccQ	RP-HPLC (column: Luna C18 250x4.6 mm)	FLD	LOD: 0.03-0.07 mg L^{-1} LOQ: 0.08-0.2 mg L^{-1}	-	(63)
Cad, Hexa, His, Phe, Spm, Tryp, Tyr	Yes BCEC-Cl	RP-HPLC (column: Hypersil C18 200x4.6mm)	FLD	LOD: 0.001-0.008 mg L^{-1} LOQ: 0.004-0.026 mg L^{-1}	2.9-4.1%	(64)
Cad, Hexa, His, Phe, Put, Spm, Spmd, Tyr	Yes EAC	RP-HPLC (column: Hypersil BDS C18 200x4.6 mm)	FLD	LOD: (2.7-6.9) $x10^{-4}$ mg L^{-1} LOQ: -	1.3-1.9%	(65)
Agm, But, Cad, Det, Dmet, Hex, His, Ibut, Ipent, Met, Phe, Prop, Put, Spm, Spmd, Tryp, Tyr	Yes tosyl chloride	RP-HPLC (column: Gemini C18 150x4.6 mm)	MS/MS	LOD: $2.3x10^{-5}$-83 mg L^{-1} LOQ: $7.5x10^{-5}$-270 mg L^{-1}	<15.0%	(66)

Table 4.3 (Continued).

Amines	Derivatization	Separation Technique	Detection	LOD/LOQ	Reproducibility Spiked Sample (RSD)	Ref
Cad, Eth, Etha, His, Put, Spm, Spmd	Yes NaOH (post-column)	IC (column: IonPac CS18 250x2.0 mm)	AMP (Au electrode)	LOD: 0.009-0.11 mg L^{-1} LOQ: 0.03-0.30 mg L^{-1}	-	(37)
Agm, Cad, His, Put, Spm, Spmd, Tyr	Yes NaOH (post-column)	IC (column: Dionex IonPac CS17 250x2.0 mm)	AMP (Au electrode)	LOD: 0.77-2.12 mg L^{-1} LOQ: -	1.2-11.0%	(36)
Cad, His, Put, Spmd	No	IC (column: Dionex IonPac CS17 250x4.0 mm)	CONDUC (suppression)	LOD: 0.15-0.50 mg kg^{-1} LOQ: 0.50-1.0 mg kg^{-1}	2.4-3.7%	(34)
Agm, Cad, His, Put, Spm, Spmd, Tea, Tma	No	IC (column: Dionex IonPac CS17 250x4.0 mm)	CONDUC (suppression)	LOD: 0.02-0.07 mg kg^{-1} LOQ: 0.07-0.23 mg kg^{-1}	<0.32%	(35)
But, Eth, Met, Prop	No	IPC (column: C18 100x4.6 mm)	POT (Cu electrode)	LOD: 0.72-1.90 mg L^{-1} LOQ: 3.11-7.31 mg L^{-1}	-	(38)
But, Eth, Hex, Met, Pent, Prop	No	IC (column: Alltech universal 100x4.6 mm)	POT (ISE based on macrocycle ionophores)	LOD: 0.01-2.70 mg L^{-1}	<6.0% (But, standard)	(39)
Cad, Put	No	IC (column: Alltech universal 100x4.6 mm)	POT (ISE based on macrocycle ionophores)	LOD: 0.06-0.07 mg L^{-1} LOQ: -	-	(39)
But, Eth, Hex, Met, Pent, Prop	No	IC (column: Dionex Ionpac CS12A 250x4.0 mm)	POT (ISE based on dibenzo-18-crown-6-KI and TCPB)	LOD: 0.004-0.007 mg L^{-1} LOQ: -	2.2-4.0%	(40)
Eth, Cad, His, Met, Phe, Put, Spm, Spmd, Tryp, Tyr	No	IPC (column: Luna Omega Polar C18 150x4.6mm)	POT (ISE based on CB[6] and TCPB)	LOD: 0.03-0.20 mg L^{-1} LOQ: 0.09-0.61 mg L^{-1}	0.2-9.4%	This work

AccQ: 6-aminoquinolyl-N-hydroxysuccinimidyl carbamate; Agm: agmatine; AMP: amperometric detector; Amy: amylamine; BCEC-Cl: 2-(11H-benzo[a]carbazol-11-yl) Ethyl carbonochloridate; But: butylamine; Cad: cadaverine; CONDUC: conductivity detector; Det: diethylamine; Dmet: dimethylamine; EAC: ethyl-acridine-sulfonyl chloride; Eth: Ethylamine; Etha: ethanolamine; FLD: fluorescence detector; Hex: Hexylamine; Hexa: 1,6-hexamethylenediamine; His: histamine; RP-HPLC: reversed-phase high-performance liquid chromatography; Ibut: isobutylamine; IC: ion-chromatography; IPC: ion-pair chromatography; Ipent: isopentylamine; Met: methylamine; MS: Mass spectrometry detector; Phe: phenylethylamine; POT: potentiometric detector; Prop: propylamine; Put: putrescine; Spm: spermine; Spmd: spermidine; Tea: trimethylamine; Tma: trimethylamine; Tryp: tryptamine; Tyr: tyramine; UV: ultraviolet detector; 5-HT, serotonin.

4.2.3.4. Analysis of tomato samples

The validated method was applied for the quantification of BAs in different tomato samples, including fresh tomato, canned chopped tomato, and canned pulp tomato (**Table 4.4**). Some representative chromatograms of tomato samples analysis are displayed in **Figure 4.7**.

For non-processed food, the presence of BAs above a certain level is indicative of undesired microbial activity (42, 67). Nonetheless, the total amine content found in fresh tomato (7.11 mg L^{-1}) is far from the toxic levels to human health, which is acceptable for ingestion. Besides, the most abundant amine found was putrescine, followed by tryptamine, phenylethylamine, and tyramine. Concerning processed food such as pulp tomato, 50% more BAs were found (7.69 mg L^{-1}) compared to the chopped tomato (5.12 mg L^{-1}). This result was expected once the former is more processed than the second. Moreover, all BAs were detected in the pulp tomato while spermine and phenylethylamine were not detected in the chopped tomato. Histamine, one of the most toxicological relevant BAs, was detected at higher levels in the pulp tomato but still lower than the regulated values (42).

Finally, the data obtained shows that none of the analyzed samples represent a possible risk for consumer health, although additional risk factors such as amine oxidase-inhibiting drugs, alcohol, and gastrointestinal diseases may enhance the toxicity of BAs (22).

Table 4.4 BAs content (mg L^{-1}) in tomato samples (mean value, *n*=*3*).

Sample	Eth	Put	Cad	His	Spmd	Spm	Tyr	Phe	Tryp	Total
Fresh	0.30	1.60	0.34	0.77	N.D	0.71	0.80	1.04	1.56	7.11
Chopped	0.34	0.92	0.20	0.18	1.07	N.D	1.40	N.D	1.00	5.12
Pulp	0.24	2.52	0.08	1.61	0.48	0.40	0.87	0.60	0.88	7.69

N.D. Not detected.

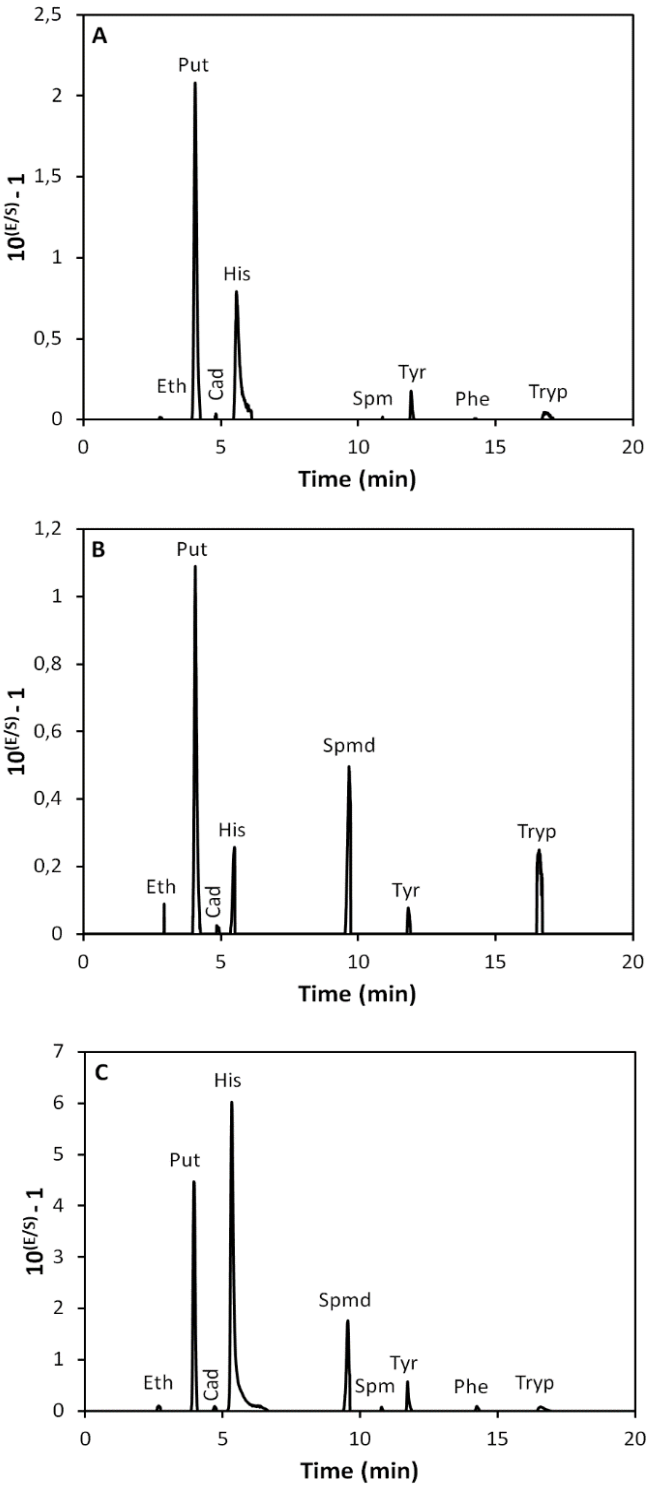

Figure 4.7 Individual chromatograms obtained with the proposed method for the analysis of tomato samples: **(A)** fresh tomato, **(B)** canned chopped tomato, and **(C)** canned pulp tomato. Chromatographic conditions: Gradient elution: solvent A – 5.0×10^{-3} mol L^{-1} SBS in 1.0×10^{-2} mol L^{-1} lithium formate buffer and solvent B – 1.0×10^{-3} mol L^{-1} lithium formate buffer: ACN (v/v, 90:10, pH=4). Column: Luna® Omega 5 µm Polar C18, 150 x 4.6 mm I.D. (Phenomenex). Flow-rate: 1.2 mL min^{-1}. Injection volume: 100 µL.

4.2.4. Conclusion

In this work, an amine-selective electrode based on CB[6] as an ionophore was successfully used as a detector in a fit-for-purpose HPLC procedure for the determination of BAs. The proposed method based on LC/potentiometry allowed the simultaneous detection of ten underivatized BAs namely: methylamine, ethylamine, putrescine, cadaverine, histamine, spermidine, spermine, tyramine, phenylethylamine, and tryptamine. The separation was successfully achieved using the SBS as an ion-pair agent. The optimal conditions allowed the separation of all BAs in less than 20 min with good peak resolution. The methodology was validated according to the ICH guidelines, showing LOD and LOQ values ranging from 0.03 to 0.20 mg L^{-1} and 0.09 to 0.61 mg L^{-1}, respectively. The great precision was characterized by the RSD% lower than 9.1% and 13.3% for the repeatability intra and inter-day, respectively. The analysis of spiked tomato samples showed recovery values from 85.8±0.0% to 108.5±0.0%, proving the great accuracy of the proposed method. The proposed system is thus an attractive and reliable approach for simple, fast, and greener determination of BAs in foodstuff.

4.2.5. References

1. Schultz FA, Mathis DE. Ion-selective electrode detector for ion-exchange liquid chromatography. Anal Chem. 1974;46(14):2253-5.

2. M. C. Franks DLP. A technique for the determination of trace anions by the combination of a potentiometric sensor and liquid chromatography, with particular reference to the determination of halides. Analyst. 1974;99(1181):503-14.

3. Haddad PR, Alexander PW, Trojanowicz M. High-performance liquid-chromatography of organic-acids with potentiometric detection using a metallic copper electrode. J Chromatogr. 1984;315(Dec):261-70.

4. Alexander PW, Haddad PR, Trojanowicz M. Potentiometric detection in ion chromatography using a metallic copper indicator electrode. Chromatographia. 1985;20(3):179-84.

5. Haddad PR, Alexander PW, Trojanowicz M. Ion chromatography of inorganic anions with potentiometric detection using a metallic copper electrode. J Chromatogr. 1985;321(2):363-74.

6. Chen ZL, Alexander PW, Haddad PR. Liquid chromatography of carboxylic acids using potentiometric detection with a tungsten oxide electrode. Anal Chim Acta. 1997;338(1-2):41-9.

7. Chen ZL, Alexander PW. Potentiometric detection of metal ions separated by liquid chromatography using a tungsten oxide electrode. Electroanalysis 1997;9(11):818-21.

8. Isildak I. Potentiometric detection of monovalent anions separated by ion chromatography using all solid-state contact PVC matrix membrane electrode. Chromatographia. 1999;49(5-6):338-42.

9. Lee DK, Lee HJ, Cha GS, Nam H, Paeng KJ. Ion chromatography detector based on solid-state ion-selective electrode array. J Chromatogr A. 2000;902(2):337-43.

10. Trojanowicz M. Recent developments in electrochemical flow detections--a review part II. Liquid chromatography. Anal Chim Acta. 2011;688(1):8-35.

11. Zielinska D, Poels I, Pietraszkiewicz M, Radecki J, Geise HJ, Nagels LJ. Potentiometric detection of organic acids in liquid chromatography using polymeric liquid membrane electrodes incorporating macrocyclic hexaamines. J Chromatogr A. 2001;915(1-2):25-33.

12. Bazylak G, Nagels LJ. Potentiometric detection of exogenic beta-adrenergic substances in liquid chromatography. J Chromatogr A. 2002;973(1-2):85-96.

13. Daems D, Van Camp G, Fernandez M, Guisez Y, Prinsen E, Nagels LJ. Use of potentiometric detection in (ultra) high performance liquid chromatography and modelling with adsorption/desorption binding kinetics. Anal Chim Acta. 2013;777:25-31.

14. Gil RL, Amorim CG, Montenegro M, Araujo AN. Potentiometric detection in liquid chromatographic systems: an overview. J Chromatogr A. 2019;1602:326-40.

15. Linares DM, Martín M, Ladero V, Alvarez MA, Fernández M. Biogenic amines in dairy products. Crit Rev Food Sci Nutr. 2011;51(7):691-703.

16. Ruiz-Capillas C, Jiménez-Colmenero F. Biogenic amines in meat and meat products. Crit Rev Food Sci Nutr. 2005;44(7-8):489-599.

17. Costantini A, Vaudano E, Pulcini L, Carafa T, Garcia-Moruno E. An overview on biogenic amines in wine. Beverages. 2019;5(1):19.

18. Kalač P, Šavel J, Křížek M, Pelikánová T, Prokopová M. Biogenic amine formation in bottled beer. Food Chem. 2002;79(4):431-4.

19. Barone C, Barebera M, Barone M, Parisi S, Zaccheo A. Chemical evolution of nitrogen-based compounds in mozzarella cheeses. Switzerland: Springer International Publishing; 2017.

20. Suzzi G, Torriani S. Editorial: Biogenic amines in foods. Front Microbiol. 2015;6(472).

21. Shalaby AR. Significance of biogenic amines to food safety and human health. Food Res Int. 1996;29(7):675-90.

22. Ruiz-Capillas C, Herrero AM. Impact of biogenic amines on food quality and safety. Foods. 2019;8(2).

23. Wei F, Xu X, Zhou G, Zhao G, Li C, Zhang Y, et al. Irradiated chinese rugao ham: changes in volatile N-nitrosamine, biogenic amine and residual nitrite during ripening and post-ripening. Meat Sci 2009;81(3):451-5.

24. Papageorgiou M, Lambropoulou D, Morrison C, Kłodzińska E, Namieśnik J, Płotka-Wasylka J. Literature update of analytical methods for biogenic amines determination in food and beverages. Trac-Trend Anal Chem. 2018;98:128-42.

25. Onal A, Tekkeli SE, Onal C. A review of the liquid chromatographic methods for the determination of biogenic amines in foods. Food Chem. 2013;138(1):509-15.

26. de Figueiredo TC, de Assis DCS, Menezes LDM, da Silva GR, Lanza IP, Heneine LGD, et al. HPLC–UV method validation for the identification and quantification of bioactive amines in commercial eggs. Talanta. 2015;142:240-5.

27. Zhang Y, Li Y, Zhu XJ, Li M, Chen HY, Lv XL, et al. Development and validation of a solid-phase extraction method coupled with HPLC-UV detection for the determination of biogenic amines in Chinese rice wine. Food Addit Contam Part A Chem Anal Control Expo Risk Assess. 2017;34(7):1172-83.

28. Angulo MF, Flores M, Aranda M, Henriquez-Aedo K. Fast and selective method for biogenic amines determination in wines and beers by ultra high-performance liquid chromatography. Food Chem. 2020;309:125689.

29. Ishimaru M, Muto Y, Nakayama A, Hatate H, Tanaka R. Determination of biogenic amines in fish meat and fermented foods using column-switching high-performance liquid chromatography with fluorescence detection. Food Anal Methods. 2019;12(1):166-75.

30. Liu SJ, Xu JJ, Ma CL, Guo CF. A comparative analysis of derivatization strategies for the determination of biogenic amines in sausage and cheese by HPLC. Food Chem. 2018;266:275-83.

31. Sagratini G, Fernández-Franzón M, De Berardinis F, Font G, Vittori S, Mañes J. Simultaneous determination of eight underivatised biogenic amines in fish by solid phase extraction and liquid chromatography–tandem mass spectrometry. Food Chem. 2012;132(1):537-43.

32. Ochi N. Simultaneous determination of eight underivatized biogenic amines in salted mackerel fillet by ion-pair solid-phase extraction and volatile ion-pair reversed-phase liquid chromatography-tandem mass spectrometry. J Chromatogr A. 2019;1601:115-20.

33. Sirocchi V, Caprioli G, Ricciutelli M, Vittori S, Sagratini G. Simultaneous determination of ten underivatized biogenic amines in meat by liquid chromatography-tandem mass spectrometry (HPLC-MS/MS). J Mass Spectrom. 2014;49(9):819-25.

34. Cinquina AL, Calì A, Longo F, De Santis L, Severoni A, Abballe F. Determination of biogenic amines in fish tissues by ion-exchange chromatography with conductivity detection. J Chromatogr A. 2004;1032(1-2):73-7.

35. Palermo C, Muscarella M, Nardiello D, Iammarino M, Centonze D. A multiresidual method based on ion-exchange chromatography with conductivity detection for the determination of biogenic amines in food and beverages. Anal Bioanal Chem. 2013;405(2-3):1015-23.

36. Favaro G, Pastore P, Saccani G, Cavalli S. Determination of biogenic amines in fresh and processed meat by ion chromatography and integrated pulsed amperometric detection on Au electrode. Food Chem. 2007;105(4):1652-8.

37. Rivoira L, Castiglioni M, Bruzzoniti MC. Chromatographic determination of biogenic amines in four typical Italian cheeses: correlations with processing and nutritional characteristics through a chemometric approach. J Sci Food Agric. 2019;99(11):4963-8.

38. Chen ZL, Alexander PW. Potentiometric detection of aliphatic amines by flow injection analysis and ion-interaction chromatography with a metallic copper electrode. J Chromatogr A. 1997;758(2):227-33.

39. Poels I, Nagels LJ. Potentiometric detection of amines in ion chromatography using macrocycle-based liquid membrane electrodes. Anal Chim Acta. 2001;440(2):89-98.

40. Aydin R, Asan A, Attar A, Isildak I. Trace analysis of amines in cheese serum with liquid chromatographic potentiometric detection by using amine-selective electrode. Arab J Chem. 2019;12(8):4533-40.

41. FDA. Fish and fishery products hazards and controls guidance. 4th ed. IFAS - Extension Bookstor: FDA; 2019.

42. EFSA panel on biological hazards (BIOHAZ), scientific opinion on risk based control of biogenic amine formation in fermented foods. EFSA Journal. 2011;9(10):93.

43. Lagona J, Mukhopadhyay P, Chakrabarti S, Isaacs L. The Cucurbit[n]uril Family. Angew Chem Int Ed. 2005;44(31):4844-70.

44. Zhang S, Grimm L, Miskolczy Z, Biczók L, Biedermann F, Nau WM. Binding affinities of cucurbit[n]urils with cations. Chem Commun. 2019;55(94):14131-4.

45. Barrow SJ, Kasera S, Rowland MJ, del Barrio J, Scherman OA. Cucurbituril-based molecular recognition. Chem Rev. 2015;115(22):12320-406.

46. Pereira AR, Araujo AN, Montenegro M, Amorim C. A simpler potentiometric method for histamine assessment in blood sera. Anal Bioanal Chem. 2020;412(15):3629-37.

47. Waters. Taking the complexity out of SPE method development 2017 [Available from: http://www.waters.com/webassets/cms/library/docs/720005685en.pdf.

48. Amorim CG, Araujo AN, Montenegro MC. Exploiting sequential injection analysis with lab-on-valve and miniaturized potentiometric detection epinephrine determination in pharmaceutical products. Talanta. 2007;72(4):1255-60.

49. Haddad PR. Chapter 3 Ion-exchange stationary phases for ion chromatography. In: Haddad PR, editors. Journal of Chromatography Library. Volume 46. Amsterdam: Elsevier; 1990. p. 29-77.

50. Ståhlberg J. Chromatography: liquid | Ion pair liquid chromatography. In: Poole C, Cooke M, Wilson ID, editors. Encyclopedia of separation science. 1st. ed. Oxford: Academic Press; 2000. p. 676-84.

51. Phenomenex. Technical tip: ion-pairing agents 2015 [Available from: https://phenomenex.blog/2015/10/18/technical-tip-ion-pairing-agents/].

52. Arlorio M, Coïsson JD, Martelli A. Ion-pair HPLC determination of biogenic amines and precursor aminoacids. Application of a method based on simultaneous use of heptanesulphonate and octylamine to some foods. Chromatographia. 1998;48(11):763-9.

53. Sun J, Guo HX, Semin D, Cheetham J. Direct separation and detection of biogenic amines by ion-pair liquid chromatography with chemiluminescent nitrogen detector. J Chromatogr A. 2011;1218(29):4689-97.

54. Chemical and physical properties [Available from: https://pubchem.ncbi.nlm.nih.gov].

55. Bartha Á, Vigh G, Billiet H, Galan Ld. Effect of the type of ion-pairing reagent in reversed-phase ion-pair chromatograph. Chromatographia. 1985;20(10):587-90.

56. Company S. Switching the mobile phase from acetonitrile to methanol [Available from: https://www.shimadzu.com/an/service-support/technical-support/analysis-basics/tips/acetonitrile/2-1.html].

57. Poole CF, Lenca N. Reversed-phase liquid chromatography. In: Fanali S, Haddad PR, Poole CF, Riekkola M-L, editors. Liquid Chromatography. 2nd ed. Amsterdam: Elsevier 2017. p. 91-123.

58. ICH. ICH harmonised tripartite guideline: Validation of analytical procedures: text and methodology Q2 (R1) ICH, Geneva, Switzerland, 2005 [Available from: https://www.ich.org/page/quality-guidelines].

59. De Wael K, Daems D, Van Camp G, Nagels LJ. Use of potentiometric sensors to study (bio)molecular interactions. Anal Chem. 2012;84(11):4921-7.

60. Daems D, van Nuijs AL, Covaci A, Hamidi-Asl E, Van Camp G, Nagels LJ. Potentiometric detection in UPLC as an easy alternative to determine cocaine in biological samples. Biomed Chromatogr. 2015;29(7):1124-9.

61. Milheiro J, Ferreira LC, Filipe-Ribeiro L, Cosme F, Nunes FM. A simple dispersive solid phase extraction clean-up/concentration method for selective and sensitive quantification of biogenic amines in wines using benzoyl chloride derivatisation. Food Chem. 2019;274:110-7.

62. Li J, Guan RF, Wei XM, Chen JC, Hu YQ, Liu DH, et al. Detection of ten biogenic amines in Chinese commercial soybean paste by HPLC. Int J Food Prop. 2018;21(1):1344-50.

63. Ordonez JL, Callejon RM, Troncoso AM, Garcia-Parrilla MC. Evaluation of biogenic amines profile in opened wine bottles: Effect of storage conditions. J Food Compost Anal. 2017;63:139-47.

64. Wu H, Li G, Liu S, Ji Z, Zhang Q, Hu N, et al. Simultaneous determination of seven biogenic amines in foodstuff samples using one-step fluorescence labeling and dispersive liquid–liquid microextraction followed by HPLC-FLD and method optimization using response surface methodology. Food Anal Methods. 2015;8(3):685-95.

65. Li G, Dong L, Wang A, Wang W, Hu N, You J. Simultaneous determination of biogenic amines and estrogens in foodstuff by an improved HPLC method combining with fluorescence labeling. LWT - Food Sci Technol. 2014;55(1):355-61.

66. Nalazek-Rudnicka K, Wasik A. Development and validation of an LC-MS/MS method for the determination of biogenic amines in wines and beers. Monatshefte Fur Chemie. 2017;148(9):1685-96.

67. Chiacchierini E, Restuccia D, Vinci G. Evaluation of two different extraction methods for chromatographic determination of bioactive amines in tomato products. Talanta. 2006;69(3):548-55.

4.2.6. Supplementary material

Results and discussion

Optimization of the hydrodynamic conditions

The detector performance can be markedly affected by the hydrodynamic conditions such as the flow rate and the sample injection volume due to the nature of the potentiometric response (1). On the chromatographic side, the flow rate of the mobile phase and the injection volume may also affect both k and α, and lastly, the resolution and the chromatographic run time (2).

Accordingly, the effect of different flow rates (0.8, 1.0, 1.2, 1.4, and 1.6 mL min^{-1}) was first examined. The obtained k values for methylamine, histamine, spermidine, tyramine, and spermine were quite similar in all the tested flow rates but an increase was observed for phenylethylamine and tryptamine (**Figure S1**). When the flow rate changed from 0.8 to 1.6 mL min^{-1}, the k values increased from 7.5 to 12.8 and 8.5 to 13.8, respectively, which indicates higher retention of these analytes. In contrast, the low k values obtained for methylamine and histamine (<1) indicate a poor interaction with the stationary phase, which can hinder their determination in real samples. Regarding the effect on the detector performance, higher flow rates led to an increase in the peak height for phenylethylamine and tryptamine but a decrease for the others. These findings can be explained by the kinetic response of the potentiometric detector, governed by the lipophilicity of the amines (XLogP3). While lipophilic amines are easily extracted into the membrane, decreasing the response time, hydrophilic amines need more time to interact with the membrane and so the higher flow rates affect negatively the response and decrease the peak heights. For this reason, it was not possible to detect the hydrophilic amines at concentrations below 1.0×10^{-5} mol L^{-1}. Therefore, a flow rate of 1.2 mL min^{-1} showed to be the most suitable condition regarding the separation of analytes as well as the detector performance.

The effect of the injection volume (20, 50, and 100 µL) was then investigated by the injection of standard mixtures of BAs at different concentration levels. An increase of the k values was observed for all amines with the increase of the injection volume, especially from 20 to 100 µL. Additionally, higher peak heights were noticed in all analyzed concentrations with the 100 µL volume and hence it was maintained to obtain a better detection limit (**Figure S2**).

Ionic strength of mobile phase

The ionic strength of the mobile phase has an important effect in the interaction of the ion-pair agent with the carbon chains of the column and lastly, in the retention parameters of the analytes. As shown in **Figure S3**, the increase of lithium formate buffer concentration, from 1.0×10^{-3} to 1.0×10^{-2} mol L^{-1}, led to a decrease of k values for most of the BAs, which is explained by the decrease of the ion-pair concentration at the column surface (3). This behavior was mainly observed for hydrophilic amines but a slight increase of k values was noticed for phenylethylamine and tryptamine. Attending to these differences, gradient elution with different ionic strengths was considered to attain the separation in the shorter running time possible. The buffer solution concentration of 1.0×10^{-2} mol L^{-1} for solvent A and 1.0×10^{-3} mol L^{-1} for solvent B enabled the retention and potentiometric detection of nine BAs (putrescine and cadaverine were co-eluted with histamine) in less than 12 min. Nonetheless, further studies were still required to obtain the complete resolution of all amines and thus the replacement of ACN for MeOH was considered (4).

Figures

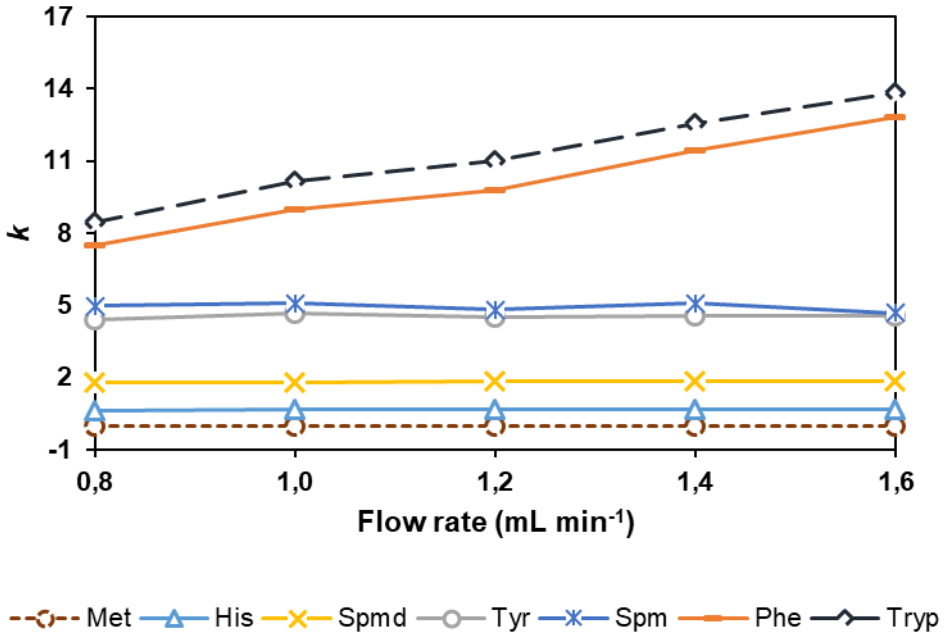

Figure S1 Retention factors for a standard mixture of biogenic amines as a function of the mobile phase flow rate.

Injected concentration: 1.0×10^{-4} mol L^{-1}. Gradient elution: mobile phase A – 5.0×10^{-3} mol L^{-1} SBS in 1.0×10^{-2} mol L^{-1} lithium formate buffer: ACN (v/v, 97.5:2.5, pH=4) and mobile phase B – 1.0×10^{-2} mol L^{-1} lithium formate buffer: ACN (v/v, 90:10, pH=4). Column: Luna® 5 µm C8(2), 150 x 4.6 mm I.D., (Phenomenex). Injection volume: 100 µL.

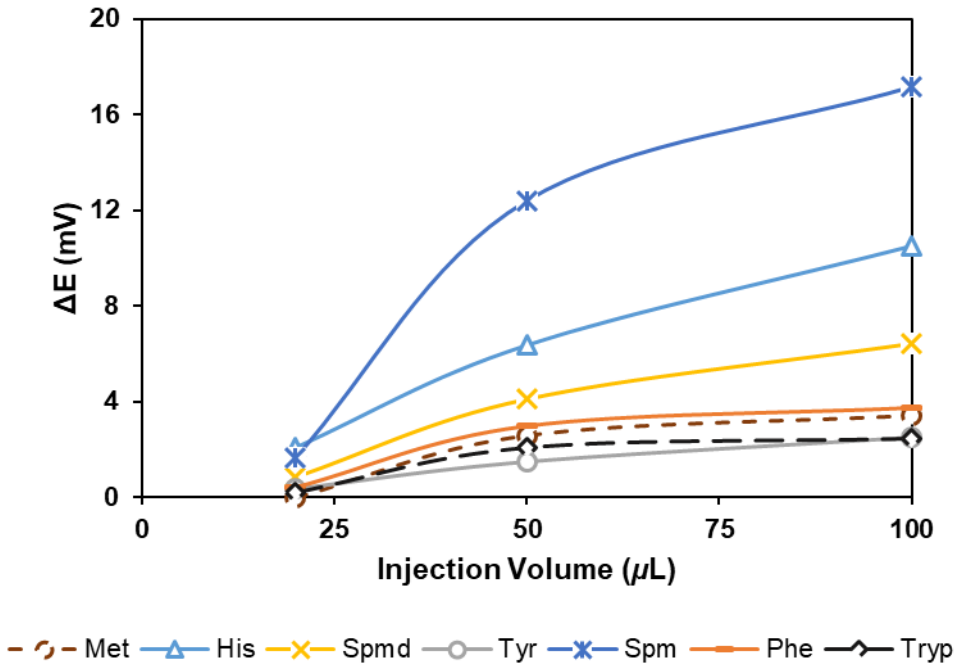

Figure S2 Detector performance for a standard mixture of biogenic amines as a function of the injection volume.

Injected concentration: 1.0×10^{-5} mol L^{-1}. Gradient elution: mobile phase A – 5.0×10^{-3} mol L^{-1} SBS in 1.0×10^{-2} mol L^{-1} lithium formate buffer: ACN (v/v, 97.5:2.5, pH=4) and mobile phase B – 1.0×10^{-2} mol L^{-1} lithium formate buffer: ACN (v/v, 90:10, pH=4). Column: Luna® 5 µm C8(2), 150 x 4.6 mm I.D. (Phenomenex). Flow rate: 1.2 mL min^{-1}.

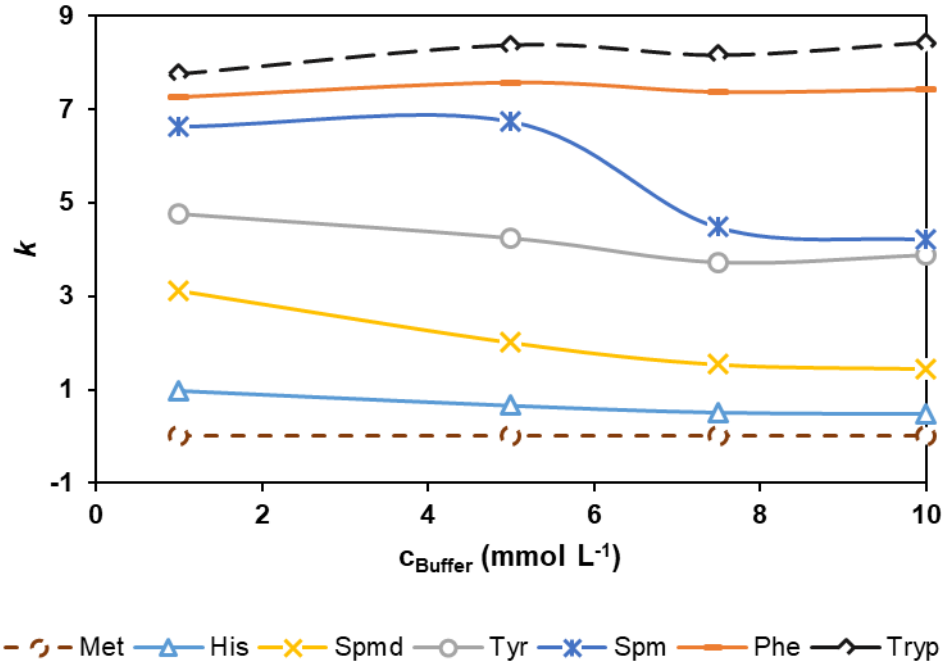

Figure S3 Retention factors of biogenic amines as a function of the ionic buffer concentration.

Injected concentration: 1.0×10^{-4} mol L^{-1}; Gradient elution: solvent A – 5.0×10^{-3} mol L^{-1} SBS in different lithium formate buffer concentration: ACN (v/v, 97.5:2.5, pH=4) and solvent B – different lithium formate buffer concentration: ACN (v/v, 90:10, pH=4). Column: Luna® 5 µm C8(2), 150 x 4.6 mm I.D. (Phenomenex). Flow rate: 1.2 mL min^{-1}. Injection volume: 100 µL.

Tables

Table S1 Summary of the analysis of spiked tomato samples.

		Sample					
Analyte	**Spiked level (µmol L^{-1})**	**Chopped Tomato**	**RSD%**	**Pulp Tomato**	**RSD%**	**Fresh Tomato**	**RSD%**
Eth	3	99.3 ± 0.0	0.3	95.4 ± 0.0	2.5	98.7 ± 0.0	0.9
	10	85.8 ± 0.0	2.8	93.2 ± 0.0	1.6	96.7 ± 0.0	4.3
	30	89.5 ± 0.0	4.4	100.3 ± 0.0	2.8	102.0 ± 0.0	0.8
Put	3	95.8 ± 0.1	9.3	87.0 ± 0.0	1.2	105.9 ± 0.0	1.7
	10	86.3 ± 0.0	3.0	92.6 ± 0.1	8.2	93.2 ± 0.0	4.7
	30	91.1 ± 0.1	5.5	86.6 ± 0.0	3.0	98.9 ± 0.0	2.3
Cad	3	106.7 ± 0.0	4.5	88.2 ± 0.0	3.1	86.0 ± 0.0	4.6
	10	93.1 ± 0.1	7.5	86.7 ± 0.0	2.1	95.4 ± 0.1	5.7
	30	99.9 ± 0.1	8.2	90.8 ± 0.0	4.4	97.6 ± 0.0	2.3
His	3	98.3 ± 0.0	5.0	91.6 ± 0.0	3.1	108.5 ± 0.0	1.5
	10	92.6 ± 0.0	5.3	88.1 ± 0.0	4.9	97.1 ± 0.1	7.3
	30	86.5 ± 0.0	3.3	89.5 ± 0.0	4.6	95.1 ± 0.0	3.6
Spmd	3	93.9 ± 0.0	2.9	95.9 ± 0.0	2.8	95.1 ± 0.0	0.6
	10	93.1 ± 0.1	5.6	87.6 ± 0.1	6.9	90.6 ± 0.1	8.6
	30	100.3 ± 0.1	6.9	87.1 ± 0.0	4.9	87.5 ± 0.0	3.7
Spm	3	100.5 ± 0.0	1.2	97.6 ± 0.0	1.1	99.1 ± 0.0	0.4
	10	102.7 ± 0.0	4.3	101.2 ± 0.0	2.2	104.4 ± 0.1	6.2
	30	98.6 ± 0.1	2.8	106.0 ± 0.0	1.7	102.7 ± 0.0	0.9
Tyr	3	85.6 ± 0.0	0.9	98.2 ± 0.0	3.6	98.9 ± 0.0	0.2
	10	87.7 ± 0.0	5.4	86.6 ± 0.0	1.7	90.4 ± 0.1	9.4
	30	89.6 ± 0.1	8.7	89.5 ± 0.0	2.4	88.4 ± 0.0	4.4
Phe	3	97.2 ± 0.0	1.0	100.0 ± 0.0	0.7	99.5 ± 0.0	0.2
	10	92.8 ± 0.0	4.5	86.6 ± 0.0	1.7	93.5 ± 0.0	1.2
	30	91.2 ± 0.0	4.5	86.2 ± 0.0	3.6	98.6 ± 0.0	4.5
Tryp	3	86.3 ± 0.0	2.3	98.4 ± 0.0	0.5	106.8 ± 0.0	1.1
	10	102.4 ± 0.1	5.7	102.7 ± 96.6	3.2	98.8 ± 0.0	3.8
	30	88.3 ± 0.0	3.8	96.6 ± 0.1	6.2	87.5 ± 0.0	1.4

An interesting observation relies on the higher values of recovery obtained for putrescine and histamine in fresh tomato compared to chopped and pulp tomato. Accordingly, a possible explanation may be related to the fact that while fresh tomatoes were directed used without any food processing, the canned chopped and pulp tomato were processed. These different treatments certainly contribute for change their chemical composition, affecting

consequently the recovery values since they are calculated based on the addition of non-degraded analyte.

References

1. Toth K, Stulik K, Kutner W, Feher Z, Lindner E. Electrochemical detection in liquid flow analytical techniques: characterization and classification - (IUPAC Technical Report). Pure Appl Chem. 2004;76(6):1119-38.

2. Samuelsson J, Edström L, Forssén P, Fornstedt T. Injection profiles in liquid chromatography. I. A fundamental investigation. J Chromatogr A. 2010;1217(26):4306-12.

3. Ståhlberg J. Chromatography: liquid | Ion pair liquid chromatography. In: Poole C, Cooke M, Wilson ID, editors. Encyclopedia of separation science. 1st ed. Oxford: Academic Press; 2000. p. 676-84.

4. Hopkins T. The role of methanol and acetonitrile as organic modifiers in reversed-phase liquid chromatography. Chromatography today. 2019;12(1):24-6.

4.3. HPLC-potentiometric method for determination of biogenic amines in alcoholic beverages: a reliable approach for food quality control

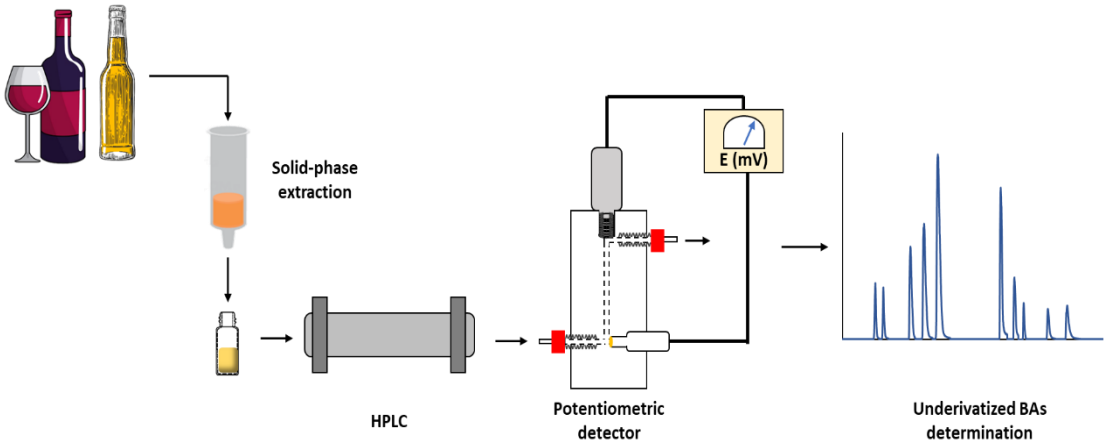

Section 4.3 describes the improvement of the analytical performance of the previous HPLC-Potentiometric method for the determination of biogenic amines and its application in the analysis of alcoholic beverages[3].

[3] This is a partial transcription of the article *Renato L. Gil, Célia G. Amorim, Maria C.B.S.M. Montenegro, Alberto N. Araújo; HPLC-potentiometric method for determination of biogenic amines in alcoholic beverages: A reliable approach for food quality control; Food chemistry, 2022, 372, 131288; doi: 10.1016/j.foodchem.2021.131288*;

4.3.1. Introduction

Biogenic amines (BAs) comprehend a special group of low molecular weight compounds with biological activity. Further insight on chemical structure subdivides them between aliphatic (e.g. cadaverine – Cad, ethylamine – Eth, putrescine – Put, methylamine – Met, spermine – Spm, and spermidine – Spmd), aromatic (e.g. tyramine – Tyr and phenylethylamine – Phe), and heterocyclic amines (e.g. histamine – His and tryptamine – Tryp). While some BAs play important roles in human physiology, others are considered as metabolic by-products found essentially in foodstuffs such as cheese, wine, beer, chocolate, vegetables, fishery products, and aged meat (1). That presence results from bacteria thriving along with food processing and storage, which convert free amino acids into BAs via decarboxylase or deiminase activities (2). In turn, ingestion of BAs at determined concentrations might trigger toxic symptoms such as headache, hypertension, diarrhea, nausea, red rash, and localized inflammation (1, 3). Effects can be even more harmful whether the catabolic activity of monoamine oxidase and diamine oxidase enzymes present in the human body is somehow compromised. For instance, the consumption of ethanol (e.g. alcoholic beverages), tobacco, and monoamine oxidase-inhibiting drugs (e.g. antidepressants) increase an individual's susceptibility (4). BAs presence in foodstuff has become of concern to producers, consumers, and enforcement authorities for quality control and food safety (5). These are hence compelling arguments justifying the detection and quantification of BAs in fermented food products.

Several analytical methods for BAs determination have been reported, mostly based on HPLC coupled to either UV-Vis (6, 7) or fluorimetric detection (8-10). Chemical derivatization involving the amine group is usually performed to gain selectivity and sensitivity, though using toxic reagents such as dansyl chloride, benzoyl chloride, or o-phthalaldehyde (11). Alternatively, direct BAs analysis is feasible by HPLC-MS/MS tandem technique operated by skilled technicians but at a high-cost expense (12, 13). Electroanalytical detectors based on amperometry (14, 15) were also proposed, though needing post-column pH adjustment with hydroxide. At alkaline pH, compounds bearing an N atom with unshared pair of electrons such as with BAs can be catalytically adsorbed on the surface of the electrodes poised at positive potentials, stoichiometrically oxidized, and desorbed (14). In the case of conductimetric detection (16, 17), a suppressor system is necessary for the amine determination at low levels, affecting the analytical signal reproducibility. Therefore, new analytical methodologies for simple, sensitive, and fast determination of BAs need to be developed and validated.

Potentiometric ion-selective electrodes (ISEs) have great potential as detection systems because of their versatility of use, cost-effectiveness, and miniaturization ability. A pioneering work revealed the ability of solid-contact electrodes based on macrocycle molecules to detect organic amines by cation-exchange chromatography (18). This aspect was put forward in the determination of aliphatic amines in cheese serum by ion-interaction chromatography, resorting to a solid-contact ISE based on dibenzo-18-crown-6 ether (19). Recently, the determination of BAs in tomato samples by ion-pair chromatography coupled to a solid-contact amine-selective electrode based on cucurbit[6]uril as an ionophore was proposed in a companion paper. Despite their powerful features, potentiometric sensors are still not viewed as routine detectors for HPLC and thus researchers should put more effort to demonstrate the competitiveness with other detectors (20). The trade-off is the achievement of fast, friendly, and reliable procedures, where chemical derivatization steps are eliminated and simple, low-cost and sensitive electrodes are easily prepared to use.

This work intends to determine a greater number of amines, improve the analytical performance of our previously reported potentiometric detector (21), and verify the usefulness of the method for controlling alcoholic beverages. To achieve this goal, the separation and detection conditions of underivatized BAs were optimized concerning the mobile phase and sensing membrane composition. The final methodology was then validated following the Eurachem and International Conference on Harmonization guidelines.

4.3.2. Materials and methods

4.3.2.1. Chemicals and reagents

Methylamine hydrochloride (Met, ≥98%, ref. M0505), ethylamine hydrochloride (Eth, 98%, ref. 232831), putrescine dihydrochloride (Put, ≥97%, P5780), cadaverine dihydrochloride (Cad, 95%, D22606), histamine dihydrochloride (His, ≥99%, H7250), spermidine trihydrochloride (Spmd, ≥98%, ref. S2501), spermine tetrahydrochloride (Spm, ≥99%, ref. 85610), tyramine hydrochloride (Tyr, ≥98%, ref. T2879), 2-phenylethylamine hydrochloride (Phe, ≥98%, ref. P6513), tryptamine hydrochloride (Tryp, ≥99%, ref. 246557), lithium chloride (LiCl, ref. 310468), lithium hydroxide (LiOH, ref. 442410), ammonium hydroxide solution (NH_4OH, ref. 320145), and butane-1-sulfonic acid sodium salt (SBS, ref. 1183030025) were purchased from Sigma-Aldrich (Algés, Portugal). Formic acid (HCOOH, ≥98%, ref. 06450), and glacial acetic acid (CH_3COOH, ref. 33209) were from Fluka (Porto

Salvo, Portugal). Acetonitrile (ACN, ref. 1.00029.2500P) and methanol (MetOH, ref. 1.06035.2500P), both HPLC Gradient grade, were acquired from VWR (Amadora, Portugal). Ultra-pure water with conductivity <0.055 µS cm^{-1} was used (Heal Force, Shangai China).

For the solid conductive support preparation, graphite powder (<50µm, ref. 1.04206) and Araldite M (ref. 10951) were purchased from Sigma-Aldrich (Algés, Portugal) whereas the hardener Ren HY 5162 (ref. 068620205) was from Huntsman (Barcelona, Spain). For the amine-selective membrane, high molecular weight polyvinyl chloride (PVC, ref. 81392), o-nitrophenyloctyl ether (o-NPOE, ref. 365130), cucurbit[6]uril hydrate (CB[6], ref. 94544), potassium tetrakis(p-chlorophenyl)borate (TCPB, ref. 60591), multi-walled carbon nanotubes (MWCNTs, 110-170nm x 5-9 µm, ref. 659258), and tetrahydrofuran (THF, ref. 186562) were obtained from Sigma-Aldrich (Algés, Portugal).

4.3.2.2. Mobile phase and standard solutions

Lithium formate buffer (pH=4) and acetic acid solutions at $1.0x10^{-2}$ mol L^{-1} were weekly prepared in ultra-pure water. The solvent A of the mobile phase was prepared by dissolving an accurately weighed amount of SBS powder in the acetic acid solution to obtain a final concentration of $5.0x10^{-3}$ mol L^{-1}. Besides, solvent B was prepared by firstly diluting the acetic solution in ultra-pure water for a concentration of $1.0x10^{-3}$ mol L^{-1}, which was then mixed with ACN in the proportion of 90:10 (v/v), respectively. Mixed cellulose esters membrane, hydrophilic, 0.22 µm (ref. GSWP04700) from Millipore (Algés, Portugal) were used to filter the mobile phases. Stock solutions of amines were prepared in the acetic acid solution for a concentration of $1.0x10^{-2}$ mol L^{-1} and stored in the fridge at 4 °C. Dilutions of the stock solutions in solvent A of the mobile phase were performed extemporaneously before injection.

4.3.2.3. Sample preparation

Alcoholic beverage samples were purchased from the local market, which includes beer, white and red wine. All samples were firstly degassed in an ultrasonic bath for 20 min. Then, 10 mL aliquots of each sample were filtered through a 0.2 µm Nylon syringe filter (ref. 28145-487, VWR, Amadora, Portugal) and stored at 4° C (no more than one week). Before analysis, further cleanup was proceeded by solid-phase extraction (SPE) using cartridges Water Oasis PRIME MCX (3cc, 60mg, ref. 186008918, Waters, Lisboa, Portugal) according

to Y. Zhang et al. (22). About 1.0 mL of each sample was loaded in the cartridge, afterward washed twice with 1.0 mL of ultra-pure water. The compounds of interest were quantitatively recovered after elution in triplicate with 1.0 mL of a MetOH: NH_4OH solution (95:5, v/v). The eluate was dried under N_2 flow and finally reconstituted in 1.0 mL of the initial mobile phase. All solutions were filtered before injection in the chromatographic system.

4.3.2.4. Apparatus

The HPLC-potentiometry instrumentation used for the determination of BAs is depicted in **Figure 4.8**. The HPLC system comprised a Waters 600 Solvent Delivery Pump (Waters Liquid Chromatography) and a Rheodyne 7725i six-port external sample injector (IDEX Health & Science, LLC) where a sample loop of 100 µL was mounted.

Potential measurements were carried out using a 6-Channel Precision Electrochemistry EMF Interface (LawsonLabs, Inc. USA). The potentiometric signals vs. time (i.e. chromatograms) were recorded by the graphics software from LawsonLabs, Inc. USA. Hand-made miniaturized indicator electrodes (ISEs) and a commercial miniaturized reference electrode filled with a 3.0 mol L^{-1} KCl (model 6.0727.0 0 0, Metrohm, Switzerland) were used in the HPLC measurements. A double-junction Ag/AgCl reference electrode (Orion 90-02-00, Thermo Scientific) with its external compartment filled with a $1.0x10^{-2}$ mol L^{-1} LiCl solution was used in the measurements under static conditions.

4.3.2.5. Chromatographic conditions

The separation was carried out on Luna Omega Polar C18 column (150 x 4.6 mm, 5 µm, from Phenomenex) using a mobile phase composed of solvent A ($5.0x10^{-3}$ mol L^{-1} SBS in $1.0x10^{-2}$ mol L^{-1} CH_3COOH, pH=2.5) and solvent B (10% ACN/$1.0x10^{-3}$ mol L^{-1} CH_3COOH, v/v, pH=2.5). The gradient program applied was as follows: 0–5.0min, 0% B; 5.0–10.0min, 0–100% B, linear increase; 10.0–17.0min, 100% B; 17.0–17.5min, 100–0% B; 17.5–25.0min 0% B. The flow rate was kept at 1.2 mL min^{-1}, and the LC column was maintained at controlled room temperature (±2ºC).

4.3.2.6. Detection cell

A low-dead volume wall-jet flow-cell was used, holding both the indicator and the reference electrode (**Figure 4.8**). A brief description of the flow cell can be found elsewhere (21).

The fabrication of the miniaturized potentiometric ISEs was based on a procedure described elsewhere (23) and started with preparing an optimized graphite composite to reduce the electrical resistance and improve the electrode characteristics. Firstly, a non-conductive epoxy resin was prepared by mixing Araldite-M and the hardener HY in a 1:0.4 weight ratio. Then, this mixture was blended with graphite powder in a 1.85:1 weight ratio (graphite:epoxy resin) to obtain a paste with appropriate homogeneity and consistency. The resulting conductive composite was inserted at the end of a polytetrafluoroethylene (PTFE) rod (1.6 mm I.D. x 4.0 mm O.D. x 15 mm length), whereas an exposed copper wire of an electrically shielded cable was inserted from the opposite ending to establish the electrical contact. The electrodes were left to dry over 24h at room temperature. Finally, the surface was polished with sandpaper P120 until a specular gloss was obtained.

The amine-selective membrane consisted of 1.0% (w/w) of CB[6] as ionophore, 0.3% (w/w) of TCPB as ionic additive, 2.0% (w/w) of MWCNTs as ion-to-electron transducer, and 66.7% (w/w) of o-NPOE as plasticizer of PVC 30.0% (w/w). The membrane cocktail was prepared by accurately weighing amounts of CB[6], TCPB, MWCNTs, oNPOE, and PVC into a glass vial. A 300 mg mass of the mixture was dissolved in 3.0 mL of THF. The use of CB[6] as an ionophore is justified by its ability to form inclusion complexes with BAs (21). However, as reported by other authors (24), CB[6] also forms inclusion complexes with inorganic cations, namely the ones present in the mobile phase. In an attempt to minimize the effect of those ions a second membrane cocktail only based on TCPB (1.0% w/w) as electroactive species was prepared.

Finally, the corresponding cocktail was applied onto the conductive surface of the miniaturized electrodes by drop-coating 5 µL with an automatic pipette. After each application, the solvent was allowed to evaporate for 20 min at room temperature. The procedure was repeated three times and the ISEs were left to dry for at least 2 h before conditioning in the solvent A of the mobile phase. When not in use, each electrode was kept immersed in the conditioning solution.

In HPLC measurements, the electrode was firstly inserted in the wall-jet flow-cell and conditioned with the running mobile phase until a stable baseline was observed (~30 min).

To facilitate the comparison between chromatograms, the sensor response was offset to 0 mV before injections.

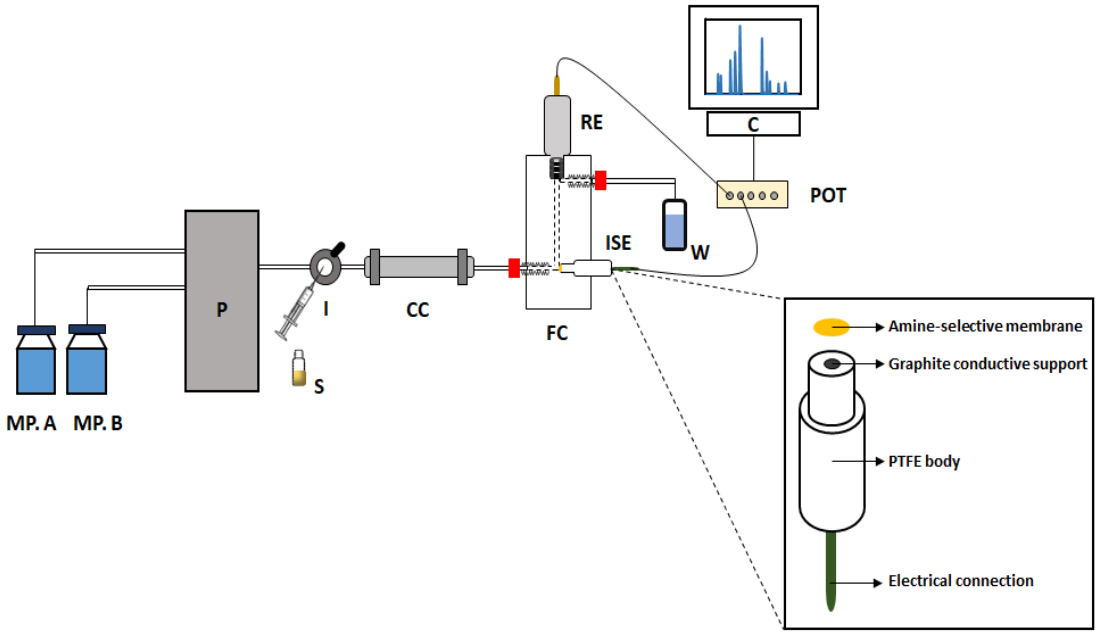

Figure 4.8 Illustration of the HPLC-potentiometry setup for determination of BAs. MP – Mobile phase (A and B); P – HPLC pump; I – Injection valve; S – sample; CC – Chromatographic column; FC – Potentiometric flow-cell; ISE – Ion-selective electrode; RE – Reference electrode; POT – Potentiometer; C – Computer; W – Waste. Inset: Miniaturized ISE based on graphite conductive substrate prepared by the drop-casting of an amine-selective membrane.

4.3.2.7. Method validation

The proposed method was validated in compliance with the Eurachem (25) and International Conference on Harmonization (26) guidelines. The linearity and linear range, limits of detection (LOD) and quantification (LOQ), precision, and accuracy were evaluated. The chromatographic parameters, namely retention time, peak symmetry, number of theoretical plates, capacity factor, selectivity factor, and peak resolution were calculated using standard formulas about the liquid chromatographic process (27).

The linearity and linear range were assessed from calibration curves obtained after the triplicate injection of standard solutions of BAs covering the concentration range of $1.0\text{x}10^{-7}$ – $1.0\text{x}10^{-4}$ mol L^{-1} (*n=8*). Firstly, the potential variation ($E(mV)$) as a function of the logarithm of the concentration of the BAs was fitted by the Nikolsky-Eisenman (NE) type function (see equation 2). Secondly, the potentiometric signal was converted in a

transformed response $tR = 10^{E/S} - 1$ (28), where E is the potentiometric signal in mV and S is the slope of the NE equation, which was plotted against the BAs concentration. The coefficients of determination (R^2) were calculated from the intra-assay calibration curves.

The LOD and LOQ were defined as three and ten times the signal-to-noise ratio, respectively, obtained from the injection of standard solutions of BAs covering the calibration range.

The precision was assessed through repeatability and intermediate precision of the potentiometric signal and retention time. The repeatability was determined by triplicate analysis of standard solutions of BAs at three concentration levels ($3.0x10^{-6}$, $1.0x10^{-5}$, and $3.0x10^{-5}$ mol L^{-1}) performed on the same day, whereas the intermediate precision was evaluated by quintuplicate analysis at one concentration level ($1.0x10^{-5}$ mol L^{-1}) performed on consecutive days. The inter-electrode reproducibility was evaluated by the triplicate analysis of standard solutions of BAs at three concentration levels ($1.0x10^{-6}$, $1.0x10^{-5}$, and $1.0x10^{-4}$ mol L^{-1}) using three different sensor units. The obtained results were expressed as relative standard deviation (RSD%).

The accuracy was determined through the triplicate analysis of spiked samples at three fortification levels ($1.0x10^{-6}$, $3.0x10^{-6}$, and $1.0x10^{-5}$ mol L^{-1}) before and after the sample preparation procedure. The results were expressed as recovery values accordingly (29):

$$Recovery\ (\%) = \frac{BA_{Recovered}}{BA_{Post\ spiked}}\ x\ 100\% \qquad (1)$$

in which $BA_{Recovered}$ is the concentration of BAs measured in the extracts obtained from the samples spiked before the SPE and $BA_{Post\ spiked}$ is the concentration of BAs measured in the extracts spiked after the SPE.

4.3.3. Results and discussion

4.3.3.1. Potentiometric detector performance in static conditions

Nanomaterials, namely carbon nanotubes, have been widely used for their unique properties such as large surface area/volume ratio, mechanical strength, and excellent electrical conductivity (30). Their use in sensors has been associated with gains in sensitivity, limits of detection, and electron transfer kinetics (30, 31). In this context, the sensing membrane previously reported by our group (21) was enriched with 2.0% (w/w) of MWCNTs to improve the sensor characteristics. The potentiometric response was

evaluated for ten BAs using the mobile phase with lithium formate buffer as background electrolyte to mimic the detection conditions in HPLC. The BAs were divided according to the number of charges into monoamines (Eth, Met, Phe, Tryp, and Tyr), diamines (Cad, His, and Put), and polyamines (Spm and Spmd). The potentiometric performance characteristics for each amine are summarized in **Table 4.5**. For all assayed amines the calibration curves (**Figure S4)** follow the NE equation, providing linear response ranges from $1.0x10^{-5}$ to $1.0x10^{-2}$ mol L^{-1} with R^2 higher than 0.9950. Noteworthy, the analytical ranges attained were wider for His and Tyr, over four orders of magnitude. Practical detection limits (PDL), calculated as the concentration at the point of intersection of the extrapolated lines of the nonresponsive and linear-response segments of the calibration plot (32), were also diverse and ranged from $(4.3\pm1.8)x10^{-7}$ to $(7.4\pm0.4)x10^{-5}$ mol L^{-1}, respectively for Phe and Met. The slope values varied according to the number of amine groups in each BA. For instance, Eth is a mono-charged cation while His is a double-charged one and thus, according to the NE equation, the slope should be theoretically equal to 59 and 30 mV dec^{-1} at 25ºC, respectively. Nonetheless, 52.2 and 28.0 mV dec^{-1} were attained for Eth and His with the proposed detector, respectively.

Table 4.5 Summary of the potentiometric response characteristics of the proposed detector for BAs under static conditions.

Amine	Slope (mV dec^{-1})	R^2	LLLR (mol L^{-1})	PDL (mol L^{-1})	Linear Range (mol L^{-1})
Met	47.3±0.3	0.9962±0.0008	$1.0x10^{-4}$	$(7.4\pm0.4)x10^{-5}$	$1.0x10^{-4}$ – $1.0x10^{-2}$
Eth	52.2±0.2	0.9988±0.0001	$5.0x10^{-5}$	$(2.0\pm0.4)x10^{-5}$	$5.0x10^{-5}$ – $1.0x10^{-2}$
Tyr	43.2±0.7	0.9975±0.0013	$2.0x10^{-6}$	$(2.0\pm0.3)x10^{-6}$	$2.0x10^{-6}$ – $1.0x10^{-2}$
Phe	61.3±1.7	0.9953±0.0059	$1.2x10^{-5}$	$(4.3\pm1.8)x10^{-7}$	$1.0x10^{-5}$ – $1.0x10^{-2}$
Tryp	64.1±1.5	0.9982±0.0008	$3.0x10^{-5}$	$(6.3\pm2.0)x10^{-7}$	$3.0x10^{-5}$ – $1.0x10^{-2}$
Put	24.5±0.2	0.9960±0.0005	$5.0x10^{-5}$	$(1.8\pm0.5)x10^{-5}$	$5.0x10^{-5}$ – $1.0x10^{-2}$
Cad	27.4±0.2	0.9980±0.0006	$2.5x10^{-5}$	$(1.2\pm0.0)x10^{-5}$	$2.5x10^{-5}$ – $1.0x10^{-2}$
His	28.0±0.8	0.9990±0.0010	$1.0x10^{-6}$	$(1.0\pm0.5)x10^{-6}$	$1.0x10^{-6}$ – $1.0x10^{-2}$
Spmd	15.4±0.7	0.9962±0.0010	$9.1x10^{-6}$	$(5.0\pm0.8)x10^{-6}$	$9.1x10^{-6}$ – $1.0x10^{-2}$
Spm	8.8±0.6	0.9950±0.0022	$2.0x10^{-5}$	$(3.7\pm0.7)x10^{-6}$	$2.0x10^{-5}$ – $1.0x10^{-2}$

LLLR – Lower limit of linear response; PDL – practical detection limit.

The presence of interfering ions, which may be any substance different than the target ions, affects the measured potential of the electrochemical cell (32). Those substances can give a similar response to the ions being measured, resulting in an apparent increase in their activity (or concentration). Another possibility concerns the electrolytes present at a high concentration that give rise to appreciable liquid junction potential differences, which

significantly decreases the activity coefficient of the target ions. The NE equation (2) translates how interfering ions introduce signal bias (32):

$$E\ (mV) = E^0 \pm \frac{RT}{z_i F} \ln(a_i + K_{i,j}^{pot} a_j^{z_i/z_j}) \qquad (2)$$

wherein the analyte ion is usually labeled i, and j is the interfering ion. In this equation, E^0 is the potential difference of the indicator and reference electrodes under standard conditions plus liquid-junction and material interfacial potentials, R is the gas constant, T is the absolute temperature, a_i and z_i are the activity and charge number of the target analyte ion i, and F is the Faraday constant. $K_{i,j}^{pot}$ is the potentiometric selectivity coefficient, which is a numerical measure of the sensor ability to discriminate the analyte ion i from interfering ion j, while a_j and z_j are the activity and charge number of the interfering ion j, respectively (32, 33).

Nonetheless, the NE equation is reduced to a simple form where the interfering compounds are only provided from the mobile phase and the ionic strength is adjusted (equation 3) (28):

$$E\ (mV) = E^0 + S \log(c_{analyte} + Cst) \qquad (3)$$

being S the slope of the straight line relating $E\ (mV)$ with $log\ c_{analyte}$, and Cst the contribution of interfering ions of the mobile phase to the analytical signal, which is dependent on its concentration, charge, and the respective potentiometric selectivity coefficients (28). Highly interfering ions will thus cause a decrease in the sensitivity of the method (slope) in all the linear response ranges of BAs.

Accordingly, it was hypothesized if the interfering ions present in the mobile phase, particularly lithium from formate buffer, could explain the differences obtained for slopes towards the theoretical value (**Table 4.5**). In recent work, the potentiometric selectivity coefficient for His was determined in the presence of lithium background at 1.0x10^{-2} mol L^{-1}, giving a $K_{His,Li}^{pot}$ of (9.05±4.50)x10^{-3} (34). This output indicates that a Lithium/His concentration ratio higher than 100 compromises the sensitivity and determination of His, especially at the low levels required for food quality control. The affinity of CB[6] for lithium ions was also confirmed by its binding constant, which was determined by others as 2.41 (24). To overcome this limitation, a sensor free of CB[6] and only based on the TCPB (1.0% w/w) as an ion exchanger was prepared and evaluated. Although the improvement of the sensitivity demonstrated by the higher slope of the NE equation for the hydrophilic amines (Put, Cad, His, Spmd, and Spm), the lower limit of linear response (LLLR) and PDL

increased (data not shown), which is not suitable for the determination of BAs at low levels. Besides, the response to lipophilic amines (Tyr, Phe, and Tryp) was hindered in the absence of CB[6], since both the slope, LLLR, and PDL values worsened. These findings are in agreement with the ability of cucurbit[n]urils to cage cationic guests, especially bearing some hydrophobicity (35) such as the herein studied lipophilic amines.

Therefore, the presence of CB[6] is fundamental to improving the potentiometric response features. The CB[6] modulates the selectivity of the potentiometric sensor towards the interfering ions of the mobile phase and, despite the ability to complex with inorganic cations, the extraction of the BAs into the membrane is favored (36). In turn, TCPB brings permselectivity by preventing anion coextraction from the sample and reproducible response by buffering the amount of free amine in the membrane phase. Moreover, the use of MWCNTs allowed better electron transfer kinetics, which also contributed to lowering the detection limits and obtaining more reproducible results, even in the presence of interfering ions.

An important aspect of the performance of the proposed detector concerns the response time, which has a major impact under transient flow injections, such as the liquid chromatography, due to the short time of interaction between the analytes and the membrane surface. The response time was herein determined as the time that elapses between the instant at which the concentration of the target BA is changed in the solution and the first instant at which the measured potential of the electrochemical cell becomes equal to 95% of the signal at a steady-state (32). The response time was investigated for each BA at concentrations ranging from $1.0x10^{-6}$ to $1.0x10^{-2}$ mol L^{-1}. It was found a very fast response for BAs concentrations higher than $1.0x10^{-4}$ mol L^{-1} (<5 s). Nonetheless, longer response times were observed for lower concentrations, though still less than 15 s, which were still suitable for their determination by liquid chromatography. For instance, His presented a response time of around 13 s at $1.0x10^{-6}$ mol L^{-1}.

As such, the attractive figures of merit obtained with the proposed sensor justifies its use as an appropriate detector for the determination of BAs after chromatographic separation. Moreover, the impact of the mobile phase composition in the sensor response highlights the importance of its careful control to obtain even better analytical features.

4.3.3.2. Optimization of mobile phase composition

Considering that SBS at $5.0x10^{-3}$ mol L^{-1} is essential to achieve the chromatographic separation of ten BAs (21), other adjustments in the mobile phase composition were performed to optimize the figures of merit of the newly proposed sensor. Particularly, the replacement of the lithium formate buffer by acetic acid solution on the mobile phase preparation, since CB[6] has a lower binding constant to hydrogen than lithium ions (1.06 and 2.41, respectively) (24). The pH of the new mobile phase decreased from 4.0 to 2.5 but without impairing the sensor response, which is not affected by the pH in the range of 2.0 to 6.0 pH units (34). Therefore, the potentiometric response of the miniaturized electrodes was evaluated when coupled to the HPLC system, though with acetic acid as acidifying agent (**Figure S5**). The separation was carried out on a Luna Omega Polar C18 column (150 x 4.6 mm, 5 µm from Phenomenex) using a mobile phase composed of solvent A ($5.0x10^{-3}$ mol L^{-1} SBS in $1.0x10^{-2}$ mol L^{-1} CH_3COOH, pH=2.5) and solvent B (10% (v/v) ACN/$1.0x10^{-3}$ mol L^{-1} CH_3COOH, pH=2.5) in gradient mode.

Several calibrations curves were performed by injecting BAs standard solutions covering the concentration range of $1.0x10^{-7}$ to $1.0x10^{-4}$ mol L^{-1}. The absence of lithium ions in the mobile phase allowed to obtain detections limits of $3.0x10^{-7}$ mol L^{-1} for all assayed BAs, which are half an order of magnitude lower than previously reported (21). This outcome confirms the effect of background ions in the potentiometric response, especially for the determination of low analyte concentrations.

The new mobile phase was evaluated concerning chromatographic separation and showed an increase in the capacity factors for all BAs and improved peak symmetries for Met, Eth, Cad, His, Spm, Phe, and Tryp. Noteworthy, the improvement in the separation efficiency, as shown by the increase in the number of theoretical plates, highly contributed to increasing the peak resolution. Detailed information about the chromatographic parameters is summarized in **Table S1**. Overall, the introduced modification allowed a complete separation of ten BAs in less than 19 min for a total run of 25 min. The new proposed analytical methodology for a fast and sensitive determination of BAs was further validated.

4.3.3.3. Validation of the proposed method for biogenic amines determination

The optimized method was validated as described in Section 4.3.6.7., namely assessing the chromatographic parameters, linearity and linear range, the limit of detection (LOD) and quantification (LOQ), precision, and accuracy. The chromatographic parameters and analytical figures of merit for each BA are summarized in **Table S2** and **Table 4.6**, respectively. The capacity and selectivity factors obtained for all amines are fairly good, ranging from 1.1 to 13.4 and 1.1 to 2.1, respectively. Peak resolution ranged from 2.6 to 13.2, which is above the acceptable criteria (≥ 1.5).

Linear regression lines were obtained for Put, Cad, His, Spmd, Spm, and Tyr in the range from $1.0x10^{-6}$ to $1.0x10^{-4}$ mol L^{-1} and for Met, Eth, Phe, and Tryp in the range from $1.0x10^{-6}$ to $3.0x10^{-5}$ mol L^{-1}, with R^2 ranging from 0.9870 to 0.9991. LOD and LOQ values were of $3.0x10^{-7}$ and $1.0x10^{-6}$ mol L^{-1} for all BAs, which correspond to a range from 9.3 to 60.7 µg L^{-1} and from 31.1 to 202.3 µg L^{-1}, respectively.

The repeatability of the potentiometric signal at $3.0x10^{-6}$, $1.0x10^{-5}$ and $3.0x10^{-5}$ mol L^{-1} provided RSD% values ranging from 4.6 to 7.7%, 1.3 to 5.8%, and 0.1 to 3.7%, respectively, whereas the intermediate precision showed RSD% values from 3.1 to 8.3%. Regarding the retention time, RSD% values lower than 0.3% and 0.5% were obtained for repeatability and intermediate precision at $1.0x10^{-5}$ mol L^{-1}, respectively. The inter-electrode reproducibility was evaluated for three different sensor units at $1.0x10^{-6}$, $1.0x10^{-5}$ and $1.0x10^{-4}$ mol L^{-1}, showing RSD% from 3.2 to 13.3%, 0.3 to 6.6%, and 1.9 to 6.5%, respectively. According to the Horwitz equation (37), the great precision of the method is demonstrated by the acceptable RSD% values obtained for each amine.

The recovery percentage ranged from 88.7 ± 3.5 to 109.9 ± 2.5%, 86.4 ± 3.0 to 108.7 ± 7.2%, and 87.1 ± 5.9 to 107.8 ± 8.8% in red wine, white wine, and beer, respectively, with RSD% values lower than 8.2%. These obtained values are in agreement with the European requirements because they fall within the ranges of -20% to +10% for the applied target concentrations (38), proving the great accuracy of the method. Detailed information on recoveries and RSD% obtained for each sample is further summarized in **Table S3**.

The most important features of the herein described method were compared with other reported methods based on HPLC for the determination of BAs in alcoholic beverages (**Table 4.7**). The analytical figures of merit obtained with the proposed method highlight its competitiveness with those routinely based on spectroscopic detection (6, 8, 10). It is only surpassed by methods relying on MS/MS detection (13), which demands expensive

equipment and maintenance, not daily used for food quality control purposes. The simultaneous quantification of ten BAs in less than 25 min also surmounts the lower number of determined BAs and/or higher analysis time (>30 min) reported for other methods. Moreover, the reliable determination of ten BAs attained with a simple, low-cost, and sensitive potentiometric detector, without derivatization steps, allows the achievement of fast and eco-friendly procedures, being a very promising method to be implemented in the food quality control sector.

Table 4.6 Summary of validation results obtained with the proposed potentiometric detector in HPLC.

Amine	t_R [a]	Linear Equation [b]	R^2	LOD [c]	LOQ [d]	Repeatability [e] RSD%		Intermediate Precision [f] RSD%		Accuracy [g]
		y=mx+b		µg L^{-1}	µg L^{-1}	t_R	Signal	t_R	Signal	Recovery%
Met	2.5	97.1x-0.07	0.9963	9.3	31.1	0.1	3.3	0.5	6.8	86.4-107.8
Eth	3.2	98.0x-0.06	0.9951	13.5	45.1	0.0	3.7	0.5	5.2	88.3-109.9
Put	5.2	269.3x-0.88	0.9961	26.5	88.2	0.2	2.7	0.3	5.1	89.7-107.3
Cad	6.3	366.9x-0.67	0.9991	30.7	102.2	0.3	2.4	0.4	8.3	88.7-109.9
His	7.3	327.1x-0.44	0.9986	33.3	111.1	0.3	1.3	0.5	7.5	91.5-108.2
Spmd	12.2	599.1x-0.50	0.9976	46.6	145.3	0.1	1.3	0.3	7.1	91.3-104.5
Spm	13.2	436.7x-0.38	0.9922	60.5	202.3	0.1	2.5	0.5	3.1	89.3-103.7
Tyr	14.1	135.3x-0.69	0.9870	41.2	137.2	0.3	4.1	0.2	7.3	87.8-107.2
Phe	15.8	29.5x-0.06	0.9875	36.4	121.2	0.4	5.8	0.4	7.0	87.1-106.0
Tryp	17.3	20.9x-0.01	0.9956	48.1	160.2	0.3	5.3	0.3	7.4	89.5-109.9

[a] BAs concentration 1.0x10^{-4} mol L^{-1}; t_R – retention time (min); t_0 – 1.2 min; [b] *n = 3*; [c] S/N = 3; [d] S/N = 10; [e] *n = 3* for 1.0x10^{-5} mol L^{-1}; [f] *n = 5* in two consecutive days for 1.0x10^{-5} mol L^{-1}; [g] *n = 3.*

Table 4.7 Comparison of different analytical methods based on HPLC for determination of BAs in alcoholic beverages.

Matrix	Amines	Sample preparation	Derivatization	Method	Analysis time min	LOD/LOQ µg L^{-1}	Repeatability RSD%	Recovery %	Ref
Beer	Cad, Hexa, His, Phe, Put, Spm, Spmd, Tyr	Extraction with TFA	Yes: EAC	HPLC-FLD	60	LOD: 0.27-0.69 LOQ: -	1.3-1.9	94.1-104.0	(8)
Wine	Amy, But, Cad, Eth, Hex, His, Phe, Prop, Put, Spm, Spmd, Tryp	SPE	Yes Benzoyl chloride	HPLC-UV	77.5	LOD: 133-509 LOQ: 331-1540	1.8-28.7	72-99	(6)
	Agm, Cad, His, Phe, Put, Spmd, Tyr	SPE	Yes AccQ–Fluor Kit	HPLC-FLD	45	LOD: 27-70 LOQ: 83-212	-	-	(10)
Beer and Wine	Cad, Hexa, His, Phe, Spm, Tryp, Tyr	UA-DLLME	Yes: BCEC-Cl	HPLC-FLD	32	LOD: 1.1-7.8 LOQ: 3.5-26.1	2.0-3.5	91.2-107.1	(9)
	Cad, His, Phe, Put, Spm, Spmd, Tryp, Tyr	Addition of PVPP	Yes Dansyl chloride	UHPLC-UV	18	LOD: 30-180 LOQ: 200-590	0.7-4.9	57.6-109.4	(7)
	Agm, But, Cad, Det, Dmet, Hex, His, Ibut, Ipent, Met, Phe, Prop, Put, Spm, Spmd, Tryp, Tyr	Dilution with water	Yes: p-toluenesulfonyl chloride	HPLC-MS/MS	30	LOD: 0.023-83 LOQ: 0.075-270	<15	-	(13)
	Eth, Cad, His, Met, Phe, Put, Spm, Spmd, Tryp, Tyr	SPE	No	HPLC-POT	25	LOD: 9.3-60.7 LOQ: 31.1-202.3	0.4-8.2	86.4-109.9	This work

Agm: agmatine; Amy: amylamine; BCEC-Cl: 2-(11H-benzo[a]carbazol-11-yl) ethyl carbonochloridate; But: butylamine; Cad: cadaverine; Det: diethylamine; Dmet: dimethylamine; EAC: ethyl-acridine-sulfonyl chloride; Eth: Ethylamine; FLD: fluorescence detection; Hex: Hexylamine; Hexa: 1,6-hexamethylenediamine; His: histamine; Ibut: isobutylamine; Ipent: isopentylamine; Met: methylamine; MS: Mass spectrometry; Phe: phenylethylamine; Pot: potentiometry; Prop: propylamine; Put: putrescine; PVPP: polyvinylpyrrolidone; SPE: solid-phase extraction; Spm: spermine; Spmd: spermidine; TCA: trifluoroacetic acid; Tryp: tryptamine; Tyr: tyramine; UA-DLLME: ultrasound-assisted dispersive liquid liquid microextraction; UV: ultraviolet.

4.3.3.4. Real samples analysis

The BAs content in alcoholic beverages was assessed with the optimized and validated method. One sample of beer and two independent wine samples were analyzed in triplicate and the representative chromatograms are displayed in **Figure 4.9**. A higher content of amines was found in red wine (7.54±0.42 mg L^{-1}), followed by white wine (5.24±0.24 mg L^{-1}) and beer (4.58±0.20 mg L^{-1}) (**Table 4.8**). These values corroborate those previously reported for wine samples commercialized in Portugal (39). They do not entail any risk to the health of consumers as long as risk factors such as amine oxidase-inhibiting drugs, alcohol, and gastrointestinal diseases are prevented (1). Noteworthy, the low levels of Put in all assayed samples (≈0.33±0.01 mg L^{-1}) were indicative of adequate sanitary conditions during food processing (5). Concerning His, one of the most toxicological relevant BAs, it was detected at higher levels in the red wine when compared with the other samples, but still lower than the regulated values (40). Regarding other BAs concentration in wine samples, Tyr and Tryp were the most abundant in red wine, with amounts of 2.29±0.19 and 1.06±0.08 mg L^{-1}, respectively. In the case of white wine, Spmd, Spm, and Tryp were the most representative, though with levels lower than 0.97±0.02 mg L^{-1}. In the beer sample, Tyr and Tryp were also the most abundant, only surpassed by Eth (0.84±0.03 mg L^{-1}).

Table 4.8 Quantification of BAs (mg L^{-1}) in beer and wine samples (mean ± standard deviation, *n=3*).

Amine	Sample		
	Red wine	**White wine**	**Beer**
Met	0.27±0.02	0.27±0.02	0.23±0.01
Eth	0.39±0.01	0.16±0.00	0.84±0.03
Put	0.36±0.02	0.33±0.01	0.30±0.02
Cad	0.36±0.03	0.31±0.01	0.25±0.01
His	0.82±0.03	0.26±0.00	0.21±0.01
Spmd	0.71±0.01	0.97±0.02	0.34±0.01
Spm	0.76±0.00	0.95±0.08	0.58±0.01
Tyr	2.29±0.19	0.68±0.04	0.74±0.02
Phe	0.52±0.04	0.55±0.03	0.50±0.01
Tryp	1.06±0.08	0.75±0.02	0.59±0.04
Total	7.54±0.42	5.24±0.24	4.58±0.20

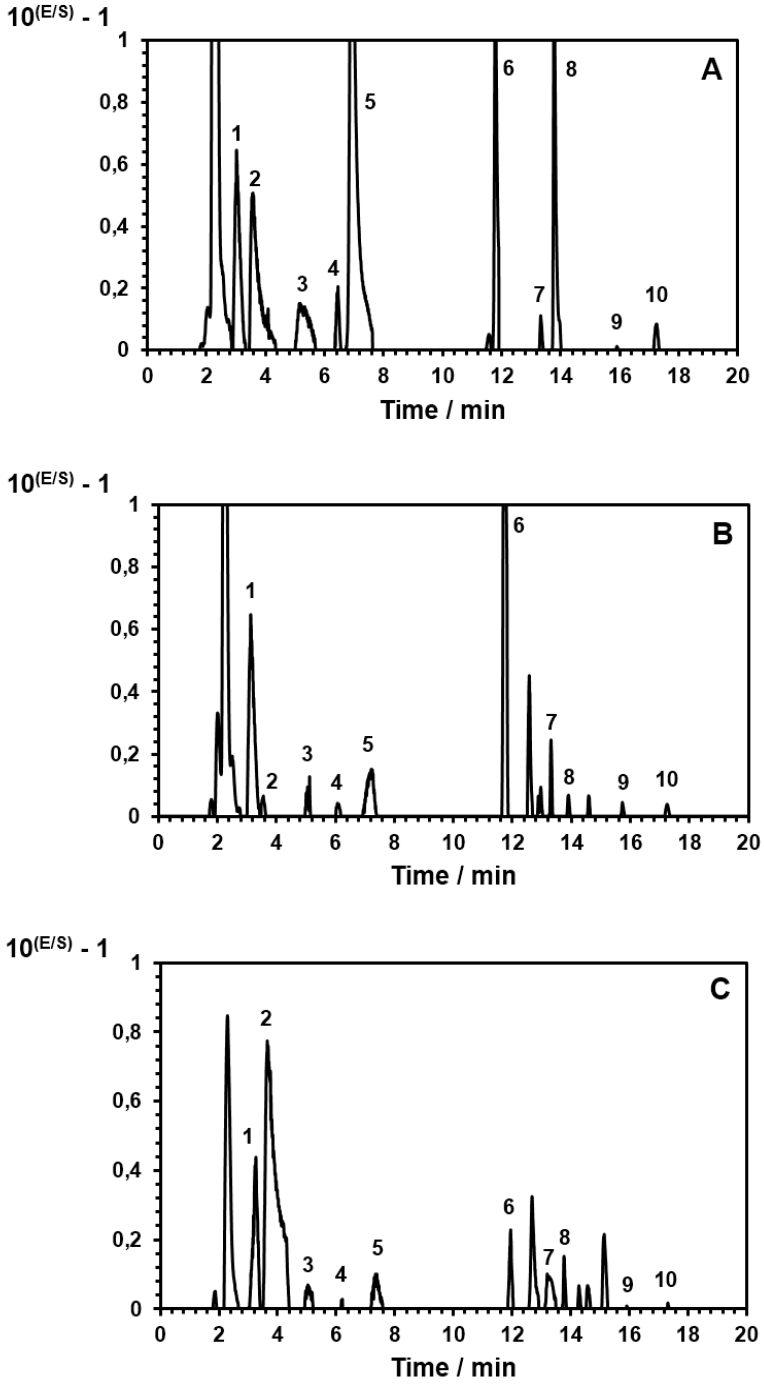

Figure 4.9 Individual chromatograms obtained with the proposed HPLC-potentiometric method for the analysis of red wine **(A)**, white wine **(B)**, and beer **(C)**. 1 – Met; 2 – Eth; 3 – Put; 4 – Cad; 5 – His; 6 – Spmd; 7 – Spm; 8 – Tyr; 9 – Phe; 10 – Tryp. Gradient elution: A – 5.0×10^{-3} mol L^{-1} SBS in 1.0×10^{-2} mol L^{-1} CH_3COOH and B – 1.0×10^{-3} mol L^{-1} CH_3COOH:ACN (v/v, 90:10). Column: Luna Omega 5µm Polar C18 150x4.6mm, I.D. (Phenomenex). Flow-rate: 1.2 mL min^{-1}. Injection volume: 100 µL.

4.3.4. Conclusion

In this work, an HPLC-potentiometric method for the determination of BAs in alcoholic beverages is presented. For such, the incorporation of multi-walled carbon nanotubes in the sensing membrane and the replacement of the acidifying agent in the mobile phase, from lithium formate buffer to acetic acid were the most relevant factors for lowering the detection limits and achieving a high separation efficiency. The proposed method allowed the simultaneous determination of ten underivatized BAs in less than 25 min. Concerning the validation results, the proposed methodology showed improved selectivity, sensitivity, precision, and accuracy. These figures of merit make the method attractive and competitive for the simple and reliable determination of BAs in alcoholic beverages, easily implemented by any laboratory for food quality control.

4.3.5. References

1. Ruiz-Capillas C, Herrero AM. Impact of biogenic amines on food quality and safety. Foods. 2019;8(2).

2. Suzzi G, Torriani S. Editorial: Biogenic amines in foods. Front Microbiol. 2015;6(472).

3. Shalaby AR. Significance of biogenic amines to food safety and human health. Food Res Int. 1996;29(7):675-90.

4. McCabe-Sellers BJ, Staggs CG, Bogle ML. Tyramine in foods and monoamine oxidase inhibitor drugs: A crossroad where medicine, nutrition, pharmacy, and food industry converge. J Food Comp Anal. 2006;19:S58-S65.

5. EFSA panel on biological hazards (BIOHAZ), scientific opinion on risk based control of biogenic amine formation in fermented foods. EFSA Journal. 2011;9(10):93.

6. Milheiro J, Ferreira LC, Filipe-Ribeiro L, Cosme F, Nunes FM. A simple dispersive solid phase extraction clean-up/concentration method for selective and sensitive quantification of biogenic amines in wines using benzoyl chloride derivatisation. Food Chem. 2019;274:110-7.

7. Angulo MF, Flores M, Aranda M, Henriquez-Aedo K. Fast and selective method for biogenic amines determination in wines and beers by ultra high-performance liquid chromatography. Food Chem. 2020;309:125689.

8. Li G, Dong L, Wang A, Wang W, Hu N, You J. Simultaneous determination of biogenic amines and estrogens in foodstuff by an improved HPLC method combining with fluorescence labeling. LWT - Food Sci Technol. 2014;55(1):355-61.

9. Wu H, Li G, Liu S, Ji Z, Zhang Q, Hu N, et al. Simultaneous determination of seven biogenic amines in foodstuff samples using one-step fluorescence labeling and dispersive liquid–liquid microextraction followed by HPLC-FLD and method optimization using response surface methodology. Food Anal Methods. 2015;8(3):685-95.

10. Ordonez JL, Callejon RM, Troncoso AM, Garcia-Parrilla MC. Evaluation of biogenic amines profile in opened wine bottles: Effect of storage conditions. J Food Compost Anal. 2017;63:139-47.

11. Liu SJ, Xu JJ, Ma CL, Guo CF. A comparative analysis of derivatization strategies for the determination of biogenic amines in sausage and cheese by HPLC. Food Chem. 2018;266:275-83.

12. Ochi N. Simultaneous determination of eight underivatized biogenic amines in salted mackerel fillet by ion-pair solid-phase extraction and volatile ion-pair reversed-phase liquid chromatography-tandem mass spectrometry. J Chromatogr A. 2019;1601:115-20.

13. Nalazek-Rudnicka K, Wasik A. Development and validation of an LC-MS/MS method for the determination of biogenic amines in wines and beers. Monatshefte Fur Chemie. 2017;148(9):1685-96.

14. Favaro G, Pastore P, Saccani G, Cavalli S. Determination of biogenic amines in fresh and processed meat by ion chromatography and integrated pulsed amperometric detection on Au electrode. Food Chem. 2007;105(4):1652-8.

15. Draisci R, Volpe G, Lucentini L, Cecilia A, Federico R, Palleschi G. Determination of biogenic amines with an electrochemical biosensor and its application to salted anchovies. Food Chem. 1998;62(2):225-32.

16. Cinquina AL, Calì A, Longo F, De Santis L, Severoni A, Abballe F. Determination of biogenic amines in fish tissues by ion-exchange chromatography with conductivity detection. J Chromatogr A. 2004;1032(1-2):73-7.

17. Palermo C, Muscarella M, Nardiello D, Iammarino M, Centonze D. A multiresidual method based on ion-exchange chromatography with conductivity detection for the determination of biogenic amines in food and beverages. Anal Bioanal Chem. 2013;405(2-3):1015-23.

18. Poels I, Nagels LJ. Potentiometric detection of amines in ion chromatography using macrocycle-based liquid membrane electrodes. Anal Chim Acta. 2001;440(2):89-98.

19. Aydin R, Asan A, Attar A, Isildak I. Trace analysis of amines in cheese serum with liquid chromatographic potentiometric detection by using amine-selective electrode. Arab J Chem. 2019;12(8):4533-40.

20. Gil RL, Amorim CG, Montenegro M, Araujo AN. Potentiometric detection in liquid chromatographic systems: an overview. J Chromatogr A. 2019;1602:326-40.

21. Gil RL, Amorim CG, Montenegro MCBSM, Araújo AN. Determination of biogenic amines in tomato by ion-pair chromatography coupled to an amine-selective potentiometric detector. Electrochim Acta. 2021:138134.

22. Zhang Y, Li Y, Zhu XJ, Li M, Chen HY, Lv XL, et al. Development and validation of a solid-phase extraction method coupled with HPLC-UV detection for the determination of biogenic amines in Chinese rice wine. Food Addit Contam Part A Chem Anal Control Expo Risk Assess. 2017;34(7):1172-83.

23. Amorim CG, Araujo AN, Montenegro MC, Silva VL. Cyclodextrin-based potentiometric sensors for midazolam and diazepam. J Pharm Biomed Anal. 2008;48(4):1064-9.

24. Zhang S, Grimm L, Miskolczy Z, Biczók L, Biedermann F, Nau WM. Binding affinities of cucurbit[n]urils with cations. Chem Commun. 2019;55(94):14131-4.

25. Magnusson B, Örnemark U. Eurachem Guide: The fitness for purpose of analytical methods – A laboratory guide to method validation and related topics 2014 [Available from: https://www.eurachem.org/images/stories/Guides/pdf/MV_guide_2nd_ed_EN.pdf].

26. ICH. ICH harmonised tripartite guideline: Validation of analytical procedures: text and methodology Q2 (R1) ICH, Geneva, Switzerland, 2005 [Available from: https://www.ich.org/page/quality-guidelines].

27. Pool CF. The Essence of Chromatography. 1st ed. Amsterdam: Elsevier; 2003.

28. Sekula J, Everaert J, Bohets H, Vissers B, Pietraszkiewicz M, Pietraszkiewicz O, et al. Coated wire potentiometric detection for capillary electrophoresis studied using organic amines, drugs, and biogenic amines. Anal Chem. 2006;78(11):3772-9.

29. Waters. Taking the complexity out of SPE method development 2017 [Available from: http://www.waters.com/webassets/cms/library/docs/720005685en.pdf].

30. Crespo GA, Macho S, Rius FX. Ion-selective electrodes using carbon nanotubes as ion-to-electron transducers. Anal Chem. 2008;80(4):1316-22.

31. Yuan D, Anthis AHC, Ghahraman Afshar M, Pankratova N, Cuartero M, Crespo GA, et al. All-solid-state potentiometric sensors with a multiwalled carbon nanotube inner transducing layer for anion detection in environmental samples. Anal Chem. 2015;87(17):8640-5.

32. Richard P. Buch EL. Recomendations for nomenclature of ion-selective electrodes (IUPAC Recommendations 1994). Pure Appl Chem. 1994;66(12):2527-36.

33. Umezawa Y, Buhlmann P, Umezawa K, Tohda K, Amemiya S. Potentiometric selectivity coefficients of ion-selective electrodes Part I. Inorganic cations - (Technical report). Pure Appl Chem. 2000;72(10):1851-2082.

34. Pereira AR, Araujo AN, Montenegro M, Amorim C. A simpler potentiometric method for histamine assessment in blood sera. Anal Bioanal Chem. 2020;412(15):3629-37.

35. Barrow SJ, Kasera S, Rowland MJ, del Barrio J, Scherman OA. Cucurbituril-based molecular recognition. Chem Rev. 2015;115(22):12320-406.

36. Yang L, Kan J, Wang X, Zhang Y, Tao Z, Liu Q, et al. Study on the binding interaction of the α,α′,δ,δ′-tetramethylcucurbit[6]uril with biogenic amines in solution and the solid state. Front Chem. 2018;6(289).

37. Horwitz W. Evaluation of analytical methods used for regulation of foods and drugs. Anal Chem. 1982;54(1):67A-76A.

38. Union E. Commission Decision of 12 August 2002 implementing Council Directive 96/23/EC concerning the performance of analytical methods and the interpretation of results. Off J Eur Communities; 2002. p. 8-36.

39. Leitão MC, Marques AP, San Romão MV. A survey of biogenic amines in commercial Portuguese wines. Food Control. 2005;16(3):199-204.

40. Costantini A, Vaudano E, Pulcini L, Carafa T, Garcia-Moruno E. An overview on biogenic amines in wine. Beverages. 2019;5(1):19.

4.3.6. Supplementary material

Figures

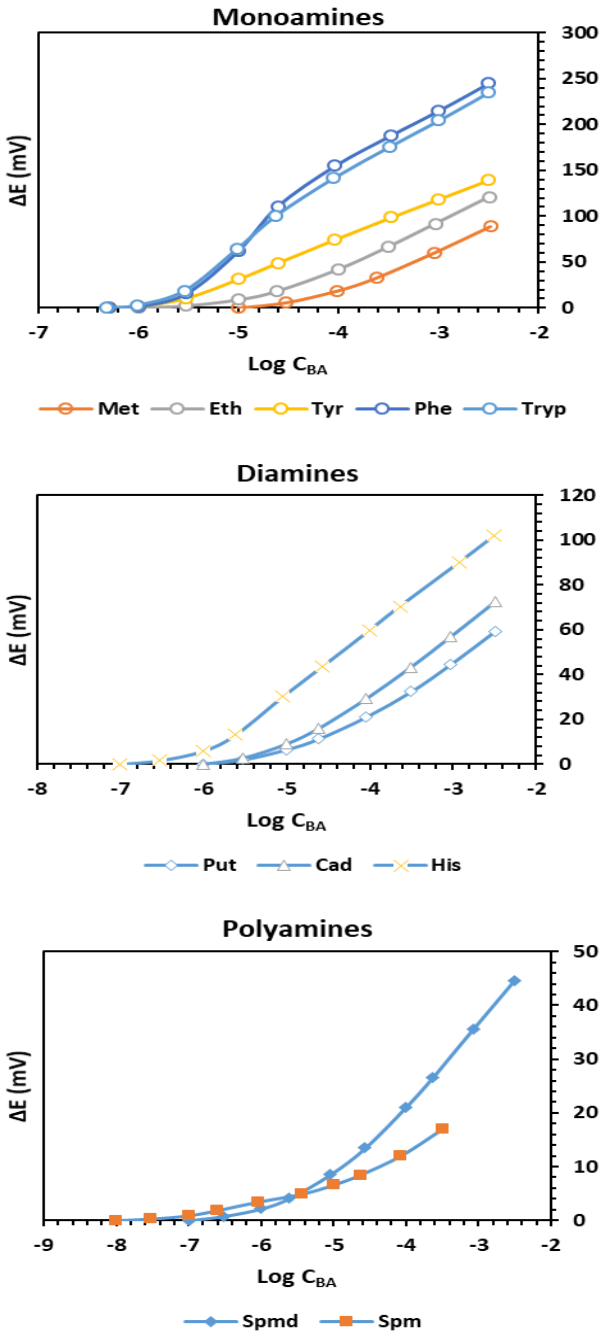

Figure S4 Individual calibration curves obtained under static conditions for monoamines (Methylamine – Met, Ethylamine – Eth, Tyramine – Tyr, Phenylethylamine – Phe, and Tryptamine – Tryp), diamines (Putrescine – Put, Cadaverine – Cad, and Histamine – His), and polyamines (Spermidine – Spmd and Spermine – Spm).

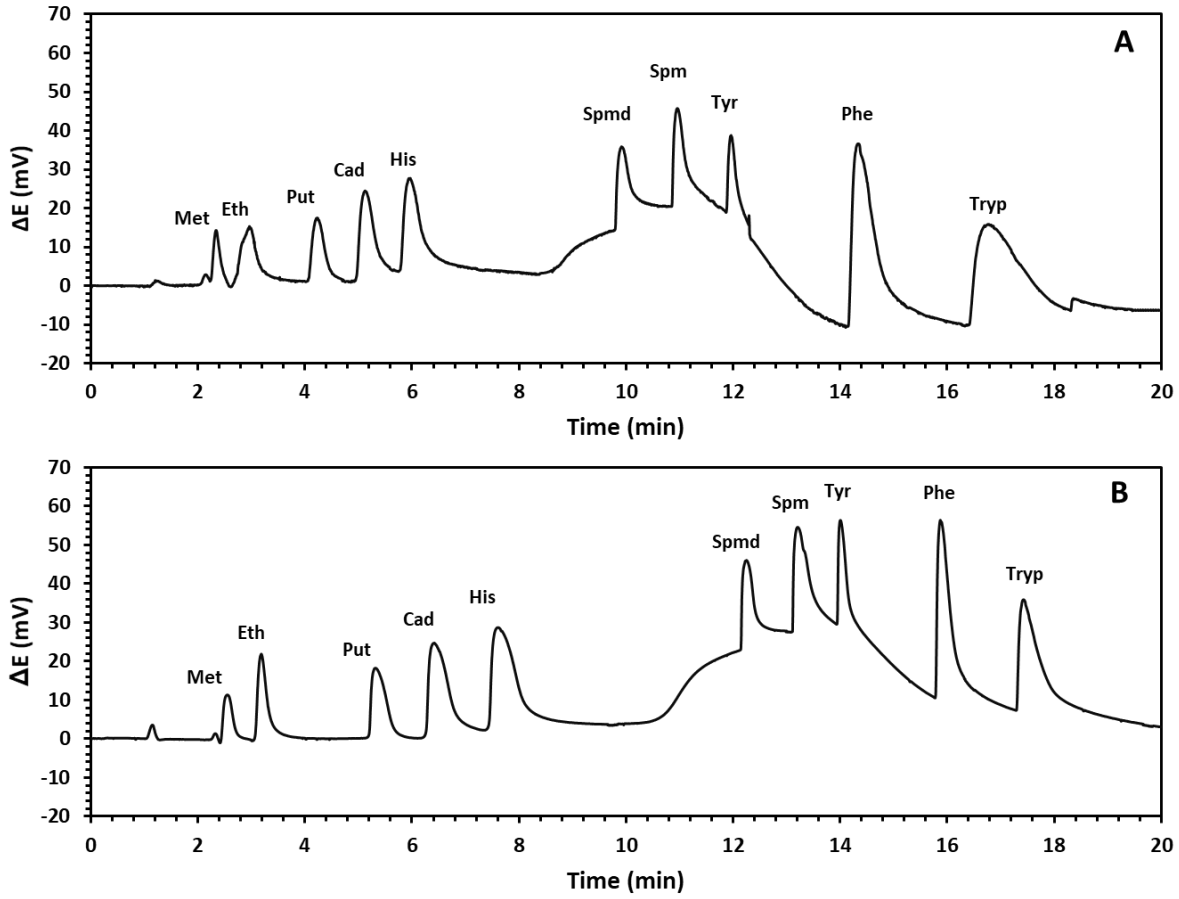

Figure S5 Comparative chromatograms of a standard mixture of BAs obtained with lithium formate buffer **(A)** and acetic acid **(B)** as acidifying agents of the mobile phase. Injected concentration: $1.0x10^{-4}$ M. Gradient elution: solvent A – $5.0x10^{-3}$ mol L^{-1} SBS in $1.0x10^{-2}$ mol L^{-1} acidifying agent and solvent B – $1.0x10^{-3}$ mol L^{-1} acidifying agent:organic modifier (v/v, 90:10). Column: Luna Omega 5µm Polar C18 150x4.6mm, i.d., Ea (Phenomenex). Flow-rate: 1.2 mL min^{-1}. Injection volume: 100 µL.

Tables

Table S2 Summary of the chromatographic retention parameters obtained after the separation with lithium formate buffer and acetic acid as acidifying agents of the mobile phase.

	Lithium formate buffer						**Acetic acid**					
Amine	t_R	A_s	N_{eff}	k	α	R_s	t_R	A_s	N_{eff}	k	α	R_s
Met	2.27	1.6	1331	0.9	1.6	1.6	2.54	1.3	2954	1.1	1.5	3.4
Eth	2.87	1.8	557	1.4	1.7	2.7	3.15	1.6	5497	1.6	2.1	8.6
Put	4.13	1.4	1470	2.4	1.3	1.9	5.25	1.6	4377	3.4	1.3	3.0
Cad	4.99	2.1	1601	3.2	1.2	1.4	6.28	1.8	4514	4.2	1.2	2.6
His	5.78	3.4	1282	3.8	1.9	7.7	7.34	2.0	4415	5.1	1.8	13.2
Spmd	9.89	2.0	8438	7.2	1.1	1.7	12.18	2.0	27355	9.2	1.1	3.7
Spm	10.95	3.7	2728	8.1	1.1	1.8	13.23	1.9	37897	10.0	1.1	3.9
Tyr	11.91	1.8	33443	8.9	1.2	5.3	14.11	1.8	96987	10.8	1.1	7.7
Phe	14.29	3.6	7831	10.9	1.2	2.1	15.80	2.4	58823	12.2	1.1	5.0
Tryp	16.57	2.9	1965	12.8	-	-	17.29	2.4	41420	13.4	-	-

t_R – retention time (min); A_s – peak symmetry; N_{eff} – number of theoretical plates; k – retention factor; α – separation factor; R_s– peak resolution.

Table S3 Recovery (%) of the HPLC-potentiometric method for determination of BAs in alcoholic beverages (*n=3*).

Amine	Spiked level	Red wine		White wine		Beer	
	(μmol L^{-1})	Recovery %	RSD %	Recovery %	RSD %	Recovery %	RSD %
Met	1	105.0	5.8	94.8	8.0	107.8	8.2
	3	106.2	3.8	104.2	8.2	95.4	4.4
	10	93.4	7.1	86.4	3.5	107.6	4.9
Eth	1	105.8	2.3	88.3	2.6	94.7	4.1
	3	109.9	4.4	90.3	2.5	107.4	7.4
	10	89.7	5.1	94.3	7.5	87.1	6.8
Put	1	95.8	4.2	99.7	3.9	107.1	5.6
	3	107.3	7.3	96.6	5.1	89.7	5.1
	10	96.5	6.3	94.7	2.9	92.7	3.3
Cad	1	102.1	7.1	95.8	2.0	102.5	5.7
	3	109.9	2.2	101.8	1.5	89.1	4.7
	10	88.7	1.7	94.8	2.0	99.2	3.2
His	1	101.6	4.1	93.8	1.5	91.5	3.7
	3	108.2	7.4	99.1	0.9	100.6	3.6
	10	94.7	2.0	102.0	2.5	90.7	6.8
Spmd	1	103.2	2.0	92.5	2.0	95.0	1.7
	3	91.3	4.3	92.2	6.0	104.5	6.8
	10	98.4	1.0	100.7	8.0	99.1	4.3
Spm	1	101.2	0.4	89.9	7.9	92.9	6.8
	3	96.9	5.6	92.2	4.9	103.7	7.3
	10	100.9	1.3	93.7	5.0	89.3	4.8
Tyr	1	95.6	8.1	89.7	5.6	95.5	2.4
	3	95.9	4.2	87.8	5.2	107.2	8.2
	10	95.1	7.8	88.1	3.2	98.6	4.0
Phe	1	93.8	7.6	87.1	5.3	99.4	1.8
	3	90.4	2.0	97.6	3.5	106.0	5.5
	10	103.0	6.2	102.0	6.2	100.3	3.1
Tryp	1	107.5	7.2	89.7	3.1	100.0	6.9
	3	109.9	0.6	108.7	6.6	97.9	8.0
	10	103.4	0.5	89.5	4.6	91.8	7.3

4.4. Cucurbit[8]uril-based potentiometric sensor coupled to HPLC for determination of tetracycline residues in milk samples

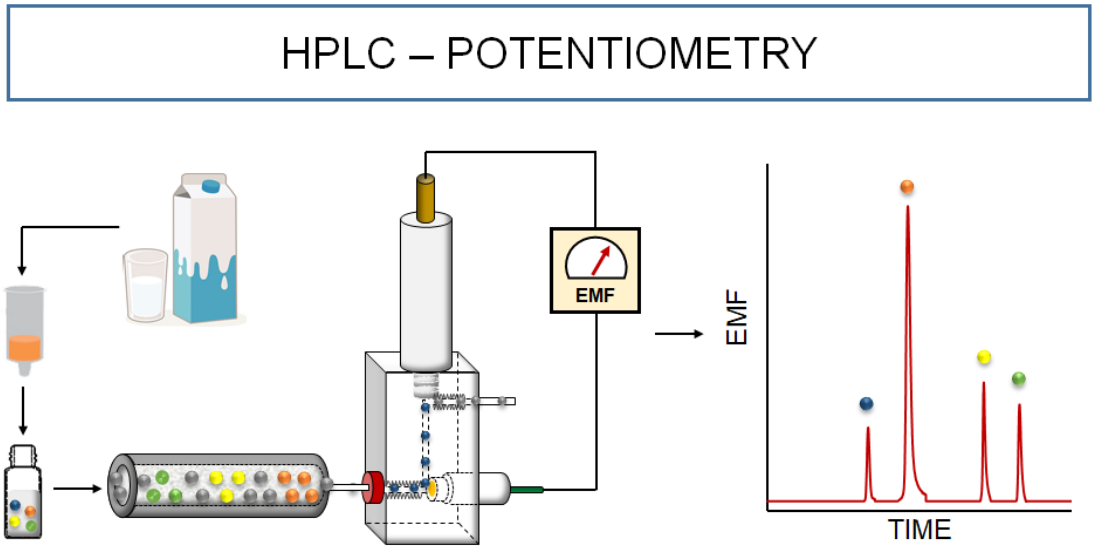

Section 4.4 describes a novel tetracycline-selective electrode based on cucurbit[8]uril as a macrocyclic host and its use as a detector of reversed-phase chromatography for the determination of tetracycline antibiotics in milk samples[4].

[4] This is a partial transcription of the article *Renato L. Gil, Célia G. Amorim, Maria C.B.S.M. Montenegro, Alberto N. Araújo; Cucurbit[8]uril-based potentiometric sensor coupled to HPLC for determination of tetracycline residues in milk samples; Chemosensors, 2022, 10(3), 98; doi: 10.3390/chemosensors10030098*;

4.4.1. Introduction

Tetracycline antibiotics (TCs) are broad-spectrum pharmaceutical drugs that exhibit activity against a wide range of microorganisms (1). The most used compounds within this antibiotic group are chlortetracycline, doxycycline, oxytetracycline, and tetracycline. The low toxicity profile and low cost enhance their extensive use as veterinary drugs for the prevention and treatment of several microbial diseases (2) as well as growth promoters in intensive animal farming (3). This widespread use of TCs may cause the presence of residues in foods of animal origin, whose intake results in harmful effects on human health such as allergic reactions, gastrointestinal disturbance, liver damage, poor fetal development, and pigmentation of teeth (4,5). Moreover, the consumption of low-level doses for long periods induces the selective predominance of drug-resistant microorganisms with time, which puts public health in jeopardy (6).

To ensure food safety and reduce the exposure of people to veterinary drugs, regulatory authorities have set maximum residue limits (MRLs) allowed in foods for human consumption. The MRLs for TCs residues, according to the US Food and Drug Administration (FDA), are 2 mg kg^{-1} in muscle, 6 mg kg^{-1} in the liver, and 0.3 mg kg^{-1} in milk (7), whereas the Codex Alimentarius Commission of the FAO/WHO has adopted MRLs of 0.2 mg kg^{-1} in muscle, 0.6 mg kg^{-1} in the liver, and 0.1 mg L^{-1} in milk (8). These low MRL values demand the use of analytical methods with suitable sensitivity and detectability to determine these residues in foodstuff.

Different analytical methodologies for the determination of TCs in milk samples have been reported in the literature, with an emphasis on HPLC coupled to a photodiode array (9). The complexity of the chromatograms nonetheless requires a positive correspondence of compounds to the peaks by comparing the sample and reference spectra. Fluorimetric detection improves both selectivity and sensitivity but requires post-column derivatization (10). On the other hand, LC-MS/MS methods with the best figures of merit have been developed for the determination of TCs residues (11–13). However, the high cost and the requirement of skilled technicians are not easy to circumvent, which makes this method unaffordable for routine analysis. Although effective methods are already implemented, more simple, rapid, inexpensive, and reliable analytical methodologies are needed to fulfill the requirements of governmental agencies and consumer organizations (9).

Of particular interest is the potentiometric technique based on ion-selective electrodes (ISEs) due to their versatility of use, simplicity of instrumentation, cost-effectiveness, and miniaturization ability (14,15). The coupling of potentiometric detection with liquid

chromatography was considered decades ago by using metallic copper electrodes (16–18) for the determination of inorganic ions in ion chromatography systems. Later on, Luc Nagels and his group extended the applications to organic ionic substances, including organic acids (19), basic drugs (20,21), and alkaloids (22), resorting to polymeric membrane electrodes based on conductive support. Despite their powerful features, potentiometric sensors are still not viewed as routine detectors in HPLC and thus researchers should put more effort into demonstrating their competitiveness with other detectors.

Several ISEs using different types of recognition elements have been described in the literature to accomplish the determination of TCs. Electroactive ion-pair complexes were initially proposed for the determination of chlortetracycline (23) and tetracycline (24), though the poor limits of detection (LOD) strongly limited their application. Alternatively, molecularly imprinted polymers (MIPs) for the determination of oxytetracycline (25) and tetracycline (26,27) were also considered. Nevertheless, the poor LOD (25,26), the long response time (≈ 200 s), and the inner filling solution configuration hindered its use in microfluidic platforms (27). The use of macrocyclic receptors as recognition elements to form inclusion complexes by a host-guest mechanism (28,29), such as α-cyclodextrin (30) and β-cyclodextrin (31), has been referred to as a convenient approach in the development of tetracycline-selective electrodes (TC-SE) with improved sensitivity and detection limits. Nevertheless, none of these potentiometric sensors were used together with chromatographic separation, and thus the simultaneous detection of different TCs with suitable LOD was still a real limitation.

Recently, the cucurbit[n]urils (CB[n]s) family has attracted significant attention due to their interesting molecular recognition properties (32). CB[n]s are barrel-shaped macrocyclic hosts with a hydrophobic inner cavity accessed via two polar carbonyl-rimmed openings (33). While the cavity provides a hydrophobic void to host neutral hydrophobic molecules, the carbonyl rims represent docking sites for positively charged groups and stabilize the host-guest complex through ion-dipole and hydrogen-bonding interactions (34). Different CB[n]s/organic compound complexes have been described in the literature by using spectroscopic (35–37) and electroanalytical techniques (38–40). Particularly in potentiometric detection, CB[6] was considered for the development of etilefrine (41) and atropine (42) selective electrodes for pharmaceutical control as well as biogenic amine determination in different food samples (43,44). However, based on the authors' knowledge, to date, no TC-selective electrode has been reported based on CB[n] as a recognition element to determine the presence of TCs in food matrices.

Therefore, this work intends to develop a simple, cost-effective, and reliable method for the determination of TCs by HPLC coupled with potentiometric detection. To achieve this goal,

a novel TC-selective electrode based on CB[8] as an ionophore was developed and integrated into a microfluidic wall-jet flow-cell, which was used as a detector in a reversed-phase HPLC system. The final methodology was validated following the international guidelines and was applied to the analysis of milk samples.

4.4.2. Experimental Section

4.4.2.1. Chemicals and materials

All chemicals were of analytical reagent grade. Chlortetracycline hydrochloride (CTC, ≥91.0%, ref. C4881), doxycycline hyclate (DXC, ≥93.5%, ref. D9891), oxytetracycline hydrochloride (OTC, >96.5%, ref. O5875), tetracycline hydrochloride (TTC, 95.0%, ref. T3383), oxalic acid dihydrate (ref. 1.00495), citric acid (ref. 251275), sodium phosphate dibasic dihydrate (ref. 71662), and ethylenediaminetetraacetic acid disodium salt dihydrate (EDTA, ref. E5134) were purchased from Sigma–Aldrich (Algés, Portugal). Sulphuric acid was from PanReac AppliChem (96%, H_2SO_4, ref. 131058) while acetonitrile (ACN, ref. 1.00029.2500P) and methanol (MetOH, ref. 1.06035.2500P) of LiChrosolv hyper grade were acquired from VWR (Amadora, Portugal). Ultra-pure water with conductivity <0.055 μS cm^{-1} was produced in our laboratory (Heal force, Easy model, Shanghai, China) and used whenever needed.

The stock standard solutions of TCs were prepared in an aqueous oxalic acid solution (0.05 M) at the concentration level of 0.01 M and stored in the freezer at −20 °C before use. The working standard solutions were prepared daily by the subsequent dilution of the stock solution. The EDTA/McIlvaine Buffer was prepared according to the literature (45) by mixing a 0.1 M aqueous solution of citric acid with a 0.1 M aqueous solution of anhydrous dibasic sodium phosphate (100:62.5, v/v). Then, the corresponding mass of disodium EDTA for a final concentration of 0.1 M was added, and the pH was adjusted to 4.1 with a 5 M sodium hydroxide solution (measured with a sensION pH meter, Hach, Portugal).

For the electrode conductive support preparation, graphite powder (<50μm, ref. 1.04206) and Araldite M (ref. 10951) were purchased from Sigma–Aldrich (Algés, Portugal), whereas the hardener Ren HY 5162 (ref. 068620205) was from Huntsman (Barcelona, Spain). For the sensing membranes preparation, high molecular weight polyvinyl chloride (PVC, ref. 81392), cucurbit[8]uril hydrate (CB[8], ref. 545228), potassium tetrakis(p-chlorophenyl)borate (TCPB, ref. 60591), 2-fluorophenyl 2-nitrophenyl ether (FNDPE, ref. 47390), multi-walled carbon nanotubes (MWCNTs, 110–170 nm x 5–9 μm, ref. 659258),

and tetrahydrofuran (THF, ref. 186562) were obtained from Sigma–Aldrich (Algés, Portugal).

4.4.2.2. Sample preparation

Milk samples were purchased from a local supermarket (Porto, Portugal), which included UHT skimmed milk, UHT semi-skimmed milk, and fresh semi-skimmed milk, and were stored at 4 °C (for no more than one week). Firstly, 1.0 mL of each milk sample was mixed with 5.0 mL of EDTA/McIlvaine Buffer in a 15 mL centrifuge tube. The solutions were agitated for 1 min using a vortex, followed by centrifugation at 4750 rpm for 15 min at 4 °C. Any floating lipid layer and precipitate were disposed of, being the remaining supernatant cleaned-up with solid-phase extraction (SPE) cartridges OASIS PRIME hydrophobic–lipophilic-balanced (HLB) from Waters (3 cc, 60 mg, ref. 186008056) assembled in a Visiprep™ SPE Vacuum Manifold (ref. 57030-U, Supelco). The supernatant was loaded into the SPE cartridge at a flow rate of 1.0 mL min^{-1}. After the sample was percolated, the cartridges were washed with 2.0 mL of ultra-pure water and dried for 1 min drawing a full vacuum. The target analytes were eluted twice by 1.0 mL of HPLC grade methanol at the same flow rate. The extract was dried under a gentle nitrogen stream and was finally reconstituted in 1.0 mL of aqueous oxalic acid at 0.05 M. All solutions were filtered through 0.22 µm Nylon syringe filters (FilterLab, ref. JNY022013N) before injection in the chromatographic system.

4.4.2.3. Apparatus

The HPLC-ISE analysis was performed on a Waters 600E Multisolvent Delivery System (Waters, Milford, MA, USA) equipped with a Waters 600 controller, a Waters 600E pump, a Waters 2487 Dual Absorbance Detector, and a Rheodyne 7725i six-port external manual injector (IDEX Health & Science, LLC, Middleboro, MA, USA). Millennium 32 Chromatography Manager Software (Waters, Milford, MA, USA) was used to control the HPLC components and data processing in the UV detector.

Handmade miniaturized indicator electrodes and a commercial miniaturized reference electrode filled with a 3.0 M KCl (model 6.0727.0 0 0, Metrohm, Herisau, Switzerland) were used for the potentiometric measurements, which were carried out using a 6-Channel Precision Electrochemistry EMF Interface (LawsonLabs, Inc., Malvern, PA, USA). A double-junction Ag/AgCl reference electrode (Orion 90-02-00, Thermo Scientific, Waltham, MA,

USA) with its external compartment filled with a 0.01 M KCl solution was used in the experiments in batch mode. The potentiometric signals vs. time data were recorded by the graphics software from LawsonLabs, Inc., Malvern, PA, USA.

4.4.2.4. Chromatographic conditions

A Luna C8(2) column (150 mm x 4.6 mm I.D., 5 µm from Phenomenex, Torrance, CA, USA) was used at controlled room temperature (±2 °C) to perform the separation using a mobile phase composed of solvent A (0.005 M H_2SO_4:ACN, 90:10, v/v) and solvent B (0.005 M H_2SO_4:ACN, 80:20, v/v). A gradient elution was used following the program: 0% B from 0 to 13.00 min; 0–100% B from 13.00 to 13.01 min; 100% B from 13.01 to 24.00 min; 100–0% B from 24.00 to 24.01 min. The injection volume and the flow rate were optimized to be 100 µL and 1.30 mL min^{-1}, respectively.

4.4.2.5. Detection cell

The column outlet was connected in-line to the Waters Absorbance Detector at a wavelength of 355 nm, according to the literature (45,46), which was used to validate the potentiometric measurements. The microfluidic potentiometric wall-jet flow-cell (**Figure 4.10**) holding both the miniaturized TC-selective electrode and the reference electrode was in-line connected after the UV detector using PEEK tubing (L x O.D. x I.D. = 300 mm x 1/16 in. x 0.25 mm). The flow-cell consisted of an acrylic block (length – 40 mm, width – 22 mm, and height – 22 mm) incorporating four single holes: two for the inlet and outlet of the mobile phase, one enabling to screw the reference electrode, and the last for coupling the miniaturized TC-selective electrode. The internal channel was drilled with an internal diameter of 0.8 mm. For the inlet and outlet, a blue ferrule and male red nut (1/16, IDEX Health & Science) were used to connect the PEEK tubing.

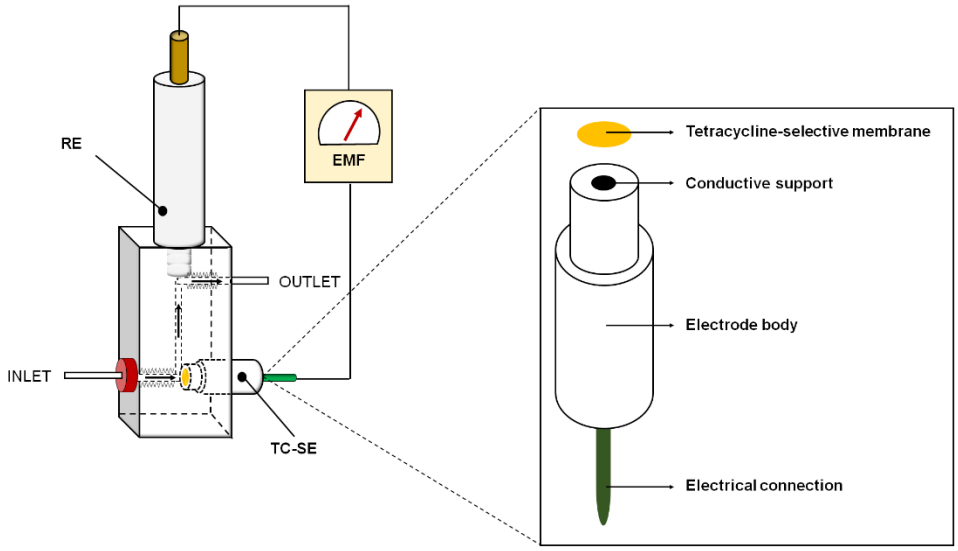

Figure 4.10 Illustration of the microfluidic wall-jet potentiometric cell used for the determination of tetracycline antibiotics. TC-SE – Tetracycline-selective electrode; RE – Reference electrode. Inset: Miniaturized TC-SE based on graphite conductive substrate prepared by the drop-casting of a tetracycline-selective membrane.

4.4.2.6. Preparation of TC-selective electrodes

Handmade TC-selective electrodes of solid contact were fabricated following a procedure described elsewhere (44,47). Briefly, a non-conductive epoxy resin was prepared by mixing Araldite-M and hardener HY (1:0.4 w/w), which was blended with graphite powder to obtain a composite with appropriate homogeneity and consistency. The final proportion was 1:1.85 w/w of epoxy resin and graphite, respectively. A portion of the conductive composite was introduced in one end of a Perspex tube (6.0 mm I.D. x 10.0 mm O.D. x 150.0 mm length) and a polytetrafluoroethylene rod (1.6 mm I.D. x 4.0 mm O.D. x 15.0 mm length) for the fabrication of conventionally shaped and miniaturized electrodes, respectively. An electrically shielded cable with the copper wire exposed was inserted from the opposite endings to establish the electrical contact. The electrodes were left to dry over 24 h at room temperature and, finally, the surface was polished with sandpaper of different grit sizes until a specular gloss was obtained.

Ion-selective membranes (ISMs) were prepared by mixing accurately weighed amounts of the polymer (PVC), plasticizer (FNDPE), ionophore (CB[8]), ionic additive (TCPB), and nanostructured materials (MWCNTs) in glass vials to obtain the compositions shown in

Table 4.9. A total of 300 mg of the mixture was dissolved in 3.0 mL of THF and shaken in a vortex before use. The conductive electrode surface was modified by dropping the corresponding ISMs until covering all the support contact areas (≈100 µL). The THF was left to evaporate for 30 min before the next deposition. The procedure was repeated a further five times and, finally, the electrodes were left to dry overnight before conditioning in an aqueous 0.05 M solution of oxalic acid. For miniaturized electrodes, 4 x 5 µL of the corresponding ISM was drop-coating onto the conductive support with an automatic pipette. Each layer was allowed to dry for 20 min before the next addition. Finally, the electrodes were conditioned overnight (~12 h) in an aqueous 0.005 M solution of sulphuric acid. When not in use, each electrode was kept immersed in the corresponding conditioning solution.

Table 4.9 Ion-selective membranes (ISMs) composition.

	Components in the ISM (wt%)				
ISM	**PVC**	**FNDPE**	**CB[8]**	**TCPB**	**MWCNTs**
A	31.00	68.97	–	0.03	0.00
B	31.00	68.07	0.90	0.03	0.00
C	31.00	67.07	0.90	0.03	1.00
D	31.00	66.07	0.90	0.03	2.00

PVC – polyvinyl chloride; FNDPE –2-fluorophenyl 2-nitrophenyl ether; CB(8) – cucurbit(8)uril hydrate; TCPB – potassium tetrakis(p-chlorophenyl)borate; MWCNTs – multi-walled carbon nanotubes.

4.4.3. Results and discussion

4.4.3.1. Evaluation of the conventionally-shaped TC-selective electrodes

The potentiometric response of conventionally shaped electrodes prepared with different membranes (without CB[8] – ISM A and with CB[8] – ISM B) was firstly evaluated towards four different TCs in batch conditions. The background solution of 0.05 M oxalic acid solution at a pH of 2.0 allowed for the total ionization of TCs and the ionic strength adjustment. **Figure S6** shows the typical time trace of the EMF values of both electrodes for the stepwise addition of various concentrations of each of the TCs. The EMF values observed at the steady-state were plotted against the corresponding logarithmic TCs' concentration, showing a Nerstian behavior for all target compounds (**Figure S7**). The general calibration parameters (**Table 4.10**), namely slope, linear response range, and LOD, showed high similarity between the sensing membrane without (ISM A) and with the addition of ionophore

(ISM B). Noteworthy, the intra- and inter-electrode potentiometric responses were highly reproducible (*n=3* for electrodes and successive calibrations), since the given relative standard deviation (RSD%) of the obtained slopes was better than 3.0% and 4.1% for ISM A and ISM B, respectively.

Table 4.10 Calibration parameters of the conventionally shaped electrodes prepared without (ISM A) and with ionophore (ISM B) in batch mode for different tetracycline antibiotics.

Calibration parameter	ISM	CTC	DXC	OTC	TTC
Slope[a], mV dec^{-1}	A	62.5 ± 1.1	58.6 ± 0.9	54.0 ± 0.6	52.9 ± 1.6
	B	63.4 ± 2.1	59.0 ± 0.1	56.2 ± 0.9	53.8 ± 2.2
Linear response range, M	A	3.0x10^{-7}–1.0x10^{-3}	3.0x10^{-7}–1.0x10^{-3}	6.0x10^{-6}–1.0x10^{-3}	1.0x10^{-6}–1.0x10^{-3}
	B	3.0x10^{-7}–1.0x10^{-3}	3.0x10^{-7}–1.0x10^{-3}	6.0x10^{-6}–1.0x10^{-3}	1.0x10^{-6}–1.0x10^{-3}
Limit of detection [a], M	A	(1.3 ± 0.6) x 10^{-7}	(1.7 ± 0.3) x 10^{-7}	(2.9 ± 0.0) x 10^{-6}	(3.6 ± 0.2) x 10^{-7}
	B	(1.5 ± 1.3) x 10^{-7}	(1.8 ± 0.7) x 10^{-7}	(2.5 ± 0.0) x 10^{-6}	(4.3 ± 0.5) x 10^{-7}

[a] Standard deviation value was calculated from three subsequent calibrations of the same electrode.

Nonetheless, regarding the application of the potentiometric sensor in liquid chromatography, the dynamic response characteristics of the TC-selective electrodes must be emphasized, since they can affect the analytical performance under hydrodynamic flow analysis (48). An important aspect concerns the response time, which has a major impact under transient flow injections due to the short time of interaction between the analytes and the membrane surface. The response time for each of the TCs was determined following IUPAC recommendation (49) at concentrations ranging from 1.0x10^{-7} to 1.0x10^{-3} M. As expected, a fast response was obtained for higher TC concentrations, especially for ISE containing CB[8] as an ionophore (<10 s, ISM B). However, longer response times were observed at concentrations lower than 1.0x10^{-6} M (<30 s), though still lower than those obtained with the ionophore-free sensing membrane (<60 s, ISM A).

On the other hand, attending to the complexation ability of CB[8] with the TCs, the reduction in the Gibbs energy ($\Delta G_{complex}$) in the presence of the host molecule should, in principle, generate a larger signal when used under transient flow injections. As such, improved sensitivity and detectability can be attained, which was already demonstrated by other authors dealing with potentiometric detection in liquid chromatography (50,51).

Therefore, the use of CB[8] as an ionophore for the development of a new TC-selective electrode, highlighting its ability to detect different TCs with great analytical features and a

short response time, foresees its application as a detector in a liquid chromatographic system for food control.

4.4.3.2. Evaluation of the miniaturized TC-selective electrode coupled to HPLC system

After the characterization of the potentiometric sensors in batch conditions, the miniaturized TC-selective electrodes were assembled in a microfluidic wall-jet flow-cell and coupled to the HPLC system. Several experimental conditions such as i) the composition of the mobile phase; ii) gradient program, including hydrodynamic conditions; iii) incorporation of nanostructured materials into the ISM, were optimized to achieve the best chromatographic separation conditions of the four TCs without compromising the sensitivity and detectability (43).

Optimization of mobile phase composition

Various elution solvents were first investigated under isocratic conditions at a fixed flow rate of 1.0 mL min^{-1}, namely by evaluating different mixtures of aqueous acid solutions (phosphoric, oxalic, hydrochloric, or sulphuric acid) with ACN (80:20, v/v). While phosphoric, oxalic, and hydrochloric acid concentrations were prepared at 0.05 M, sulphuric acid was prepared at 0.005 M, and the pH was adjusted to 2.0 using HCl/NaOH solution. As shown in **Figure S8A**, the lowest retention factor (k) values were achieved for sulphuric acid, ranging from 0.7 to 5.0 for OTC and DXC, respectively, which enabled a shorter analysis time. Moreover, the separation factor (α) was determined for two subsequent peaks and no effect was noticed when changing the acid agent (**Figure S8B**). Therefore, aqueous sulphuric acid was selected as an acidifying agent and the content of ACN (10, 20, and 30%, v/v) was investigated under isocratic conditions. However, a lack of chromatographic selectivity or an increase in the analysis time was observed. To surpass this constraint, gradient elution was considered.

For that, two solvents were selected containing 0.005 M of H_2SO_4 and ACN at a different proportion (A: 90:10; B: 80:20; v/v). Several combinations of the time/mobile phase composition were carried out to optimize the chromatographic separation in terms of resolution and running time as well as to obtain the best analytical performance of the potentiometric detector. In HPLC-ISE methodologies, a compromise between the optimal

separation and detection conditions should be expected because of the impact of the mobile phase composition in the potentiometric detector rather than the spectroscopic detectors.

Optimization of hydrodynamic conditions

The flow rate and sample injection volume were optimized to obtain the best separation and detection conditions, adjusting the gradient elution whenever necessary. For that, different flow rates (1.0, 1.3, and 1.5 mL min^{-1}) were firstly examined by the triplicate injection of standard solutions of TCs at $1.0x10^{-6}$, $1.0x10^{-5}$, and $1.0x10^{-4}$ M. According to the chromatograms, the retention times of OTC and DXC (i.e., first and last peak eluted, respectively) were reduced from 12.2/31.8 min to 9.8/24.6 min and 8.4/22.5 min when the flow rate was 1.0, 1.3, and 1.5 mL min^{-1}, respectively, without significant effect in the retention and separation factors. Nevertheless, higher flow rates improved the peak resolution (R_S) through an increase in the effective plate number (N_{eff}), though affecting the potentiometric detector performance. In this context, when the flow rate changed from 1.0 to 1.3 mL min^{-1}, an increase in the signal magnitude (i.e., peak height in mV) was observed for all target TCs (see **Figure S9**), which is ascribed to the wall-jet flow-cell configuration (52). On the other hand, the shorter residence time of the analyte plug in the microfluidic flow-cell, combined with the longer response time of the electrode, negatively affected the peak heights for the higher flow rate (53). Therefore, a flow rate of 1.3 mL min^{-1} was selected as the most suitable condition regarding the TCs separation and the detector performance. Overall, the optimal conditions allowed a complete separation of four TCs in less than 24.0 min, following the gradient program: 0% B from 0 to 13.00 min; 0–100% B from 13.00 to 13.01 min; 100% B from 13.01 to 24.00 min; 100–0% B from 24.00 to 24.01 min. The OTC and TTC were firstly eluted in solvent A, presenting retention times of 9.3 and 12.9 min, respectively. The strong interaction of CTC and DXC with the stationary phase required an increase in the ACN content for an efficient elution, attaining retention times of 21.1 and 24.5, respectively. Nevertheless, ACN content higher than 20% (v/v) was not considered in this study to avoid the dissolution of the membrane components (50).

On a similar basis, the effect of the injection volume (20, 50, and 100 µL) was investigated. As shown in **Figure S10**, a positive correlation was observed between the injection volume and the peak height for all the studied compounds. While an increase in the peak height was observed for CTC and DXC along with the increasing injection volume, the response for OTC and TTC only improved until 50 µL. Notably, the magnitude of the signal was very similar for injection volumes of 50 and 100 µL, which suggest either sample overload or a

slow detector response. To obtain the sensitivity and LOD desired for a simultaneous determination of four TCs in milk samples, 100 µL volume was selected.

The analytical parameters of the proposed TC-selective electrodes under flow conditions are slightly different than those obtained in static measurements (**Table S4**, ISM B). Under flow conditions, the residence and response time, the rate of diffusion and the exchange reaction of the eluent ions, the sample dispersion, and dilution, namely in flow-cell, affects the analytical performance of the proposed potentiometric detector, as has already been reported by other authors (22,48,53–55). To overtake these constraints, the use of carbon nanotubes in the sensing membrane was considered.

Effect of carbon nanotubes

Carbon nanotubes have been widely used as nanostructured materials in electrochemical sensors' preparation because of their remarkable properties such as large surface-area-to-volume ratio, mechanical strength, chemical stability, and excellent electrical conductivity (56). Their use has been associated with gains in the analytical performance of sensors, namely in LOD, sensitivity, and medium-term stability (57). In this work, the incorporation of MWCNTs in the ISM was investigated at different proportions (0.0, 1.0, and 2.0 wt%, see **Table 4.9**), and the general calibration parameters of the potentiometric sensors for the target TCs were evaluated under the optimal chromatographic conditions. As shown in **Table 4.11**, the incorporation of the MWCNTs (ISM C and D) improved the analytical features of the TC-selective electrodes, evidenced by the better slopes, LODs (calculated as a signal-to-noise ratio of 3), and repeatability of the peak heights for all the analytes. Their electrostatic interaction and hydrogen bonding with the target TCs as well as their contribution to improving the double-layer capacitance of the conductive surface of the electrode where the ion-to-electron transduction takes place allowed for the improvement of the magnitude of the signals within the linear response range by decreasing the response time (58), which contributed to an increase in the slope (comparing ISM B and ISM C in **Table 4.11**). However, it was not enough to reach the steady-state signal at the optimal measuring conditions, and, thus, the slopes were still lower than those obtained in static measurements (**Table 4.10**), especially for OTC, TTC, and DXC. Attending to the absence of a proper nomenclature of potentiometric detection in hydrodynamic separation systems, the LOD was calculated as generally defined in HPLC, using a signal-to-noise ratio of 3 (59). Nevertheless, the LOD values determined following the IUPAC recommendation were also calculated (49) (see **Table S5**). When using the signal-to-noise approach, the LODs

observed for the TCs with the ISM containing 1.0 wt% of MWCNTs (ISM C) were shifted to values below the MRL in milk defined by food authorities, attaining values down to $3.0x10^{-8}$ M for TTC, CTC, and DXC, and $1.0x10^{-7}$ M for OTC. Moreover, the improved repeatability of the analytical signal ($1.0x10^{-4}$ M, *n=3*) was demonstrated by the RSD% values of 0.2–5.8% against 0.4–42.1% in the electrodes prepared without MWCNTs (ISM B). However, when the proportion of MWCTNs was duplicated (ISM D), no gains were attained, and thus the TC-selective electrode prepared with the ISM C was selected for validation purposes.

Table 4.11 Effect of the incorporation of MWCNTs in the analytical performance of the miniaturized TC-selective electrodes coupled in the HPLC system.

Calibration parameter	ISM	MWCNTs (wt%)	OTC	TTC	CTC	DXC
Slope[a], mV dec^{-1}	B	0.0	11.2 ± 0.3	24.9 ± 5.8	34.7 ± 6.2	21.0 ± 7.0
	C	1.0	14.5 ± 0.3	31.0 ± 3.4	53.1 ± 5.5	41.3 ± 1.4
	D	2.0	13.9 ± 2.3	33.0 ± 4.5	52.4 ± 6.5	41.5 ± 3.0
LOD[b], M	B	0.0	$1.0x10^{-7}$	$1.0x10^{-7}$	$1.0x10^{-7}$	$1.0x10^{-7}$
	C	1.0	$1.0x10^{-7}$	$3.0x10^{-8}$	$3.0x10^{-8}$	$3.0x10^{-8}$
	D	2.0	$1.0x10^{-7}$	$1.0x10^{-7}$	$1.0x10^{-7}$	$1.0x10^{-7}$
Precision[c], RSD%	B	0.0	0.4	18.6	19.7	42.1
	C	1.0	5.8	0.2	3.4	1.8
	D	2.0	4.8	2.5	5.2	1.7

[a] Standard deviation value was calculated from three subsequent calibrations of the same electrode; [b] Based on a signal-to-noise ratio of 3; [c] Repeatability of the peak height calculated after triplicate injection of standard solution at $1.0x10^{-4}$ M

4.4.3.3. Method validation

The chromatographic parameters of the proposed HPLC method coupled to the potentiometric and UV detector are summarized in **Tables S6** and **S7**, respectively, namely retention times (t_R), retention factor (k), separation factor (α), effective plate number (N_{eff}), peak resolution (R_s), and tailing factor (T_f). The repeatability of retention times showed excellent results, providing RSD% values lower than 2.6% after the analysis in five independent days. The retention factors were fairly good, ranging from 1.2 to 1.6 for both types of detectors. The higher effective plate number obtained for CTC and DXC presented better separation efficiency, which is ascribed to the higher content of ACN during their elution. However, a slightly smaller value was obtained for all target TCs with the HPLC-ISE methodology, which may be attributed to the adsorption/desorption phenomena of the analytes at the membrane surface of the TC-selective electrode (22,60). This fact also

explains the differences obtained in the peak symmetry, demonstrated by the tailing factors of 1.4 to 1.6 and 1.1 to 1.2 for potentiometric and UV detectors, respectively. Although an increase in the ACN content in the mobile phase could accelerate the rate of dissociation (i.e., desorption phenomena) (22), it was not considered to avoid the dissolution of the membrane components. Overall, great peak resolution values were obtained for both types of detectors, ranging from 6.3 to 13.8 and from 7.4 to 16.0 for potentiometric and UV types, respectively, which are above the acceptable criteria (≥1.5).

Analytical figures of merit

The optimized method was validated according to the requirements of the International Council for Harmonisation of Technical Requirements for Pharmaceuticals for Human Use (ICH) (61) and the European Union (EU) (62) by evaluating the following analytical parameters: linear range, linearity, the limit of detection (LOD), the limit of quantification (LOQ), precision, accuracy, and specificity. The results of the potentiometric detector are summarized in **Table 4.12**, while those obtained with the UV detector are in **Table S8**.

The calibration curves were assessed by the injection of standard solutions of TCs at concentration levels in the range of $1.0\text{x}10^{-8}$–$1.0\text{x}10^{-4}$ M (*n=8*), and the corresponding chromatograms are presented in **Figure S11A, B** for the potentiometric and UV detector, respectively. A transformed response $tR = 10^{E/S} - 1$, where E is the potentiometric signal in mV and S is the slope of the Nikolsky–Eisenman equation, was used as the analytical signal of the potentiometric detector and plotted against the TCs' concentration (63). Linear regression lines were obtained for TTC, CTC, and DXC in the range from $1.0\text{x}10^{-7}$ to $1.0\text{x}10^{-5}$ M while, for OTC, it was in the range from $2.0\text{x}10^{-7}$ to $1.0\text{x}10^{-5}$ M, with coefficients of determination (R^2) ≥ 0.9973. Regarding the UV detector, the peak area was used as an analytical signal and plotted against the TCs' concentrations, attaining linear regression for all target TCs in the range from $1.0\text{x}10^{-8}$ to $1.0\text{x}10^{-5}$ M, with coefficients of determination (R^2) ≥ 0.9977.

The LOD and LOQ of the potentiometric detector were determined as the lowest injected concentration of the TCs giving a signal-to-noise ratio of 3 and 10, respectively, while the standard deviation of the blank and the slope of the calibration curve was used for the UV detector. In the former, LOD and LOQ values were $1.0\text{x}10^{-7}$ and $2.0\text{x}10^{-7}$ M for OTC, whereas, for TTC, CTC, and DXC, they were $3.0\text{x}10^{-8}$ and $1.0\text{x}10^{-7}$ M, respectively. These values correspond to a range of 13.3 to 46.0 μg L^{-1} and 44.4 to 92.1 μg L^{-1} for LOD and

LOQ, respectively. For comparison, the LOD and LOQ values obtained with the UV detector were $3.0x10^{-9}$ and $1.0x10^{-8}$ M for all target TCs, respectively. Nonetheless, as far as the authors know, this is the very first TC-selective electrode, coupled to HPLC, capable of determining TCs' residues around the MRL level (100 μg L^{-1}).

The precision of the HPLC method was assessed by the triplicate injection of standard solutions of TCs at concentrations of $3.0x10^{-7}$, $1.0x10^{-6}$, and $1.0x10^{-5}$ M on the same day and three different days. The intra- and inter-day precision results were expressed by the RSD% of the potentiometric and absorbance signal at each concentration level (**Tables 4.12 and S8**). In the intra-day, the RSD% ranged from 7.4 to 10.2%, 6.0 to 8.3%, and 4.1 to 7.1% for the potentiometric detector, while, for the UV detector, it ranged from 4.4 to 8.2%, 3.7 to 4.2%, and 2.9 to 4.2% at increasing TC concentration, respectively.

Table 4.12 Analytical figures of merit obtained with the proposed TC-selective electrode as detector in HPLC.

Validation parameters	**OTC**	**TTC**	**CTC**	**DXC**
Calibration curve		tR vs. [TC] μM		
Linear range, M	$2.0x10^{-7}$–$1.0x10^{-5}$	$1.0x10^{-7}$–$1.0x10^{-5}$	$1.0x10^{-7}$–$1.0x10^{-5}$	$1.0x10^{-7}$–$1.0x10^{-5}$
R^2	0.9987±0.0012	0.9986±0.0006	0.9973±0.0026	0.9983±0.0027
Slope	0.093±0.013	0.416±0.044	0.091±0.013	0.085±0.008
Intercept	-0.023±.0012	-0.083±0.015	0.006±0.013	0.010±0.008
LOD, M (μg L^{-1})	$1.0x10^{-7}$ (46.0)	$3.0x10^{-8}$ (13.3)	$3.0x10^{-8}$ (14.4)	$3.0x10^{-8}$ (13.3)
LOQ, M (μg L^{-1})	$2.0x10^{-7}$ (92.1)	$1.0x10^{-7}$ (44.4)	$1.0x10^{-7}$ (47.9)	$1.0x10^{-7}$ (44.4)
Precision (RSD%)				
		Intra-day		
3.0 x 10^{-7} M	10.2	7.9	12.5	7.4
1.0 x 10^{-6} M	6.0	8.3	6.7	6.6
1.0 x 10^{-5} M	6.6	4.1	7.1	4.9
		Inter-day		
3.0 x 10^{-7} M	4.4	11.7	13.1	13.5
1.0 x 10^{-6} M	1.6	10.0	7.2	4.9
1.0 x 10^{-5} M	1.7	3.7	5.1	7.2
		Inter-electrode		
3.0 x 10^{-7} M	12.0	10.7	5.1	2.9
1.0 x 10^{-6} M	5.9	9.4	8.3	12.9
1.0 x 10^{-5} M	6.2	3.7	8.9	6.2

Regarding the inter-day precision, the RSD% ranged from 4.4 to 13.5%, 1.6 to 10.0%, and 4.1 to 7.1% for the HPLC-POT, while for the HPLC-UV, it ranged from 6.1 to 11.5%, 5.3 to 19.1%, and 1.2 to 11.4%, respectively. The variations obtained for all the tested compounds

agree with the European requirements because they are lower than 20% and 10% for the applied target concentrations, proving the great precision of the method (62). Moreover, in the case of the potentiometric detector, the inter-electrode reproducibility (*n=3*) was also evaluated on a similar basis and showed RSD% values for the analytical signal ranging from 2.9 to 12.0%, 5.9 to 12.9%, and 3.7 to 8.9% at concentrations of 3.0×10^{-7}, 1.0×10^{-6}, and 1.0×10^{-5} M respectively.

Application in real sample analysis

To assess the accuracy and applicability of the proposed method, different milk samples containing 0, 50, 100, or 200 μg L^{-1} of standard solution were analyzed concerning the four TCs. The recoveries were calculated according to the following equation:

$$Recovery\ (\%) = \frac{TC_{Found} - TC_{Initial}}{TC_{Spiked}}\ x\ 100$$

in which TC_{Found} is the concentration of TCs measured in the extracts of the spiked milk samples, $TC_{Initial}$ is the intrinsic concentration of TCs in milk samples, and TC_{spiked} is the amount of TCs added to the milk samples. As observed in **Table 4.13**, TCs were not found in the collected milk samples and the recoveries ranged from 87.1 to 102.3%, 81.3 to 108.5%, and 84.1 to 103.9% in UHT skimmed milk, UHT semi-skimmed milk, and fresh semi-skimmed milk samples, respectively, with overall RSD% lower than 9.6%. These obtained values prove the required accuracy imposed by the European requirements, which only accept recovery values within the range between 80% and 110% for the applied target concentrations (62). For comparison purposes, the spiked milk samples were also analyzed with the UV detector and the obtained concentrations of the two groups were equal as statically demonstrated by the calculated p-values for the bilateral t-test with a 95% confidence level (**Table S9**).

To complete the method validation, the specificity was evaluated by comparing the chromatograms of the extracts obtained from spiked samples with those obtained from blank milk samples and working standard solutions containing a mixture of all TCs. **Figure 4.11** demonstrates that no interference between the matrix endogenous substances and the target TCs was found for the fresh semi-skimmed milk samples.

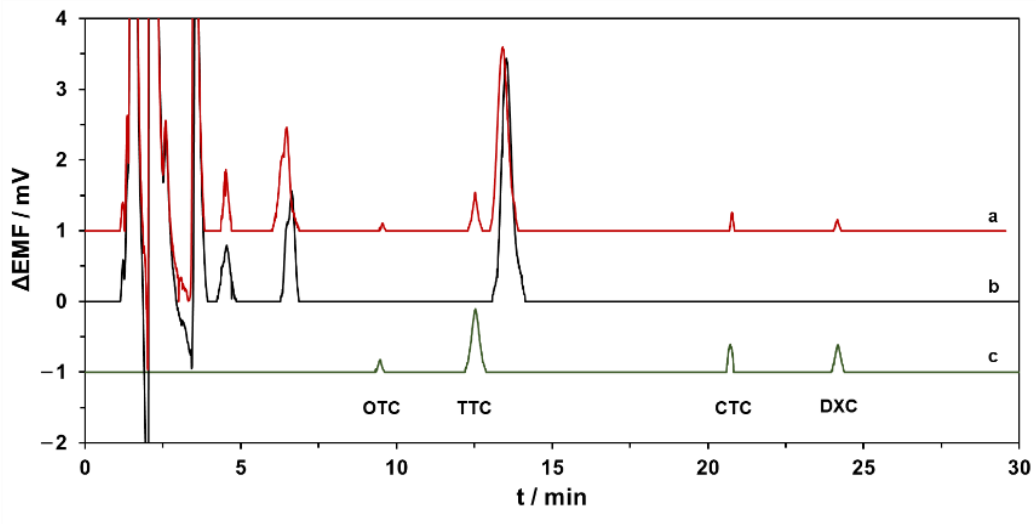

Figure 4.11 Chromatograms obtained with the proposed HPLC-ISE method after the injection of **(a)** extract of fresh semi-skimmed milk spiked at 100 μg L^{-1} (MRL level); **(b)** extract of blank fresh semi-skimmed milk; **(c)** standard solution of TCs at 3.0×10^{-7} M (≈140 μg L^{-1}).

Table 4.13 Recovery values of the proposed HPLC-ISE for the determination of TCs in spiked milk samples (*n=3* for each concentration).

		UHT skimmed milk			UHT semi-skimmed milk			Fresh semi-skimmed milk		
Analytes	**Added µg L^{-1}**	**Found µg L^{-1}**	**RSD%**	**RV %**	**Found µg L^{-1}**	**RSD%**	**RV %**	**Found µg L^{-1}**	**RSD%**	**RV %**
OTC	0	N.D.	-	-	N.D.	-	-	N.D.	-	-
	50	<LOQ	-	-	<LOQ	-	-	<LOQ	-	-
	100	100.1±3.2	3.2	100.1	103.3±4.9	4.8	103.3	98.0±6.9	7.1	98.0
	200	204.6±10.7	5.2	102.3	178.0±6.2	3.5	89.0	180.4±15.0	8.3	90.2
TTC	0	N.D.	-	-	N.D.	-	-	N.D.	-	-
	50	49.1±4.2	8.6	98.3	50.1±1.4	2.8	100.1	51.9±1.6	3.1	103.8
	100	91.0±6.1	6.7	91.0	87.7±5.3	6.0	87.7	84.1±3.2	3.8	84.1
	200	174.3±16.8	9.6	87.1	194.4±8.6	4.4	97.2	183.1±13.9	7.6	91.5
CTC	0	N.D.	-	-	N.D.	-	-	N.D.	-	-
	50	46.9±3.0	6.4	93.8	47.6±1.2	2.6	95.2	49.2±3.0	6.1	98.4
	100	88.5±7.9	8.9	88.5	88.7±2.0	2.3	88.7	103.9±4.5	4.3	103.9
	200	197.0±15.4	7.8	98.5	192.4±5.6	2.9	96.2	185.4±11.5	6.2	92.7
DXC	0	N.D.	-	-	N.D.	-	-	N.D.	-	-
	50	45.9±3.2	6.9	91.8	48.5±2.1	4.3	96.9	44.1±1.9	4.3	88.2
	100	95.6±2.0	2.1	95.6	108.5±2.1	1.9	108.5	88.1±3.1	3.5	88.1
	200	190.1±12.2	6.4	95.0	162.7±6.8	4.2	81.3	177.4±10.7	6.0	88.7

N.D. – Not detected; RV – Recovery.

4.3.3.4. Comparison of the proposed method with other conventional methods reported in the literature

The performance and the advantages of the herein proposed HPLC-ISE method were compared with the most recent methods based on HPLC for the determination of TCs' residues in milk samples (see **Table S10**). By comparing the analytical features, sample volume, and instrumental technique, the LC-MS/MS methods are strengthened by their powerful resolution, selectivity, and sensitivity (11,12). Among those advantages, MS/MS-based methods also allow multiclass detection (13,64), though the higher price of acquisition and maintenance, combined with the need for specialized human resources, limit their use in routine analysis for food quality control laboratories. Notably, the LOD/LOQ obtained with the proposed method enabled the determination of TCs below the MRL without a preconcentration step, which favorably contrasts with HPLC-UV methods (65,66). As such, the possibility of reducing the volume of the sample, and especially of the reagents during the determination, makes it a greener methodology. On the other hand, the HPLC-ISE method demonstrated great accuracy (recoveries from 81.3 to 108.5%) and precision (RSD < 9.6%) in the determination of TCs' residues around the MRL level in milk. Moreover, the simplicity and cost-effectiveness of the proposed potentiometric detector enhanced its use as an easy and affordable alternative to routine detectors.

Concerning the efficiency of the extraction method, the proposed SPE with OASIS PRIME HLB cartridges attained comparable and, in some cases, better recoveries than those of the other methods (67,68). However, the total analysis time (extraction and separation) was higher than other innovative procedures based on liquid microextraction (69,70), matrix solid-phase dispersion (71), and online SPE (72), though was comparable with those based on conventional SPE with OASIS HLB (67,68).

Overall, the proposed method provided a straightforward alternative for the determination of TCs in milk samples, and, to the best of our knowledge, this is the very first TC-selective electrode, coupled with HPLC, capable of determining TCs' residues around the MRL level (100 μg L^{-1}). Additionally, the portability and miniaturization ability of potentiometric sensors, combined with innovative sample operation techniques and the downsizing of chromatographic columns, will certainly leverage the development of an integrated lab-on-chip platform for the remote screening of TCs in food samples.

4.4.4. Conclusion

In the present work, the use of cucurbit[8]uril as a macrocyclic receptor improved the analytical features (i.e., LOD, sensitivity, and precision) already described for other tetracycline-selective electrodes with different ionophores. Moreover, the incorporation of multi-walled carbon nanotubes as nanostructured materials in the sensing membrane improved the detection limit as well as the repeatability of the analytical signal of the potentiometric detector under the optimized chromatographic conditions.

Therefore, a simple, cost-effective, and reliable HPLC-ISE method is proposed for the simultaneous determination of four tetracycline antibiotics in milk samples at levels around the maximum residue limits within an analysis time of 30 min. Noteworthy, the advantages of the proposed method highlight its competitiveness towards the currently used methods, based on HPLC with diode-array and mass spectrometry detection, for the routine analysis of tetracycline residues in food samples.

4.4.5. References

1. Chopra I, Roberts M. Tetracycline antibiotics: mode of action, applications, molecular biology, and epidemiology of bacterial resistance. Microbiol Mol Biol Rev 2001;65(2):232-60.

2. Yu H, Tao Y, Chen D, Wang Y, Yuan Z. Development of an HPLC–UV method for the simultaneous determination of tetracyclines in muscle and liver of porcine, chicken and bovine with accelerated solvent extraction. Food Chem. 2011;124(3):1131-8.

3. Sczesny S, Nau H, Hamscher G. Residue analysis of tetracyclines and their metabolites in eggs and in the environment by HPLC coupled with a microbiological assay and tandem mass spectrometry. J Agric Food Chem. 2003;51(3):697-703.

4. Han RW, Zheng N, Yu ZN, Wang J, Xu XM, Qu XY, et al. Simultaneous determination of 38 veterinary antibiotic residues in raw milk by UPLC–MS/MS. Food Chem. 2015;181:119-26.

5. Mookantsa SOS, Dube S, Nindi MM. Development and application of a dispersive liquid–liquid microextraction method for the determination of tetracyclines in beef by liquid chromatography mass spectrometry. Talanta. 2016;148:321-8.

6. Phillips I. Withdrawal of growth-promoting antibiotics in Europe and its effects in relation to human health. Int J Antimicrob Agents. 2007;30(2):101-7.

7. Food and Drug Administration. Code of Federal Regulations: Title 21 Food and Drugs; FDA: Silver Spring, Maryland, USA, 2021; Part 556, Sections 150, 500, and 720.

8. Codex Alimentarius Commission of the FAO/WHO. Maximum Residue Limits for Veterinary Drugs in Foods CX/MRL; FAO/WHO: Rome, Italy, 2018; pp. 1–46.

9. Önal A. Overview on liquid chromatographic analysis of tetracycline residues in food matrices. Food Chem. 2011;127(1):197-203.

10. Kargin ID, Sokolova LS, Pirogov AV, Shpigun OA. HPLC determination of tetracycline antibiotics in milk with post-column derivatization and fluorescence detection. Inorg Mater. 2016;52(14):1365-9.

11. Wei D, Wu SC, Zhu Y. Magnetic solid phase extraction based on graphene oxide/nanoscale zero-valent iron for the determination of tetracyclines in water and milk by using HPLC-MS/MS. Rsc Advances. 2017;7(70):44578-86.

12. Igualada C, Giraldo J, Font G, Yusà V. Validation of a multi-residue UHPLC-HRMS method for antibiotics screening in milk, fresh cheese, and whey. J Food Compost Anal. 2022;106:104265.

13. Zhang L, Shi L, He Q, Li Y. A rapid multiclass method for antibiotic residues in goat dairy products by UPLC-quadrupole/electrostatic field orbitrap high-resolution mass spectrometry. J Anal Sci Techno. 2021;12(1):14.

14. Bobacka J, Ivaska A, Lewenstam A. Potentiometric ion sensors. Chem Rev. 2008;108(2):329-51.

15. Zdrachek E, Bakker E. Potentiometric sensing. Anal Chem. 2019;91(1):2-26.

16. Alexander PW, Haddad PR, Trojanowicz M. Potentiometric detection in ion chromatography using a metallic copper indicator electrode. Chromatographia. 1985;20(3):179-84.

17. Haddad PR, Alexander PW, Trojanowicz M. Ion chromatography of Mg, Ca, Sr and Ba ions using a metallic copper electrode as a potentiometric detector. J Chromatogr A. 1984;294:397-402.

18. Haddad PR, Alexander PW, Trojanowicz M. Ion chromatography of inorganic anions with potentiometric detection using a metallic copper electrode. J Chromatogr. 1985;321(2):363-74.

19. Zielinska D, Gil A, Pietraszkiewicz M, Pietraszkiewicz O, Van de Vijver D, Nagels LJ. Podand and macrocyclic amine receptors with urea functionalities for potentiometric detection of organic acids in HPLC. Anal Chim Acta. 2004;523(2):177-84.

20. Bazylak G, Nagels LJ. Simultaneous high-throughput determination of clenbuterol, ambroxol and bromhexine in pharmaceutical formulations by HPLC with potentiometric detection. J Pharmaceut Biomed. 2003;32(4-5):887-903.

21. Vissers B, Bohets H, Everaert J, Cool P, Vansant EF, Du Prez F, et al. Characteristics of new composite- and classical potentiometric sensors for the determination of pharmaceutical drugs. Electrochim Acta. 2006;51(24):5062-9.

22. Daems D, Van Camp G, Fernandez M, Guisez Y, Prinsen E, Nagels LJ. Use of potentiometric detection in (ultra) high performance liquid chromatography and modelling with adsorption/desorption binding kinetics. Anal Chim Acta. 2013;777:25-31.

23. Uuml, Glein R, Br, Auml, Uchle C, Hampp N. Ion-selective electrodes for the determination of the antibiotic drug chlortetracycline. Anal Sci. 1994;10(6):959-62.

24. El-Ansary AL, Issa YM, Tag-Eldin AS. Tetracycline sensitive membrane electrodes based on poly (vinyl chloride) matrices and their use in drug analysis. Anal Letters. 1999;32(11):2177-90.

25. Moreira FTC, Kamel AH, Guerreiro JRL, Sales MGF. Man-tailored biomimetic sensor of molecularly imprinted materials for the potentiometric measurement of oxytetracycline. Biosens Bioelectron. 2010;26(2):566-74.

26. Coelho Moreira FT, Lara Guerreiro JR, Azevedo VL, Kamel AH, Ferreira Sales MG. New biomimetic sensors for the determination of tetracycline in biological samples: Batch and flow mode operations. Anal Methods. 2010;2(12):2039-45.

27. Gai P, Guo Z, Yang F, Duan J, Hao T, Wang S. Highly-sensitive ion selective electrode based on molecularly imprinted polymer particles for determination of tetracycline in aqueous samples. Russ J Electrochem. 2011;47(8):940.

28. Amorim CG, Araujo AN, Montenegro MC, Silva VL. Cyclodextrin-based potentiometric sensors for midazolam and diazepam. J Pharm Biomed Anal. 2008;48(4):1064-9.

29. Shishkanova TV, Sykora D, Sessler JL, Kral V. Potentiometric response and mechanism of anionic recognition of heterocalixarene-based ion selective electrodes. Anal Chim Acta. 2007;587(2):247-53.

30. Ali TA, Mohamed GG, El-Sonbati AZ, Diab MA, Elkfass AM. A potentiometric sensor for determination of doxycycline hydrochloride in pharmaceutical preparation and biological fluids. Russ J Electrochem. 2018;54(12):1081-95.

31. Cunha CO, Silva RCR, Amorim CG, Junior SA, Araujo AN, Montenegro MCBSM, et al. Tetracycline potentiometric sensor based on cyclodextrin for pharmaceuticals and waste water analysis. Electroanal. 2010;22(24):2967-72.

32. Barrow SJ, Kasera S, Rowland MJ, del Barrio J, Scherman OA. Cucurbituril-based molecular recognition. Chem Rev. 2015;115(22):12320-406.

33. Lagona J, Mukhopadhyay P, Chakrabarti S, Isaacs L. The Cucurbit(n)uril family. Angew Chem Int Ed. 2005;44(31):4844-70.

34. Das D, Assaf KI, Nau WM. Applications of cucurbiturils in medicinal chemistry and chemical biology. Front Chem. 2019;7(619).

35. Chang Y-X, Qiu Y-Q, Du L-M, Li C-F, Guo M. Determination of ranitidine, nizatidine, and cimetidine by a sensitive fluorescent probe. Analyst. 2011;136(20):4168-73.

36. Sueldo Occello VN, Veglia AV. Cucurbit(6)uril nanocavity as an enhanced spectrofluorimetric method for the determination of pyrene. Anal Chim Acta. 2011;689(1):97-102.

37. Guo J, Shi L, Liu M. Ultrastable cucurbit(6)uril-based multifunctional supramolecular assembly for efficient detection of nitroaromatic compounds and antibiotics. New J Chem. 2021;45(38):18221-8.

38. del Pozo M, Mejías J, Hernández P, Quintana C. Cucurbit(8)uril-based electrochemical sensors as detectors in flow injection analysis. Application to dopamine determination in serum samples. Sens Actuators B Chem. 2014;193:62-9.

39. Liu J, Lambert H, Zhang Y-W, Lee T-C. Rapid estimation of binding constants for cucurbit(8)uril ternary complexes using electrochemistry. Anal Chem. 2021;93(9):4223-30.

40. Cheng W, Ma J, Kong D, Zhang Z, Khan A, Yi C, et al. One step electrochemical detection for matrix metalloproteinase 2 based on anodic stripping of silver nanoparticles mediated by host-guest interactions. Sens Actuators B Chem. 2021;330:129379.

41. Amorim CG, Araujo A, Montenegro MD. Use of cucurbit(6)uril as ionophore in ion selective electrodes for etilefrine determination in pharmaceuticals. Electroanal. 2019;31(11):2171-8.

42. Ferreira C, Palmeira A, Sousa E, Amorim CG, Araujo AN, Montenegro MC. Supramolecular atropine potentiometric sensor. Sensors. 2021;21(17).

43. Gil RL, Amorim CG, Montenegro MCBSM, Araújo AN. Determination of biogenic amines in tomato by ion-pair chromatography coupled to an amine-selective potentiometric detector. Electrochim Acta. 2021:138134.

44. Gil RL, Amorim CG, Montenegro MCBSM, Araújo AN. HPLC-potentiometric method for determination of biogenic amines in alcoholic beverages: A reliable approach for food quality control. Food Chem. 2022;372:131288.

45. Waters. Application note. 2013. (Available from:https://www.waters.com/webassets/cms/library/docs/720004582en.pdf).

46. Wen Y, Wang Y, Feng Y-Q. Simultaneous residue monitoring of four tetracycline antibiotics in fish muscle by in-tube solid-phase microextraction coupled with high-performance liquid chromatography. Talanta. 2006;70(1):153-9.

47. Cuartero M, Amorim CG, Araújo AN, Ortuño JA, Montenegro MCBSM. A SO2-selective electrode based on a Zn-porphyrin for wine analysis. Anal Chim Acta. 2013;787:57-63.

48. Tóth K, Fucskó J, Lindner E, Fehér Z, Pungor E. Potentiometric detection in flow analysis. Anal Chim Acta. 1986;179:359-70.

49. Richard P. Buch EL. Recomendations for nomenclature of ion-selective electrodes (IUPAC Recommendations 1994). Pure Appl Chem. 1994;66(12):2527-36.

50. Poels I, Nagels LJ. Potentiometric detection of amines in ion chromatography using macrocycle-based liquid membrane electrodes. Anal Chim Acta. 2001;440(2):89-98.

51. Zielinska D, Poels I, Pietraszkiewicz M, Radecki J, Geise HJ, Nagels LJ. Potentiometric detection of organic acids in liquid chromatography using polymeric liquid membrane electrodes incorporating macrocyclic hexaamines. J Chromatogr A. 2001;915(1-2):25-33.

52. Amorim CG, Souza RC, Araujo AN, Montenegro MCBSM, Silva VL. SI lab-on-valve analysis of histamine using potentiometric detection for food quality control. Food Chem. 2010;122(3):871-6.

53. Toth K, Stulik K, Kutner W, Feher Z, Lindner E. Electrochemical detection in liquid flow analytical techniques: characterization and classification - (IUPAC Technical Report). Pure Appl Chem. 2004;76(6):1119-38.

54. Montenegro, M.C.B.S.M.; Araújo, A.N. Flow Potentiometry. In Advances in Flow Analysis; Trojanowicz, M. Ed.; Wiley-VCH: Weinheim, Germany, 2008.

55. Amorim CG, Araújo AN, Montenegro MCBSM, Silva VL. Sequential injection lab-on-valve procedure for the determination of amantadine using potentiometric methods. Electroanal. 2007;19(21):2227-33.

56. Saleh Ahammad AJ, Lee J-J, Rahman MA. Electrochemical sensors based on carbon nanotubes. Sensors. 2009;9(4):2289-319.

57. Yuan D, Anthis AHC, Ghahraman Afshar M, Pankratova N, Cuartero M, Crespo GA, et al. All-solid-state potentiometric sensors with a multiwalled carbon nanotube inner transducing layer for anion detection in environmental samples. Anal Chem. 2015;87(17):8640-5.

58. Crespo GA, Macho S, Rius FX. Ion-selective electrodes using carbon nanotubes as ion-to-electron transducers. Anal Chem. 2008;80(4):1316-22.

59. Brunetti B DE. About estimating the limit of detection by the signal to noise approach. Pharm Anal Acta. 2015;06(04).

60. Daems D, De Wael K, Vissenberg K, Van Camp G, Nagels L. Potentiometric sensors doped with biomolecules as a new approach to small molecule/biomolecule binding kinetics analysis. Biosens Bioelectron. 2014;54:515-20.

61. ICH. ICH harmonised tripartite guideline: Validation of analytical procedures: text and methodology Q2 (R1) ICH, Geneva, Switzerland, 2005 (Available from: https://www.ich.org/page/quality-guidelines).

62. Union E. Commission Decision of 12 August 2002 implementing Council Directive 96/23/EC concerning the performance of analytical methods and the interpretation of results. Off J Eur Communities; 2002. p. 8-36.

63. Sekula J, Everaert J, Bohets H, Vissers B, Pietraszkiewicz M, Pietraszkiewicz O, et al. Coated wire potentiometric detection for capillary electrophoresis studied using organic amines, drugs, and biogenic amines. Anal Chem. 2006;78(11):3772-9.

64. Rossi R, Saluti G, Moretti S, Diamanti I, Giusepponi D, Galarini R. Multiclass methods for the analysis of antibiotic residues in milk by liquid chromatography coupled to mass spectrometry: A review. Food Addit. Contam. Part A. 2018;35(2):241-57.

65. Vuran B, Ulusoy HI, Sarp G, Yilmaz E, Morgul U, Kabir A, et al. Determination of chloramphenicol and tetracycline residues in milk samples by means of nanofiber coated magnetic particles prior to high-performance liquid chromatography-diode array detection. Talanta. 2021;230.

66. Tang HZ, Wang YH, Li S, Wu J, Gao ZX, Zhou HY. Development and application of magnetic solid phase extraction in tandem with liquid-liquid extraction method for determination of four tetracyclines by HPLC with UV detection. J Food Sci Technol 2020;57(8):2884-93.

67. Yue Z, Qiu Y, Liu X, Ji C. Determination of multi-residues of tetracyclines and their metabolites in milk by high performance liquid chromatography-tandem positive-ion electrospray ionization mass spectrometry. Chinese J Anal Chem. 2006;34(9):1255-9.

68. Vargas Mamani MC, Reyes Reyes FG, Rath S. Multiresidue determination of tetracyclines, sulphonamides and chloramphenicol in bovine milk using HPLC-DAD. Food Chem. 2009;117(3):545-52.

69. Kaynaker M, Antep M, Merdivan M. Determination of tetracyclines in milk, eggs and honey using in-situ ionic liquid based dispersive liquid-liquid microextraction. J Anal Chem. 2018;73(1):23-9.

70. Al-Afy N, Sereshti H, Hijazi A, Nodeh HR. Determination of three tetracyclines in bovine milk using magnetic solid phase extraction in tandem with dispersive liquid-liquid microextraction coupled with HPLC. J Chromatogr B. 2018;1092:480-8.

71. Wang SS, Zhang JF, Li CY, Chen LG. Analysis of tetracyclines from milk powder by molecularly imprinted solid-phase dispersion based on a metal-organic framework followed by ultra high performance liquid chromatography with tandem mass spectrometry. J Sep Sci. 2018;41(12):2604-12.

72. de Faria HD, Rosa MA, Silveira AT, Figueiredo EC. Direct extraction of tetracyclines from bovine milk using restricted access carbon nanotubes in a column switching liquid chromatography system. Food Chem. 2017;225:98-106.

4.4.6. Supplementary material

Experimental section

Potentiometric measurements. All experiments were carried out at room temperature of 22±1°C. To calibrate each tetracycline-selective electrode, the dynamic potentiometric response was obtained at increasing concentrations of tetracycline antibiotics solution and then, the corresponding logarithmic concentrations *(c_{TC})* were plotted versus the steady-state EMF value (ionic strength adjusted with 0.05 M of oxalic acid solution). The data were fitted to the Nernst equation to obtain the sensitivity (slope) and intercept (49). The limit of detection (LOD) of the potentiometric electrodes was calculated as the concentration related to the cross point between the extrapolation of the lines defining the nonresponsive range and linear-response range of the electrode (49). The response time was determined as the time that elapses between the instant at which the concentration of the target TC is changed in the solution and the first instant at which the measured EMF of the electrochemical cell becomes equal to 95% of the signal at a steady-state (49).

Tables

Table S4 Linear fittings (EMF response in mV *versus* logarithmic concentration) for the tetracycline-selective electrode (ISM B) in batch and flow conditions.

Calibration parameter		OTC	TTC	CTC	DXC
Slope[a], mV dec^{-1}					
	Batch	56.2±0.9	53.8±2.2	63.4±2.1	59.0±0.1
	Flow	11.2±0.3	24.9±5.8	34.7±6.2	21.0±7.0
LRR, M					
	Batch	6.0×10^{-6} – 1.0×10^{-3}	1.0×10^{-6} – 1.0×10^{-3}	3.0×10^{-7} – 1.0×10^{-3}	3.0×10^{-7} – 1.0×10^{-3}
	Flow	1.0×10^{-5} – 1.0×10^{-4}	1.0×10^{-5} – 1.0×10^{-4}	1.0×10^{-5} – 1.0×10^{-4}	1.0×10^{-5} – 1.0×10^{-4}
LOD[a,b], M					
	Batch	$(2.5\pm0.0)\times10^{-6}$	$(4.3\pm0.5)\times10^{-7}$	$(1.5\pm1.3)\times10^{-7}$	$(1.8\pm0.7)\times10^{-7}$
	Flow	$(7.5\pm0.2)\times10^{-6}$	$(5.2\pm0.2)\times10^{-6}$	$(8.2\pm0.1)\times10^{-6}$	$(7.1\pm1.5)\times10^{-6}$

[a] Standard deviation value was calculated from three subsequent calibrations of the same electrode;
[b] Based on conventional definition used in potentiometry (49)

LRR: Linear response range; LOD: Limit of detection.

Table S5 Limits of detection (calculated by IUPAC recommendation (49)) of the miniaturized TC-selective electrodes prepared with different amounts of MWCNTs.

Calibration parameter	ISM	MWCNTs (wt%)	OTC	TTC	CTC	DXC
LOD (IUPAC)[c], M						
	B	0.0	7.5×10^{-6}	5.2×10^{-6}	8.2×10^{-6}	7.1×10^{-6}
	C	1.0	5.5×10^{-6}	1.9×10^{-6}	7.5×10^{-6}	7.9×10^{-6}
	D	2.0	5.2×10^{-6}	3.4×10^{-6}	7.9×10^{-6}	7.7×10^{-6}

Table S6 Chromatographic parameters of the target tetracycline antibiotics using the proposed HPLC-potentiometric method.

Analyte	t_R	N_{eff}	k	α	R_s	T_f
Oxytetracycline	9.3	5900	8.0			1.4
				1.4	6.3	
Tetracycline	12.9	6121	11.5			1.6
				1.6	13.8	
Chlortetracycline	21.2	48926	18.3			1.5
				1.2	8.2	
Doxycycline	24.7	44519	21.4			1.4

t_R, retention time, in minutes; N_{eff}, effective plate number; k, retention factor; α, separation factor, between every two successive peaks; R_s, peak resolution, between every two successive peaks; T_f, tailing factor.

Table S7 Chromatographic parameters of the target tetracycline antibiotics using the HPLC-UV method.

Analyte	t_R	N_{eff}	k	α	R_s	T_f
Oxytetracycline	9.3	8221	8.0			1.2
				1.4	7.4	
Tetracycline	12.9	8233	11.5			1.1
				1.6	16.0	
Chlortetracycline	21.2	67084	18.3			1.1
				1.2	9.0	
Doxycycline	24.7	47146	21.4			1.1

t_R, retention time, in minutes; N_{eff}, effective plate number; k, retention factor; α, separation factor, between every two successive peaks; R_s, peak resolution, between every two successive peaks; T_f, tailing factor.

Table S8 Analytical figures of merit obtained with the proposed HPLC method using the UV detector (355 nm).

Validation parameters	OTC	TTC	CTC	DXC
Calibration curve		Peak area (U.A. x s) vs [TC] µM		
Linear range, M	$1.0x10^{-8}$–$1.0x10^{-5}$	$1.0x10^{-8}$–$1.0x10^{-5}$	$1.0x10^{-8}$–$1.0x10^{-5}$	$1.0x10^{-8}$–$1.0x10^{-5}$
R^2	0.9995±0.0002	0.9994±0.0001	0.9992±0.0007	0.9977±0.0031
Slope	0.067±0.007	0.081±0.009	0.034±0.004	0.047±0.008
Intercept	0.001±.0.006	0.001±0.008	0.000±0.003	-0.004±0.004
LOD, M (µg L^{-1})	$3.0x10^{-9}$ (1.4)	$3.0x10^{-9}$ (1.3)	$3.0x10^{-9}$ (1.4)	$3.0x10^{-9}$ (1.3)
LOQ, M (µg L^{-1})	$1.0x10^{-8}$ (4.6)	$1.0x10^{-8}$ (4.4)	$1.0x10^{-8}$ (4.8)	$1.0x10^{-8}$ (4.4)
Precision (RSD%)				
		Intra-day		
3.0×10^{-7} M	4.4	5.4	3.8	8.2
1.0×10^{-6} M	3.7	3.8	4.2	4.0
1.0×10^{-5} M	2.9	3.3	3.8	4.2
		Inter-day		
3.0×10^{-7} M	6.1	11.5	10.8	9.4
1.0×10^{-6} M	7.5	5.3	19.1	14.3
1.0×10^{-5} M	4.0	2.6	1.2	11.4

Table S9 Results obtained for determination of TCs in spiked milk samples by HPLC using the proposed potentiometric detector compared with the UV detector (*n=3* for each concentration).

Analytes		Samples								
		UHT skimmed milk			UHT semi-skimmed milk			Fresh semi-skimmed milk		
	Added µg L^{-1}	HPLC-POT	HPLC-UV	p-value[a]	HPLC-POT	HPLC-UV	p-value[a]	HPLC-POT	HPLC-UV	p-value[a]
OTC	50	<LOQ	46.7±1.4	–	<LOQ	52.9±2.8	–	<LOQ	49.0±2.0	–
	100	100.1±3.2	102.3±3.6	0.478	103.3±4.9	101.3±3.5	0.607	98.0±6.9	98.0±1.0	0.990
	200	204.6±10.7	193.8±0.6	0.223	178.0±6.2	179.9±3.5	0.677	180.4±15.0	177.1±15.2	0.802
TTC	50	49.1±4.2	48.4±0.8	0.806	50.1±1.4	48.2±1.7	0.231	51.9±1.6	49.4±1.2	0.097
	100	91.0±6.1	96.1±2.4	0.247	87.7±5.3	86.1±3.6	0.678	84.1±3.2	81.6±0.7	0.258
	200	174.3±16.8	163.3±3.3	0.383	194.4±8.6	197.4±4.2	0.617	183.1±13.9	183.6±3.5	0.952
CTC	50	46.9±3.0	41.3±2.7	0.074	47.6±1.2	48.3±4.0	0.778	49.2±3.0	52.4±2.7	0.144
	100	88.5±7.9	96.3±0.7	0.231	88.7±2.0	85.7±1.1	0.083	103.9±4.5	101.8±0.5	0.510
	200	197.0±15.4	195.7±2.4	0.901	192.4±5.6	188.1±3.6	0.331	185.4±11.5	179.2±2.3	0.456
DXC	50	45.9±3.2	52.3±3.8	0.087	48.5±2.1	51.9±2.0	0.111	44.1±1.9	45.2±1.6	0.503
	100	95.6±2.0	97.0±0.7	0.319	108.5±2.1	111.5±1.0	0.087	88.1±3.1	85.4±1.4	0.242
	200	190.1±12.2	184.7±4.6	0.513	162.7±6.8	165.2±4.4	0.624	177.4±10.7	171.7±2.4	0.459

[a] p-value calculated from the bilateral t-test with 95% confidence level.

Table S10 Comparison of the proposed method with other published methods for the determination of TCs in milk samples.

Analytes	Extraction method	Sample volume	Instrumental technique	Analysis time	LOD/LOQ	PF	Intra-day RSD%	Recovery %	Ref.
CTC, DXC, MTC, TTC	IL-DLLME	5 mL	HPLC-DAD	27 min	0.12-0.45/- μg L^{-1}	25-98	0.6-1.2	75.8-109.2	(69)
CTC, OTC, TTC	MSPD	0.18 g	HPLC-MS/MS	18 min	0.2-0.3/0.7-1.1 μg kg^{-1}	N.G.	3.8-6.9	84.7-92.8	(71)
CTC, DMC, DXC, OTC, TTC	dSPE	3 g	UHPLC-HRMS	> 30 min	-/25 μg kg^{-1}	N.G.	9-19	101-109	(12)
CTC, DXC	Prime HLB- SPE	1 g	HPLC-MS/MS	> 60 min	0.5-1.0/5.0-10.0 μg kg^{-1}	N.G.	5.1-9.5	70.3-102.4	(13)
CTC, DXC, OTC, TTC	RACNTs-SPE	0.5 mL	HPLC-DAD	12 min	7.5-13.2/25.0-44.0 μg L^{-1}	N.G.	3.9-17.6	47.0-59.0	(72)
CTC, DMC, OTC, TTC,	Mag-SPE	10 mL	HPLC-MS/MS		8.1-83.2/17.4-182.7 ng L^{-1}	50	1.1-5.4	87.0-101.8	(11)
TTC	Mag-SPE	5 mL	HPLC-DAD	> 30 min	3.5/9.8 μg L^{-1}	100	3.8	94.6-105.4	(65)
CTC, DXC, OTC, TTC	Mag-SPE	1 mL	HPLC-DAD	> 45 min	40/50 μg L^{-1}	4	1.1-2.2	87.8-107.5	(66)
DXC, OTC, TTC	Mag-SPE-DLLME	1 mL	HPLC-UV	> 60 min	1.8-2.9/6.1-9.8 μg L^{-1}	66.7	0.1-6.9	70.6-121.5	(70)
DXC, CTC, OTC, TTC	HLB- SPE	5 g	HPLC-MS/MS	> 60 min	1-10/50 μg kg^{-1}	10	1.8-8.3	74.4-101	(67)
CTC, OTC, TTC	HLB-SPE	5 mL	HPLC-DAD	> 60 min	20/60 μg L^{-1}	10	2.7-4.9	83-112	(68)
CTC, DXC, OTC, TTC	Prime HLB- SPE	1 mL	HPLC-POT	> 60 min	13.3-46.0/44.4-92.1 μg L^{-1}	Not applied	0.5-11.2	81.3-108.5	This work

CTC – chlortetracycline; DAD – diode-array detector; DLLME – dispersive liquid liquid microextraction; DMC – demeclocycline; dSPE – dispersive solid phase extraction; DXC – doxycycline; HRMS – high resolution mass spectrometry; IL – ionic liquid; MSPD – matrix solid phase dispersion; MagSPE – Magnetic solid phase extraction; MS/MS - tandem mass spectrometric detector; MSPD – matrix solid phase dispersion; MTC – methacycline; N.G. not given; OTC – oxytetracycline; PF – pre-concentration; POT – potentiometric detector; RACNTs – restricted accesses carbon nanotubes; SPE – solid phase extraction; TTC – tetracycline; UV – ultraviolet detector.

Figures

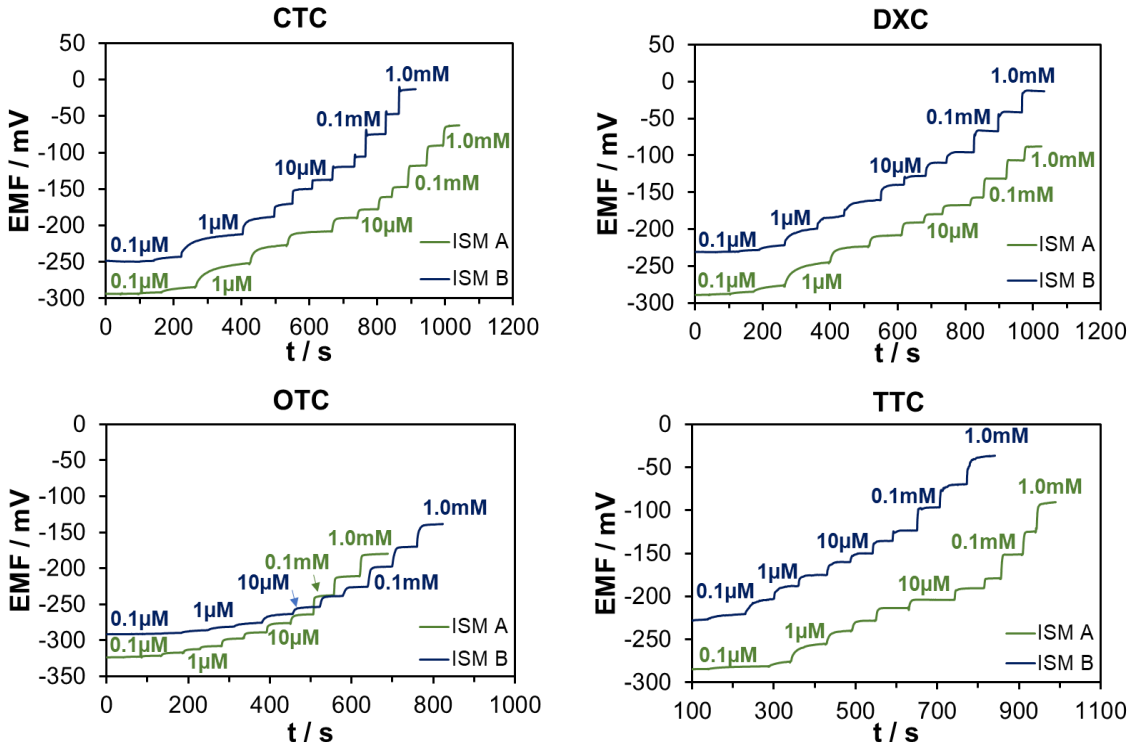

Figure S6 Dynamic potentiometric responses for ion-selective electrodes prepared without (ISM A) and with CB(8) (ISM B) in batch conditions at the increasing concentration of chlortetracycline (CTC), doxycycline (DXC), oxytetracycline (OTC), and tetracycline (TTC).

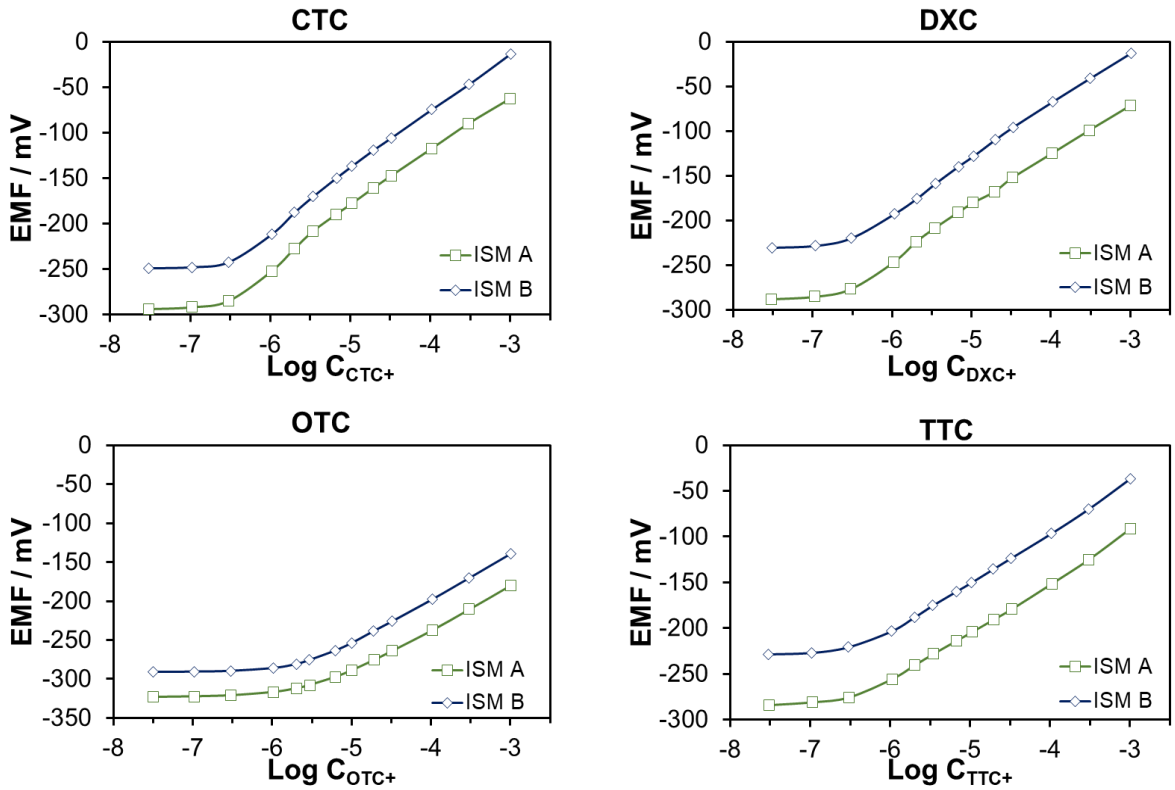

Figure S7 Calibration curves of EMF responses of CTC, DXC, OTC, and TTC obtained with the ion-selective electrodes prepared without (ISM A) and with CB(8) (ISM B) in batch conditions.

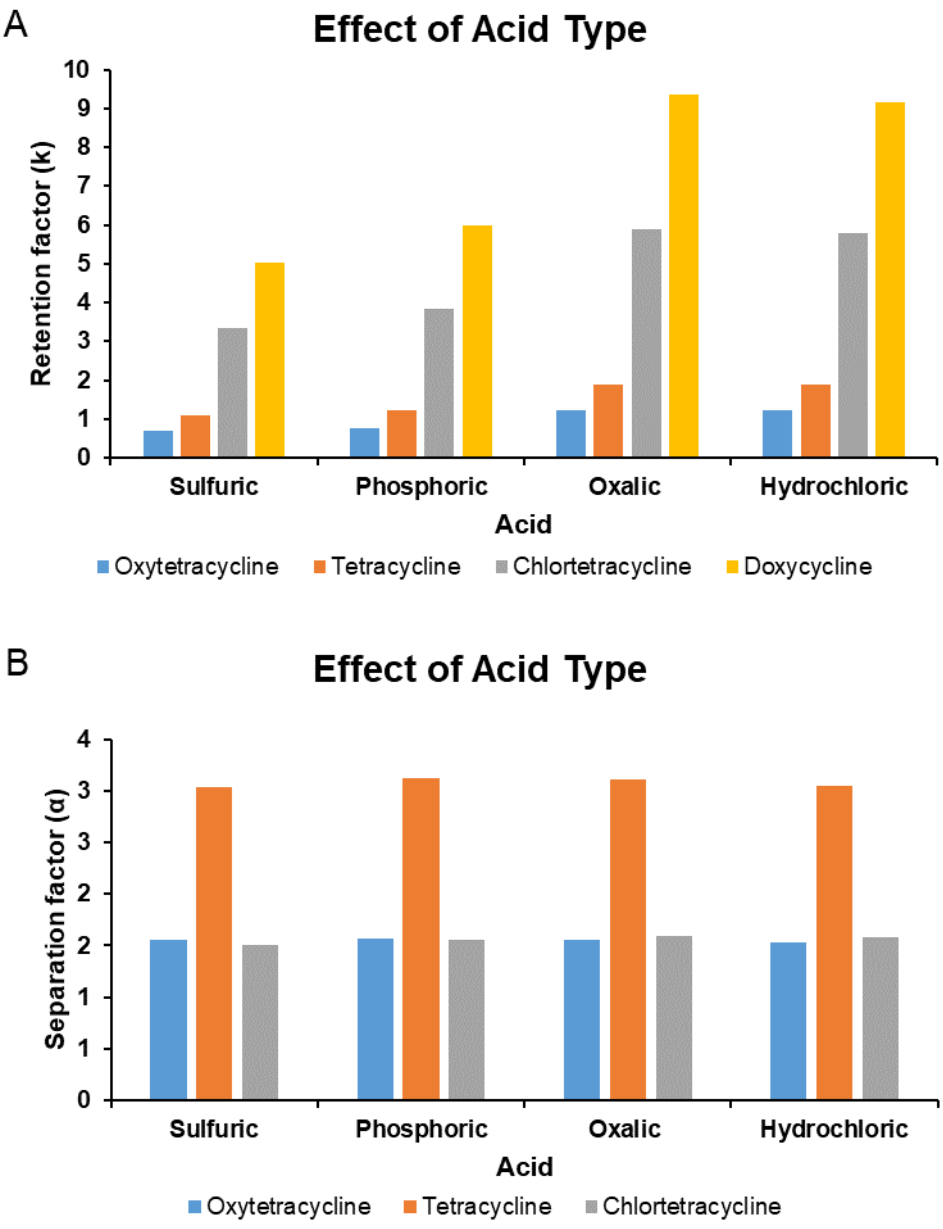

Figure S8 Effect of the acidifying agent of the mobile phase in the (A) retention and (B) separation factors.

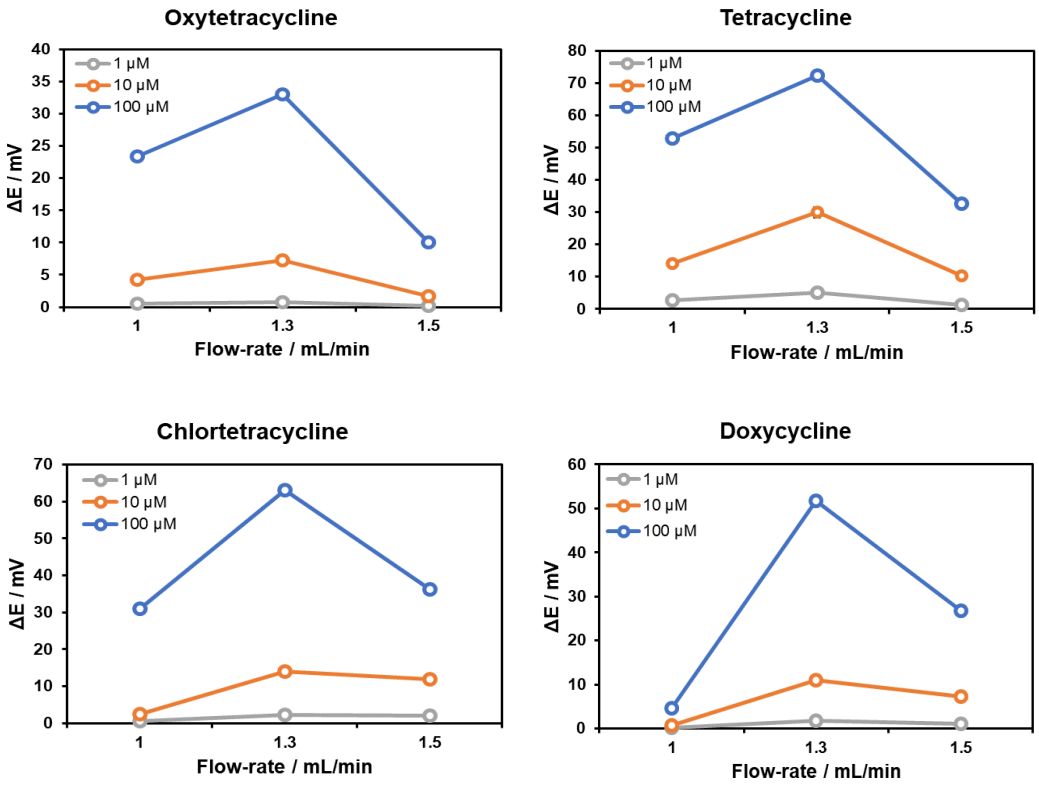

Figure S9 Detector performance (peak heights in mV) for standard solutions of four tetracycline antibiotics at 1.0, 10.0, and 100.0 µM as a function of the mobile phase flow rate.

Gradient elution: solvent A – 0.005 M H_2SO_4:ACN (90:10, v/v) and solvent B – 0.005 M H_2SO_4:ACN (80:20, v/v); Column: Luna 5 µm C8(2), 150 x 4.6 mm I.D. (Phenomenex); Injection volume: 100 µL.

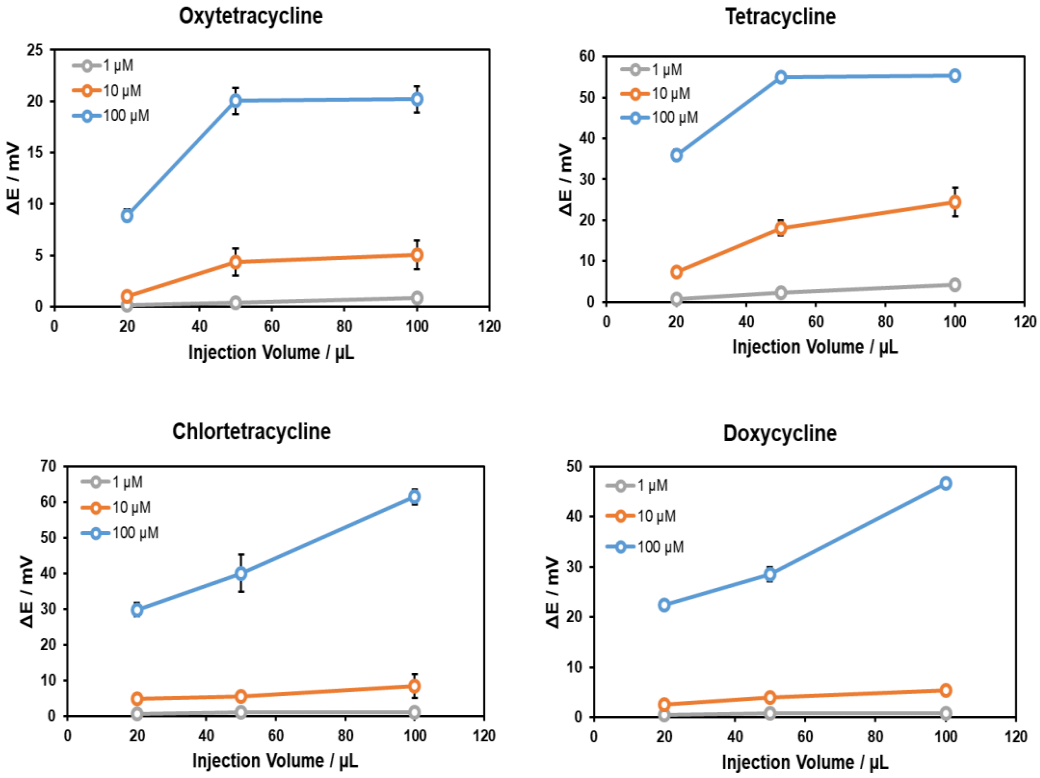

Figure S10 Detector performance (peak heights in mV) for standard solutions of four tetracycline antibiotics at 1.0, 10.0, and 100.0 µM as a function of the injection volume.

Gradient elution: solvent A – 0.005 M H_2SO_4:ACN (90:10, v/v) and solvent B – 0.005 M H_2SO_4:ACN (80:20, v/v); Column: Luna 5 µm C8(2), 150 x 4.6 mm I.D. (Phenomenex); Flow rate: 1.3 mL min^{-1}.

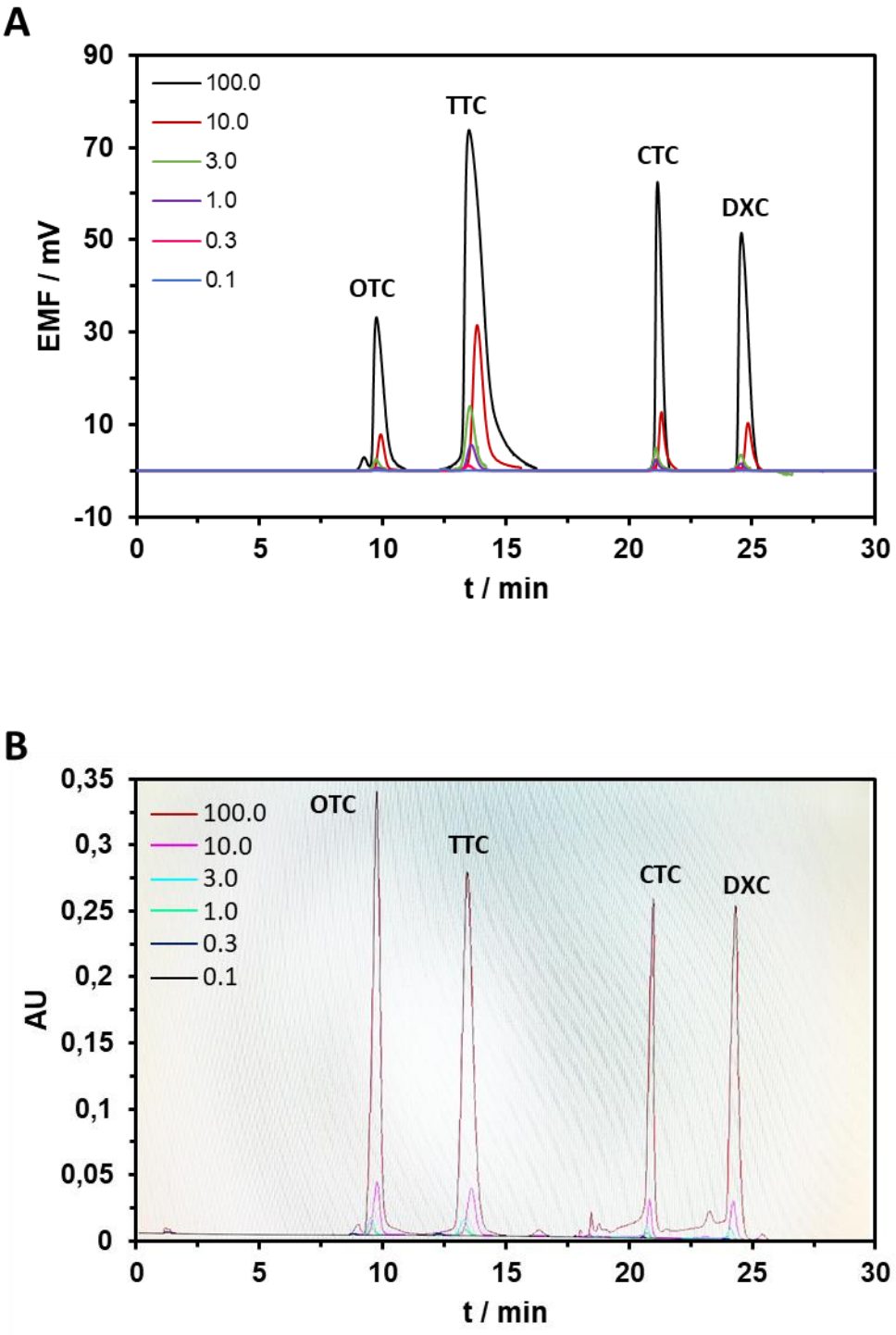

Figure S11 Chromatograms at increasing concentrations (0.1, 0.3, 1.0, 3.0, 10.0, 100.0 µM) of TCs obtained with the proposed tetracycline potentiometric detector (A) and the UV detector (wavelength 355 nm) in HPLC.

Gradient elution: solvent A – 0.005 M H_2SO_4:ACN (90:10, v/v) and solvent B – 0.005 M H_2SO_4:ACN (80:20, v/v); Column: Luna 5 µm C8(2), 150 x 4.6 mm I.D. (Phenomenex); Flow rate: 1.3 mL min^{-1}.

Chlortetracycline (CTC), doxycycline (DXC), oxytetracycline (OTC), and tetracycline (TTC).

4.5. Addressing the detection of ammonium ion in environmental water samples via tandem potentiometry–ion chromatography

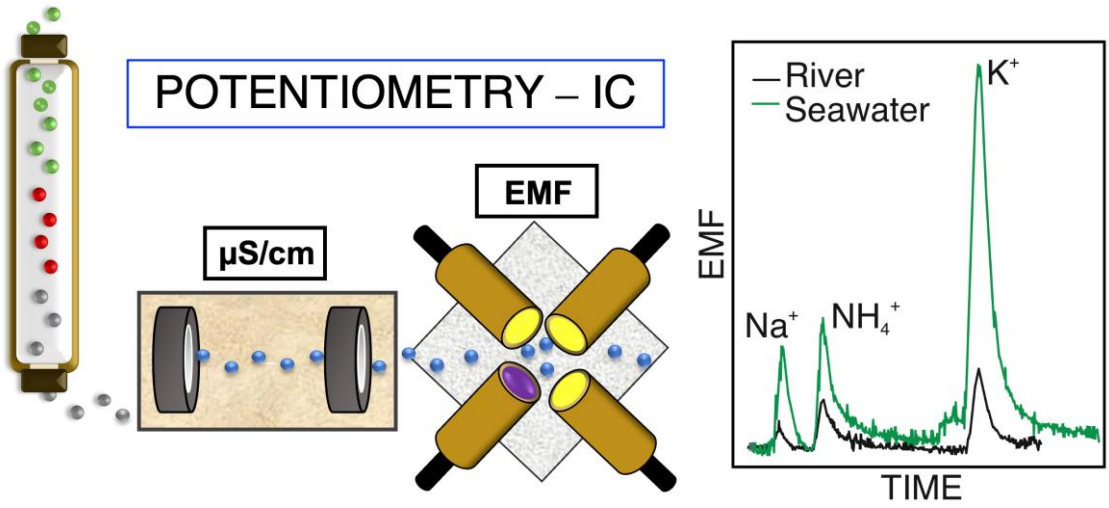

Section 4.5 describes the improvement of the analytical performance of ammonium-selective electrodes based on nonactin as ionophore by their synergic coupling with ion-chromatography for the determination of ammonium ions at micromolar levels in water samples[5].

[5] This is a partial transcription of the article *Renato L. Gil, Célia G. Amorim, Maria Cuartero, Addressing the detection of ammonium ion in environmental water samples via tandem potentiometry–ion chromatography; ACS Measurement Science Au 2022; doi: 10.1021/acsmeasuresciau.1c00056*; copyright 2022, with permission from ACS.

4.5.1. Introduction

The ammonium ion (NH_4^+) is one of the primary compounds involved in the biogeochemical cycle of nitrogen (N) in aquatic environments (1, 2). Despite its distribution in freshwaters being highly variable regionally, seasonally, and spatially within streams and lakes, the concentration of total ammonia nitrogen (TAN) in well-oxygenated waters is usually low (typical values ranging from 7 to 60 μg TAN L^{-1}) (1). When the N-cycle becomes unbalanced, detrimental consequences manifest for the water life: high NH_4^+ levels (> 2 mg TAN L^{-1}) are known to translate into undesired eutrophication and poor water quality (1, 2). Excessive NH_4^+ levels may occur through direct means (municipal effluent discharges and the animal waste) or indirect sources (nitrogen fixation, air deposition, and runoff from agricultural lands) (3). Altogether, the NH_4^+ content is considered an important environmental indicator, and monitoring it is crucial for effective water ecosystem preservation (2).

Analytical methodologies for NH_4^+ detection have been developed for many years (4, 5). Spectrophotometric, conductometric, and potentiometric readouts stand out for the specific application of water analysis among the available techniques. Potentiometric ion-selective electrodes (ISEs), based on ion-selective membranes (ISMs), are particularly interesting because of their capacity for decentralized measurements (6). Indeed, a recent review has thoroughly discussed the analytical features and applications of NH_4^+-selective electrodes reported in the last decade (7). Considering the ionophore (or receptor) as the core element of the ISM, effective NH_4^+ recognition has been accomplished over many years (7). At present, nonactin is the most utilized ionophore, despite its significant drawback of forming complexes with other cations of similar ionic size and charge to NH_4^+, such as potassium (K^+) and sodium (Na^+) ions. Thus, the presence of excess K^+ and Na^+ compared to NH_4^+ in the sample could hinder accurate determination with ISEs, rendering the effective detection of NH_4^+ difficult in either aqueous or other samples. To overcome this issue of selectivity, several strategies have been proposed in the literature aside from the search for more selective ionophores (7).

Athavale *et al*. reported a mathematical treatment to correct the recorded ISE potential, which considered the K^+ levels in freshwater together with the NH_4^+/K^+ selectivity coefficient (8). Briefly, all-solid-state ISEs were integrated into a submersible device, and the mathematical treatment was used to measure the NH_4^+ in lakes. While this approach provided accurate profiles from the depth where the NH_4^+ concentration was greater than 10 micromolar, the detection of lower concentrations remained unfeasible. Similarly, potentiometric electronic tongues for NH_4^+ detection have been proposed, which again

require the previous determination of the selectivity coefficients. The Diamond and Del Valle groups have targeted synthetic water samples, as well as river water and wastewater with this approach, claiming accurate measurements only at the millimolar level (9, 10). Speciation of N compounds has been also pursued with electronic tongues (11). Despite very valuable efforts reported in the literature until now demonstrating the utility of a statistical analysis of potentiometric data (12-15), especially in the direction of sample classification, the accurate quantification of NH_4^+ remains a challenge in environmental water samples yet.

Some very interesting analytical concepts have been developed to reduce or eliminate interference in the sample before applying potentiometric NH_4^+ detection (7). Such strategies have been applied to clinical samples rather than environmental water, such as for the method of indirect creatinine determination reported by Liu *et al* (16). All-solid-state ISEs for NH_4^+ were modified with the creatinine deiminase enzyme on top of the ISM and an outer anion-exchange membrane, which prevents the cations passing from the sample to the core of the sensing element (the ISM with the enzyme) (16). Hence, the potentiometric response represents only the NH_4^+ formed in the quantitative enzymatic creatinine reaction without any K^+/Na^+ interference. Effectively, separation science may offer suitable opportunities for NH_4^+ detection in the form of a broad portfolio of techniques to separate ions in the complex matrix *via* differences in affinity (17).

This paper presents an analytical methodology for accurately determining NH_4^+ in environmental water samples based on tandem potentiometry–ion chromatography (IC). A multi-electrode flow cell containing three miniaturized all-solid-state ISEs functionalized with nonactin as the ionophore is proposed as the detector. The cell is coupled in-line with an IC system based on a cation-exchange column. In addition, a traditional conductivity detector is implemented, which allows the validation of this new methodology. Given the selectivity limitations traditionally presented by nonactin-based ISEs, the column is exploited to provide the unequivocal separation of NH_4^+ from the main interfering ions (K^+ and Na^+) in real water samples. In addition, the potentiometric cell is explored for multi-cation detection in environmental water samples.

4.5.2. Experimental section

4.5.2.1. Preparation of the ion-selective electrodes and reference electrode

Miniaturized handmade glassy carbon electrode bodies were fabricated as detailed in the *Supporting Information* (18). All-solid-state ISEs for NH_4^+, K^+, and Na^+ were prepared via the functionalization of the glassy carbon electrodes with the ion-to-electron transducer (multiwalled carbon nanotubes, MWCNTs) and ISMs as follows (**Figure 4.12a**). Membrane cocktails containing a polymeric matrix, plasticizer, cation exchanger, and the corresponding ionophore dissolved in tetrahydrofuran (THF) were prepared to fabricate NH_4^+-, K^+- and Na^+-selective electrodes, as detailed in the *Supporting Information*. The surface of the glassy carbon electrode was first modified by drop casting 4 x 5 µL of 1 mg mL^{-1} MWCNT solution in ethanol (16). Each layer was allowed to dry for 10 min before the next was added. Then, the ISM was formed by drop casting 4 x 5 µL of the corresponding membrane cocktail on top of the MWCNT film. Each layer was allowed to dry for 20 min. Finally, the electrodes were conditioned at least overnight in a 10^{-3} mol L^{-1} solution of the respective cation analyte.

The reference electrode was fabricated by modifying the surface of the glassy carbon electrode with a silver/silver chloride (Ag/AgCl) ink (C21310007D3, GWENT Group, UK) (18), followed by oven-curing at 100°C for 10 min. The reference membrane (RM, composition in the *Supporting Information*) was drop casted on the Ag/AgCl coating (4 x 5 µL); each layer dried for 10 min before depositing the next one. The reference electrode was left to dry overnight and conditioned in 3 M KCl for at least 48 h. The electrode was stored in a 3 M KCl solution when not in use.

4.5.2.2. Preparation of the multi-electrode potentiometric flow cell

Three miniaturized ISEs were inserted in the multielectrode flow cell together with the reference electrode (18). The flow cell was a cube made of an acrylic block with six drilled holes: two on opposite sides for the inlet and outlet, one for the reference electrode, and three others to host the ISEs (**Figure 4.12b**). The electrodes were incorporated using a plastic screw (flangeless yellow ferrule and a male green nut, 1/8, IDEX Health & Science). The electrical connection was made outside the cube with small crocodile clamps connected to each electrode. For the inlet and outlet, a blue ferrule and a male red nut (1/16, IDEX Health & Science) were used to connect the PTFE tubing.

4.5.2.3. Potentiometry–ion chromatography system

The potentiometry–IC tandem measurements (**Figure 4.12c**) were conducted using an 850 Professional IC system (Metrohm Nordic) combined with a high-pressure pump and a six-port high-pressure injection valve. A guard-column (Metrosep C6 Guard/4.0; 5 x 2.0 mm I.D., 5 µm; Metrohm, Switzerland) was placed before the analytical cation-exchange column (Metrosep C6; 150 x 4.6 mm I.D., 4 µm, Metrohm, Switzerland). The outlet of the cation-exchange column was connected to the Metrohm conductivity detector. MagicNet chromatography data system software (Metrohm, Switzerland) was used to control the IC components and for data processing in the conductivity detector. The multielectrode flow cell was coupled in-line with the outlet of the conductivity detector using PEEK tubing (L x O.D. x I.D. = 300 mm x 1/16 in. x 0.25 mm, Metrohm) introduced in the ferrule and nut of the inlet of the cell.

The mobile phase used for the potentiometric measurements was 2.5×10^{-3} mol L^{-1}, as recommended by the column manufacturer for a proper functioning and ions' separation. Notably, different batches of the mobile phase solution were found to provide slightly different retention times for analogous ion peaks in the same sample. The injection volume and flow rate were optimized to be 10 µL and 0.9 mL min^{-1}, respectively.

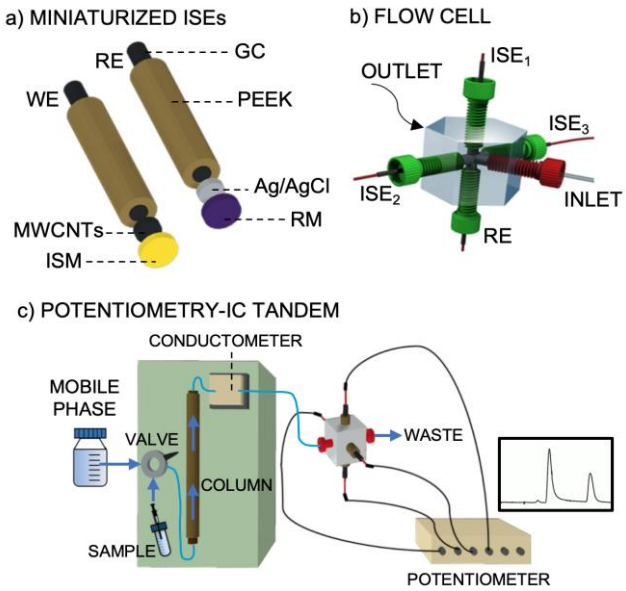

Figure 4.12 (a) Miniaturized ISEs based on glassy carbon (GC). The working electrode (WE) was prepared with MWCNTs and the ISM. The reference electrode (RE) was prepared with Ag/AgCl ink and the RM on top. **(b)** Multi-electrode flow cell with three ISEs and the RE, the inlet, and the outlet. **(c)** Tandem potentiometry–IC: the sample is injected through the valve and carried by the mobile phase through the chromatographic column.

4.5.3. Results and discussion

4.5.3.1. Analytical evaluation of miniaturized potentiometric sensors for ammonium

The analytical performance of the NH_4^+-selective electrodes was first evaluated under batch conditions (background electrolyte: $2.5x10^{-3}$ mol L^{-1} nitric acid) against the commercial Ag/AgCl reference electrode. **Figure 4.13a** shows the dynamic potentiometric response of the NH_4^+-selective electrode at increasing activities of NH_4^+. Fitting the logarithmic NH_4^+ activity *versus* the corresponding steady-state potential to the Nernst equation (inset of **Figure 4.13a**) revealed that the electrode followed a Nernstian behavior, with a slope of 54.6 mV dec^{-1}, with a linear range of response (LRR) from $3.0x10^{-6}$ to $3.0x10^{-3}$ mol L^{-1} and a limit of detection (LOD) of $6.1x10^{-7}$ mol L^{-1}. The response time (t_{95}) (19) was rapid, from 2.3 to 2.9 s within the LRR. Furthermore, the response was found to be very reproducible considering subsequent calibrations for the same electrode (slope of 54.1 ± 0.9 mV dec^{-1} and an intercept of 447.0 ± 2.3 mV, *n=3*) and equally prepared electrodes (slope of 54.5 ± 1.8 mV dec^{-1} and an intercept of 439.9 ± 9.4 mV, *n=3*), with variation coefficients for the calibration parameters of < 4%. Analogous calibration parameters, but with a slight shift in the offset potential, were achieved with the miniaturized handmade reference electrode (dotted line **Figure 4.13a**): slope of 55.5 ± 0.7 mV dec^{-1}, LRR of $3.0x10^{-6}$ – $3.0x10^{-3}$ mol L^{-1} and LOD of $(2.0 \pm 0.5)x10^{-7}$ mol L^{-1} (*n=3* electrodes).

Three NH_4^+-selective electrodes were inserted in the microfluidic cell with the handmade reference electrode (**Figure 4.12b**) for characterization under flow-mode conditions using a peristaltic pump (0.5 mL min^{-1}, $2.5x10^{-3}$ mol L^{-1} nitric acid background). **Figure 4.13b** displays the dynamic response at increasing NH_4^+ activities and the calibration graph corresponding to one of the three NH_4^+-selective electrodes as an example. The average calibration parameters of the three electrodes were: a slope of 52.5 ± 1.2 mV dec^{-1}, LRR from $3.0x10^{-5}$ to $1.0x10^{-2}$ mol L^{-1}, an intercept of 410.0 ± 20.3 mV, and a LOD of $(7.5 \pm 0.2)x10^{-6}$ mol L^{-1}. A slightly lower slope was found, with the LRR starting from an NH_4^+ activity one order of magnitude higher than in the batch mode. The LOD was also one order of magnitude higher in the flow mode. Overall, the response was slightly worse in the microfluidic cell, likely due to the flow-cell configuration *per se* (tangential mode) and the hydrodynamic conditions of the measurements. Other authors found that the tangential mode hindered achieving approximately 95% of the steady-state signal, especially in low ion analyte activities. In addition, relatively low flow rates (such as 0.5 mL min^{-1}) do not propitiate the removal of infinitesimal concentrations at the membrane surface, with the

result that low analyte concentrations require longer times to attain the steady-state signal (20).

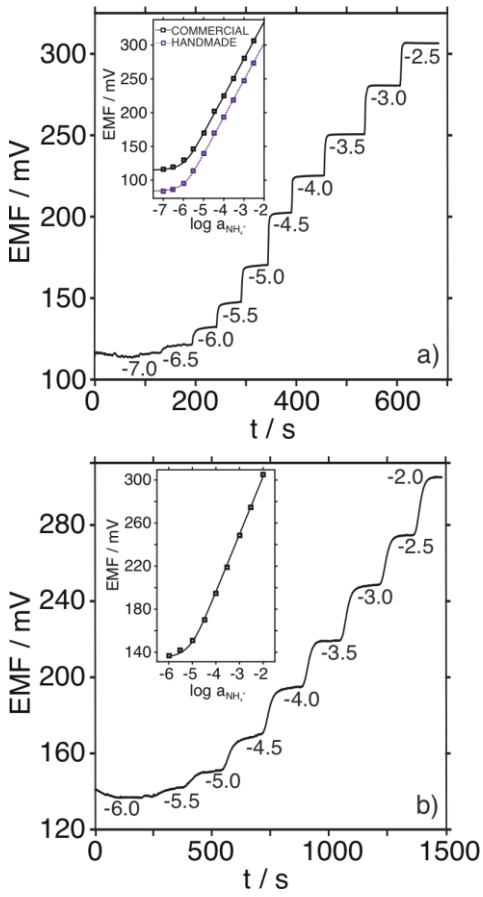

Figure 4.13 (a) The dynamic response of one NH_4^+-selective electrode in batch mode at increasing NH_4^+ activity and using the commercial Ag/AgCl reference electrode. Inset: corresponding calibration plot and that obtained with the handmade reference electrode. **(b)** The response of one NH_4^+-selective electrode in the flow cell (0.5 mL min^{-1}). Inset: Corresponding calibration graph.

Potentiometric selectivity coefficients were determined for Mg^{2+}, Ca^{2+}, Li^+, Na^+, and K^+ ions using the well-known separate solution method (21). Notably, the apparent values were calculated since, this method assumes the slope in the calibration graph of the interfering cation is equal to that of the primary one, which was not the case. In addition, the interfering cations were tested in order of their lipophilicity and with NH_4^+ (the most preferred cation) in the last place to avoid bias in the values (21). The potential provided by 10^{-3} activity of each interfering cation and for NH_4^+ were used to calculate the apparent logarithmic selectivity coefficients: $logK^{pot}_{NH_4^+,X} = -4.15 \pm 0.22, -4.30 \pm 0.16, -2.50 \pm 0.12, -2.20 \pm 0.28\ and\ -0.98 \pm 0.12$ for X=Mg^{2+}, Ca^{2+}, Li^+, Na^+, and K^+ (*n=3*), respectively. The K^+ ion was found to give the strongest interference, showing a similar value of the logarithmic selectivity

coefficient to those previously reported for ISEs containing nonactin as the ionophore (from −0.42 to −1.8) (7).

Considering typical K^+ concentrations in freshwater and seawater (0.1 and 10 mmol L^{-1}, respectively) together with the calculated logarithmic coefficient, the minimum LODs that could be reached for NH_4^+ are estimated to be *ca*. 10^{-5} and 10^{-3} mol L^{-1} (calculated as $[K^{pot}_{NH_4^+,K^+} \cdot c_{K^+}]$). As a result, the potentiometric cell developed in this work is unsuitable for seawater analysis and can only be applied to freshwater samples with NH_4^+ exceeding 10^{-5} mol L^{-1}, i.e., heavily contaminated samples. To overcome this limitation, the tandem potentiometric–IC is investigated, wherein the effective separation of NH_4^+ from any interfering cations present is expected.

4.5.3.2. Coupling the potentiometric cell with the ion chromatography system

The separation capability of the proposed tandem potentiometry–IC was first evaluated with a mixture containing equal activities ($1.0x10^{-3}$ mol L^{-1}) of Li^+, Na^+, K^+, and NH_4^+. The black lines in **Figures 4.14a** and **b** indicate the chromatograms observed with both the conductivity detector and one of the NH_4^+-selective electrodes in the potentiometric cell (sample volume: 10 µL, flow rate: 0.9 mL min^{-1}). Peak identification was performed from solutions of each cation (data not shown).

The order of elution for the cations was: Li^+ (5.8 min), Na^+ (8.4 min), NH_4^+ (9.6 min), and K^+ (14.4 min), with the retention times being *ca*. 4 s longer for the potentiometric detector than for the conductivity detector, because of their position in the experimental setup. While the chromatogram provided by the conductivity detector yields similar peak areas for the four cations, the chromatogram provided by the potentiometric cell displayed a higher potential readout for NH_4^+ than for the other cations (**Table S11**). Indeed, the peaks for Li^+ and Na^+ were very weak. Furthermore, when the NH_4^+ content in the sample was decreased to $1.0x10^{-6}$ mol L^{-1} while maintaining the levels for the rest of the cations ($1.0x10^{-3}$ mol L^{-1}), the peaks for Li^+, Na^+, and K^+ did not change, but the peak height for NH_4^+ decreased in both the potentiometric and conductivity chromatograms (**Figures 4.14a** and **b** and **Table S12**).

Then, the peak for $1x10^{-6}$ mol L^{-1} was well-observed with the potentiometric detector, but it was difficult to be identified and/or quantified by the conductivity detector. Notably, in the

case of the potentiometric detector, the returning to the base signal in the NH_4^+ peak appears to be slower for increasing activity, which seems to not disturb the K^+ signal as demonstrated with the overlapping K^+ peaks in **Figure 4.14b**. Importantly, this behavior is not expected to influence the accuracy of the NH_4^+ analysis even at high activity/concentrations (around mmol L^{-1}), since the signal does return to the initial baseline at the end of the chromatogram.

Next, the effect of the injected sample volume and flow rate on the chromatograms was investigated. For this purpose, samples with increasing activity of NH_4^+ (from $1.0x10^{-6}$ to $1.0x10^{-3}$ mol L^{-1}, *n=3*) were analyzed using two different sample volumes (10 and 20 µL, flow rate of 0.9 mL min^{-1}) and three flow rates (0.5, 0.7, and 0.9 mL min^{-1}, sample volume of 10 µL). **Figures 4.14c–4.14f** compare the chromatograms observed with the same electrode at $1.0x10^{-3}$ mol L^{-1} under the different volume and flow rate conditions, together with the averaged calibration graphs (*n=3*) at increasing NH_4^+ activity.

In the case of the injected sample volume, and considering a 10^{-3} mol L^{-1} NH_4^+ activity (**Figure 4.14c**), the peak was higher (81.7 mV versus 158.0 mV) and wider (time difference at 5% of the peak maximum of 2.4 min versus 4.2 min) when the volume was increased from 10 to 20 µL. Also, the retention time was slightly longer (9.8 min versus 10.3 min). This trend appeared for all tested NH_4^+ activities (**Figure S12**). In principle, an increase in peak height, width, and retention time is expected with increasing sample volume as the analyte plug injected into the detector increases in length. Consequently, the separation efficiency was slightly better with the 10 µL sample (**Table S13**: number of plates of 2544 *versus* 1146 for NH_4^+ activity >10^{-5} mol L^{-1}). However, the average calibration graph (*n=3*) with a 20 µL sample volume displayed a hyper-Nernstian slope (62.1 mV versus 57.3 mV for 20 and 10 µL, respectively, **Figure 4.14d**) as well as a lower LOD ($1x10^{-7}$ versus $6x10^{-6}$ mol L^{-1}, **Figure 4.14d**). The peaks at lower NH_4^+ activities appear slightly more distinct with the 20 µL volume than the 10 µL volume (**Figure S12**).

Concerning the flow rate, we found increasing retention times (9.5, 11.9, and 16.4 min) and widths (1.7, 2.2, and 2.9 min) for the NH_4^+ peak with decreasing flow rate (**Figure 4.14e**), corresponding to decreased separation efficiency (number of theoretical plates of 1584, 2254, and 3040 for 0.5, 0.7, and 0.9 mL min^{-1}, respectively, **Table S14**). Nevertheless, we did not find any significant difference in the averaged calibration parameters (*n=3*) of the different flow rates (**Figure 4.14f**; the corresponding chromatograms are provided in **Figure S13**). Given these results, a sample volume of 10 µL and a flow rate of 0.9 mL min^{-1} were

selected for further experiments as a compromise between separation efficiency, calibration parameters, and analysis time.

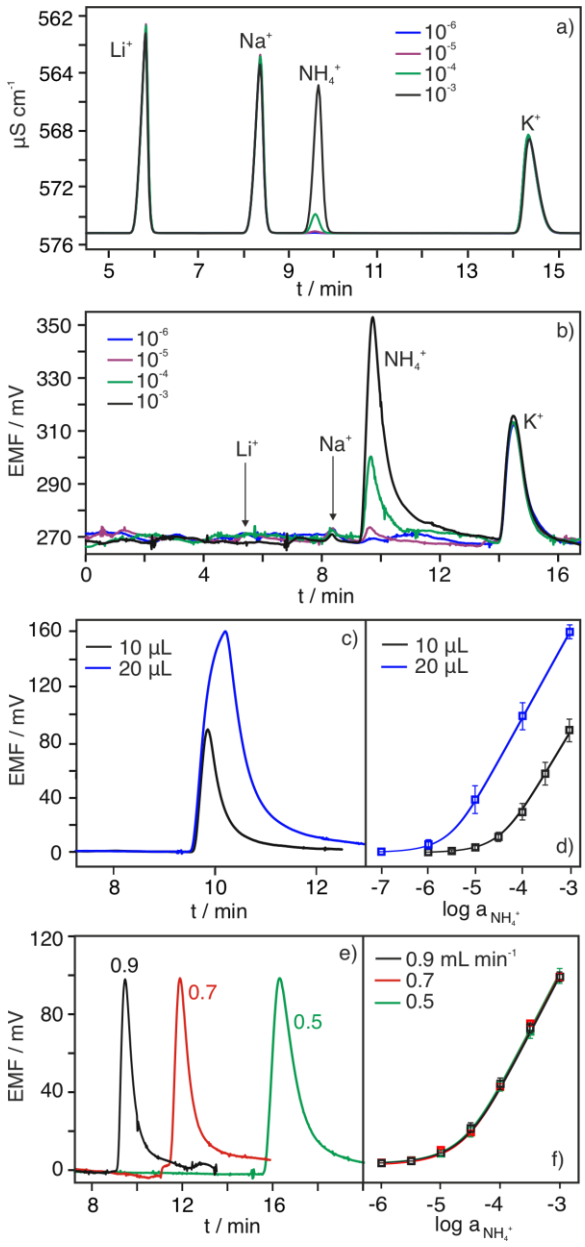

Figure 4.14 (a) Conductivity chromatograms at increasing NH_4^+ activities and fixed 1x10^{-3} mol L^{-1} of the other cations (10 µL volume, 0.9 mL min^{-1}). **(b)** Potentiometric chromatograms at increasing NH_4^+ activity and 1x10^{-3} mol L^{-1} of the rest of the cations (10 µL volume, 0.9 mL min^{-1}). **(c)** Potentiometric chromatograms with 10 and 20 µL injected volume of NH_4^+ at 1x10^{-3} mol L^{-1} (0.9 mL min^{-1}). **(d)** Averaged calibration graphs (*n=3*). **(e)** Potentiometric chromatograms with 1x10^{-3} mol L^{-1} of NH_4^+ at 0.5, 0.7, and 0.9 mL min^{-1} (10 µL volume). **(f)** Averaged calibration graphs (*n=3*). Background: 2.5x10^{-3} mol L^{-1} nitric acid.

4.5.3.3. Analytical performance of the tandem potentiometry–ion chromatography

The sensitivity, LRR, LOD, limit of quantification (LOQ), and reproducibility were investigated at the optimized experimental conditions. Potentiometric chromatograms at increasing NH_4^+ activity (10^{-7} – 10^{-3} mol L^{-1}) are presented in **Figure 4.15a**. The averaged calibration graph for the potentiometric cell (*n=3* electrodes) revealed a slope of 59.5 ± 1.2 mV dec^{-1} within the LRR ($3.0x10^{-5}$ – 10^{-3} mol L^{-1}) and a LOD of $2.5x10^{-6}$ mol L^{-1} (**Figure 4.15b**). Pursuing the detection of lower NH_4^+ levels, we investigated a transformation for the calibration graph *via* linearization of the entire logarithmic response (18). We used the linear fitting of the $(10^{E/S} - 1)$ magnitude (where E refers to the potential and S to the slope in the LRR when plotting the potential versus log a_i) against the NH_4^+ concentration (**Figure 4.15c**), as previously reported for other chromatographic–potentiometric tandem systems (22).

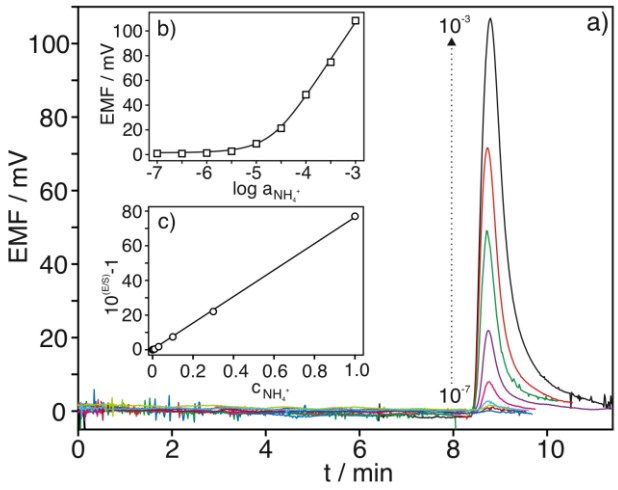

Figure 4.15 (a) Chromatograms at increasing NH_4^+ activity. **(b)** Corresponding averaged calibration graph (*n=3*). **(c)** Linearization of the averaged calibration graph. ($2.5x10^{-3}$ mol L^{-1} nitric acid, 10 µL sample volume, flow rate of 0.9 mL min^{-1}).

Following this approach, an expanded LRR from 10^{-6} to 10^{-3} mol L^{-1} NH_4^+ with a sensitivity of 76.6 ± 2.2 L $mmol^{-1}$ (R^2 = 0.9986) was found. The LOD and LOQ were calculated as the concentration corresponding to a signal-to-noise ratio of three and ten times, respectively, yielding values of $3.0x10^{-7}$ and $1.0x10^{-6}$ mol L^{-1}. Under the same experimental conditions, the LOD and LOQ with the conductivity detector were calculated as $1.0x10^{-6}$ and $3.0x10^{-6}$ mol L^{-1} (**Figure S14**). The reproducibility was evaluated by the triplicate injection of $3.0x10^{-6}$, $1.0x10^{-5}$, and $3.0x10^{-4}$ mol L^{-1} NH_4^+ measured with three NH_4^+-selective electrodes and the injection of $1.0x10^{-5}$ mol L^{-1} NH_4^+ over four consecutive days. Intra-

electrode reproducibility for the peak potentials revealed a variation coefficient <5%. Inter-electrode reproducibility showed a variation coefficient of <9%. Finally, variations of *ca*. 0.5% and 7% were observed for the calibration parameters of the NH_4^+-selective electrodes in the second and fourth days of their continuous usage, respectively.

4.5.3.4. Analysis of natural water samples (see Table S15 for sample identification)

Recovery studies were accomplished with a river water sample (R1.0, **Table S16**) spiked with $1.0x10^{-5}$ (R1.1) and $5.0x10^{-5}$ (R1.2) mol L^{-1} NH_4^+ concentrations. Each sample was analyzed in triplicate using both the potentiometric and conductivity detectors (**Table 4.14** and **Table S16**). The recovery percentages were acceptable for both detectors, showing the appropriate accuracy of the potentiometry–IC methodology.

Table 4.14 Quantification of ammonium levels in different natural water samples using the potentiometry–IC and conductivity–IC setups[a].

Sample	Potentiometry–IC		Conductivity–IC		
	μmol L^{-1}	RSD	μmol L^{-1}	RSD	%Diff
R1.0	5.5	2.3	4.2	7.9	31
R1.1	13.0	2.8	14.0	1.2	7
R1.2	56.5	1.8	57.0	0.9	1
R2	2.6	8.4	ND	–	–
R3	5.2	5.3	6.7	8.4	22
R4	4.7	3.1	ND	–	–
L1	3.6	9.8	ND	–	–
L2	4.0	7.1	ND	–	–
L3	12.5	3.6	12.8	7.5	2
S1	4.2	8.3	ND	–	–
S2	9.9	3.7	8.9	9.3	6
S3	4.0	6.7	ND	–	–
S4	23.7	2.6	22.9	7.4	3

[a] ND = non-detectable. %Diff = percentage of the difference between the results provided by potentiometry and conductivity. RSD = relative standard deviation.

Furthermore, the NH_4^+ content in ten water samples from different locations in Portugal, Sweden, and Spain (**Table S15**) was estimated. Some representative chromatograms are

shown in **Figure 4.16**. Notably, the NH_4^+ peak was visible in all samples, approaching the level of noise (and potentiometric baseline) if the NH_4^+ content was close to the micromolar level. Peaks for K^+ and Na^+ were also observed in all the tested samples, presenting higher levels in the seawater samples. Nevertheless, there was no detected overlap with the NH_4^+ peak that could adversely affect its detection. The quantification of NH_4^+ was possible in all samples using the potentiometric detector, whereas the conductivity detector only detected NH_4^+ concentrations higher than $5x10^{-6}$ mol L^{-1}. In those samples where a comparison was feasible, the results from both detectors agreed better at higher NH_4^+ concentrations. Overall, the potentiometric cell could detect and quantify lower NH_4^+ concentrations than the conductivity detector. The RSD% provided by both techniques were similar and always <10%. An interesting advantage of the potentiometric detector developed here is simultaneously combining ISEs that are selective for different ions in the same cell for multi-ion detection. Accordingly, NH_4^+-, Na^+-, and K^+-selective electrodes were incorporated into the potentiometric cell as a preliminary proof-of-concept. The chromatograms and the corresponding calibration graphs obtained by using solutions containing the three cations at the same (increasing) concentrations are displayed in **Figure 4.17.** As observed, all the cations can be selectively detected by the corresponding electrode with no interference from the other cations. In more detail, the Na^+-selective electrode presented a negligible response for NH_4^+ and a very low response for K^+, whereas the K^+-selective electrode displayed a negligible response for Na^+ and some response for NH_4^+.

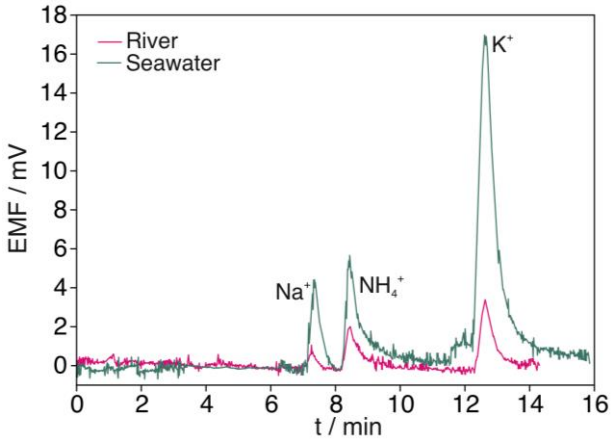

Figure 4.16 Chromatograms observed for two water samples: freshwater (river) and seawater.

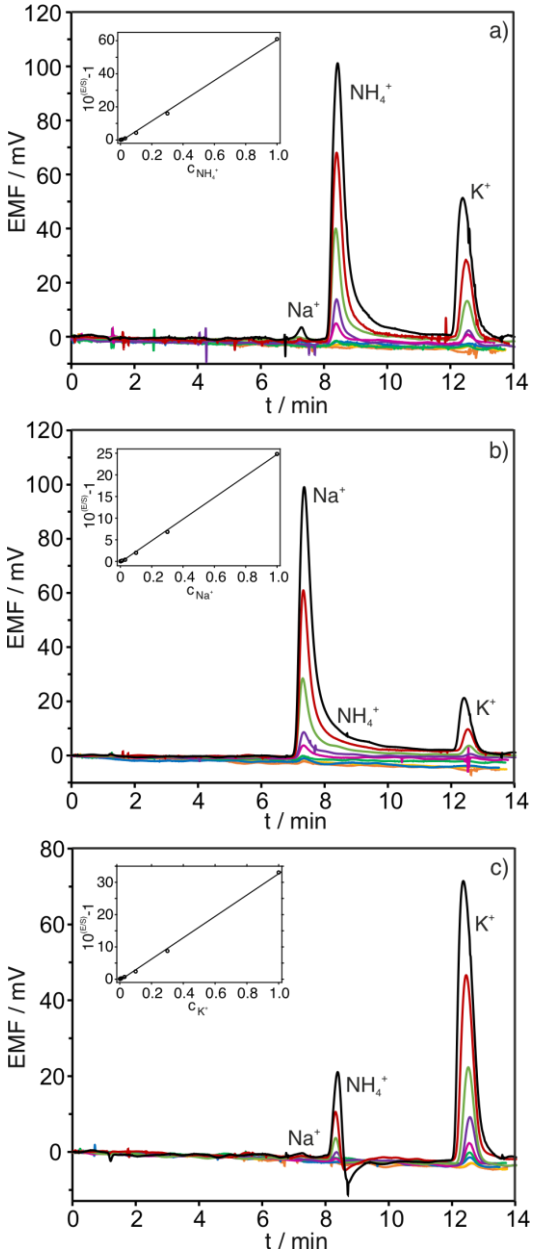

Figure 4.17 Chromatograms at increasing NH_4^+, Na^+ and K^+ activity provided by the **(a)** ammonium-selective electrode, **(b)** sodium-selective electrode and **(c)** potassium-selective electrode. Insets: Linearized calibration graph. ($2.5x10^{-3}$ mol L^{-1} nitric acid, 10 µL sample volume, flow rate of 0.9 mL min^{-1}).

Regarding the calibration graph, in the case of Na^+ and K^+ electrodes, the LRR of the typical potentiometry plot (*i.e.*, EMF versus logarithmic activity) was found to include the levels expected in water samples (0.1 – 100 mmol L^{-1}) and hence, implementing the linearization approach is not necessary (see **Figure S15** for the calibration graphs and **Table S17** for the corresponding calibration parameters). However, aiming at only one type of calibration, we used the linearized version of the calibration graph (as described above) for each of the three cations (NH_4^+, Na^+, and K^+) with the corresponding electrode. The calibration

parameters in the LRR are collected in **Table S18**. Linear regression lines were obtained for NH_4^+, Na^+, and K^+ in the concentration range from 10^{-6} to 10^{-3} mol L^{-1} with sensitivities of 61.2 ± 2.5 (R^2 = 0.9983), 24.9 ± 0.4 (R^2 = 0.9979), and 33.1 ± 0.6 (R^2 = 0.9973), respectively. The LOD and LOQ were calculated as the concentration corresponding to a signal-to-noise ratio of three and ten times, respectively, producing values of $3.0x10^{-7}$ (LOD) and $1.0x10^{-6}$ (LOQ) mol L^{-1} for the three cations.

The river samples R1.0, R1.1, and R1.2 were analyzed with the multi-cation potentiometric cell, revealing appropriate recovery percentages ranging from 81 to 102% for the potentiometric detector and from 73 to 140% for the conductivity one (**Table 4.15**). Considering the results provided by the conductivity detector, an excellent agreement was found, with a percentage of difference always lower than the 18%, except for the R1.0 sample that presented a 26% difference (**Table 4.15**). These results confirmed the great potential of the potentiometry–IC tandem for multi-ion detection.

Table 4.15 Quantification of ammonium, sodium, and potassium levels in different natural water samples using the potentiometry–IC and conductivity–IC setups[a].

Sample	Cation	Potentiometry–IC			Conductivity–IC			%Diff
		µmol L^{-1}	RSD	%Rec	µmol L^{-1}	RSD	%Rec	
R1.0	NH_4^+	4.1	2.6	–	5.2	8.8	–	26
	Na^+	140.3	0.4	–	148.4	1.0	–	6
	K^+	13.2	3.6	–	12.6	2.9	–	5
R1.1	NH_4^+	12.2	3.6	82	14.4	4.4	92	18
	Na^+	149.8	3.1	95	162.4	1.3	140	8
	K^+	21.3	6.1	81	19.9	5.0	73	7
R1.2	NH_4^+	47.8	3.6	88	53.8	6.7	97	12
	Na^+	191.1	4.0	102	206.3	2.5	116	8
	K^+	57.6	4.1	89	65.6	8.1	106	14

[a] %Rec=percentage of recovery. %Diff=percentage of the difference between the results provided by potentiometry and conductivity.

4.5.3.5. Analysis of the developed tandem potentiometry–ion chromatography method with respect to the state-of-the-art

To the best of our knowledge, the first attempts to coupling potentiometry to IC for (multi)ion detection used inner-filing solution-type ISEs (23-26). While the design of the electrode hindered the miniaturization of the entire system; these works have demonstrated the great potential of potentiometry to detect ions after chromatographic separation, as it was sometimes superior to the analytical performance of the conductivity detector (27, 28). It is worth mentioning that three main strategies have been followed in terms of the membrane composition: (i) the membrane contains a single ionophore that is selective for only one ion; (ii) a multi-ionophore membrane that is selective for at least two ions; and (iii) a membrane with a non-selective profile (23, 26-29).

The concept of a multi-ionophore membrane was translated to the solid-contact electrode type by Lee *et al*., who demonstrated the simultaneous analysis of K^+, NH_4^+, Na^+, and Ca^{2+} with a membrane containing four ionophores, one for each cation (30). However, the separation between NH_4^+, Na^+, and K^+ peaks was incomplete, likely due to the complex cross-selectivity profile normally found for this type of membrane. For NH_4^+ in particular, the observed LOD was close to 10^{-5} M, which is more than one order of activity higher than that presented in this paper. Notably, NH_4^+ detection in real samples was not demonstrated.

Five years later, Isildak *et al*. presented tubular-shaped membrane electrodes with non-selective profiles for either cation or anion detection after chromatographic separation (27, 31). Their cation detector was able to identify Na^+, NH_4^+, K^+, Rb^+, Cs^+, and Tl^+ with well-separated peaks but with what appears to be a continuously drifting baseline, based on the figures. The electrode was used in conjunction with a double-junction calomel reference electrode, which was not a solid-contact type because this technology was not yet common. For NH_4^+, the LOD was *ca.* 6 µM, which is again higher than that achieved in this paper and hence unsuitable for NH_4^+ detection in any water sample. The NH_4^+ concentration in two water samples (river and seawater) was calculated to be close to 20 µM, while the cation was not detectable in a tap water sample. Unfortunately, the results in real water samples were not validated with parallel measurements using a gold standard technique.

Shen *et al*. have reported chromatographic separation coupled to a solid-contact sensor array (i.e., conducting wires covered by the membrane) in which each electrode was selective for one cation: Na^+, NH_4^+, K^+, Mg^{2+}, and Ca^{2+} (32, 33). The authors achieved a constant baseline without any noticeable drift by including a 1 µM concentration of each cation in the eluent solution (i.e., the background for the potentiometric measurements). The sensors presented LRRs from 0.05 to 1 mM. The ammonium content in some synthetic

samples and a hydroponic solution was analyzed. However, the LRR did not allow the detection of NH_4^+ in a series of commercial and natural water samples.

The most recent paper reporting on NH_4^+ detection in mixtures dates from 2016 and is based on a solid-contact electrode (copper wire) modified with a carbon composite containing the membrane components (34). In this case, the membrane presented a nonselective profile and, after chromatographic separation, the NH_4^+ and K^+ peaks appear with a high degree of overlap, and thus, the LRR ranged between $5x10^{-5}$ and 10^{-2} M, which is not suitable for NH_4^+ detection in water samples. However, it is suitable for K^+ detection.

Overall, the potentiometry–IC approach developed in the present paper is proposed within a state-of-the-art context that lacks a functional solution to detect NH_4^+ together with other cations in any water sample. The technology put forward regarding the potentiometry–chromatography system that can additionally include a conductivity detector is a unique method to validate all the measurements and demonstrates the advantages of the potentiometric readout over conductimetry. The performance of the potentiometric sensors used to detect NH_4^+ (but also K^+ and Na^+) is superior to the other sensors. Importantly, the potentiometric cell presents huge versatility for the detection of any ion.

4.5.4. Conclusion

We demonstrate the necessity of the tandem potentiometry–IC system together with the linearization of the potentiometric response to address NH_4^+ detection at micromolar levels in any water sample where other cations (such as K^+ and Na^+) are present at higher levels. To pursue the decentralization of such analytical determination in diverse water environments, a miniaturized potentiometric detector based on a multi-electrode flow cell was fabricated and characterized to provide the best analytical performances after in-line coupling with chromatographic separation. Advantageously, the potentiometric detector can be equipped with three similar ISEs to obtain reproducibility in the NH_4^+ quantification or three electrodes, each selective for different ions, for multi-ion detection within the same sample. Preliminary results revealed the accurate and simultaneous detection of NH_4^+, Na^+, and K^+ in river samples. Soon, the implementation of the potentiometry–IC analytical concept in true *in situ* measurements is foreseen *via* potentiometric-ion-chromatography-on-a-chip technology. Simultaneous multi-ion detection is expected to be feasible in any kind of water (even such a complex matrix as seawater) and with high temporal and spatial resolution, thanks to further implementation in water platforms considering microfluidics.

4.5.5. References

1. Wetzel RG. The Nitrogen Cycle. In: Wetzel RG, editor. Limnology. 3rd ed. San Diego: Academic Press; 2001. p. 205-37.

2. U.S. Environmental Protection Agency Aquatic Life Ambient Water Quality Criteria for Ammonia- Freshwater. In: EPA-822-R-13-001, editor. Washington D.C.2013.

3. Xia X, Zhang S, Li S, Zhang L, Wang G, Zhang L, et al. The cycle of nitrogen in river systems: sources, transformation, and flux. Environ Sci Process Impacts. 2018;20(6):863-91.

4. Lin K, Zhu Y, Zhang Y, Lin H. Determination of ammonia nitrogen in natural waters: Recent advances and applications. Trends Environ Anal Chem. 2019;24:e00073.

5. Zhu Y, Chen J, Yuan D, Yang Z, Shi X, Li H, et al. Development of analytical methods for ammonium determination in seawater over the last two decades. Trends Anal Chem. 2019;119:115627.

6. Moretto LM, Kalcher K. Environmental Analysis by Electrochemical Sensors and Biosensors; New York: Springer; 2014.

7. Cuartero M, Colozza N, Fernández-Pérez BM, Crespo GA. Why ammonium detection is particularly so-challenging and insightful with ionophore-based potentiometric sensors – an overview of the last 20-year-progress. Analyst. 2020;145: 3188-3210.

8. Athavale R, Kokorite I, Dinkel C, Bakker E, Wehrli B, Crespo GA, et al. In situ ammonium profiling using solid-contact ion-selective electrodes in eutrophic lakes. Anal Chem. 2015;87(24):11990-7.

9. de Viteri FJS, Diamond D. Ammonium detection using an ion-selective electrode array in flow-injection analysis. Electroanalysis. 1994;6(1):9-16.

10. Gallardo J, Alegret S, de Roman MA, Munoz R, Hernandez PR, Leija L, et al. Determination of ammonium ion employing an electronic tongue based on potentiometric sensors. Anal Lett. 2003;36(14):2893-908.

11. Nuñez L, Cetó X, Pividori MI, Zanoni MVB, del Valle M. Development and application of an electronic tongue for detection and monitoring of nitrate, nitrite and ammonium levels in waters. Microchem J. 2013;110:273-9.

12. Mimendia A, Gutiérrez JM, Leija L, Hernández PR, Favari L, Muñoz R, et al. A review of the use of the potentiometric electronic tongue in the monitoring of environmental systems. Environ Model Softw. 2010;25(9):1023-30.

13. Li D, Xu X, Li Z, Wang T, Wang C. Detection methods of ammonia nitrogen in water: A review. Trends Anal Chem. 2020;127:115890.

14. Chen X, Zhou G, Mao S, Chen J. Rapid detection of nutrients with electronic sensors: a review. Environ Sci Nano. 2018;5(4):837-62.

15. Gutiérrez M, Gutiérrez JM, Alegret S, Leija L, Hernández PR, Favari L, et al. Remote environmental monitoring employing a potentiometric electronic tongue. Int J Environ Anal Chem. 2008;88(2):103-17.

16. Liu Y, Cánovas R, Crespo GA, Cuartero M. Thin-Layer potentiometry for creatinine detection in undiluted human urine using ion-exchange membranes as barriers for charged interferences. Anal Chem. 2020;92(4):3315-23.

17. Gil RL, Amorim CG, Montenegro M, Araujo AN. Potentiometric detection in liquid chromatographic systems: an overview. J Chromatogr A. 2019;1602:326-40.

18. Cuartero M, Pankratova N, Cherubini T, Crespo GA, Massa F, Confalonieri F, et al. In situ detection of species relevant to the carbon cycle in seawater with submersible potentiometric probes. Environ Sci Tech Let. 2017;4(10):410-5.

19. Richard P. Buch EL. Recomendations for nomenclature of ion-selective electrodes (IUPAC Recommendations 1994). Pure Appl Chem. 1994;66(12):2527-36.

20. Tóth K, Fucskó J, Lindner E, Fehér Z, Pungor E. Potentiometric detection in flow analysis. Anal Chim Acta. 1986;179:359-70.

21. Bakker E. Determination of unbiased selectivity coefficients of neutral carrier-based cation-selective electrodes. Anal Chem. 1997;69(6):1061-9.

22. Daems D, van Nuijs AL, Covaci A, Hamidi-Asl E, Van Camp G, Nagels LJ. Potentiometric detection in UPLC as an easy alternative to determine cocaine in biological samples. Biomed Chromatogr. 2015;29(7):1124-9.

23. Trojanowicz M, Meyerhoff ME. Replacement ion chromatography with potentiometric detection using a potassium-selective membrane-electrode. Anal Chim Acta. 1989;222(1):95-107.

24. Hyun Han S, Shin Lee K, Sig Cha G, Liu D, Trojanowicz M. Potentiometric detection in ion chromatography using multi-ionophore membrane electrodes. J Chromatogr A. 1993;648(1):283-8.

25. Kwon K-H, Paeng K-J, Lee DK, Lee IC, Hong US, Sig Cha G. Neutral carrier-based ion-selective electrode with similar sensitivity to different monovalent cations as a detector in ion chromatography. J Chromatogr A. 1994;688(1-2):350-6.

26. Hong US, Kwon HK, Nam H, Cha GS, Kwon KH, Paeng KJ. Simultaneous determination of alkali and alkaline-earth metals by ion chromatography with neutral carrier-based ion-selective electrode detector. Anal Chim Acta. 1995;315(3):303-10.

27. Isildak I, Covington AK. Ion-selective electrode potentiometric detection in ion-chromatography. Electroanalysis. 1993;5(9-10):815-24.

28. Jackson PE. Ion Chromatography in Environmental Analysis. Encyclopedia of Analytical Chemistry. New Jersey: John Wiley & Sons; 2006.

29. Cuartero M, Crespo GA. Using potentiometric electrodes based on nonselective polymeric membranes as potential universal detectors for ion chromatography: investigating an original research problem from an inquiry-based-learning perspective. J Chem Educ. 2018;95(12):2172-81.

30. Lee KS, Shin JH, Cha MJ, Cha GS, Trojanowicz M, Liu D, et al. Multiionophore-based solid-state potentiometric ion sensor as a cation detector for ion chromatography. Sensor Actuator B Chem. 1994;20(2-3):239-46.

31. Isildak I, Asan A. Simultaneous detection of monovalent anions and cations using all solid-state contact PVC membrane anion and cation-selective electrodes as detectors in single column ion chromatography. Talanta. 1999;48(4):967-78.

32. Shen HD, Cardwell TJ, Cattrall RW. The application of a chemical sensor array detector in ion chromatography for the determination of Na^+, NH_4^+, K^+, Mg^{2+} and Ca^{2+} in water samples. Analyst. 1998;123(10):2181-4.

33. Lee DK, Lee HJ, Cha GS, Nam H, Paeng KJ. Ion chromatography detector based on solid-state ion-selective electrode array. J Chromatogr A. 2000;902(2):337-43.

34. Dumanli R, Attar A, Erci V, Isildak I. Simultaneous analysis of monovalent anions and cations with a sub-microliter dead-volume flow-through potentiometric detector for ion chromatography. J Chromatogr Sci.. 2016;54(4):598-603.

4.5.6. Supplementary material

Experimental section

Reagents, materials, and instrumentation. Ammonium ionophore I (Nonactin), Sodium ionophore X (4-tert-Butylcalix[4]arene-tetraacetic acid tetraethyl ester), Potassium ionophore I (valinomycin), sodium tetrakis[3,5-bis(trifluoromethyl)phenyl]borate (NaTFPB), and carboxylic acid functionalized multiwalled carbon nanotubes (MWCNTs) were purchased in selectophore grade from Sigma-Aldrich. High molecular weight poly(vinyl chloride) (PVC), polyvinyl butyral (PVB), dioctylsebacate (DOS), tetrahydrofuran (THF), ammonium chloride, magnesium chloride, calcium chloride, lithium chloride, sodium chloride, potassium chloride (KCl), and nitric acid (69%, HNO_3) were obtained from Sigma Aldrich.

All solutions were prepared by dissolving the appropriate salts in 18.2 MΩ cm^{-1} doubly deionized water (Milli-Q water systems, Merck Millipore). The mobile phase in the IC system consisted of 2.5 mmol L^{-1} nitric acid solution prepared by dilution of the corresponding concentrated form. Natural water samples (river, lake, and seawater) from Portugal, Sweden, and Spain were collected at the surface of the corresponding aquatic resource with a falcon tube. The samples were filtered through 0.45 µm pore-size filters coupled to syringes and then stored in the fridge at 4 °C.

The cocktail for the NH_4^+ ISM was obtained by dissolving 1.0 mg of ammonium ionophore I (nonactin), 0.5 mg of NaTFPB, 66.5 mg of DOS, and 32.0 mg of PVC in 1 mL of THF. For the Na^+ ISM, 1.2 mg of sodium ionophore X, 0.5 mg NaTFPB, 66.0 mg DOS, and 33.0 mg of PVC were dissolved in 1 mL of THF. In the case of the K^+ ISM, 1.3 mg of potassium ionophore I, 0.5 mg of NaTFPB, 66.0 mg of DOS, and 33.0 mg of PVC were dissolved in 1 mL of THF. The cocktail for the reference membrane (RM) was prepared by dissolving 50 mg of sodium chloride and 78 mg of PVB in 1 mL of methanol.

The potential of the developed ISEs was measured with a high input impedance (10^{15}Ω) EMF16 multichannel data acquisition device (Lawson Laboratories, Inc.) against either a double-junction Ag/AgCl/3M KCl/1M LiOAc reference electrode (6.0726.100, Metrohm Nordic, Sweden) or the hand-made solid-state reference electrode.

Before its coupling to the IC system, an ISMATEC peristaltic pump (Model IPC N-4 ISM 935) and PTFE tubing (L x O.D. x I.D. = 300 mm x 1/16 in. x 100 µm, Supelco) were used for the analytical characterization of the potentiometric cell.

Preparation of the ion-selective electrodes and reference electrode bodies. Miniaturized handmade glassy carbon electrodes (**Figure 1a**) were fabricated by gluing a glassy carbon rod (I.D. = 1.98 mm and 20 mm long, SIGRADUR®) inside a PEEK tube (Supelco) and maintaining a length of 5 mm of the rod outside the PEEK tube to make the electrical connections. The surface of the carbon rod inside the PEEK was polished first with sandpaper (301D P400) until a flat surface was reached and then with alpha-alumina (0.5 microns) to reach a specular brightness of the glassy carbon material.

Potentiometric measurements. All experiments were carried out at room temperature of 22±1°C. To calibrate each ammonium-selective electrode, the dynamic potentiometric response was obtained at increasing concentrations of NH_4^+ in the sample solution and then, the corresponding logarithmic activities (a_i) were plotted versus the steady-state potential. Activity coefficients were calculated based on the Debye-Hückel theory to transform concentrations into activities and vice versa (1-3). The data were fitted to the Nernst equation to obtain the sensitivity (slope) and intercept (i.e., whether the date was not treated under the linearization protocol) (4). Unless otherwise indicated, the limit of detection (LOD) of the potentiometric electrodes was calculated as the activity related to the cross point between the extrapolation of the lines defining the nonresponsive range and linear-response range of the electrode (5).

Tables

Table S11 Signal output provided by the potentiometry–IC and conductivity–IC setups.

Cation	Concentration (mol L^{-1})	Potentiometry–IC		Conductivity–IC		
		t_R (min)	Peak Height (mV)	t_R (min)	Peak Height (µS cm^{-1})	Peak Area (µS cm^{-1} min^{-1})
Li^+	1.0x10^{-3}	5.9	0.33	5.8	14.00	2.26
Na^+	1.0x10^{-3}	8.4	2.35	8.4	11.81	2.55
NH_4^+	1.0x10^{-3}	9.7	80.89	9.6	10.36	2.33
K^+	1.0x10^{-3}	14.5	44.38	14.4	6.60	2.36

t_R: Retention time

Table S12 Signal output of increasing NH_4^+ concentration provided by the potentiometry–IC and conductivity–IC setups (concentration of Li^+, Na^+, and K^+ were fixed at 1.0 x 10^{-3} mol L^{-1}).

Cation	Concentration (mol L^{-1})	Potentiometry–IC		Conductivity–IC		
		t_R (min)	Peak Height (mV)	t_R (min)	Peak Height (µS cm^{-1})	Peak Area (µS cm^{-1} min^{-1})
NH_4^+	1.0x10^{-6}	9.8	1.65	9.6	0.03	0.01
	1.0x10^{-5}	9.6	5.13	9.6	0.12	0.03
	1.0x10^{-4}	9.7	30.23	9.6	1.34	0.29
	1.0x10^{-3}	9.7	80.89	9.7	10.36	2.33

t_R: Retention time

Table S13 Chromatographic parameters obtained for the ammonium peak using the potentiometry–IC setup at different injection volumes.

	Injection volume					
	10 µL			20 µL		
NH_4^+ (mol L^{-1})	1.0x10^{-5}	1.0x10^{-4}	1.0x10^{-3}	1.0x10^{-5}	1.0x10^{-4}	1.0x10^{-3}
t_R	9.7	9.7	9.8	9.9	9.9	10.3
k	6.5	6.5	6.5	6.6	6.6	6.9
Peak width	1.3	2.1	2.4	2.0	2.7	4.2
A_s	2.5	3.5	3.3	2.7	2.9	2.3
N_{eff}	3581	2389	1663	1780	1225	434

t_R: retention time in minutes; k: retention factor; Peak width was measured as the difference between the time in minutes at 5% of the peak maximum; A_s: peak symmetry;N_{eff}: effective plate number.

Table S14 Chromatographic parameters obtained for the ammonium peak using the potentiometry–IC setup at different flow rates (average of 1.0 x 10^{-3}, 1.0 x 10^{-4}, and 1.0 x 10^{-5} mol L^{-1} of NH_4^+).

	Flow rate (mL min^{-1})		
	0.5	**0.7**	**0.9**
t_R	15.4	11.0	8.5
k	10.8	7.5	5.5
Peak width	2.9	2.2	1.7
A_s	2.5	2.6	3.1
N_{eff}	1584	2254	3040

t_R: retention time in minutes; k: retention factor; Peak width was measured as the difference between the time in minutes at 5% of the peak maximum; A_s: peak symmetry;N_{eff}: effective plate number.

Table S15 Identification of environmental water samples and approximate location.

Sample	Type	Country	Geographic coordinates
R1	River	Portugal	41°35'45.6"N 8°27'49.7"W
R2	River	Sweden	59°51'48.3"N 17°37'51.0"E
R3	River	Spain	37°59'25.09"N 1°5'18.76"W
R4	River	Spain	37°59'4.14"N 1°10'18.50"W
L1	Lake	Sweden	59°18'43.6"N 18°00'58.6"E
L2	Lake	Spain	38°02'07.0"N 1°40'18.3"W
L3	Lake	Spain	38°13'14.8"N 1°58'28.4"W
S1	Seawater	Sweden	59°18'54.0"N 18°01'28.5"E
S2	Seawater	Sweden	59°19'40.7"N 18°03'22.3"E
S3	Seawater	Sweden	59°21'36.0"N 18°05'24.8"E
S4	Seawater	Spain	38°50'05.1"N 0°07'54.6"E

Table S16 Recovery values of the potentiometry–IC and conductivity–IC setups for ammonium determination in a spiked river sample (*n=3*).

Sample	Added (µM)	Potentiometry–IC			Conductivity–IC		
		Found (µM)	RSD	% Recovery[a]	Found (µM)	RSD	% Recovery[a]
R1.0	0	5.5		–	4.2		–
R1.1	10	13.0	2.8	75.3	14.0	1.2	98.5
R1.2	50	56.5	1.8	102.1	57.0	0.9	105.5

[a] The recovery percentage was calculated according to the formula:

$$Recovery\ (\%) = \frac{NH_4^+{}_{Found} - NH_4^+{}_{Initial}}{NH_4^+{}_{Added}}\ x\ 100\%$$

Table S17 Linear fittings (potential versus logarithmic activity) within the LRR for NH_4^+-, Na^+- and K^+-selective electrodes incorporated in the microfluidic cell in the potentiometry–IC setup (*n=2*). Coefficients of variation in % are provided in parenthesis.

	Slope (mV dec^{-1})	Intercept (mV)	R^2	LRR (mol L^{-1})	LOD (mol L^{-1})
$NH4^+$ - ISE	57.3 ± 0.3 (0.4)	272.5 ± 0.3 (0.1)	0.9966 ± 0.0006 (0.1)	3.0x10^{-5} to 1.0x10^{-3}	(1.9 ± 0.0)x10^{-5} (2.7)
Na^+ - ISE	71.1 ± 0.5 (0.7)	312.9 ± 2.8 (0.9)	0.9984 ± 0.0004 (0.0)	1.0x10^{-4} to 1.0x10^{-3}	(4.2 ± 0.3)x10^{-5} (7.0)
K^+ - ISE	48.7 ± 0.6 (1.3)	219.9 ± 3.6 (1.7)	0.9947 ± 0.0036 (0.4)	1.0x10^{-4} to 1.0x10^{-3}	(3.5 ± 0.2)x10^{-5} (4.6)

LRR: Linear response range; LOD: Limit of detection.

Table S18 Calibration parameters for NH_4^+-, Na^+- and K^+-selective electrodes incorporated in the microfluidic cell in the potentiometry–IC setup (*n=3*) using the linearized approach for the calibration procedure. Coefficients of variation in % are provided in parenthesis.

	Slope (mM^{-1})	**Intercept (-)**	**R^2**	**LRR (mol L^{-1})**	**LOQ (mol L^{-1})**	**LOD (mol L^{-1})**
$NH4^+$ - ISE	61.2 ± 2.5 (4.1)	-0.8 ± 0.0 (3.8)	0.9983 ± 0.0000 (0.0)	$1.0x10^{-6}$ to $1.0x10^{-3}$	$1.0x10^{-6}$	$3.0x10^{-7}$
Na^+ - ISE	24.9 ± 0.4 (1.7)	-0.3 ± 0.0 (6.6)	0.9979 ± 0.0002 (0.0)	$1.0x10^{-6}$ to $1.0x10^{-3}$	$1.0x10^{-6}$	$3.0x10^{-7}$
K^+ - ISE	33.1 ± 0.6 (1.9)	-0.4 ± 0.1 (26.4)	0.9973 ± 0.0012 (0.1)	$1.0x10^{-6}$ to $1.0x10^{-3}$	$1.0x10^{-6}$	$3.0x10^{-7}$

LRR: Linear response range; LOQ: Limit of quantification; LOD: Limit of detection.

Figures

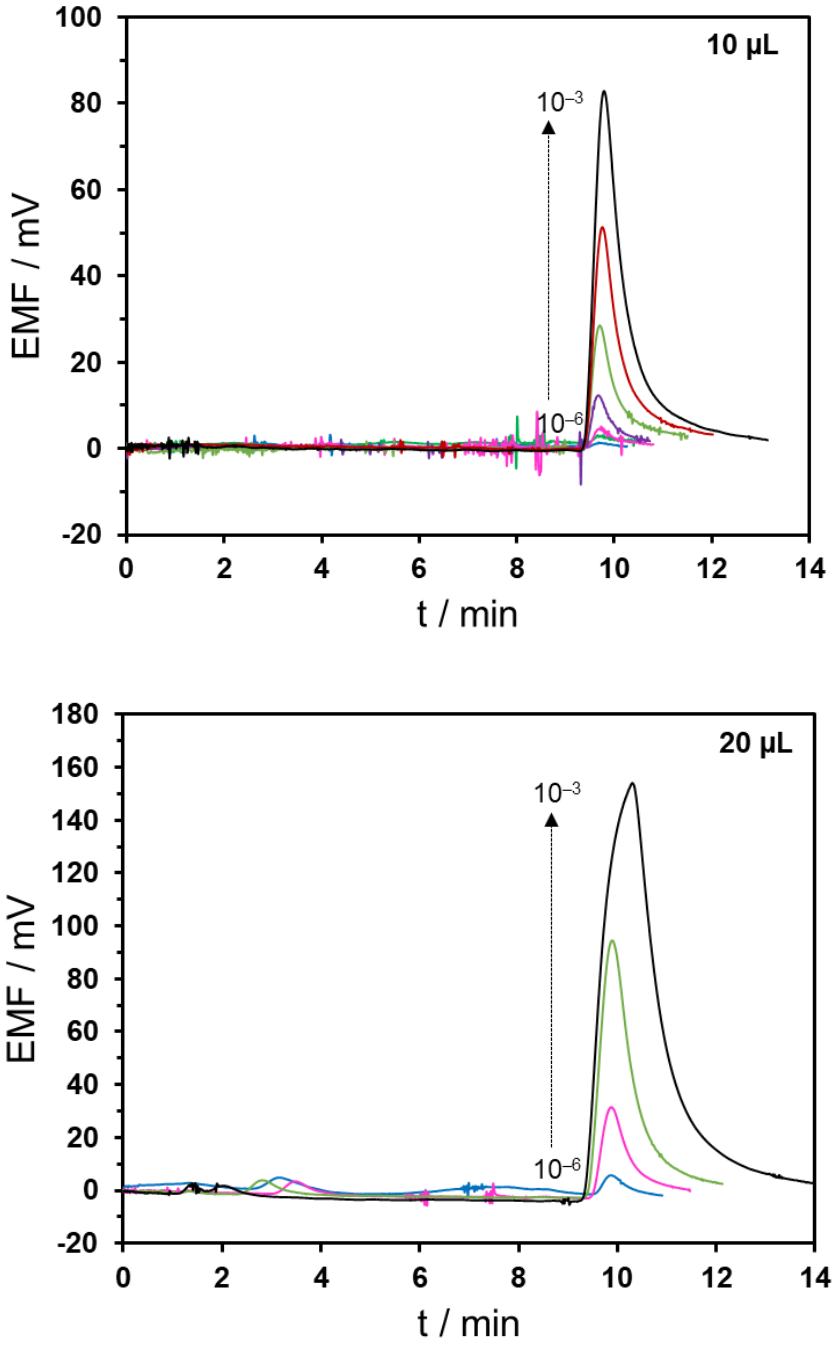

Figure S12 Potentiometric chromatograms with 10 and 20 µL injected sample volume at increasing NH_4^+ activity ($2.5x10^{-3}$ mol L^{-1} nitric acid, 0.9 mL min^{-1}).

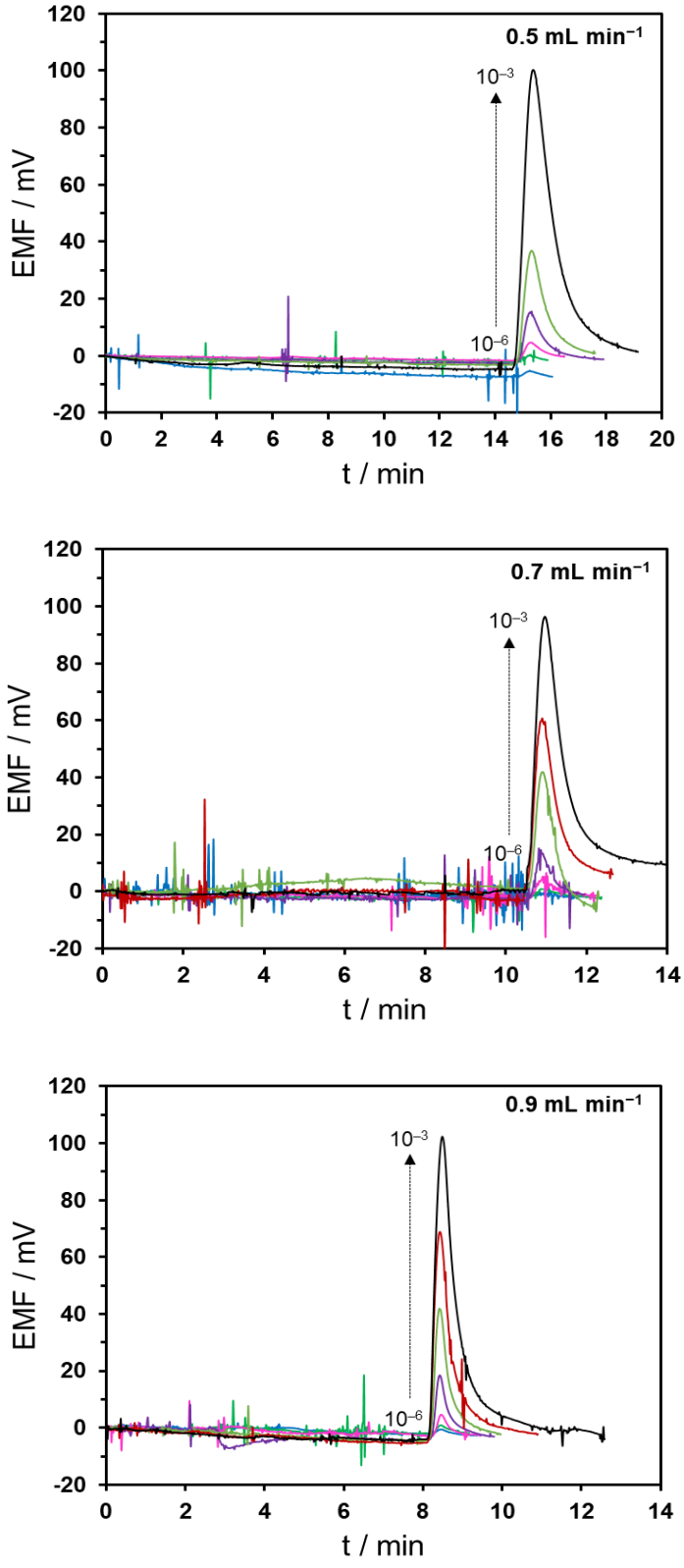

Figure S13 Potentiometric chromatograms with 0.5, 0.7 and 0.9 mL min^{-1} at increasing NH_4^+ activity ($2.5x10^{-3}$ mol L^{-1} nitric acid, 10 µL volume).

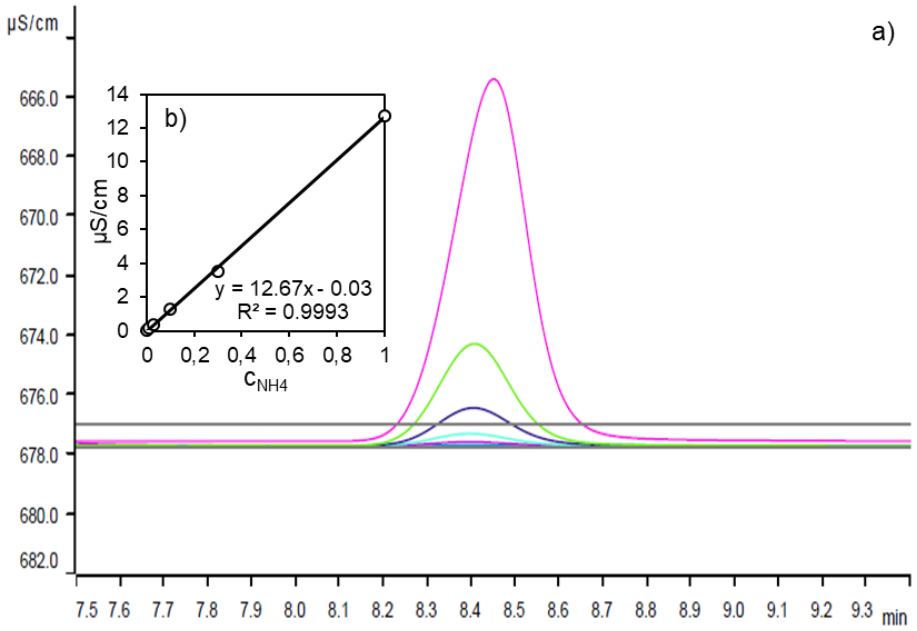

Figure S14 (a) Conductimetric chromatograms at increasing NH_4^+ activity. (b) Corresponding calibration graph (2.5x10^{-3} mol L^{-1} nitric acid, 10 µL sample volume, flow rate of 0.9 mL min^{-1}).

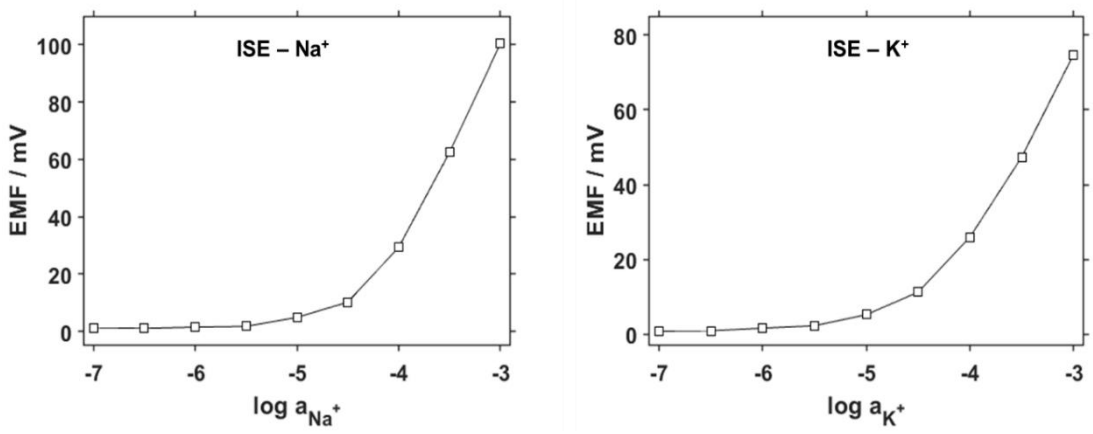

Figure S15 Calibration graphs (potential versus logarithmic activity) for Na^+- and K^+-selective electrodes incorporated in the microfluidic cell in the potentiometry–IC setup at increasing Na^+ and K^+ activity (2.5x10^{-3} mol L^{-1} nitric acid, 10 µL sample volume, flow rate of 0.9 mL min^{-1}).

References

1. Meier PC. Two-parameter debye-hückel approximation for the evaluation of mean activity coefficients of 109 electrolytes. Anal Chim Acta. 1982;136:363-8.

2. Cuartero M, Pankratova N, Cherubini T, Crespo GA, Massa F, Confalonieri F, et al. In situ detection of species relevant to the carbon cycle in seawater with submersible potentiometric probes. Environ Sci Tech Let. 2017;4(10):410-5.

3. Pankratova N, Crespo GA, Afshar MG, Crespi MC, Jeanneret S, Cherubini T, et al. Potentiometric sensing array for monitoring aquatic systems. Environ Sci Process Impacts. 2015;17(5):906-14.

4. Bakker E, Pretsch E. Modern potentiometry. Angew Chem Int Ed Engl. 2007;46(30):5660-8.

5. Richard P. Buch EL. Recomendations for nomenclature of ion-selective electrodes (IUPAC Recommendations 1994). Pure Appl Chem. 1994;66(12):2527-36.

Chapter 5

Conclusion

5.1. General conclusions

Liquid chromatography is probably the most used technique in routine analytical laboratories for the separation and analysis of chemical mixtures. The high versatility is demonstrated by the analysis of a wide range of compounds in different samples including pharmaceutical drugs, foodstuff, plastics, water samples, and tissue extracts.

LC has shown great usefulness in food quality control, mostly coupled with spectroscopic detection techniques for the routine determination of organic species. However, the need for chemical derivatization procedures to improve both sensitivity and detectability resorts to toxic agents, that are chemically non-stable and increase the analysis time. On the other hand, the use of hyphenated LC/MS/MS methodologies to overcome these drawbacks requires high-cost instrumentation, the use of internal standards, and the need for highly skilled technicians, which hinder its use in routine quality assays for the quantification of chemical species. A simpler, faster, and less expensive detection technique in LC for food quality control is still a real limitation.

Electroanalytical detection has great potential to fulfill these requirements. While amperometric and conductimetric detectors are well established in LC, with commercially available instrumentation, the use of potentiometric detectors seems to be overlooked. Although great advances were achieved over the years, potentiometric detection was not yet accepted as a routine electroanalytical technique. In chromatographic methods, a compromise between the optimal separation and detection conditions is expected, hindered by the chemical impact of the mobile phase composition on potentiometric detectors, despicable in other detection techniques. In this context, inorganic ions (i.e. buffers) incorporated in the mobile phase may be highly interfering if the ion-selective electrode (ISE) has not selectivity enough to the target analytes while the organic modifiers (i.e.

methanol and acetonitrile), generally used in reversed-phase chromatography, cause the degradation of the sensing membrane, decreasing the detector performance. On the other hand, the dynamic response characteristics of potentiometric sensors are highly dependent on the flow-cell configuration, the response time, and the rate of diffusion and exchange reaction between the eluent and the sensing membrane. Altogether, these determining factors make the use of potentiometric detection in LC a challenging approach, which is supported by the lack of fully validated analytical methodologies reported in the scientific literature.

The different works presented in this thesis aim to overcome these constraints and to demonstrate the feasibility of potentiometric detectors in LC, for quality control routine analysis. Focus on the development of the analytical applications for cationic analytes with alike chemical structures, cucurbit[n]urils (CB[n]) were investigated as recognition elements due to their ability to interact and form complexes with positively charged guests. Particularly, ISEs based on CB[6] and CB[8], combined with a lipophilic cation-exchanger (potassium tetrakis(4-chlorophenyl)borate) to improve ion extraction to the organic membrane phase, enabling the development of amine- and tetracycline-selective electrodes, respectively. The potentiometric sensors were miniaturized and assembled in a microfluidic wall-jet flow-cell, and used as a detector in the LC system. The separation and detection conditions were optimized concerning the composition of the mobile phase, type of stationary phase, hydrodynamic parameters, and the incorporation of carbon nanomaterials in the sensing membrane.

The reliable and simultaneous determination of aliphatic, aromatic, and heterocyclic biogenic amines was accomplished by ion-pair chromatography coupled with an amine-selective electrode based on CB[6] as a neutral macrocyclic host and a lipophilic cation-exchanger (section 4.2). Particularly, the determination of putrescine, cadaverine, spermidine, and spermine was demonstrated for the first time in LC-potentiometry systems. Nevertheless, the chromatographic separation of this set of biogenic amines with different lipophilic features, combined with the constraints imposed by the ISE detector, revealed a challenge. Ion-pair chromatography was selected as a potential strategy and thus, sulfonate ion-pair agents (methane, butane, and heptane) were incorporated in the mobile phase to change the chromatographic selectivity of a C8 column. Although the good retention and separation provided by the butane-sulfonic acid, the chromatographic resolution still needed to be improved. In this context, the concentration of the ion-pair agent and eluent buffer, the elution mode, the type/content of organic modifier, the stationary phase, and the hydrodynamic conditions were optimized concerning the resolution, detector performance,

and analysis time. Notably, the optimal conditions allowed the separation of all BAs in less than 20 min with good peak resolution, using a gradient elution of butane-sulfonic acid, lithium formate buffer, and acetonitrile. The methodology showed detection and quantification limits ranging from 31.1 to 202.3 μg L^{-1} and 93.3 to 606.9 μg L^{-1}, respectively. In the particular case of histamine, which is listed as a toxin by the FDA and the EFSA, the limit of detection cover the minimum admissible values requested. On the other hand, good precision was demonstrated by the relative standard deviation (RSD%) values lower than 9.1% and 13.3% for the intra- and inter-day measurements, respectively. Finally, the proposed method was successfully applied for the quantification of biogenic amines in different tomato products.

In another work (section 4.3), the incorporation of multi-walled carbon nanotubes in the amine-selective membrane improved the previous analytical features described for the proposed potentiometric detector, lowering the limits of detection/quantification and obtaining more reproducible results. On the other hand, the replacement of the acidifying agent in the mobile phase, from lithium formate buffer to acetic acid, decreases the presence of interfering ions, contributing to the improvement of the analytical results and the achievement of higher separation efficiency. The introduced modifications shifted the detection and quantification limits to 9.3 – 60.7 μg L^{-1} and 31.1 – 202.3 μg L^{-1}, respectively, and decreased the RSD% values for intra- and inter-day precision. The usefulness of the proposed method was proved by the quantification of biogenic amines in different alcoholic beverages. The remarkable advantage of the proposed analytical methodologies relies on the direct determination of underivatized biogenic amines, suppressing the need for chemical derivatization steps, which contributes to faster and more environmentally friendly analytical methodologies. The simple preparation of the amine-selective electrodes makes the proposed potentiometric detector a cost-effective alternative in any laboratory for food quality control.

Later on, it was investigated the determination of four tetracycline antibiotics in milk samples using a tetracycline-selective electrode coupled to reversed-phase liquid chromatography (section 4.4). Firstly, the potentiometric response observed for chlortetracycline, doxycycline, oxytetracycline, and tetracycline proved the potential of CB[8] as a macrocyclic host for the development of a new tetracycline-selective electrode. After miniaturization and coupling the tetracycline-selective electrode on the chromatographic system, the mobile phase composition, elution mode, and the hydrodynamic parameters were optimized. The separation was attained in less than 30 min using a gradient mobile phase of sulphuric acid and acetonitrile. On the other hand, the incorporation of multi-walled carbon nanotubes in

the sensing membrane improved the sensitivity, detectability, and precision of the potentiometric detector. The limits of detection and quantification ranged from 13.3 to 46.0 μg L^{-1} and 44.4 to 92.1 μg L^{-1}, respectively. Notably, this is the very first potentiometric detector coupled to LC for the quantification of tetracycline antibiotics, showing the ability to detect levels around the maximum residue limit imposed by international authorities (100 μg L^{-1} in milk).

In a different approach, the synergic coupling of potentiometric detection with LC was demonstrated by the analytical determination of ammonium ions at low micromolar levels in water samples in the presence of high levels of potassium and sodium, using nonactin-based potentiometric sensors (section 4.5). Particularly, the ammonium-selective electrodes were assembled in a microfluidic thin-layer flow cell, which was used as a detector in ion chromatography. Notably, the separation of both cations was achieved in less than 15 min by isocratic elution with a mobile phase of nitric acid. The detection and quantification limits were 5.4 and 18.0 μg L^{-1}, respectively. Advantageously, the used microfluidic flow cell could be equipped with three ISEs for reproducibility purposes or with different ISEs for multi-ion detection within the same sample. In this context, ammonium-, sodium-, and potassium-selective electrodes were incorporated into the flow cell as a preliminary proof-of-concept, revealing an accurate detection of the respective ions in river samples. Moreover, multi-ion detection is expected to be feasible in any kind of water (drinking water or even more complex matrix such as seawater).

The high complexity of samples analyzed through this thesis still requires the use of sample clean-up procedures, namely solid-phase extraction in both determinations of biogenic amines (section 4.2 and 4.3) and tetracycline antibiotics (section 4.4). Exceptionally, the determination of ammonium ions in environmental water samples required only a filtration step before injection to remove solid particles (section 4.5). Nevertheless, the sample pretreatment step was lower than 90 min, including the extraction of the target analytes from different samples, dryness of the eluate, and reconstitution of the residue.

Overall, the LC-potentiometric methodologies proposed in the present thesis are in agreement with international guidelines in terms of precision and accuracy. Their simple, robust, affordable, and user-friendly instrumentation makes the potentiometric detection techniques a straightforward alternative to the expensive, complex, and laborious analytical methods implemented in routine analysis in the food quality sector.

The portability and miniaturization ability of potentiometric sensors, combined with innovative sample operation techniques and downsizing of chromatographic columns, will

certainly leverage the development of an integrated lab-on-chip platform for the remote analysis of different samples, enabling the decentralization of such analytical determinations from the lab context.

5.2. Future perspectives

The advantages of the synergic coupling of potentiometric detection with liquid chromatographic systems herein discussed highlight the interest for further investigation in the determination of other relevant analytes in different fields, such as catecholamines in clinical diagnosis, contaminants in pharmaceutical products, and antibiotics in environmental samples. One particular challenge is the determination of hydrophilic analytes with adequate detectability and sensitivity similar to those already obtained for lipophilic compounds. Further work is also required to demonstrate the robustness and universality of potentiometric detectors. In this context, the use of nanomaterials in the preparation of potentiometric sensors will contribute to these achievements due to their attractive properties.

The most promising application stands by the development of a portable lab-on-chip chromatography platform for decentralized analysis, maintaining the resolution of separation and analytical features of the detector. Although the extensive investigation accomplished so far, no microfluidic platform for chromatographic separation with potentiometric detection was reported in the scientific literature. Chromatographic separation can be obtained by packaging silica-based particles on the microfluidic channels or by a chemical modification of the channel surface to provide suitable selectivity for the target analytes. On the other hand, different sensor construction can be evaluated, such as paper-based electrodes, to be accommodated in microfluidic platforms.

So far, subtractive manufacturing technology has been the method of election, which involves laborious process planning, high precision, and generating material wastage. Additive manufacturing (3D printing) will contribute to suppressing these drawbacks, making simpler and faster the fabrication of prototypes that could be easily tested and modified if necessary. On the other hand, engineering processes will also be required for the miniaturization of pumps and injection valves to create a fully portable platform.

Appendix

Appendix A. Short CV

1991	Born on the 18th of March in Mirandela, Portugal.
1996 – 2001	Primary school education – Lamas de Orelhão, Mirandela.
2001 – 2009	Preparatory and secondary school education – Mirandela.
2009 – 2014	MSc. Degree in Pharmaceutical Sciences – University of Porto, Portugal.
2015 – 2017	Pharmacist – Farmácias Holon, Portugal.
2018 – 2022	Ph.D. Degree in Pharmaceutical Sciences – University of Porto, Portugal.

Papers directly resulting from the Doctoral Thesis

1. Gil, R. L.; Amorim, C. G.; Montenegro, M.; Araujo, A. N. Potentiometric detection in liquid chromatographic systems: an overview. Journal of Chromatography A 2019, 1602, 326-340. DOI: 10.1016/j.chroma.2019.06.006.
2. Gil, R. L.; Amorim, C. G.; Montenegro, M. C. B. S. M.; Araújo, A. N. Determination of biogenic amines in tomato by ion-pair chromatography coupled to an amine-selective potentiometric detector. Electrochimica Acta 2021, 138134. DOI: 10.1016/j.electacta.2021.138134.
3. Gil, R. L.; Amorim, C. G.; Montenegro, M. C. B. S. M.; Araújo, A. N. HPLC-potentiometric method for determination of biogenic amines in alcoholic beverages: A reliable approach for food quality control. Food Chem. 2022, 372, 131288. DOI: 10.1016/j.foodchem.2021.131288.
4. Gil, R. L.; Amorim, C. G.; Cuartero, M. Addressing the detection of ammonium ion in environmental water samples via tandem potentiometry–ion chromatography. ACS Measurement Science Au 2022. DOI: 10.1021/acsmeasuresciau.1c00056.
5. Gil, R. L.; Amorim, C. M, P. G; Montenegro, M. d. C. B. S. M.; Araújo, A. N. Cucurbit[8]uril-based potentiometric sensor coupled to HPLC for determination of tetracycline residues in milk samples. Chemosensors 2022, 10, 98. DOI: 10.3390/chemosensors10030098.

Papers indirectly resulting from the Doctoral Thesis

1. Gil, R.; Amorim, C. G.; Araújo, A. N.; Montenegro, M. C. B. S. M. Process Analysis: Electroanalytical Techniques in Encyclopedia of Analytical Science, (3rd ed.), Worsfold, P.; Poole, C.; Townshend, A.; Miró, M., Editors.; Amsterdam: Elsevier, 2018, pp 384–388.
2. Amorim, C. G.; Gil, R. L.; Cevallos-Mendoza, J.; Araújo, A. N.; Rodríguez-Díaz, J. M.; da Conceição Montenegro, M. 3D Printing Technology in the Environment. In Advances in the Domain of Environmental Biotechnology, 2021; pp 131-160.
3. Gil, R. L.; Amorim, C. G.; Rodríguez-Díaz, J. M.; Araújo, A. N.; Montenegro, M. C. B. S. M. Nanofibers in Medical Microbiology. In Nanotechnology for Advances in Medical Microbiology, 2021; pp 87-117.

Oral communications

1. R. Gil*, C.G. Amorim, M.C.B.S.M. Montenegro, A.N. Araújo. *Potentiometric detection in liquid chromatographic systems*. XXIV Encontro Luso-Galego de Química. November 2018. Porto (Portugal)
2. M.C.B.S.M. Montenegro*, R. Gil, C.G. Amorim, A.N. Araújo. *Potentiometric detection in flow analysis systems: the particular case of liquid chromatography*. II Convención Científica Internacional UCLV 2019, VII Simpósio Internacional de Química 2019. June 2019, Santa Clara (Cuba).
3. R. Gil*, C.G. Amorim, M.C.B.S.M. Montenegro, A.N. Araújo. *Biogenic amines determination by ion-pair chromatography using potentiometric detection*. XXV Encontro Luso-Galego de Química. November 2019. Santiago de Compostela (Spain).
4. R. Gil*, C.G. Amorim, M.C.B.S.M. Montenegro, A.N. Araújo. *Determination of ten underivatized biogenic amines by ion pair chromatography using potentiometric detection*. 71st Annual Meeting of the International Society of Electrochemistry. September 2020. Online.
5. R. Gil*, C.G. Amorim, M.C.B.S.M. Montenegro, A.N. Araújo. *Potentiometric detection in liquid chromatographic systems: analytical applications for food analysis*. LAQV Webinar. October 2021. Online.

Posters

1. R. Gil*, M.C. Sarraguça, C.G. Amorim, M.C.B.S.M. Montenegro, A.N. Araújo. *Lithium determination in human serum with improved accuracy using potentiometric detection*. 26th National Meeting of the Portuguese Chemical Society. June 2019, Porto (Portugal)
2. A. Mantovani, R. Gil, A.N. Araújo, M.C.B.S.M. Montenegro, C.G. Amorim*. *Ranitidine selective electrode based on curcubit[6]uril for pharmaceutical quality control*. XXV Encontro Luso-Galego de Química. November 2019. Santiago de Compostela (Spain).
3. I. Costa*, R. L. Gil, C. G. Amorim, M.C.B. Montenegro, A. N. Araujo. *Study of cucurbit[n]urils as ionophores for the potentiometric detection of biogenic amines with high impact in clinical diagnosis*. 14th Young Research Meeting of University of Porto (IJUP). May 2021. Online.

Awards

3rd prize – Business Ignition Programme 2020 (U. Porto Innovation).

Self-contained heterogeneous separation/potentiometric sensing devices for the screening of alike compounds in food matrices

Renato Lopes Gil

Faculdade de Farmácia